La Formation Ayabacas (limite Turonien-Coniacien, Sud-Pérou) : collapse sous-marin en réponse à l'amorce de l'orogenèse andine

Pierre Callot

THÈSE

En vue de l'obtention du

DOCTORAT DE L'UNIVERSITÉ DE TOULOUSE

Délivré par *l'Université Toulouse III – Paul Sabatier*
Discipline ou spécialité : *Sciences de la Terre - Géologie*

Présentée et soutenue par *Pierre CALLOT*
Le *26 juin 2008*

Titre :

La Formation Ayabacas (limite Turonien-Coniacien, Sud-Pérou) : collapse sous-marin en réponse à l'amorce de l'orogenèse andine

---

JURY

M. Dominique Chardon, Professeur, Toulouse, Président
M. Etienne Jaillard, Directeur de recherche, Grenoble, Rapporteur
M. Thierry Mulder, Professeur, Bordeaux, Rapporteur
M. Roger Urgeles Esclasans, Maître de conférence, Barcelone, Examinateur

---

Ecole doctorale : *Sciences de l'Univers, de l'Environnement et de l'Espace*
Unité de recherche : *Laboratoire des Mécanismes de Transferts en Géologie (LMTG)*
Directeur(s) de Thèse : *Francis Odonne et Thierry Sempéré*

THÈSE

En vue de l'obtention du

DOCTORAT DE L'UNIVERSITÉ DE TOULOUSE

Délivré par *l'Université Toulouse III - Paul Sabatier*
Discipline ou spécialité : *Sciences de la Terre - Géologie*

Présentée et soutenue par Pierre CALLOT

Le 26 juin 2008

La Formation Ayabacas (limite Turonien-Coniacien, Sud-Pérou) : collapse sous-marin en réponse à l'amorce de l'orogenèse andine

JURY

M. Dominique Chardon	*Professeur, Toulouse*	*Président*
M. Etienne Jaillard	*Directeur de recherche, Grenoble*	*Rapporteur*
M. Thierry Mulder	*Professeur, Bordeaux*	*Rapporteur*
M. Roger Urgeles Esclasans	*Maître de conférence, Barcelone*	*Examinateur*

Ecole doctorale : *Sciences de l'Univers, de l'Environnement et de l'Espace*
Unité de recherche : *Laboratoire des Mécanismes et Transferts en Géologie (LMTG)*
Directeurs de Thèse : *Francis ODONNE (Professeur, Toulouse) & Thierry SEMPERE (Chargé de recherche, Toulouse)*

"…when you have eliminated the impossible, whatever remains, however improbable, must be the truth."

''…lorsque vous avez éliminé l'impossible, ce qui reste, si improbable soit-il, est nécessairement la vérité.''

Sir Arthur Conan Doyle (1859 - 1930),
à plusieurs reprises dans les romans mettant en scène Sherlock Holmes

Remerciements

A l'issue de plus de trois ans de thèse, nombreux sont ceux qui ont apporté leur petite pierre à l'édifice et méritent mes remerciements. Je vais probablement en oublier quelques-uns, je les prie de m'en excuser…

En priorité je tiens à exprimer ma gratitude à la famille ''élargie'' : mes parents tout d'abord, pour leur soutien actif tant du point de vue moral que financier et pour la relecture de la thèse ; la Famille Mandret au grand complet (Claire, Philippe, Marine et le petit Paul) ; ma chère petite sœur Laure à qui Lima et même Toulouse semblaient bien loin ; et enfin ma petite chérie Cintya, qui a notamment supporté le pire (les 10 derniers mois de la thèse…) et qui a alors fait tout son possible et même plus pour me faciliter la vie.

J'adresse aussi mes plus vifs remerciements à mes deux directeurs de thèse, Francis Odonne et Thierry Sempéré, pour m'avoir proposé ce sujet passionnant et m'avoir si bien soutenu, notamment dans la rédaction des articles, depuis la Maîtrise pour Francis, et tout au long de la thèse pour tous les deux. Mes remerciements vont également à l'ensemble du jury : Etienne Jaillard et Thierry Mulder qui ont rapporté mon travail, Dominique Chardon qui a présidé la soutenance et Roger Urgeles dont j'ai apprécié les nombreuses remarques constructives.

Au Pérou, je tiens tout particulièrement à remercier l'INGEMMET et les géologues péruviens qui m'ont accueilli pendant 15 mois. Je voudrais également dire merci à tout le personnel de la représentation de l'IRD à Lima et notamment son directeur Pierre Soler pour sa bonne humeur et son soutien constant, Miriam Soto qui a toujours fait le maximum pour régler tous les problèmes avec les administrations françaises et péruviennes (et il y en a eu !), Alexandra Roulet pour avoir toujours facilité l'aspect comptable des missions, les chauffeurs péruviens José, Enrique et Hernan(do) qui m'ont supporté pendant les longs séjours sur le terrain.

Je suis également très reconnaissant envers Laurence et Olivier Audin-Hourton, Hugo et Alexandra Perfettini ainsi que François Pujos pour leur accueil et leur aide au Pérou. Merci également à Jean-Loup Guyot pour la spéléo à Soloco, et à tous les amis péruviens que j'ai rencontrés au Pérou : Astrid, le trio Yvette Yvan Yvo, Jhon, Karina, Marco, Jovita, Milka, la Famille Anapán Becerra,…

Beaucoup méritent aussi mille mercis au sein du laboratoire LMTG ! Yves Godderis, Carine Lézin, Bernard Andreu, Elie-Jean Debroas, Agnès Maillard et Michel de Saint-Blanquat pour leur soutien au cours de la thèse ou dans la préparation des enseignements. Christiane Cavaré Hester pour son aide lors de mes petits soucis avec Illustrator, pour les scans et pour les impressions. Yann, Manu et Yoann pour les canons à Vienne… Et enfin tous les latinos ou ''assimilés latinos'' du labo pour les bons moments passés au labo ou en dehors ces dernières années : Teresa, Laurent, Carolina, Ana, Benjamin, Ysabel, Rolo, Riccardo, Vincent, Marcelo, Waldo, Magalie,… et tous ceux que j'oublie. Un remerciement spécial pour Marianne qui m'aura accompagné jusqu'au bout, nous avons loupé de peu la soutenance le même jour !

Je veux aussi remercier tous les amis de la fac : Claire, Flo et Laure (sans ordre de préférence, inutile de vous battre, c'est par ordre alphabétique…), Vivien et Yoyo pour la colocation, Bertrand, Natacha, Clo, Gaël (le Sgag), et tous ceux qui sont venus dans nos WE (soi-disant) géologie du 1er Mai… Un grand merci à la Famille ''Denèle'', Claire et Christian, Magali et Julio, pour m'avoir si souvent et si chaleureusement accueilli en Ariège.

Enfin, je n'aurais probablement pas fait de géologie sans la spéléo. Ma reconnaissance va à tous mes amis de sorties sous terre, et plus particulièrement Alain Massuyeau qui m'a tant apporté, notamment au cours des premières années, lors des initiations avec Thomas ; Bruno Nurisso pour sa bonne humeur, ses bonnes blagues et tout le reste ; Mickey Douat, Philippe Pélissier, Richard Maire et de nombreux membres de l'ARSIP qui m'ont donné le goût de la découverte (ah, les grandes discussions devant un feu de camp ou au Chalet du Bracas pendant l'AG !) ; et je salue bien sûr mes deux compagnons de galère des grosses virées, Gaël Enaud et Olivier Lacroix.

Résumé

La Formation Ayabacas est une unité resédimentée, affectée de déformations spectaculaires, qui affleure irrégulièrement dans les Andes du sud du Pérou. Elle résulte du collapse sous-marin, aux alentours de la limite Turonien-Coniacien (~91-89 Ma), de la quasi-totalité de la plate-forme carbonatée qui s'était mise en place au cours de deux transgressions, entre l'Albien inférieur et l'Albien supérieur (~108,5 - ~102 Ma) pour la première, et entre le Cénomanien supérieur et le Turonien supérieur (~95 - ~90 Ma) pour la seconde. Le collapse a affecté une surface d'au moins 80 000 km^2 et les dépôts, parfois absents à l'amont, atteignent plus de 500 m d'épaisseur à l'aval. Il a été déplacé, au cours d'un événement unique à l'échelle des temps géologiques, un volume de matériaux estimé à > 10 000 km^3. Ces dimensions, de l'ordre de celles des glissements sous-marins géants récents, font du collapse Ayabacas le plus grand glissement sous-marin fossile actuellement connu.

Le collapse s'organise du NE au SW en six zones basées sur les faciès de déformation, en relation avec deux importants systèmes structuraux d'échelle lithosphérique (une septième zone, à l'extrême NE, correspondant aux dépôts non déstabilisés). Dans les parties amont du collapse (zones 1 à 3, au NE), les dépôts forment une méga-brèche, avec des éléments de taille décamétrique à kilométrique (principalement des nappes et des radeaux calcaires, souvent plissés plastiquement ; plus rarement des blocs rigides dérivés de formations crétacées et paléozoïques) flottant dans un mélange de petits clastes carbonatés ou siliciclastiques et de matériaux pélitiques rougeâtres. Ce mélange de matériaux enclins à se liquifier et à se déformer plastiquement a servi de semelle de glissement aux plus gros éléments. Ces zones se caractérisent également par des déformations et des faciès bréchiques quelle que soit l'échelle d'observation. Les parties aval, au SW, sont exclusivement carbonatées, avec un empilement de masses calcaires de tailles croissantes, une disparition de la semelle de glissement très ductile et une organisation croissante des dépôts marquant un amortissement du collapse.

Le collapse Ayabacas, qui s'est produit sur une marge qui paraissait *a priori* stable, est atypique comparé aux autres glissements actuels ou fossiles. Intervenant immédiatement avant la rapide continentalisation du bassin d'arrière-arc sud-péruvien, et donc l'émergence des Andes, le collapse est une des conséquences de changements géodynamiques à l'échelle de la cellule de convection mantellique du Pacifique, qui ont notamment entraîné une brusque modification des conditions de subduction dans le sud du Pérou. Ce bouleversement a provoqué une flexure de la lithosphère de l'arrière-arc et un découpage du substratum ante-Ayabacas en blocs basculés par des failles normales, créant des pentes favorables au collapse de la plate-forme.

Abstract

The Ayabacas Formation, which crops out irregularly in the Andes of southern Peru, is a resedimented unit displaying spectacular deformation. It results from the submarine collapse, near the Turonian-Coniacian boundary (~90 Ma), of the carbonate platform that had developed during two transgressions, in the early to late Albian (~108.5 - ~102 Ma) and from the late Cenomanian to late Turonian (~95 - ~90 Ma). The collapse extended over more than 80 000 km^2 and its deposits, which are locally lacking in the head, reached > 500 m in thickness in the toe. More than 10 000 km^3 of sedimentary materials were displaced during a single event (at the scale of geological time). Its dimensions are comparable to those of recent giant slides and the Ayabacas collapse appears as the most extensive fossil submarine mass-wasting body currently known.

Deposits are organised from NE (head) to SW (toe) into six zones, on the basis of deformational facies and in relation with two important structural systems that were reactivated at the time of collapse. A seventh zone corresponds to the northeastern 'stable' platform. In zones 1 to 3, deposits consist in a megabreccia, with elements of 10s to 100s of metres (limestone rafts and sheets, plastically folded, and less commonly rigid blocks deriving from Cretaceous or Paleozoic units) 'floating' in a calcareous-siliciclastic mix of small clasts and red mudstones to siltstones. These materials were partly liquified and easily deformable and thus prone to ductile deformation: they acted as a sliding sole that greatly facilitated the downslope displacement of the larger elements. These zones are also characterised by deformation and brecciation at whichever scale. Zones 4 to 6, at the toe of the collapse, are exclusively calcareous and display stacked limestone masses that increase in size, due to the westward disappearance of the ductile sliding sole.

When compared with recent or fossil giant slides, the Ayabacas Formation appears as an atypical collapse because it occurred along an apparently stable backarc margin. The collapse occurred just prior to the rapid continentalization of the backarc basin of Peru, which have long been interpreted to mark the beginning of the Andean orogeny, and was one of the consequences of the significant changes that affected the Pacific mantle convection cell between ~91 and 70 Ma. Along the Peru margin, the conditions of subduction were abruptly modified starting ~91-89 Ma: decrease in slab subduction angle increased plate coupling and slab velocity, which dragged down and flexured the backarc lithosphere. This flexuration normal-faulted the backarc substratum, which triggered the giant collapse of its sedimentary cover.

Table des matières

I.

INTRODUCTION

I. Introduction

I.1. Les glissements sédimentaires sous-marins : intérêt de l'étude

Les glissements sédimentaires sous-marins sont un phénomène courant (Canals et al., 2004 ; Hünerbach et al., 2004) qui se produit à toutes les échelles dans les séries sédimentaires des marges continentales actives ou passives (Mienert et al., 2002 ; Locat & Mienert, 2003) et au niveau des édifices basaltiques des îles volcaniques (Urgeles et al., 1997, 1999). Plusieurs raisons expliquent l'intérêt scientifique qui leur a été porté, en particulier depuis les années 1980.

Tout d'abord, les glissements sédimentaires sous-marins sont reconnus comme étant un processus majeur de la redistribution des sédiments sur les marges continentales (Mienert et al., 2002; Canals et al., 2004 ; Hünerbach et al., 2004 ; Lucente & Pini, 2008). Ils peuvent déplacer des quantités extrêmement importantes de sédiments en très peu de temps, sur de grandes distances et ce malgré des pentes très faibles. Par exemple Talling et al. (2007) estiment que 125 km^3 de sédiments (soit 22,5 x 10^{13} kg, *i.e.* environ dix fois la quantité de sédiments transportés annuellement par l'ensemble des rivières du monde vers les océans (Milliman & Syvitski, 1992 ; Syvitski, 2003)) ont été transportés jusqu'à 1500 km de leur lieu de dépôt originel, en quelques heures ou quelques jours, lors d'un seul glissement au large des côtes de l'Afrique du nord-ouest, alors que la pente ne dépasse pas 0,05°. Dans le cas du courant de turbidité des Grands Bancs (Terre Neuve, Canada) en 1929, ce sont plus de 150 km^3 de sédiments qui ont été déplacés à plus de 700 km en quelques heures (Piper et al., 1999). Plusieurs glissements sous-marins géants récents ont déplacé en quelques centaines à quelques dizaines de milliers d'années plus de 1 000 km^3 de matériaux : 2 400 à 3 200 km^3 en moins de 1 000 ans pour le "Storegga Slide" (Haflidason et al., 2004, 2005), 1 100 à 1 400 km^3 pour le "Bjørnøyrenna Slide" (Vorren & Laberg, 2001), 1 400 km^3 pour le "Cape Fear Slide" (Popenoe et al., 1993), 600 à 1 100 km^3 pour le "Saharan Debris Flow" (Gee *et al*., 1999), ~1 000 km^3 pour les "Israel Slump Complexes" (Frey-Martínez *et al*., 2005) ou ~1 000 km^3 pour la "Orotava-Icod-Tino Avalanche" (Wynn *et al*., 2000). Dingle (1977) estime que certains glissements le long de la marge de l'Afrique du Sud auraient déplacé de 10 000 à 20 000 km^3 de matériaux, un ordre de grandeur équivalent à l'estimation du volume de matériaux déplacés lors du collapse de l'Ayabacas (Callot et al., 2008).

Une importante proportion des marges continentales étant sous l'influence des instabilités sédimentaires (~10 % des marges continentales des Etats-Unis, et jusqu'à 27% pour le Golfe du Mexique d'après McAdoo et al., 2000), ces dernières vont avoir un impact sur la géométrie et la distribution des dépôts sédimentaires, notamment ceux pouvant potentiellement servir de couche imperméable de scellement ou de réservoir aux hydrocarbures (Mienert et al., 2002). Les recherches pour mieux comprendre la redistribution des sédiments par les instabilités sous-marines sont donc particulièrement importantes dans le cadre de l'exploration de gisements d'hydrocarbures.

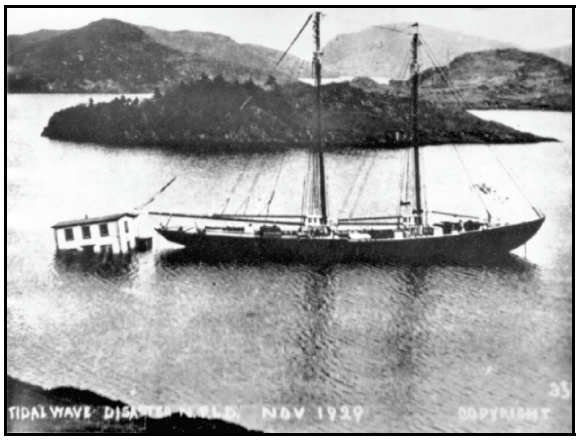

Fig. I.1 : Photographie d'un bateau remorquant une maison entraînée en mer par le tsunami qui a suivi le glissement sédimentaire sous-marin des Grands Bancs, le 18 novembre 1929. Extrait de Locat & Lee (2002).

Cependant, ce n'est pas uniquement dans le cadre de la recherche de nouveaux gisements que l'industrie s'intéresse à l'étude des glissements sédimentaires. La prospection d'hydrocarbures off-shore a migré vers des zones de plus en plus profondes, notamment vers des zones instables, comme les talus continentaux, où le risque de rupture sédimentaire augmente (Barley, 1999 ; Campbell, 1999). Par exemple, le gisement gazeux d'Ormen Lange, un des plus importants au monde, se situe au niveau de l'arrachement du Storegga Slide (bien que dans ce cas précis le risque de nouveau glissement sous-marin géant ait été écarté (Nadim et al., 2005 ; Solheim et al., 2005b)). Des plates-formes pétrolières off-shore ont également été détériorées dans le delta du Mississipi (Bea, 1971 ; McAdoo et al., 2000). Il existe donc un risque potentiel pour les installations d'exploration ou d'exploitation, car même de petits glissements pourraient les endommager (Mienert et al., 2002). Les ruptures sédimentaires sous-marines représentent également un danger pour d'autres installations sous-marines ou côtières, notamment à cause des tsunamis qu'elles sont susceptibles de provoquer. Plusieurs exemples historiques ou récents de catastrophes naturelles ont ainsi montré le rôle des glissements sous-marins et/ou des tsunamis associés. Ainsi lors du séisme de 1755, la côte du Portugal et en particulier de Lisbonne a été dévastée par un tsunami résultant probablement

d'un glissement sous-marin (Gracia et al., 2003). Un autre exemple classique est le courant de turbidité causé par le séisme de magnitude 7.2 (Piper et al., 1999) qui s'est produit le 18 novembre 1929 au niveau des Grands Bancs (Terre Neuve, Canada). Le séisme a provoqué plusieurs petits slumps rotationnels sous-marins (Piper et al., 1999) qui ont d'abord rompu presque simultanément tous les câbles télégraphiques sous-marins sur le plateau continental (Heezen & Ewing, 1952) pour se transformer ensuite graduellement en coulées de débris puis en courant de turbidité (Piper et al., 1992 ; 1999), brisant progressivement les câbles plus en aval (Heezen & Ewing, 1952 ; Heezen et al., 1954). Le glissement sous-marin a également donné naissance à un tsunami, observé jusqu'en Europe, qui a causé des destructions (Fig. I.1) et des pertes humaines sur la côte canadienne (Murty, 1977 ; Clague, 2001 ; Fine et al., 2005). Enfin un exemple plus récent est le courant de turbidité déclenché à Nice en 1979 par des travaux d'extension de l'aéroport de Nice. Une partie des terrains gagnés sur la mer se sont effondrés le 16 octobre 1979 lors d'un glissement sédimentaire, entraînant avec eux vers les fonds grands fonds sous-marins les bulldozers (à 15 km de la zone de départ ; Mulder et al., 1997) et provoquant là encore la rupture des câbles sous-marins et un tsunami (Gennesseaux et al., 1980 ; Piper & Savoye, 1993).

La compréhension des glissements sédimentaires est donc un enjeu important en sciences de la terre pour déterminer la géométrie de leurs dépôts et pour prévenir les dommages qu'ils peuvent occasionner sur les installations en mer et le long des côtes. Des liens entre évolutions climatiques naturelles de la planète et glissements sédimentaires sous-marins semblent également exister, avec des relations importantes entre gisements de méthane sous forme d'hydrates de gaz, instabilités sédimentaires et changements climatiques (Dickens et al., 1997 ; Mienert & Posewang, 1999 ; Vogt et al., 1999 ; Dickens, 2003).

I.2. Problématique et objectifs de la thèse

La problématique de cette thèse s'articule autour des déformations très particulières affectant les dépôts calcaires marins de la Formation Ayabacas, qui ont été interprétées très différemment selon les auteurs malgré des descriptions très similaires.

Ces calcaires furent nommés Formation "Ayavacas" (sic) par Cabrera La Rosa & Petersen (1936) en référence au village du même nom, situé à ~10 km au nord-est de Juliaca (Fig. I.2), près duquel se trouvent des affleurements remarquables. Sempere et al. (2000) ont corrigé cette orthographe en Formation Ayabacas, conformément à la toponymie officielle (Fig. I.3).

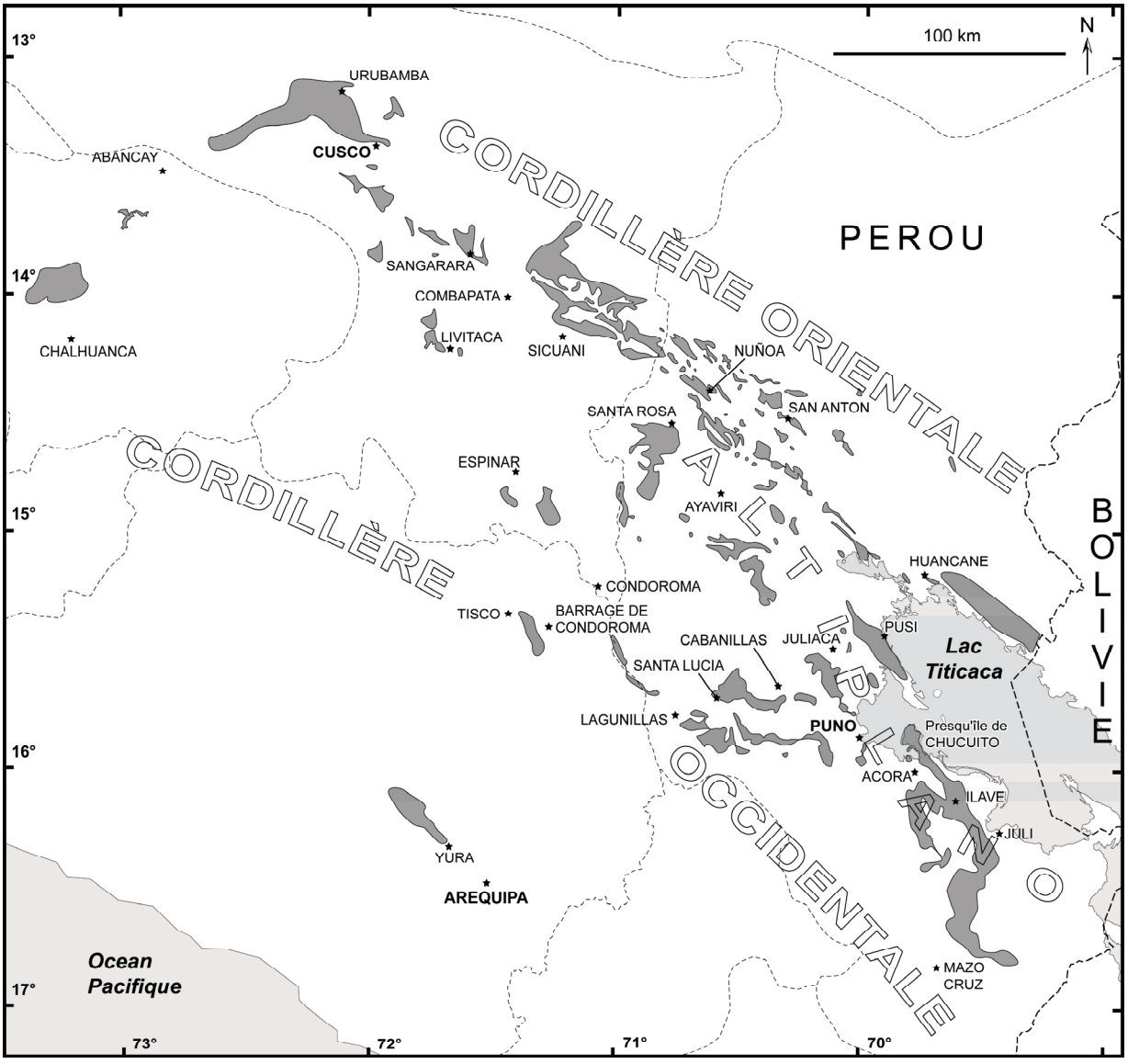

Fig. I.2 : Carte de localisation des principales villes de la zone d'étude et des zones d'affleurement de la Formation Ayabacas et d'une partie de la Formation Arcurquina. Réalisée à partir des cartes géologiques de l'INGEMMET (Instituto Geológico Minero y Metalúrgico, Perou), des photographies aériennes et des observations de terrain.

Premier auteur à décrire quelques affleurements dans la région de Pusi, Rassmuss (1935) suggère une explication tectonique à cette structure chaotique. Les observations, dans la même zone, de Cabrera La Rosa & Petersen (1936) sont plus précises et ces deux auteurs sont les premiers à décrire la formation comme une brèche, à remarquer que les bancs calcaires ont été déformés avant d'être consolidés et à souligner qu'une origine tectonique orogénique ne peut pas expliquer, à elle seule, la genèse de cette brèche. Bien que les concepts de grand glissement sous-marin soient inconnus à cette époque, ils proposent que cette brèche se soit formée sur le fond sous-marin, peut-être suite à un tsunami ou à cause de phénomènes de lithification différée. A la fin des années 1940, deux auteurs (Heim, 1947 ; Newell, 1949) ont étudié la géologie du sud du Pérou. Les descriptions de Newell (1949) concernant la Formation Ayabacas sont particulièrement éloquentes: *"the formation is intricately folded and broken, in extreme disorder*" ; "*the limestone masses (...) are identical lithologically*" ; "*relatively weak, or "incompetent" to compression (...) whereas subjacent and superjacent strong formations are very much less profoundly affected*". Cependant, ils concluent tous deux que la Formation Ayabacas est le produit de la tectonique andine, de même que Kalafatovich (1957) après son travail dans la zone de Cusco sur la Formation Yuncaypata, redéfinie par la suite comme l'équivalent local de la Formation Ayabacas (Carlotto *et al.*, 1996).

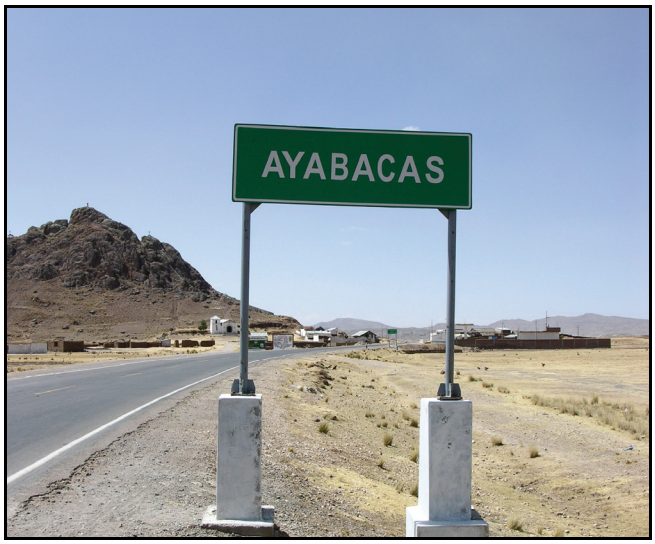

Fig. I.3 : Panneau indicateur à l'entrée du village d'Ayabacas (~10 km au NE de Juliaca) qui a donné son nom à la Formation Ayabacas.

Finalement, le premier ouvrage dans lequel la genèse de la Formation Ayabacas est associée à une instabilité sédimentaire est la thèse de Portugal (1964) sur la zone de Santa Lucia, mais dont les résultats sont finalement publiés dix ans plus tard. Dans cette publication,

Portugal (1974) écrit notamment "*I am speaking of gravity sliding or gravitational tectogenesis of an uplifted area in which the sediments have slipped down-slope and became compressed, folded, and overthrust in areas of lower elevation with the assumption that the nonconsolidated limestones have yielded plastically*". Il liste également une série de six points justifiant son interprétation de glissement tectonique non-orogénique (*nonorogenic gliding-tectonics idea*): (1) constatation d'une pente sur laquelle les glissements ont pu se produire ; (2) absence de clivage sur le flanc inverse des plis ; (3) la structure chaotique des blocs montre qu'ils se sont déplacés indépendamment les uns des autres ; (4) les plis sont empilés ; (5) des flancs amincis ont été préservés ; (6) les calcaires Ayabacas reposent sur des niveaux rouges argileux qui ont pu aider au glissement des calcaires.

Audebaud fournit des dessins explicites (Fig. I.4) et des descriptions précises des déformations dans sa thèse de 3ème cycle (Audebaud, 1967), et pressentit l'hypothèse de glissements sous-marins (cependant suivis d'importantes déformations dues à la tectonique orogénique), mais la minimisa fortement par la suite en proposant d'autres explications aux déformations particulières de la Formation Ayabacas : déformations dysharmoniques et/ou polyphasées (Audebaud & Laubacher, 1969; Audebaud, 1970, 1971a,b; Audebaud & Debelmas, 1971; Audebaud *et al*., 1973), karstification précoce formant les brèches, appareils hypovolcaniques, diapirisme (Audebaud, 1971a). Mais curieusement, il ne reprend pas, dans ces dernières publications, l'idée de glissements sous-marins majeurs, suggérant seulement la survenue de petits collapses synsédimentaires peu significatifs. A la même période, d'autres auteurs, dont l'étude se limite à la zone de Pirin, considèrent que les déformations Ayabacas ont une origine purement tectonique et sont dues à un empilement de nappes tectoniques (Chanove et al., 1969).

Des descriptions précises sont données par De Jong (1974) à l'ouest du Lac Titicaca, à proximité de Puno et Pusi. La nouvelle interprétation qu'il propose — des glissements gravitaires subaériens survenant peu après le dépôt — ne tient pas compte de, et semble difficilement compatible avec, les déformations plastiques des radeaux calcaires et les brèches hydroplastiques observés sur le terrain. Quelques années plus tard, Laubacher (1978) discute les interprétations de Chanove et al. (1969) et de De Jong (1974) dans la zone Pusi, et penche pour celle de Chanove et al. (1969), tout en admettant que l'hypothèse du glissement gravitaire de De Jong (1974) ne peut être totalement exclue. Il propose d'ailleurs des glissements gravitaires tectoniques pour expliquer la présence d'olistolithes de calcaires Ayabacas plus au sud-ouest, dans la zone de Lagunillas (Laubacher, 1978). Klinck et al. (1986) et Ellison et al. (1989) avancent également l'hypothèse des glissements gravitaires

subaériens, mais d'âge Néogène Supérieur. Au même moment, Green & Wernicke (1986) et Moore (1993) soutiennent que la Formation Ayabacas résulte d'un collapse continental produit au Miocène Supérieur par de l'extension crustale de grande ampleur, causée par l'effondrement gravitationnel de la Cordillère.

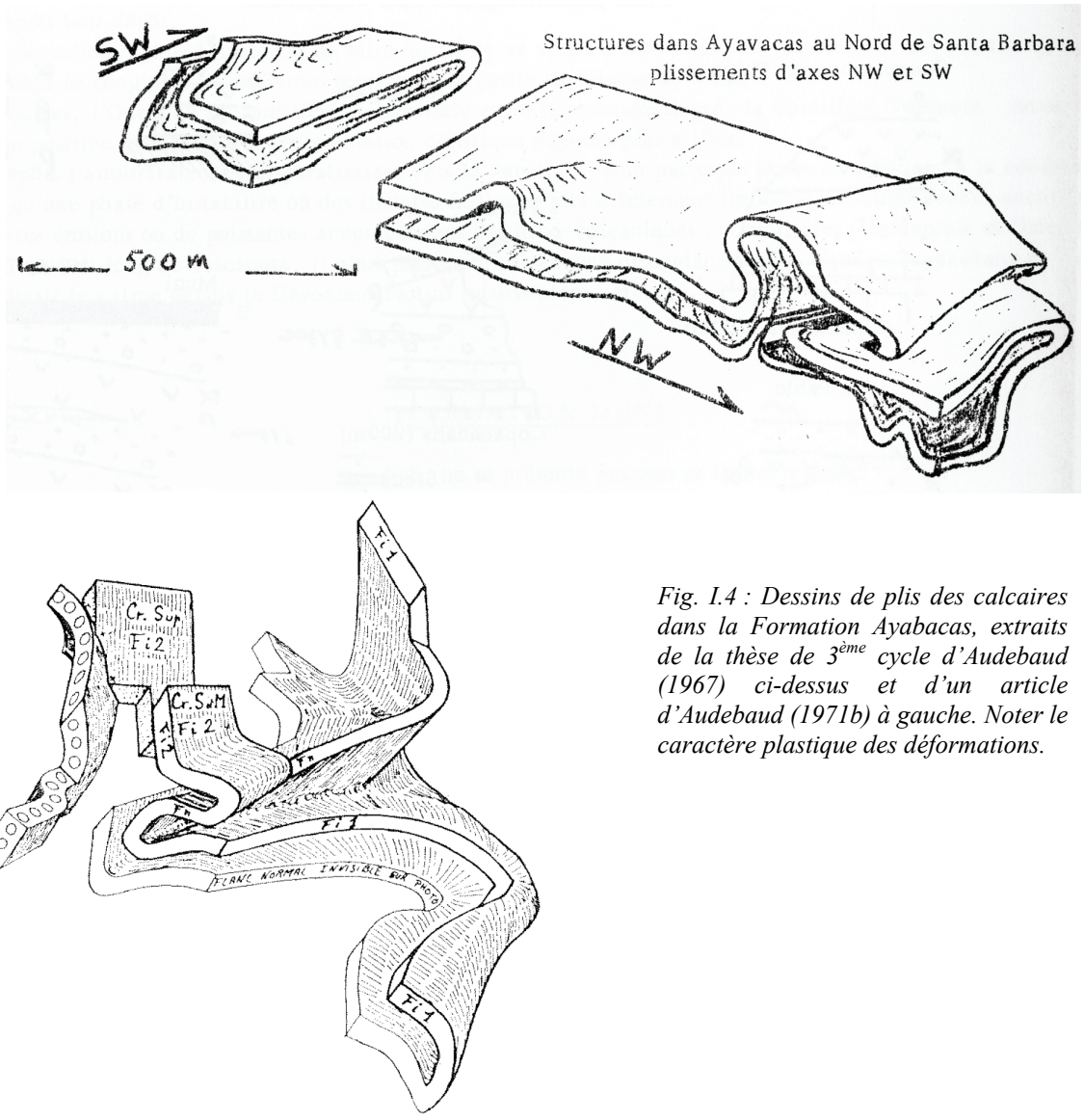

Fig. I.4 : Dessins de plis des calcaires dans la Formation Ayabacas, extraits de la thèse de 3ème cycle d'Audebaud (1967) ci-dessus et d'un article d'Audebaud (1971b) à gauche. Noter le caractère plastique des déformations.

A partir des années 1990, l'hypothèse des glissements sous-marins est de nouveau suggérée dans la région de Cusco (Carlotto et al., 1992, 1996 ; Carlotto, 2002) puis nettement affirmée plus au sud par Sempere et al. (2000) qui décrivent la Formation Ayabacas comme une méga-brèche (*megabreccia, sensu* Spence & Tucker, 1997) sédimentaire d'origine sous-marine.

Le second aspect de la problématique était de relier la Formation Ayabacas à l'histoire de la marge péruvienne, et d'expliquer pourquoi un événement catastrophique de cette ampleur

se produisit précisément à ce moment-là et à cet endroit-là. Un autre phénomène marquant occupe la même position stratigraphique que la Formation Ayabacas : dans le bassin d'arrière-arc du sud Pérou, essentiellement marin depuis le Jurassique inférieur jusqu'au Turonien, les dépôts deviennent presque exclusivement continentaux à partir du Coniacien (Jaillard, 1994, 1995 ; Jaillard et al., 1993). La Formation Ayabacas constitue donc le dernier niveau marin avant la brusque continentalisation du bassin d'arrière arc du sud Pérou, depuis longtemps interprétée comme la marque de l'initiation de l'orogénèse andine (Steinman, 1929 ; Mégard, 1978).

Suite à cette problématique, trois grands objectifs sont apparus :

Le premier objectif était d'étudier précisément la Formation Ayabacas et de définir ses caractéristiques et son organisation. Il s'agissait notamment de montrer sans ambiguïté que les déformations d'ampleur exceptionnelle qui l'affectent résultent principalement d'un collapse sous-marin. Par conséquent il fallait étudier la Formation Ayabacas dans son ensemble, et ne pas la restreindre à une zone géographique limitée comme dans la plupart des études précédentes.

Un deuxième objectif était d'améliorer la compréhension des mécanismes des glissements sous-marins permettant à une formation entière, qui s'étend sur plusieurs centaines de kilomètres le long de la marge, de s'effondrer sur au moins 150 km vers le large. Il s'agissait également de trouver des éléments expliquant le déplacement de masses stratifiées de plusieurs centaines de mètres de côté et plusieurs dizaines de mètres de haut.

Le troisième objectif était d'identifier les conditions dans lesquelles s'est mise en place la Formation Ayabacas, et de déterminer s'il existe un rapport entre les déformations très particulières affectant la Formation Ayabacas et la continentalisation du bassin d'arrière arc, ou si ces deux événements ont été totalement indépendants l'un de l'autre.

I.3. Les glissements sédimentaires sous-marins : état des connaissances

I.3.1. Classification des dépôts de glissements sédimentaires sous-marins

Le principal phénomène physique intervenant lors d'un glissement en masse est la gravité. Cependant d'autres mécanismes interviennent, notamment des phénomènes de liquéfaction lors des séismes (Nichols, 1995) et d'incorporation d'eau dans la masse glissée (Mulder & Alexander, 2001), pouvant entraîner une importante évolution du contenu ou des masses glissées d'un glissement gravitaire entre le moment de son initiation et celui de son dépôt final (Fisher, 1983 ; Mulder & Cochonat, 1996 ; Mulder & Alexander, 2001). La pente ne sera donc pas le seul facteur déterminant le type de glissement sédimentaire.

Les dépôts de transports en masse sous-marins (*submarine mass-wasting complexes* ou MWCs *sensu* Lucente & Pini, 2003, 2008 ; *mass-transport deposits* ou MTDs *sensu* Tripsanas et al., 2008 ; *mass-transport complexes* ou MTCs *sensu* Pickering & Corregidor, 2005) ont été classés suivant le mouvement en masse dont ils résultent. Les processus gravitaires sous-marins sont notablement différents des glissements subaériens et peuvent être séparés en trois catégories (Mulder & Cochonat, 1996 ; Mulder & Alexander, 2001) : (1) ceux dont le transport est généré exclusivement par la gravité (glissements de type *slides* et *slumps*) ; (2) ceux dont le transport est attribuable à un fluide mais qui restent cohésifs (*i.e.* les coulées de boues ou de débris, *mud/debris flow*) et dont le déplacement est laminaire (écoulements plastiques ou *plastic flows*) ; (3) ceux dont le transport est dû à un fluide, qui ne sont pas cohésifs et dont le déplacement est turbulent (coulées fluidisées ou liquéfiées et courants de turbidité, *fluidised/liquefied flows and turbidity currents*).

On distingue ainsi les processus suivants :

- La reptation (*creeping* en anglais). Ce processus implique un glissement lent, sur une surface de décollement, de sédiments (généralement de la boue) conservant leur cohésion mais se déformant plastiquement et très lentement sous l'effet d'une charge constante (Mulder & Cochonat, 1996). Lorsque le processus s'arrête (et s'il s'arrête), les dépôts consistent en des strates, légèrement inclinées et présentant de faibles déformations internes. Si la pente est assez forte ou si les conditions physiques évoluent (*e.g.* chocs dus à un séisme, infiltration de fluides, augmentation de la charge), la reptation peut évoluer et se transformer en glissement sédimentaire (Mulder & Cochonat, 1996 ; Lee & Chough, 2001)

- Les chutes de blocs ou de débris (*debris/rock falls* en anglais). Ce processus correspond au brusque mouvement gravitationnel le long d'une pente très abrupte de

sédiments consolidés ou de fragments du substratum. Les blocs consolidés qui se détachent (parfois hors de l'eau, on-shore) parcourent une distance qui dépend de la taille et de la forme des blocs ainsi que du gradient et de la rugosité de la surface de la pente. Les dépôts résultants, généralement constitués de blocs isolés ou de chaos de blocs sans matrice, se concentrent au bas de la pente (Prior & Doyle, 1985).

- Les avalanches de blocs ou de débris (*debris/rock avalanches* en anglais). Ce processus est similaire aux chutes de blocs, mais les avalanches de blocs sont des événements à grande échelle, catastrophiques, impliquant d'importants volumes de matériel (Mulder & Cochonat, 1996 ; Tripsanas et al., 2008). Elles se produisent fréquemment au niveau des pentes fortes des zones volcaniques (*e.g.* Moore et al., 1989 ; Urgeles et al., 1997, 1999 ; Ollier et al., 1998 ; Kessler & Bédard, 2000 ; Masson et al., 2002). Cependant des avalanches entraînant des débris de roches sédimentaires et/ou consolidées ont été également observées (Collot et al., 2001 ; Bohannon & Gardner, 2004 ; Normark et al., 2004 ; Orpin, 2004). Les blocs charriés peuvent avoir des dimensions conséquentes : couramment jusqu'à plus de 500 m de long et plusieurs dizaines de mètres de haut (Mulder et Cochonat, 1996), voire plusieurs kilomètres (18 km maximum) de long et 2 km de haut dans le cas de l'avalanche de débris géante de Ruatoria (Fig. I.5 ; Collot et al., 2001). Ces blocs peuvent parfois être entraînés sur de grandes distances, jusqu'à 100 km de leur origine (*e.g.* Moore et al., 1989 ; Collot et al., 2001).

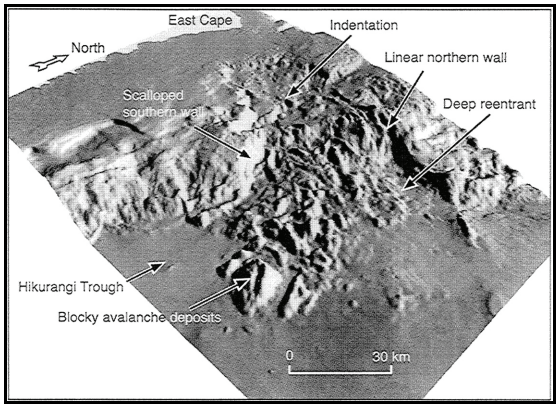

Fig. I.5 : Modèle numérique de terrain de l'avalanche de blocs sous-marine géante de Ruatoria en Nouvelle-Zélande. Les plus gros blocs mesurent jusqu'à 18 km de côté et 2 km de haut. Extrait de Collot et al. (2001).

- Les glissements *s.s.* (*slides* et *slumps* en anglais, qui correspondent respectivement aux glissements rotationnels et aux glissements translatisonnel). La traduction française "glissement" étant trop vague et pouvant prêter à confusion, nous utiliserons dans la suite du texte les termes anglais "slide" et "slump", largement utilisés même en français, le terme "glissement" étant utilisé seulement dans son sens général. Les slides et slumps sont des mouvements de masses sédimentaires cohérentes sur une surface basale cisaillante nette

(généralement un plan de stratification), limités de tous les côtés par des plans de rupture distincts, en particulier en amont par un escarpement de quelques mètres à plusieurs centaines de mètres (Coleman & Prior, 1988 ; Mulder & Cochonat, 1996). La différence entre un slide et un slump est parfois (*e.g.* Mulder & Cochonat, 1996) basée sur la valeur du rapport de Skempton *h/l* entre la profondeur h et la longueur l du glissement (Fig. I.6) : les slides sont translationnels parce que leur rapport de Skempton est inférieur à 0,15 tandis que les slumps sont rotationnels avec un rapport de Skempton > 0,33 (Skempton & Hutchinson, 1969). La plupart des glissements se révèlent être des slides translationnels (Prior & Coleman, 1984), mais le déclenchement de slides originellement translationnels est rare, ils résultent plus couramment de l'évolution et/ou du regroupement d'un ou de plusieurs slumps (Fig. I.7 ; Mulder & Cochonat, 1996). Les slides et slumps peuvent être simples ou complexes (Mulder & Cochonat, 1996). Un slide/slump est simple si le principal corps glissé ne génère pas d'autres arrachements significatifs. Au contraire un slide/slump est complexe lorsque le mouvement du principal corps glissé entraîne l'instabilité des zones voisines et que le volume de ces slides/slumps induits est équivalent au volume du slide/slump initial (Mulder & Cochonat, 1996). Les slides/slumps complexes se font classiquement par rétrogradation, avec une succession de slides/slumps se produisant progressivement vers l'amont (Fig. 1.7). La partie aval du dépôt se caractérise par deux morphologies différentes : les slides confinés frontalement et les slides émergents frontalement (*frontally confined and frontally emergent slides*, Fig. I.8 ; Frey-Martínez et al., 2006). Les slides confinés frontalement se caractérisent par une translation restreinte et ne surmontent pas les niveaux non déformés en place à l'aval. Dans le cas des slides émergents frontalement, une translation plus importante se produit, et la masse sédimentaire en mouvement chevauche les niveaux non déformés en place à l'aval pour se répandre librement et s'étaler sur le fond océanique.

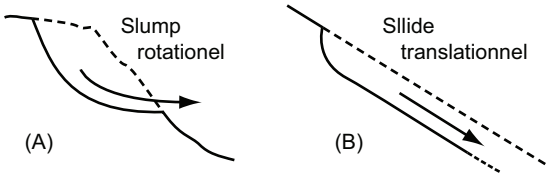

Fig. I.6 : représentation schématique d'un slump rotationnel (A) et d'un slide translationnel (B). D'après Mulder & Cochonat (1996).

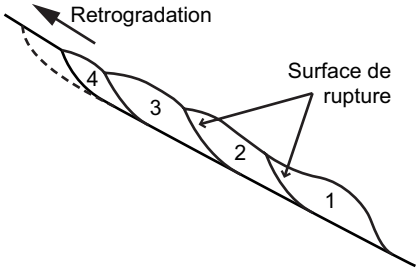

Fig. I.7 : représentation schématique de slumps rotationnels successifs (de 1 à 4), aboutissant par rétrogradation à la formation d'un slide translationnel. En pointillé, éventuel prochain slump. Modifié d'après Mulder & Cochonat (1996).

Dans le cas des slides/slumps la déformation de la masse de sédiments glissés varie de faible (bancs inclinés et micro-faillés) à modérée (convolutes, bancs plissés et/ou lenticulaires), les structures et faciès initiaux du sédiment déplacé et redéposé étant seulement partiellement reconnaissables (Coussot & Meunier, 1996). Lorsque la déformation devient suffisamment importante, avec notamment une liquéfaction partielle de la masse par des pressions de fluide interstitiel élevées, alors la masse de sédiments glissés quitte le domaine des slides/slumps et se transforme en coulée de débris (Mulder & Cochonat, 1996 ; Iverson et al., 1997).

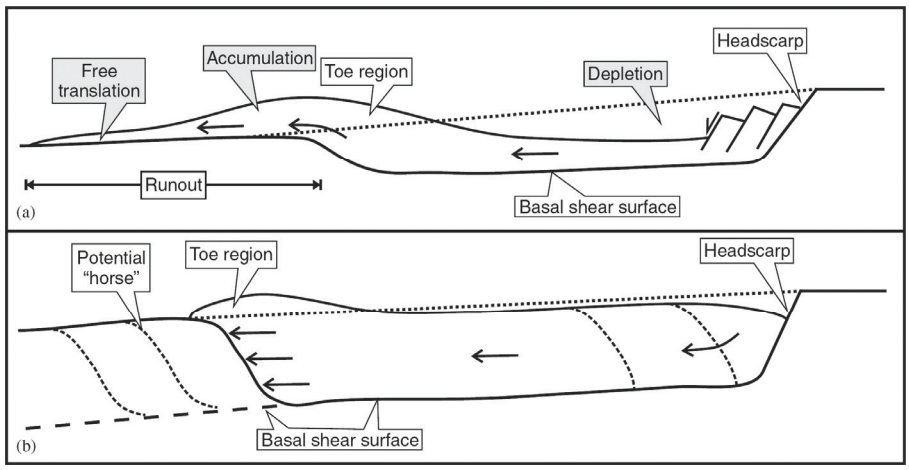

Fig. I.8 : Slides émergent frontalement (a) et confiné frontalement (b). D'après Frey-Martínez et al., 2006.

- Les coulées de débris ou de boues (*debris or mud flows* en anglais ; Fig. I.9). Elles sont constituées par une matrice plastique de matériaux cohésifs et non-liquéfiables, généralement limoneux et argileux (coulées de boue), dans laquelle flottent des fragments consolidés de roches dans le cas des coulées de débris (Postma, 1986 ; Mulder & Cochonat, 1996 ; Mulder & Alexander, 2001). C'est la cohésion de la matrice, due à la présence d'argile, qui empêche la transformation de la coulée de débris en écoulement turbulent, même lorsque le volume de sédiments et la pente sont importants (Rodine & Johnson, 1976). La coulée parvient également à transporter de grands blocs isolés, d'une part grâce à la faible différence de densité entre les blocs isolés et les débris de roches, et d'autre part grâce à la force cohésive du mélange boueux d'eau, de sédiments et d'argile (Rodine & Johnson, 1976). Les dépôts de coulées de débris sont des conglomérats, avec parfois un granoclassement inverse (Mulder & Cochonat, 1996). Leur dépôt se produit *en masse* (Lowe, 1982 ; Postma, 1986), la coulée ou une partie de la coulée se figeant lorsque la force de résistance au cisaillement de la coulée devient égale à la force due à la gravité (Mulder & Alexander, 2001).

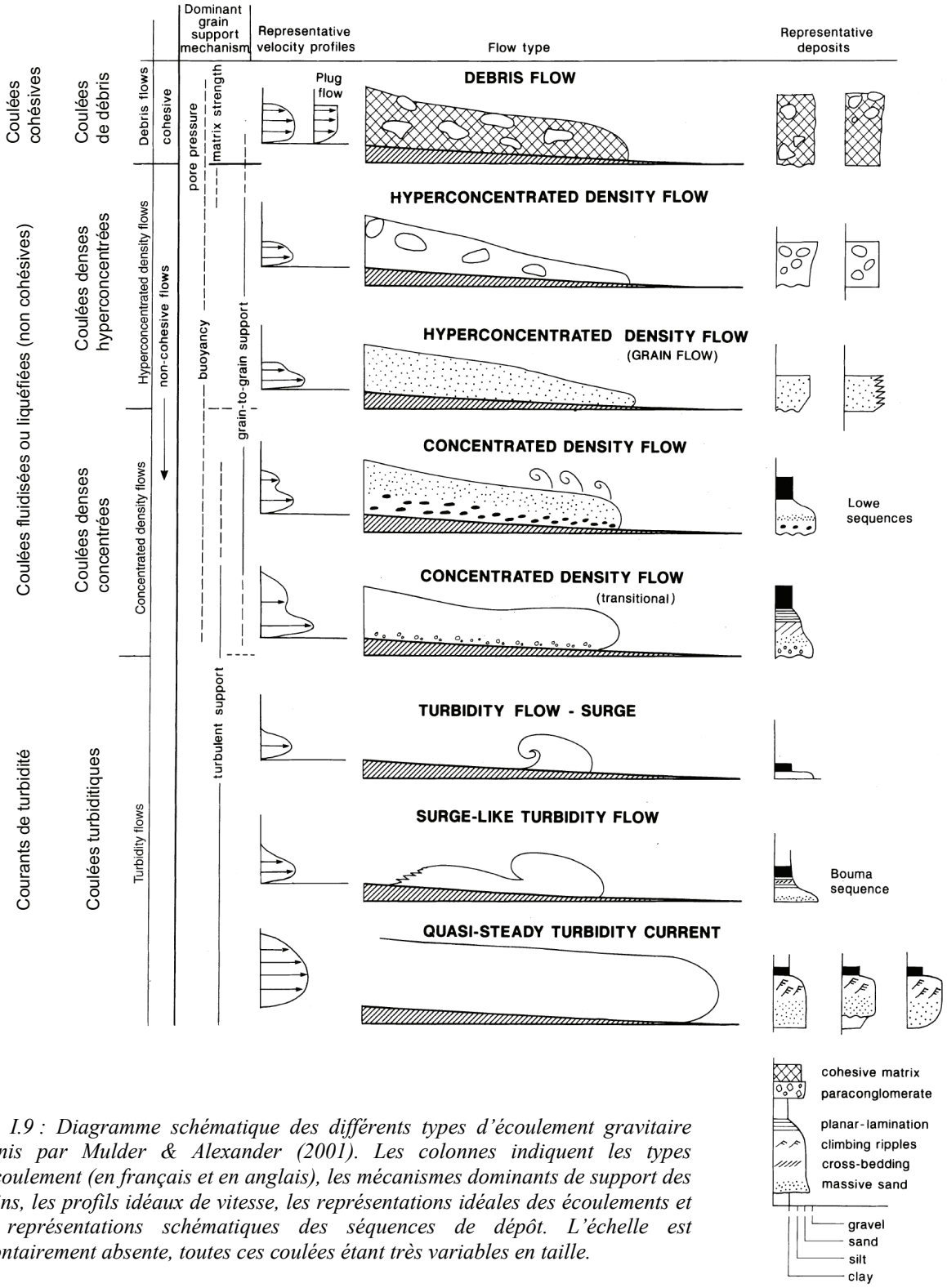

Fig. I.9 : Diagramme schématique des différents types d'écoulement gravitaire définis par Mulder & Alexander (2001). Les colonnes indiquent les types d'écoulement (en français et en anglais), les mécanismes dominants de support des grains, les profils idéaux de vitesse, les représentations idéales des écoulements et les représentations schématiques des séquences de dépôt. L'échelle est volontairement absente, toutes ces coulées étant très variables en taille.

- Les coulées fluidisées ou liquéfiées (*fluidised and liquefied flows* en anglais ; Fig. I.9). Elles sont aussi appelées coulées denses hyper-concentrées et concentrées (*hyperconcentrated and concentrated density flows*, Mulder & Alexander, 2001). Ce sont des coulées de matériaux, généralement sableux ou limoneux, qui perdent leur cohésion et

s'écoulent librement, même lorsque la pente est très faible (*e.g.* < 0,2° dans le delta du Mississipi, Prior & Coleman, 1978). Cette faible cohésion résulte soit d'une proportion plus faible de particules cohésives dans le matériel, soit de l'agitation interne des grains à cause de la vitesse élevée des matériaux sur une surface rugueuse (Mulder & Alexander, 2001). Les phénomènes de liquéfaction (suite à un séisme) et de fluidisation (suite à l'injection d'un fluide à travers le sédiment) peuvent également réduire ou éliminer la résistance au cisaillement d'un matériau en augmentant la pression interstitielle de fluide (Nichols, 1995), et permettre au matériau affecté de s'écouler comme un liquide (Allen, 1982). Ces phénomènes sont particulièrement courants dans les matériaux sableux (*e.g.* Nichols, 1995). Une coulée de boue ou de débris (cohésive) peut évoluer en coulée non cohésive par incorporation d'eau et/ou diminution de la fraction argileuse, ou par augmentation de la vitesse sans changement des teneurs en eau et en argile (Fisher, 1983). La transformation inverse est également possible en cas de ralentissement de la coulée ou d'expulsion d'eau du matériel (Middleton & Southard, 1984 *in* Mulder & Alexander, 2001). Il y a une évolution continue des coulées de boue/débris aux coulées denses hyper-concentrées puis aux coulées denses concentrées, ces dernières étant plus diluées et la turbulence fluide pouvant être le principal mécanisme de transport à l'avant (entraînant de l'érosion sous la base de la coulée) et au sommet de la coulée (Laval et al., 1988) (Fig. I.10). Les coulées denses concentrées peuvent également se transformer en continu en courants de turbidité (Mulder & Alexander, 2001).

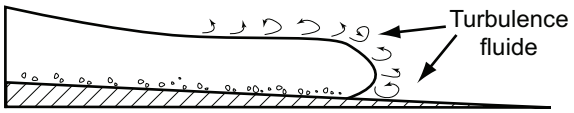

Fig. I.10 : Dans les coulées denses concentrées, la turbulence fluide peut être le principal mécanisme de transport à l'avant et au sommet de la coulée.

- Les courants de turbidité (*turbidity currents* en anglais ; Fig. I.9). Ce sont des écoulements de sédiments maintenus en suspension dans un fluide turbulent (Kneller & Buckee, 2000), classés en fonction de la durée de l'écoulement en écoulement turbiditique déferlant, écoulement quasiment déferlant et écoulement quasiment continu (*surge turbidity flow*, *surge-like turbidity flow*, *quasi-steady turbidity currents* ; Mulder & Alexander, 2001). Une coulée dense concentrée peut évoluer en courant de turbidité par incorporation d'eau de mer à l'avant de la coulée et dilution du sédiment transporté (Hallworth et al., 1993 ; Mulder & Alexander, 2001). Les courants de turbidité peuvent déplacer des sédiments en suspension sur des distances considérables, plusieurs centaines de kilomètres. Ils peuvent atteindre des vitesses élevées : la rupture successive des câbles télégraphiques sous-marins a permis de

calculer une vitesse de 60-100 km/h pour le courant de turbidité des Grands Bancs de 1929 (Kuenen, 1952 ; Evans, 2001), et plus de 100 km/h pour celui de Nice en 1979 (Gennesseaux et al., 1980 ; Piper & Savoye, 1993 ; Mulder et al., 1997). Les dépôts sédimentaires des courants de turbidité constituent les turbidites, bien que le terme turbidites soit utilisé pour définir un spectre beaucoup plus large de dépôts de transports en masse sous-marins, depuis les coulées de boues jusqu'aux coulées denses concentrées (Kneller & Buckee, 2000 ; Mulder & Cochonat, 2001).

Il est important de noter qu'un glissement n'est pas cantonné dans une catégorie et peut évoluer suivant les propriétés de ses matériaux constitutifs et les conditions du milieu (Fisher, 1983 ; Mulder & Cochonat, 1996 ; Mulder & Alexander, 2001), comme par exemple le glissement des Grands Bancs de 1929 qui a commencé par plusieurs petits slumps rotationnels sous-marins qui se sont graduellement transformés en coulées de débris puis en courant de turbidité (Fig. I.11 ; Piper et al., 1992 ; 1999). Plusieurs processus gravitaires peuvent se produire au cours d'un même glissement, qui peut donc fournir différents types de dépôts de transports en masse sous-marins. L'observation de différents types de dépôts est courante dans le cas des dépôts fossiles de transports en masse sous-marins, car les affleurements sont souvent constitués par plusieurs événements successifs mais pratiquement simultanés à l'échelle des temps géologiques, bien que parfois distinguables si les escarpements des têtes d'arrachement sont conservés (*e.g.* Callot et al., en révision). Haflidason et al. (2005) ont montré que c'était également le cas de certains grands collapses récents, comme le Storegga Slide, formés de glissements successifs qui se suivent au cours de quelques centaines ou milliers d'années.

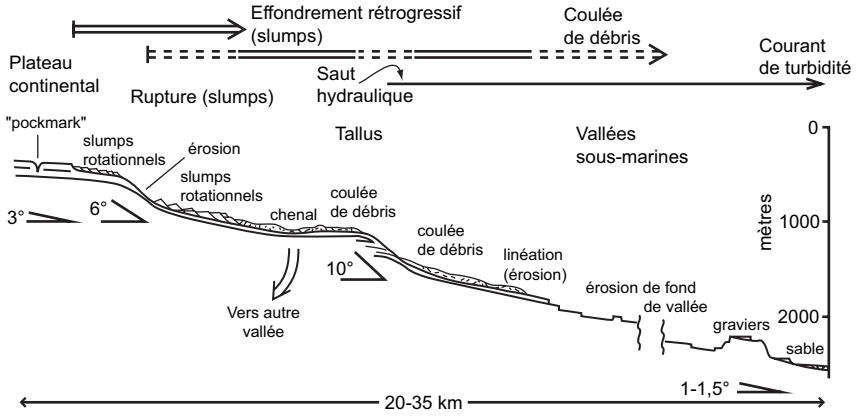

Fig. I.11 : Exemple d'évolution d'un glissement sous-marin (depuis les slumps rotationnels jusqu'au courant de turbidité) d'après l'exemple du glissement des Grands Bancs de 1929. Modifié d'après Piper et al, (1999).

A l'échelle d'une plateforme, Spence & Tucker (1997) parlent de méga-brèche (*megabreccia* en anglais), un terme général pour décrire tous les produits résultant d'instabilités gravitationnelles majeures et catastrophiques. D'après leur définition, reprise de Mountjoy et al. (1972), les méga-brèches contiennent des slides et des slumps, des sédiments fluidisés cohérents ou non, des matériaux semi-lithifiés présentant des déformations plastiques et des matériaux lithifiés de toutes tailles (de moins d'un mètre à plusieurs centaines de mètres) pouvant être transportés sur plusieurs centaines de kilomètres. Le terme « méga-brèche » semble particulièrement bien adapté pour décrire la Formation Ayabacas, en particulier dans sa partie NE.

Devant la difficulté de faire la distinction entre les différents types de glissements (notamment slide et slump), et en particulier dans le cas d'exemples fossiles dans lesquels coexistent parfois des glissements de type slide ou slump, certains auteurs suggèrent d'utiliser des termes plus génériques, comme par exemple "dépôts de transports en masse sous-marins" (*submarine mass-wasting deposits* pour Lucente & Pini, 2003, 2008 ; *mass-transport deposits* pour Tripsanas et al., 2008 ; *mass-transport complexes* pour Pickering & Corregidor, 2005). Ces termes semblent également plus adaptés pour la Formation Ayabacas, dans laquelle plusieurs types de glissements se sont produits.

I.3.2. Facteurs de stabilité des pentes et mécanismes déclenchant des glissements sédimentaires sous-marins

Plusieurs facteurs ont été reconnus comme pouvant déclencher des glissements sous-marins, ou établir des conditions favorables à la rupture. Ils sont variés et c'est souvent la conjonction de plusieurs facteurs qui détériore la stabilité de la marge jusqu'à occasionner un glissement (Hampton et al., 1996 ; Mienert et al., 2002). La stabilité d'une pile sédimentaire dépend de deux facteurs : la résistance au cisaillement du matériel constituant la pile sédimentaire, et la contrainte cisaillante à laquelle il est soumis. Toute augmentation de la contrainte cisaillante et/ou toute diminution de la résistance au cisaillement de la pile sédimentaire vont réduire la stabilité de la marge, la rupture se produisant lorsque la contrainte cisaillante dépasse la résistance au cisaillement (Hampton et al., 1996 ; Canals et al., 2004).

Il existe des phénomènes déclenchant à court terme, qui sont les facteurs de forçage nécessaires pour provoquer le glissement dans une pile sédimentaire sujette à l'instabilité suite à l'action de facteurs de causalité à long terme (Sultan et al., 2004a). La première condition pour qu'apparaisse un glissement gravitaire est bien entendu qu'il existe une pente

qui génère une contrainte cisaillante. Cependant un glissement ne se produit pas nécessairement lorsque la pente est élevée si d'autres facteurs (comme une cémentation rapide par exemple) augmentent sa résistance au cisaillement et donc sa stabilité (Kenter, 1990), et souvent, la pente seule ne permet d'expliquer ni pourquoi ni où la rupture sédimentaire advient ou non (McAdoo et al., 2000 ; Mienert et al., 2002). Par ailleurs des glissements se produisent couramment alors que la pente est très faible (inférieure à quelques degrés), que ce soit sur des marges silicoclastiques (McAdoo et al., 2000 ; Talling et al., 2007) ou carbonatées (Spence & Tucker, 1997). L'angle de la pente (*i.e.* la force de gravité) est donc un facteur de causalité à long terme, incapable de déclencher à lui seul la rupture mais condition nécessaire à celle-ci (Hampton et al., 1996 ; Sultan et al., 2004a). Les autres facteurs de causalité à long terme qui peuvent intervenir sont l'héritage sédimentaire de la marge, comme par exemple des niveaux salifères (Loncke et al., 2006), ou des niveaux riches en gaz (Bünz et al., 2005 ; Minisini et al., 2007), la progradation des deltas (Prior & Coleman, 1978, 1982, 1984), ainsi que les glissements précédents (Sultan et al., 2004a).

Diminution de la résistance au cisaillement	**Augmentation de la contrainte cisaillante**
Différences de lithification - aquifères confinés Couches salifères Gaz et hydrates de gaz dans les sédiments Erosion en bas de pente Processus biologiques/biochimiques	Augmentation de l'angle de la pente tectonique flexure de la croûte diapirisme processus volcaniques Surcharge sédimentaire brusque Surcharge sédimentaire (glaciation, progradation des deltas)
Taux de sédimentation élevé Séismes Percolation / infiltration / injection d'un fluide Variations du niveau marin relatif Action des vagues Marées Activités humaines	

Fig. I.12 : Tableau récapitulatif des principales causes et éléments déclencheurs des instabilités sédimentaires.

Outre ces facteurs à long terme, la littérature avance un nombre conséquent de facteurs à plus ou moins court terme pour expliquer l'instabilité des marges (Fig. I.12), toujours en augmentant la contrainte cisaillante et/ou en diminuant la résistance au cisaillement des matériaux (voir en particulier Hampton et al., 1996 ; Canals et al., 2004) :

(1) un taux de sédimentation élevé entraînant la formation de pression de fluide interstitiel élevée (couches en surpression) et de niveaux sous-consolidés peu résistants au

cisaillement (Mandl & Crans, 1981 ; Postma, 1983; Gardner et al., 1999; Mourgues & Cobbold, 2003 ; Vendeville & Gaullier, 2003 ; Bartezko and Kopf, 2007) ;

(2) des vitesses de lithification différentes et la présence d'aquifères confinés (Hilbrecht, 1989 ; Spence and Tucker, 1997) ;

(3) la présence de couches salifères (Brun & Fort, 2004 ; Loncke et al., 2006 ; Vernhet et al., 2006) ;

(4) une brusque surcharge sédimentaire, par exemple suite à un glissement de terrain subaérien en amont ;

(5) la création de pente jusqu'à atteindre l'angle de rupture des matériaux (*oversteepening*). Cette augmentation de la pente peut avoir différentes causes :

- des processus tectoniques, en extension (rejet de faille, blocs basculés ; Callot et al., 2008) ou en compression (Barnes & Lewis, 1991 ; McAdoo et al., 2000 ; Cochonat et al., 2002) ;
- une flexure de la lithosphère (Hoffman & Hartz, 1999 ; Sempere et al., soumis) ;
- du diapirisme et de la tectonique salifère (McAdoo et al., 2000) ;
- une croissance volcanique ou des processus d'îles volcaniques (Urgeles et al., 1997, 1999) ;

(6) l'activité sismique en général et ses conséquences (tsunamis, liquification ; Nichols, 1995), et un séisme de forte magnitude en particulier (*e.g.* le glissement des Grands Bancs de 1929 ; Piper et al., 1999) ;

(7) une érosion à la base de la pente (par des courants marins par exemple) ;

(8) la production de gaz (généralement du méthane) dans les sédiments par décomposition de la matière organique (Prior & Coleman, 1978 ; Barnes & Lewis, 1991 ; Bünz et al., 2005), et la déstabilisation d'hydrates de gaz (Laberg & Vorren, 2000 ; Sultan et al., 2004b) ;

(9) les glaciations continentales (Mulder & Moran, 1995 ; Locat & Lee, 2002), de part la surcharge de la glace ancrée sur les sédiments sous-jacents ;

(10) la percolation / infiltration / injection d'un fluide (liquide ou gaz) à travers la pile sédimentaire (Mourgues & Cobbold, 2003 ; Vendeville & Gaullier, 2003) ;

(11) les variations du niveau marin (Vernhet et al., 2006), notamment les chutes relatives du niveau marin d'après certains auteurs (Hilbrecht, 1989 ; Spence and Tucker, 1997 ; Dreyer et al., 1999) car elles ont pour conséquence d'augmenter la surcharge sédimentaire en bordure de plateau, là où la pente est la plus forte ;

(12) La progradation des sédiments, notamment au niveau des deltas (Prior & Coleman, 1978, 1982, 1984 ; Dreyer et al., 1999 ; Callot et al., en révision) ;

(13) l'action de vagues de tempêtes (Spence & Tucker, 1997 ; Locat & Lee, 2002) ;
(14) l'activité des marées entraînant des variations de la pression de fluide interstitiel (Spence & Tucker, 1997) ;
(15) des processus biologiques (Shaikh et al., 1998) ou biochimiques (Volpi et al., 2003) ;
(16) des activités humaines, en affectant les fonds ou en surchargeant la pile sédimentaire, comme par exemple la catastrophe de l'aéroport de Nice en 1979 (Gennesseaux et al., 1980 ; Piper & Savoye, 1993).

La ou les cause(s) et surtout le ou les facteur(s) déclenchant(s) sont souvent complexes à déterminer car certains facteurs ont un effet sur d'autres. Le rôle et l'importance de chacun sont très variables suivant les cas.

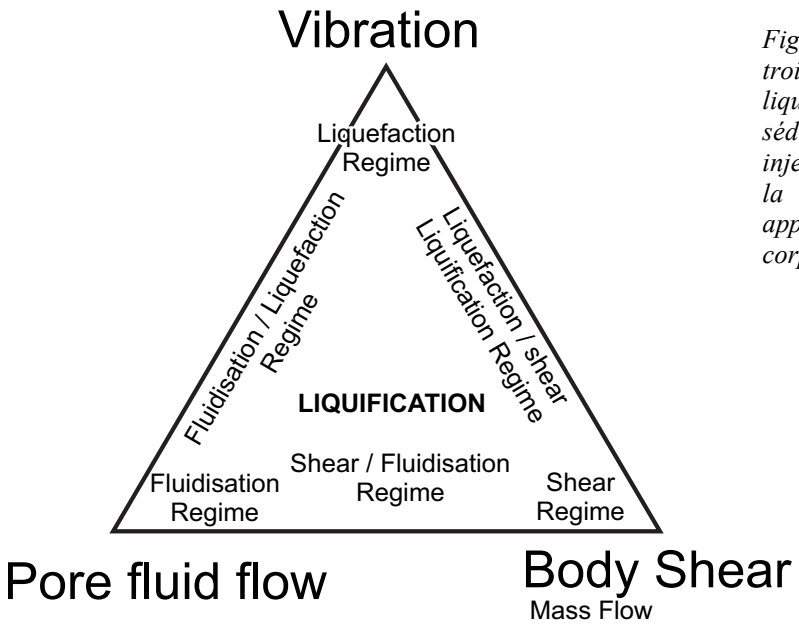

Fig. I.13 : Représentation graphique des trois types de liquification : la liquefaction (par vibration du corps sédimentaire), la fluidisation (par injection d'un fluide à travers le corps) et la liquification cisaillante (par application d'une force cisaillante sur le corps). Adapté d'après Nichols (1995).

Un phénomène particulièrement important dans le déclenchement des instabilités sédimentaires est la liquification des matériaux clastiques, qui se produit lorsque les grains ne sont plus supportés par leur contact intergranulaire, ce qui rend la résistance au cisaillement du matériau pratiquement nulle (Fig. I.13 ; Nichols, 1995). La liquification survient lorsque la conjonction de plusieurs des facteurs déclenchants vus précédemment conduit à la fluidisation ou à la liquéfaction des matériaux (Lowe, 1976) :

- la liquéfaction survient lors des séismes, lorsque le sédiment est vibré. Les grains s'entrechoquent, ils deviennent momentanément suspendus dans le fluide interstitiel. Il se produit alors une brusque chute de la résistance au cisaillement des matériaux, la cohésion devenant nulle car les grains perdent leur contact les uns par rapport aux autres. Le matériau

est alors libre de s'écouler comme un fluide (Nichols, 1995 ; Maltman & Bolton, 2003). Cela explique parfois la mise en mouvement des matériaux lorsque la pente est très faible.

- la fluidisation des sédiments a lieu lorsque des fluides s'injectent entre les grains à travers un corps sableux (Nichols, 1995 ; Maltman & Bolton, 2003). Elle est liée soit à des séismes, soit à la compaction des sédiments sous-jacents. Dans ce cas, si une couche peu perméable, telle que des argiles, recouvre ces sédiments, l'eau ne peut pas s'échapper progressivement et le gradient de pression augmente à mesure que la subsidence se produit (Fig. I.14). Lorsque le gradient de pression devient trop important, il y a rupture de la couche peu perméable, ce qui entraîne la remontée du fluide. Celui-ci peut être canalisé par des failles qu'il emprunte ou qu'éventuellement il aide à se former (Cartwright et al., 2003). Le fluide peut aussi s'échapper de façon diffuse dans la masse, en faisant flotter les grains si sa vitesse de remontée est supérieure à la vitesse de chute des grains due à la pesanteur. Cette fluidisation peut former des dykes clastiques (Dixon et al., 1995 ; Mulder & Alexander, 2001). Si elle concerne toute une couche, c'est tout un ensemble sédimentaire qui peut être mobilisé. Malgré une pente très faible, les fluides provoquent une instabilité gravitaire et permettent un glissement en masse.

- la liquification cisaillante se produit lorsqu'une force cisaillante unidirectionnelle est appliquée sur un corps sableux, qui se liquifie par réduction de la résistance au cisaillement du matériau granulaire. La liquification cisaillante est très proche de la liquéfaction, mais dans le cas de la liquéfaction la contrainte et le mouvement des grains qui en résulte sont cycliques avec de rapides changements de directions, tandis que dans le cas de la liquification cisaillante la contrainte est unidirectionnelle et résulte du déplacement en masse du corps sableux dans la direction de la contrainte.

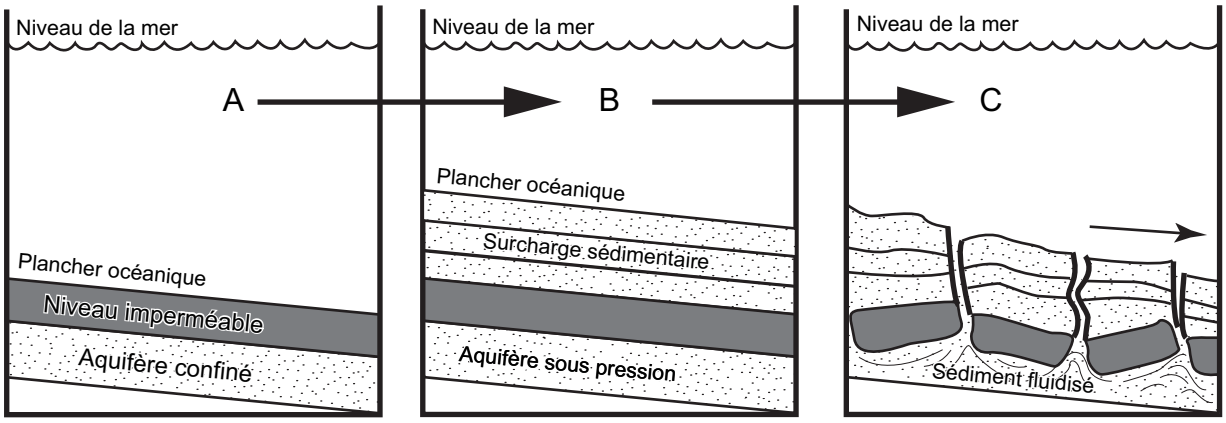

Fig. I.14 : Formation d'aquifère confiné sous-pression pouvant provoquer des instabilités sédimentaires (modifié d'après Spence & Tucker, 1997). Un niveau imperméable (par exemple des argiles ou des calcaires rapidement cimentés) se dépose au-dessus de sédiments riches en eau (A). Cet aquifère se retrouve sous pression par exemple à cause d'une surcharge sédimentaire (B). Le fluide peut alors être expulsé violemment, fracturant la couche imperméable qui scellait l'aquifère (C).

I.3.3. Les glissements sédimentaires récents

Les glissements sous-marins récents ont fait l'objet de très nombreuses études, en utilisant des méthodes géophysiques telles que les sonars et les sondeurs multifaisceaux qui donnent la bathymétrie et une image des fonds océaniques, et les profils sismiques pour étudier verticalement la pile sédimentaire (*e.g.* Bjerrum, 1971 ; Nardin et al., 1979 ; Prior & Coleman, 1982, 1984 ; Prior et al., 1984 ; McAdoo et al., 2000 ; Canals et al., 2004). Toutes ces techniques peuvent être utilisées à différentes échelles et résolutions (Masson, 2003). Généralement, plus la résolution est bonne et moins la profondeur de pénétration des ondes est importante. Ainsi, plus la tranche d'eau sera importante, plus il sera difficile d'obtenir des données à haute résolution du fond, et plus les profils sismiques seront profonds, moins la résolution sera bonne (Masson, 2003). L'étude de carottes de sédiments, prélevées dans les dépôts du transport en masse ou dans les dépôts environnants encore en place, est parfois employée et renseigne sur la nature et la rhéologie des matériaux, ainsi que sur les déformations à petite échelle (*e.g.* Gee et al, 1999 ; Barker et al., 2008 ; Henrich et al., 2008 ; Tripsanas et al., 2008). Plus récemment la sismique haute résolution en 3D a été utilisée pour l'étude des glissements sédimentaires récents (*e.g.* Huvenne et al., 2002 ; Bünz et al., 2005 ; Frey Martínez et al., 2005, 2006 ; Gee et al., 2007 ; Moscardelli and Wood, 2008). Ces méthodes géophysiques sont détaillées dans de nombreux ouvrages (*e.g.* Masson, 2003 et ses références) et ne sont pas l'objet de cette thèse.

Ces études permettent notamment de bien caractériser la morphologie générale, la surface et les volumes des masses glissées et de leurs dépôts, et la géométrie de la surface de décollement du glissement (*e.g.* McAdoo et al., 2000 ; Canals et al., 2004). Lorsqu'il est possible de dater précisément une succession de masses glissées, une évaluation de périodes favorables aux instabilités peut être donnée (*e.g.* Haflidason et al., 2005 ; Solheim et al., 2005a). L'interprétation de toutes ces données permet notamment de déterminer les causes et les facteurs déclenchants des instabilités.

Sans prétendre faire une revue exhaustive de l'ensemble des informations qui ont pu être tirées de l'étude des glissements récents, certains points méritent d'être soulignés :

(1) La distribution géographique des glissements sédimentaires (Fig. I.15) montre que ceux-ci se produisent sur tous les types de marges (actives, passives) et sous différents types de climat et d'environnement. Les zones d'exploration d'hydrocarbures et les marges des pays développés étant plus étudiées que les autres, les glissements sédimentaires ont été

logiquement plus fréquemment observés dans ces zones. Il est également important de noter que cette carte ne concerne que les grands, ou très grands, glissements.

(2) Les dimensions des glissements sont très variables, et ce même lorsque l'environnement est semblable comme on peut le voir dans les compilations de McAdoo et al. (2000) ou dans la synthèse du projet COSTA de Canals et al. (2004). Les différences peuvent être de plusieurs ordres de grandeur, comme par exemple entre le Storegga Slide et le Afen Slide qui, respectivement, affectent une surface de 90000 km^2 (Haflidason et al., 2004, 2005) et 40 km^2 (Wilson et al., 2003) et déplacent un volume de sédiments de plus de 3000 km^3 pour l'un et de 0,2 km^3 pour l'autre. Il est intéressant de noter que dans les deux cas, ils sont formés par une succession de ruptures de plus petite ampleur.

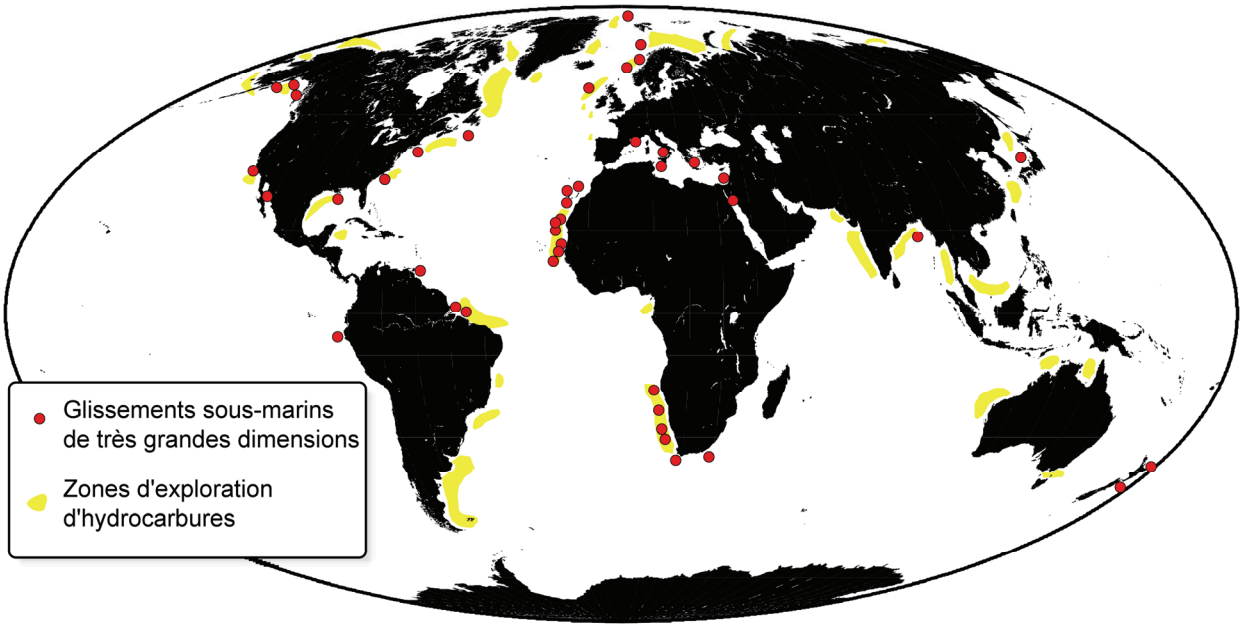

Fig. I.15 : Distribution géographique des glissements sous-marins actuels majeurs et des principales zones d'exploration d'hydrocarbures. Ces glissements se produisent sur tous les types de marges (passives, actives) et de climats. Noter que les glissements se trouvent principalement dans les zones dont les marges sont bien étudiées (zones d'exploration en hydrocarbures et côtes des pays développés). Il est raisonnablement permis de penser que des glissements sous-marins majeurs pourraient être découverts sur les marges moins intensément étudiées. D'après Stow & Mayall, (2000) et Mienert et al. (2002), et ajouts d'après Collot et al. (2001), Frey-Martínez et al. (2005, 2006), Talling et al. (2007), Moscardelli & Wood (2008).

(3) La pente de la marge est souvent faible, voire très faible, lorsque la rupture se produit (McAdoo et al., 2000 ; Canals et al., 2004 ; Hühnerbach et al., 2004 ; Masson et al., 2006 ; Talling et al., 2007). Ainsi, dans la majorité des glissements étudiés par McAdoo et al. (2000) et dans la synthèse des glissements du projet COSTA de Canals et al. (2004), l'angle moyen de la pente est inférieur à quelques degrés. Dans le glissement géant décrit par Telling et al. (2005), la pente est au maximum de 0,05°. Lorsque la pente est forte (> 10°), par exemple sur la marge de l'Oregon (McAdoo et al., 2000) ou pour le Finneidfjord Slide (Canals et al.,

2004 ; Longva et al., 2003), les glissements sont généralement de petites dimensions (volume de sédiments déplacés de quelques km^3 au maximum). Au contraire, les plus grands glissements semblent se produire sur les pentes les plus faibles (Hühnerbach et al., 2004).

(4) Des blocs lithifiés (ou au moins cohésifs) sont couramment entraînés par les glissements et se rencontrent le plus souvent dans le segment central de l'arrachement (par exemple dans tous les glissements étudiés dans le projet COSTA ; Canals et al., 2004). Les dimensions de ces blocs sont variables et ne semblent pas nécessairement reliées à la taille du glissement (Canals et al., 2004). Elles atteignent quelques centaines à quelques milliers de mètres de côté pour la plupart des glissements (Huvenne et al., 2002, Canals et al., 2004). Cependant, la résolution insuffisamment élevée des images laisse parfois une incertitude sur la présence de blocs de plus petites dimensions (Canals et al., 2004). Ainsi, lorsque les techniques utilisées permettent d'obtenir une meilleure résolution, des blocs de plus petites dimensions apparaissent : par exemple des blocs de ~60x~20 mètres ont été observés dans le Finneidfjord Slide (Longva et al., 2003), pour lequel la résolution des images est plus élevée que pour les autres glissements étudiés (Canals et al., 2004). Collot et al. (2001) indique la présence de méga-blocs particulièrement volumineux : au moins 100 blocs de plus de 1 km de côté, certains atteignent 2 km d'épaisseur, le plus grand d'entre eux mesure 18 km de long. Dans le BIG'95 Slide de dimensions relativement modestes (~2200 km^2 affectés et 26 km^3 de matériaux déplacés), Lastras et al. (2002, 2004) décrivent eux aussi des blocs de grandes dimensions, avec plus de 200 blocs de 1 à 5 km^2 mais pouvant atteindre 25 km^2, qui se sont fragmentés au cours de leur glissement.

I.3.4. Les apports de l'étude des glissements sédimentaires fossiles

L'étude des dépôts des glissements sous-marins fossiles apporte des informations complémentaires qui aident à mieux comprendre l'organisation et les processus d'instabilités sédimentaires. Ainsi les structures à l'échelle du millimètre au mètre peuvent facilement être observées dans les dépôts fossiles, alors que ces informations ne sont accessibles que par les seuls carottages de sédiments dans les dépôts en mer actuels (Tripsanas et al., 2008). L'analyse de ces structures permet de mieux comprendre leur mise en place, la rhéologie des matériaux, les mécanismes d'évolution des matériaux lors des glissements, et améliore la compréhension des mécanismes déclenchants (*e.g.* Naylor, 1981 ; Gawthorpe & Clemmey, 1985 ; Martinsen & Bakken, 1990 ; Payros et al., 1999 ; Onasch & Kahle, 2002 ; Plink-Björklund & Steel, 2004 ; Pickering & Corregidor, 2005 ; Vernhet et al., 2006 ; Montenat et

al., 2007 ; Strachan, 2008). Lorsque l'étude peut se faire à l'échelle du bassin, ou lorsqu'il est possible d'observer la succession verticale des différents événements, les dépôts fossiles permettent de déterminer l'évolution des dépôts et des structures de déformation dans l'espace (Martinsen & Bakken, 1990 ; Payros et al., 1999 ; Drzewiecki & Simó, 2002 ; Vernhet et al., 2006), ainsi que l'évolution au cours du temps de la marge et des glissements qui l'affectent (Drzewiecki & Simó, 2002 ; Plink-Björklund & Steel, 2004 ; Manzi et al., 2005 ; Pickering & Corregidor, 2005 ; Lucente & Pini, 2008). Il est également parfois possible d'estimer grossièrement la récurrence des ruptures, en supposant qu'elles se produisent à intervalles de temps réguliers (Payros et al., 1999 ; Plink-Björklund & Steel, 2004 ; Callot et al., en révision).

Un problème courant est de différencier les déformations résultant du glissement sous-marin, et celles résultant de l'histoire tectonique postérieure (*e.g.* Steen & Andresen, 1997 ; Spörli and Rowland, 2007). Une partie de l'information "initiale" peut être transformée ou effacée par la diagenèse au cours de l'enfouissement et/ou par la tectonique au cours de l'exhumation. Il est également parfois difficile de trouver des niveaux marqueurs et de relier entre eux les différents affleurements, qui sont rarement continus à l'échelle du kilomètre (Callot et al., en révision), de la dizaine voire de la centaine de kilomètres (Lucente & Pini, 2008), ce qui complique la reconstruction de la morphologie des corps glissés. Se pose enfin parfois le problème de l'interprétation des affleurements, les dépôts de transports en masse sous-marins pouvant être pris pour d'autres phénomènes géologiques, et inversement. Par exemple une partie du Groupe Otavi (Namibie), considérée par certains auteurs comme des dépôts glaciaires (*e.g.* Gevers, 1931 ; Martin, 1965 ; Hoffman et al., 1998 ; Hoffman & Schrag, 2002), est interprétée par d'autres comme des dépôts de coulées de débris sous-marines (*e.g.* Porada & Wittig, 1983 ; Martin et al, 1985 ; Eyles & Januszczak, 2007).

C'est probablement pour toutes ces raisons qu'il existe une disparité de taille entre les glissements fossiles et les glissements actuels ou récents (observés avec des méthodes géophysiques), ces derniers étant plus volumineux (Fig. I.16). Ce déficit de glissements sous-marins fossiles, encore plus important lorsqu'il fut souligné pour la première fois par Woodcock (1979a), pourrait être dû à l'exposition incomplète des grands glissements sous-marins, ce qui entraîne une sous-estimation de leurs dimensions (Macdonald et al., 1993). Camerlenghi & Pini (2008) pensent que ces corps gigantesques n'ont pas été totalement conservés lors des processus accrétion/collision et d'exhumation des orogènes. Enfin Woodcock (1979a) suppose que les dépôts de grands glissements sous-marins sont mal

interprétés et attribués à d'autres phénomènes tectoniques, idée reprise par Luccente & Pini (2008) avec l'exemple des Apennins où les grands corps résultant de glissements sous-marins ont parfois été interprétés comme des unités structurales limitées par des chevauchements. Ces dernières années, d'autres auteurs (*e.g.* Alonso et al., 2006) ont également réinterprété en dépôts gravitaires des formations précédemment considérées comme des nappes chevauchantes. Enfin Burg et al. (2008) ont très récemment reconnu un glissement géant dans le Makran (Iran), précédemment interprété comme un mélange mis en place tectoniquement (McCall & Kidd, 1982 ; McCall, 1983). Le même problème d'interprétation s'est posé pour la Formation Ayabacas, interprétée de différentes façons suivant les auteurs (détaillées dans l'article dans *Basin Research*, la partie II.2). Cette thèse apporte des éléments de réponse qui renforcent l'hypothèse du dépôt de transports en masse sous-marins.

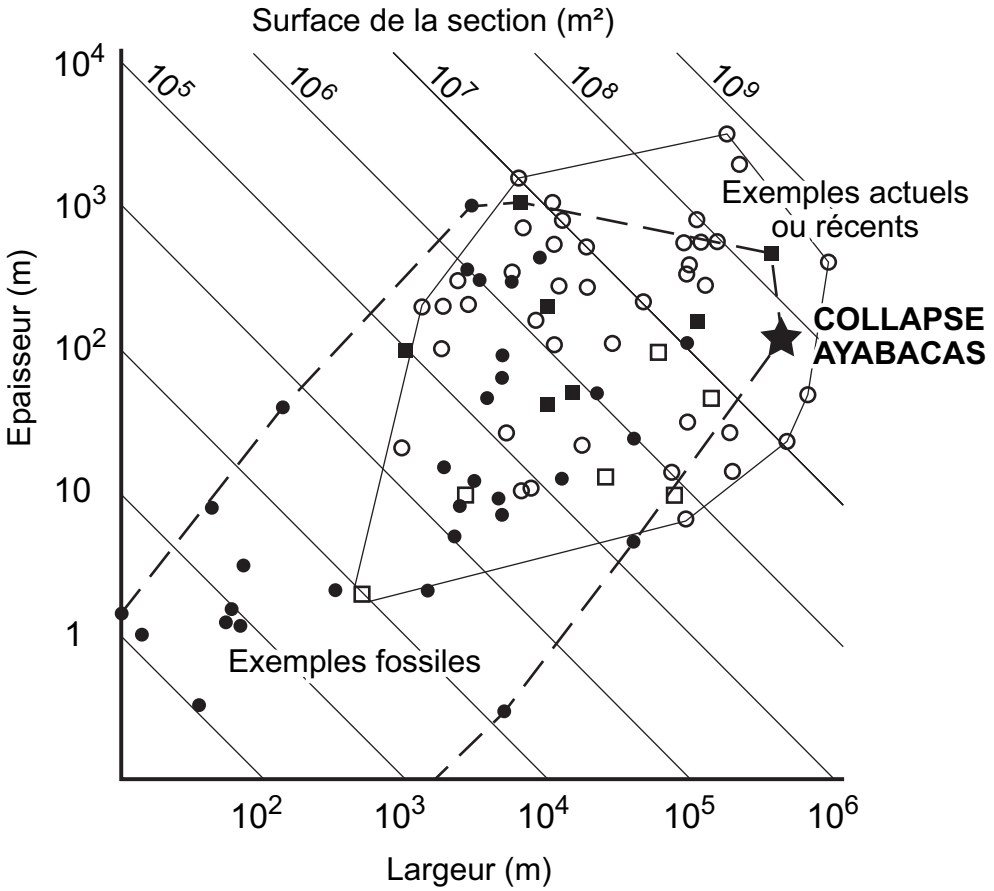

Fig. I.16 : Diagramme de l'épaisseur en fonction de la largeur des dépôts de glissements sous-marins fossiles (cercles et carrés pleins formant une enveloppe en pointillés) et récents ou actuels (cercle et carré vides formant une enveloppe en trait plein). Adapté de Lucente & Pini (2003) avec ajouts à partir de Canals et al. (2004) (carrés vides) et à partir de Payros et al. (1999), Friès & Parize (2003), Fernandez et al. (2004), Alonso et al. (2006), Falivene et al (2006) et Burg et al. (2008) (carrés pleins). Les données de Lucente & Pini proviennent également de Woodcock (1979a) et Macdonald et al. (1993). Le collapse Ayabacas, représenté par une étoile, est de dimensions équivalentes à celles des grands glissements actuels. Les deux zones délimitant les exemples fossiles et actuels se recoupent un peu mieux que dans la figure originelle de Lucente & Pini (2003), traduisant les progrès des techniques de géophysique (détection de glissements récents plus petits) et la découverte, ou une meilleure compréhension, des dépôts de glissements fossiles de grandes dimensions. Cependant, il y a toujours peu de grands dépôts fossiles en comparaison du grand nombre de glissements récents majeurs.

La disparité de tailles entre exemples récents et fossiles tend cependant à se réduire, d'une part grâce aux progrès des techniques géophysiques qui permettent de détecter des glissements récents plus petits, ce qu'avait prévu Woodcock (1979a), et d'autre part grâce à la découverte ou à la réinterprétation d'exemples fossiles (Fig. I.16). L'observation par des méthodes géophysiques de blocs de toutes dimensions (jusqu'à pluri-kilométrique) dans les collapses récents (*e.g.* Collot et al., 2001 ; Lastras et al., 2002, 2004 ; Canals et al., 2004 ; Haflidasen et al., 2004, 2005) confirme les descriptions de blocs de diverses dimensions dans les exemples fossiles (George et al., 1995 ; Friès & Parize, 2003 ; Lucente & Pini, 2003 ; Alonso et al., 2006).

I.3.5. Exemple de marqueurs des zones amont de glissements fossiles : les surfaces d'arrachement de glissements sous-marins et les déformations de sédiments associées du complexe deltaïque du Sobrarbe (Ainsa, Pyrénées espagnoles)

Dans la Formation Ayabacas, les marqueurs de la zone la plus en amont des glissements sous-marins sont souvent difficilement observables. En effet, ces affleurements se trouvent à présent dans la Cordillère Orientale, caractérisée par des écailles chevauchantes et une forte déformation tectonique orogénique, bien plus que sur l'Altiplano notamment (*e.g.* Audebaud, 1967 ; James, 1971 ; Audebaud et al., 1976 ; Laubacher, 1978 ; Dorbath et al., 1993 ; James & Sacks, 1999 ; Sempere et al., 2008). Les petites déformations synsédimentaires qui marquent les zones amont des glissements sous-marins sont peu évidentes, soit parce qu'elles n'ont pas été enregistrées, soit parce qu'elles ont été reprises et détériorées lors de la tectonique orogénique. En particulier il est très difficile de déterminer la position exacte des surfaces d'arrachement, et plus encore de déterminer leur géométrie, et il n'a pas été possible de déterminer un possible empilement de surfaces d'arrachement successives dans la Formation Ayabacas. Ces surfaces d'arrachement sont au contraire très bien exposées dans le complexe deltaïque du Sobrarbe, situé à une dizaine de kilomètres au sud-ouest d'Ainsa (Pyrénées espagnoles). Un article (actuellement en révision) ayant été rédigé lors du doctorat, cet exemple est proposé pour illustrer ce type de structure et les déformations de sédiments associées dans la zone amont d'une succession de glissements sous-marins fossiles.

Résumé en français de l'article 1 : 3D Architecture of submarine slide surfaces and associated soft sediment deformation in the Lutetian Sobrarbe deltaic complex (Ainsa, Spanish Pyrenees). *Sedimentology*, en révision.

Dans la partie centrale du bassin d'avant-pays éocène sud-pyrénéen, le complexe deltaïque du Sobrarbe représente les derniers dépôts marins du Synclinal de Santa Maria de Buil en tant que composante du Bassin d'Ainsa. C'est un bassin transporté (ou en "*piggy-back*") qui s'est mis en place lors de la croissance d'anticlinaux de rampes latérales orientés ~ nord - sud, forçant les sédiments à prograder du sud-est vers le nord-ouest. Les sédiments étaient instables et plusieurs glissements gravitaires sous-marins ont perturbé les niveaux régulièrement déposés, emportant plus en aval de 10 à 15 % des matériaux mis en place pendant les Séquences Composites "Las Gorgas" et "Barranco Solano". L'instabilité des sédiments résultait de taux de sédimentation importants (0,8 m/1000 ans en moyenne sans correction de la compaction), de la chute progressive du niveau marin relatif contrôlée par le soulèvement tectonique, et probablement de l'activité sismique (présence d'une séismite).

Cinq surfaces, résultant d'arrachements sous-marins successifs vers le nord-ouest, sont cartées et décrites dans le complexe deltaïque. Dans leur partie amont (tête du glissement), les surfaces sont aisément identifiables grâce à la discordance angulaire entre les premiers niveaux du remplissage sédimentaire post-glissement et les couches sous-jacentes sectionnées par le glissement. En allant vers l'aval, cet angle s'amenuise puis disparaît, les cicatrices des arrachements se confondent alors avec les plans de stratification, et la reconnaissance des glissements est possible grâce à d'autres marqueurs : masses déplacées, bancs de grès faillés et resédimentés, figures de déformations plastiques synsédimentaires d'échelle métrique des matériaux sous-jacents in-situ, telles que demi-grabens, failles normales, fentes de tensions remplies de sédiments (*neptunian dykes*). Ces dernières structures (*neptunian dykes*) sont interprétées comme résultant de tsunamis post-glissement. Toutes ces structures se caractérisent par une absence de minéralisation ou de fibres de calcite, et au contraire par l'éventuelle présence de bioturbations et de flutes casts, indiquant qu'au moment des glissements les matériaux étaient cohésifs mais pas complètement lithifiés.

Chaque arrachement est comblé très rapidement, avec un taux de sédimentation estimé à ~8 m/1000 ans, ce qui correspond à dix fois le taux de sédimentation moyen du complexe deltaïque du Sobrarbe. Ce taux de sédimentation, plus élevé dans les dépressions créées par un arrachement, s'explique en partie par des glissements ou des slumps rétrogressifs se produisant en amont, à la tête des arrachements. Ils fournissent des quantités importantes de matériaux et remplissent ainsi rapidement les dépressions.

L'organisation spatiale des différentes surfaces et leurs relations avec la sédimentation locale ont été reconstruites à partir des relevés de terrain et d'un modèle géologique 3D. Ce modèle, construit avec le logiciel Earth Vision, est basé sur des mesures topographiques

précises (à l'aide d'une station totale) et un modèle numérique de terrain. Il apparaît que chaque surface se produit dans une partie plus distale du complexe deltaïque et recoupe une partie du remplissage sédimentaire des glissements précédents. Au cours du temps, les glissements successifs s'empilent verticalement en deux structures de collapses complexes, et migrent vers le NNW en suivant la chute du niveau marin qui se produit entre les deux Séquences Composites. Le modèle géologique fournit également une estimation du volume de sédiments déplacés dans la zone d'étude. La première structure complexe de collapse est constituée des arrachements S1, S2 et S3, représentant un volume $32x10^6$ m^3, ce qui correspond à ~12% du volume total de sédiments déposés lors de la Séquence Composite "Las Gorgas". Les arrachements S4, S5 et S6 de la seconde structure de collapse affichent un volume de $15,4x10^6$ m^3 soit ~13% du volume de la Séquence Composite Barranco Solano.

A partir de l'ensemble des observations, un modèle conceptuel en sept étapes décrivant le développement des arrachements dans le delta du Sobrarbe a été proposé : i) un événement régressif se produit ; ii) survenue d'un glissement majeur, avec éventuellement formation d'une séismite en amont ; iii) dépôt d'une tsunamite ; iv) remplissage marneux normal de la dépression créée par le glissement ; v) possible survenue de un ou plusieurs slides ou slumps rétrogressifs mineurs à la tête du glissement, favorisant un remplissage rapide de la dépression ; vi) fin de remplissage progressivement normal de la dépression ; vii) enfouissement de l'arrachement et de son remplissage par des marnes lors d'une période de haut niveau marin relatif.

3D Architecture of submarine slide surfaces and associated soft sediment deformation in the Lutetian Sobrarbe deltaic complex (Ainsa, Spanish Pyrenees)

Short running title:

Lutetian submarine slide surfaces, Ainsa

Pierre CALLOT [(1)], Francis ODONNE [(1)], Elie-Jean DEBROAS [(1)], Agnès MAILLARD [(1)], Damien DHONT [(2)], Christophe BASILE [(3)] and Guilhem HOAREAU [(1)]

(1) LMTG, UMR 5563 – Université de Toulouse – CNRS, IRD, OMP, 14 av. E. Belin, 31400 Toulouse, France (E-mail: callot@lmtg.obs-mip.fr).

(2) MIGP, UMR 5212 CNRS – Total – Université de Pau et des Pays de l'Adour, Bat. IPRA, BP 1155, 64013 Pau Cedex.

(3) Laboratoire de Géodynamique des Chaînes Alpines, CNRS-UMR 5025, Observatoire des Sciences de l'Univers de Grenoble, Université Joseph Fourier, BP 48, 38041 Grenoble Cedex, France.

ABSTRACT

Five successive fossil submarine slides have been mapped and described in the Sobrarbe deltaic complex (Ainsa Basin, Spanish Pyrenees). They affect and remove up to 15% of the delta front. The head of the scar surfaces are clearly recognized in the field due to the angular unconformity between the infilling sediments and the underlying layers. Most of the slide scarps trend N55° with 20 to 40° dips indicating northwestward sliding. Downslope, traces of the sliding surfaces parallel stratification. However, they can be identified by displaced masses, re-sedimented sandstones, and soft sediment deformation features such metre-scale half-grabens, normal faults and tension cracks. They also all indicate a sliding displacement toward the NW.

A 3D model built from topographic data with Earth Vision software shows the architecture of the slide surfaces and provides an estimation of the volume of each sedimentary body within the limit of the studied area.

This study also indicates that: (1) the sediments have been cut and carried away before their lithification ; (2) the sedimentation rate infilling a single slump scar is estimated to be about 8 m/1000 years, *i.e.* 10 times higher than in the overall area of the Sobrarbe deltaic complex ; (3) each composite scar progressively develops and infills by retrogressive slumps; (4) the successive slide surfaces stack vertically in a collapse complex structure and migrate downward to follow sea level drop between two successive collapse complex structures; (5) the development of the scars in the Sobrarbe delta is described from a seven stages conceptual model starting with a regressive event and (6) the triggering of the Sobrarbe instabilities is controlled by high values of sedimentation rate, relative sea level falls mainly controlled by tectonic uplift, and possible likely seismic activity.

KEYWORDS:

fossil submarine slides, sedimentary instabilities, slope instabilities, soft sediment deformation, 3D modelling, Ainsa Basin, seismite, tsunamite.

INTRODUCTION

Slope instabilities are responsible for the remobilization and the distribution of sediments on continental margins. Displacement can start by the development of a cohesive slide or slump, and evolve to a debris flow as the fragmentation increases during the transport process. The end-result may be the development of laminar flow that can transform into a turbidity current that deposits sediments on the distal part of submarine fans along low-gradient slopes (Reading, 1996).

In the last few years, progress in oceanography has provided detailed views of present-day submarine landslides on continental margin (e.g. Gardner *et al*., 1999; Canals *et al*., 2004; Haflidason *et al*., 2004; Trincardi *et al*., 2004; Wilson *et al*., 2004). Thus, side-scan images, multibeam bathymetry, high resolution or 3D seismic and sub-bottom profiles have revealed the overall morphology, the basal slope and the complete 3D images of present-day slides on continental margins (Huvenne *et al*., 2002; Frey Martínez *et al*., 2005; Frey Martínez *et al*., 2006; Moscardelli and Wood, 2008).

Creeping may slowly displace considerable sediment masses over long distances (Mulder & Cochonat, 1996; Reading, 1996). But in most cases, movement starts with slides or slumps that often change in more mobile sediment gravity flows with downslope acceleration and dilution by progressive water incorporation and cohesion loss (Mulder & Alexander, 2001).

The initiation of these submarine landslides is controlled by the slope failure conditions (Mandl & Crans, 1981), that include internal and external parameters. The most important internal physical parameters are the cohesion, the internal friction coefficient of the sediments and the pore-fluid pressure (Mandl & Crans, 1981; Mello & Pratson, 1999; Mourgues & Cobbold, 2003). These parameters can evolve during diagenesis resulting in progressive porosity changes (Porebski & Steel, 2003). A sudden increase in pore-fluid pressure may result in a decrease of the sediment shear strength and in a reduction of effective shear stresses (Terzaghi, 1943; Spence & Tucker, 1997).

The main external parameters are tectonic setting, seismicity, slope geometry, sea level changes and sedimentation rates. Tectonic setting and seismicity may be responsible for sudden stress increase or sediment liquefaction (Fields et al., 1982; Greene et al., 1991; Papatheodorou & Ferentinos, 1997; Gonzalez et al., 2004). The result is a reduction in shear

strength of the sediment induced by increase of fluid pore pressure triggering slope instabilities (Allen, 1982; Nichols, 1995; Chapron *et al*., 1999; Piper *et al*., 1999; Locat & Lee, 2002; Sultan *et al*., 2004). The dip value of the slope surface may control the shear stresses applied to the sediment (Mandl & Crans, 1981). The differential loading of sediments may also result in a differential compaction that causes fluid or gas expulsion (Vendeville & Gaullier, 2003). Moreover, the instability often develops due to the simultaneous association of some of these parameters (Mienert *et al*., 2002).

Both present-day submarine landslides and fossil slides provide complementary information to help understanding instability processes. The study of present-day submarine landslides provides data on the surface geometry and extension, on the timing of the successive events that have built the sliding and on the volume of displaced sediments. When compared to present-day submarine landslides, fossil slides provide details on the internal structures, deformation and depositional processes (Lucente & Pini, 2003 ; Pickering & Corregidor, 2005; Vernhet *et al*., 2006; Spörli & Rowland, 2007; Callot *et al*., 2008). Where the outcrops are well exposed, the complete vertical succession of the different sliding events can be observed, and the subsequent study of their temporal and spatial relationships is then possible.

This paper focuses on fossil submarine landslides of the Lutetian Sobrarbe deltaic complex (Spanish Pyrenees) in order to identify the geometry of the slide surfaces that occurred during the sedimentation. The geological setting of the area has been previously established (De Federico, 1981; Dreyer *et al*., 1999) and is not developed in this work. Field exposure is very good particularly in the western limb of the Santa Maria de Buil syncline presently crossed by several small valleys that exhibit sections of the slide surfaces and some of the classical associated structures: scars, tilted blocks, syn-sedimentary faults and microfaults, small scale slump structures (Martinsen, 1989).

Each slide surface has been described in order to present the different structures and deformation processes that can be recognized. The spatial organization of the different slide surfaces and their relationships with local sedimentation has been reconstructed from a detailed field mapping and a 3D geologic model on the base of very accurate topographic measurements. The 3D geologic model permits an estimate of the initial sediment volumes that can be compared with the sediment volumes removed by the fossil slides. A conceptual model describes the development of the scars in the Sobrarbe delta.

GEOLOGICAL SETTING OF THE EOCENE SOBRARBE DELTAIC COMPLEX

In the central part of the Eocene South Pyrenean Foreland Basin, the Sobrarbe deltaic complex represents the last marine filling of the Santa Maria de Buil syncline as a part of the Ainsa Basin. It is a piggy-back basin that has developed westward during the in sequence formation of three growing lateral thrust-ramp anticlines (Figs. 1 and 2). The delta formed west of the N-S anticlinal ridge of Mediano, over the gentle growing Arcusa anticline and east of Boltaña anticline condensation zone during Lutetian to Bartonian times. The submarine uplift of these anticlines forced sediments to enter within the Buil syncline from the southeast and to prograde towards the north-northwest (Fig. 2; Puigdefàbregas *et al*., 1991; Muñoz *et al*., 1994; Dreyer *et al*., 1999).

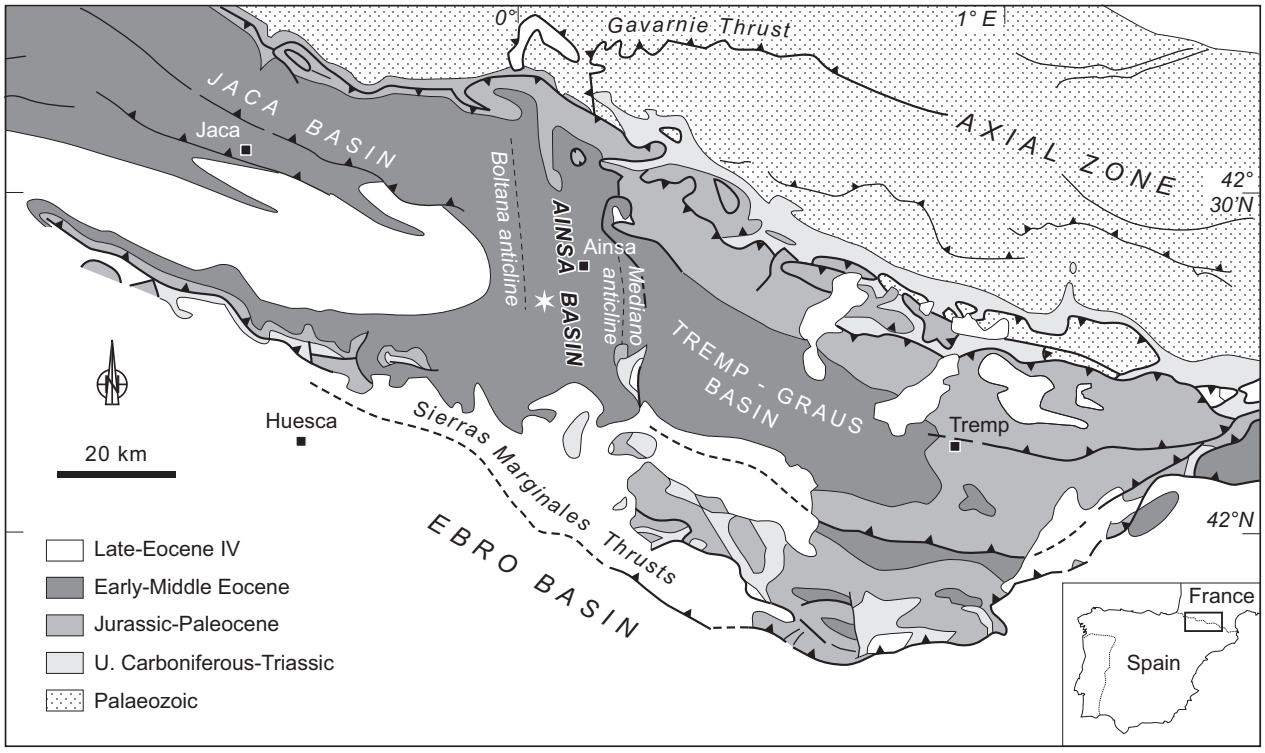

Fig. 1. Simplified geological map of the South Pyrenean Foreland Basin with location of the Ainsa Basin (North of Spain). Redrawn from Dreyer et al. (1999). Star indicates the position of the study area.

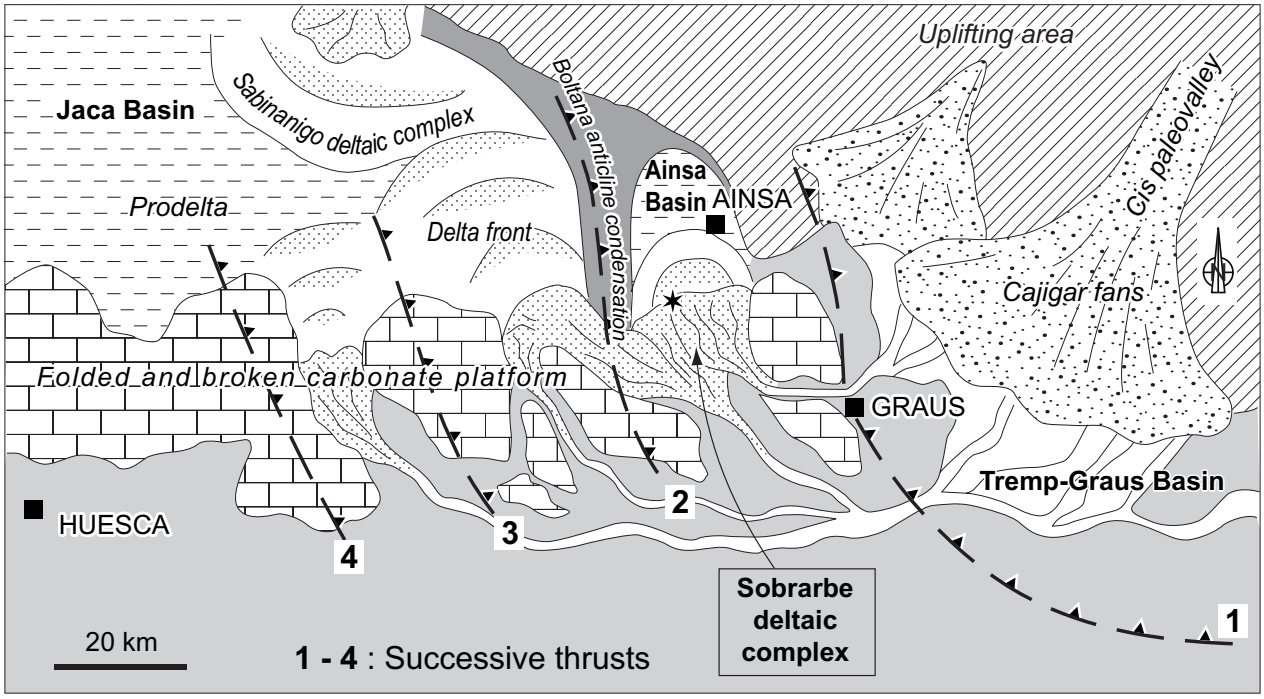

Fig. 2. Paleogeographic reconstruction of the late Lutetian Sobrarbe deltaic complex in Ainsa Basin. The successive thrusts form a series of anticlines and synclines that impose the progradation of the sedimentation to the NW. Redrawn from Dreyer et al. (1999). Star corresponds to the study area.

The sedimentary facies of the Sobrarbe deltaic complex has been described by De Federico (1981), Wadsworth (1994) and Dreyer *et al*. (1999). Six facies associations have been recognized (Dreyer *et al*., 1999). Most are mudstone-dominated and correspond to delta plain, delta front and slope deposits: (i) slope marlstones and turbidite sandstones; (ii) silty and bioturbated sandstones at the distal delta front; (iii) proximal delta front and delta plain deposits; (iv) biogenic deposits on flooding surfaces; (v) collapse zone deposits; (vi) Nummulite dominated shallow-marine carbonates.

Four composite sequences compose the northward prograding Sobrarbe deltaic complex (Fig. 3; Dreyer *et al*., 1999). They are bounded by regressive unconformities and composed of numerous minor units bounded by maximum flooding surfaces. Based on the associations of the sedimentary facies, these can be divided into lowstand, transgressive and highstand components. The studied sediments belong to the upper part of the Sobrarbe formation which includes the top of Comaron Composite Sequence, the Las Gorgas CS and the base of Barranco Solano CS and in which Dreyer et al. (1999, fig. 7) provide two local biostratigraphic timelines: (1) the "estimated top of *Nummulites sordensis/ N. crassus* biozone" and (2) the "estimated top of *N. herbi / N. aturicus* biozone". These two timelines correspond to the boundaries of the Shallow Benthic Zone 16 correlated with the late Lutetian Chron 19 (around the boundary C19r / C19n) by Serra-Kiel et al. (1998). Once updated with

the new geological time scale of Gradstein et al. (2004) these timelines indicate an age of about 40.8/40.9 Ma for the lower boundary of the SBZ 16 and about 40.4 Ma for the upper one (i.e. Lutetian/Bartonian boundary). Such an age is compatible with two other recent data: the mid Lutetian age of the Ainsa fans and the Lutetian P12 Zone age of the Guaso system deposits (Pickering & Corregidor, 2005), and the Bartonian age of the overlying fluvio-deltaic Escanilla system (Remacha & al., 2003). During this time interval of about 0.4 to 0.5 Ma, about 350 m of sediments have been deposited. The sediment-accumulation rate can be estimated to 87.5 to 70 cm/1000 years, not corrected for compaction. Such values of sedimentation rates are of the same order of magnitude of that observed in modern delta of Rhine and Nile (Martinsen, 1989; Loncke et al., 2002).

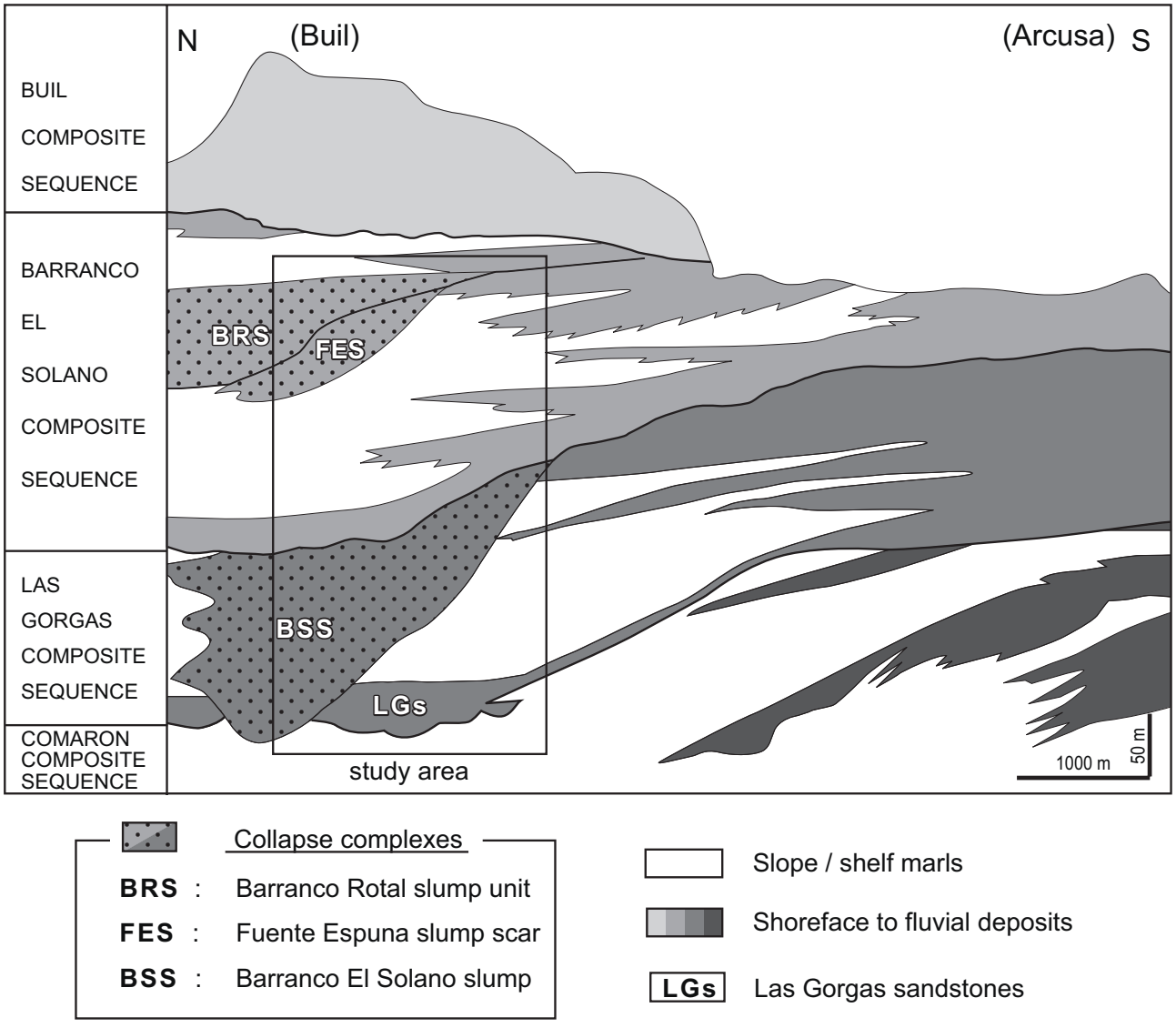

Fig. 3. Correlation diagram of the Sobrarbe deltaic complex in the Ainsa Basin. The slides developed in the Las Gorgas Composite Sequence and in the Barranco El Solano Composite Sequence. Redrawn from Dreyer et al. (1999). The box corresponds to the study area.

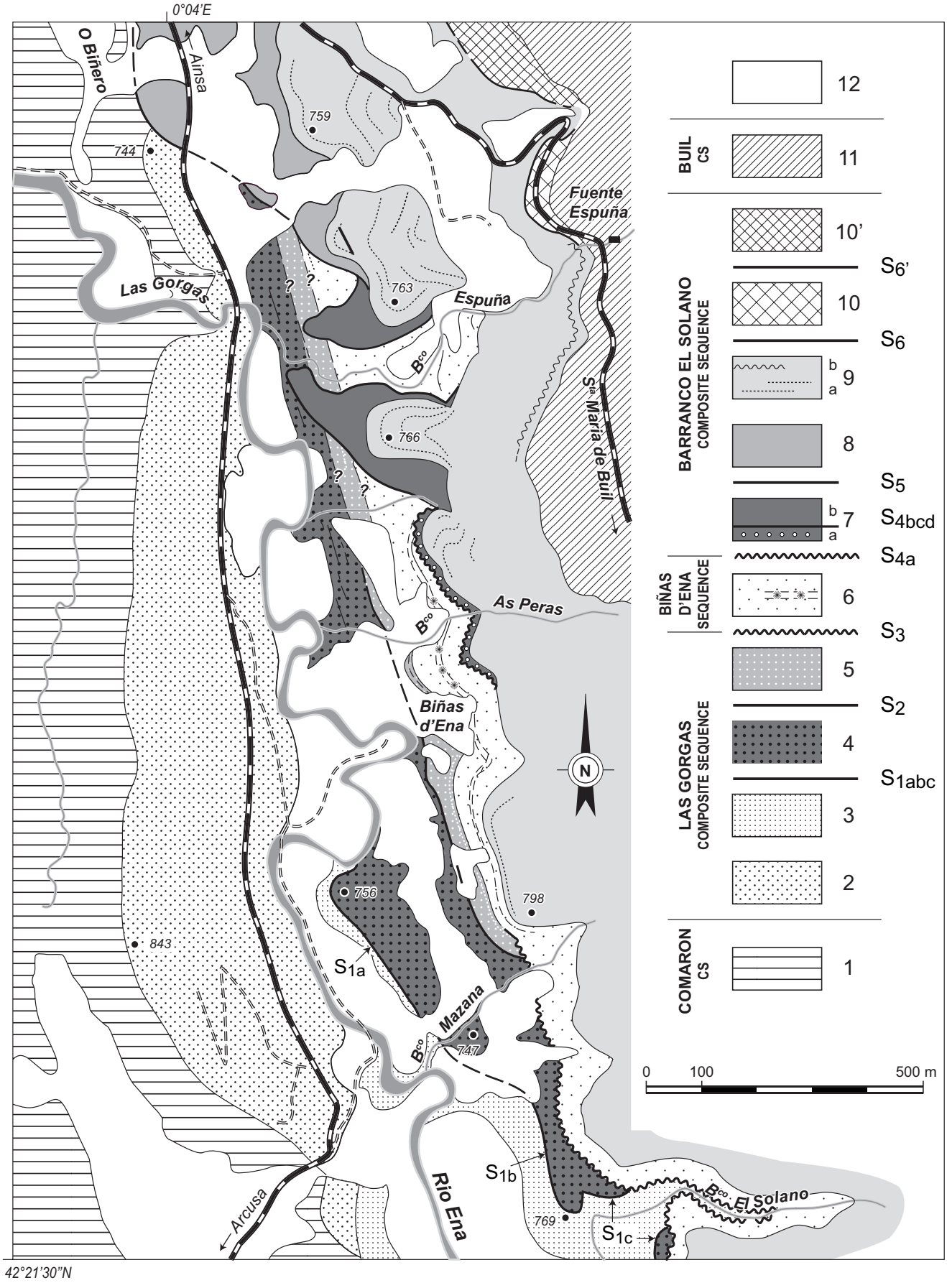
0°04'E
O Biñero
Ainsa
744
759
763
766
Fuente Espuña
Espuña
Las Gorgas
Bco
Sta María de Buil
As Peras
Biñas d'Ena
N
756
798
843
S1a
Mazana
747
S1b
S1c
Bco El Solano
769
Río Ena
Arcusa
42°21'30"N
12
BUIL CS
11
BARRANCO EL SOLANO COMPOSITE SEQUENCE
10'
S6'
10
S6
9
8
S5
7
S4bcd
S4a
BIÑAS D'ENA SEQUENCE
6
S3
5
S2
LAS GORGAS COMPOSITE SEQUENCE
4
S1abc
3
2
COMARON CS
1
0
100
500 m

Fig. 4 (previous page). Geologic map of the studied area in the western side of the Buil syncline. Six surfaces have been recognized to affect three of the four sedimentary sequences. The S1, S2 and S3 surfaces mainly developed in the Las Gorgas Composite Sequence, they were cut and they are filled by the LGCS sediments. The S4 surface developed in the LGCS sediments, the S5 surface developed in the LGCS and the Comaron CS sediments but both are filled by sediments of the Barranco El Solano Composite Sequence. The S6 surface developed in the Barranco El Solano Composite Sequence. In stratigraphic order, numbers of the legend correspond to: 1) the last deposits of the Comaron Composite Sequence (CCS); 2) the Las Gorgas sandstone body corresponding to the base of the Las Gorgas Composite Sequence (LGCS); 3) the marly distal part of the LGCS; 4) and (5) the deposits - infilling and cover - resting above S1 and S2 surfaces; 6) The sandy to marly deposits of Biñas d'Ena sequence above S3 surface with a seismite bed (*); 7) the first infilling of the Barranco Espuña S4 scar; 7a) Barranco as Peras sandstone body; 7b) Barranco Espuña re-sedimented and in situ deposits; 8) the first infilling of the O Binero S5 scar; 9) the deposits of the Barranco El Solano Composite Sequence (BSCS); 9a) last infilling of S4 and S5 scars; 9b) marlstones and Buil Nummulite banks;10) the infilling of the Fuente Espuña S6 scar; 10') the infilling of the Barranco Rotal S6' scar; 11) the last marine levels of the BSCS and the base of the Buil Composite Sequence (BCS); 12) Quaternary deposits.

Numerous gravitational slides have disrupted the layers and have removed 10 to 15% of the delta front strata (Fig. 3). Both the tectonic activity of the growing anticlines and the associated relative sea level fall are believed to have triggered such sedimentary instabilities (Dreyer *et al*., 1999 ; Pickering and Corregidor, 2003). In order to identify the spatial organization of the scar surfaces and the mechanisms responsible for the instabilities, two fossil collapse complexes were focused on: Barranco El Solano Slump and the Fuente Espuña slump scar (Dreyer & al., 1999; Fig. 3).

FIELD IDENTIFICATION OF SLIDE SURFACES

Six main surfaces have been restored and mapped in the collapse complexes of the Las Gorgas and Barranco El Solano composite sequences (Fig. 3). Their relative positions and extensions are illustrated by the geological map drawn directly on the orthophoto 211-55 of Gobierno de Aragon at 1:5000 scale (Fig. 4).

Upslope slide area

Most of the slide surfaces are revealed by a correlative upslope angular unconformity (e.g. Figs. 5 and 6). The first layers deposited in the scar successively cover the "sliding blocks" that may rest immediately above the slide surface, onlap the layers truncated by the scar and then drape the remaining slope and its uphill shoulder (Figs. 6 and 7). With the progressive infilling, the unconformity reduces upslope and the last deposits are parallel to the in-situ layers. All these deposits constitute the infill of the slide scar. The overlying deposits constitute the "cover" (Fig. 7).

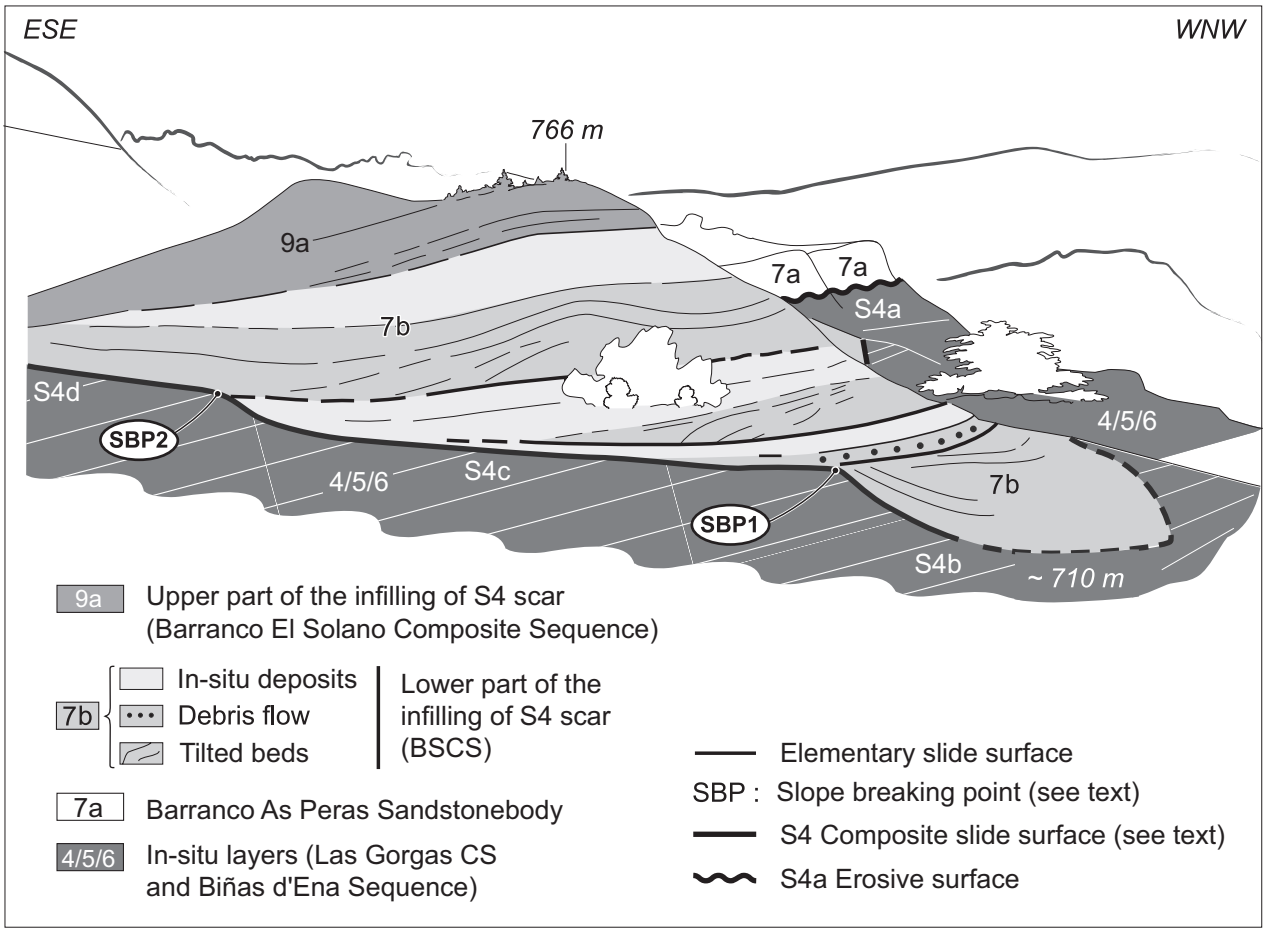

Fig. 5. Line drawing of the composite slide surface (S4) on the left bank of Barranco Espuña. The northern segment of the first order S4 surface appears to be composed of three segments separated by two slope breaking points. The infilling is subdivided by elementary slide surfaces over which are deposited tilted beds or debris flows draped by apparently in situ deposits. Three phases of retrogressive sliding and at least five main phases of infilling can be distinguished. Only the last layers of the infilling, top of 9a, exhibit the same dip values as the in-situ layers.

Downslope slide area

The angular unconformity between in-situ and infilling layers progressively reduces downslope where the geometric identification becomes difficult because both in-situ and infilling layers are essentially parallel. Other indicators of gravitational instability, such as sediment slides and slumps are shown by the presence of displaced and deformed sediments resting above the slide surface (Fig. 7, area 2) or by deformations in the in-situ sediments below the detachment surface.

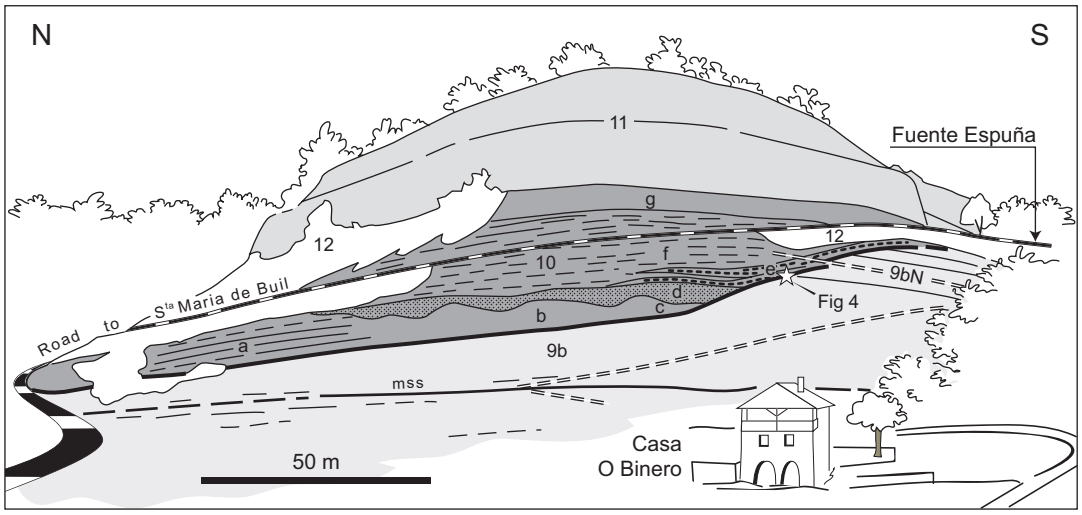

Fig. 6. Line drawing of the Fuente Espuña simple slump scar. The angular unconformity between the S6 surface and in-situ layers can be observed on both sides of the outcrop (at south near Fuente Espuña and at north in the road hairpin bend). That indicates a general scarp orientation facing to the West. 9b) named in reference to figure 4, in-situ sanstones and marlstones layers of the Barranco El Solano Composite Sequence with a minor slide surface (mss); 9bN) in-situ Nummulite banks at the top of BSCS; 10) infilling and cover of the S6 scar: a) poorly deformed sandy raft; b) fractured and partly brecciated sandstone bed; c) complex wedge of slumped layers; d) wedges of coarse to medium-grained laminated sandstones; e) Nummulite-rich re-sedimented marlstones; f) laminated marls; g)structureless marlstones with numerous Fe rich nodules; 11) the last marine levels of the BSCS and the base of the Buil Composite Sequence (BCS).

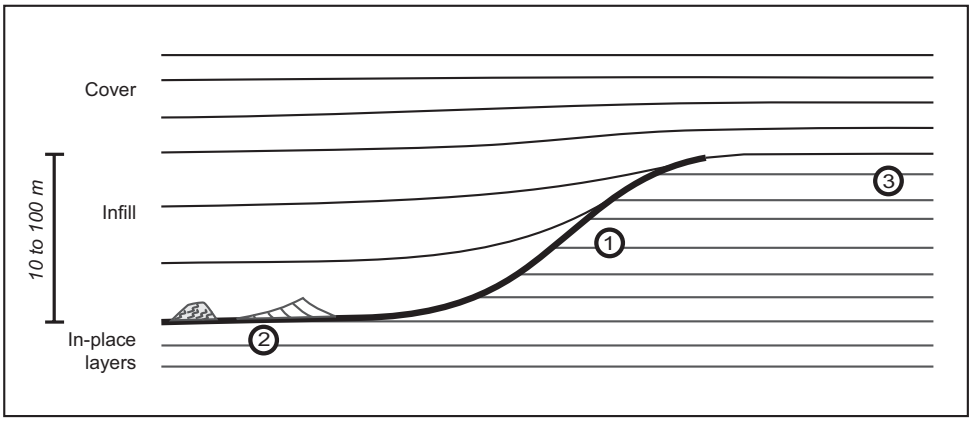

Fig. 7. Schematic line drawing of a simple slide structure. Area 1 corresponds to the head part of the sliding surface where the angular unconformity can reach 45°; Area 2 corresponds to the downslope depression where angular unconformity progressively reduces and disappears. Slide masses can be observed, that rest above the basal slip surface. They are composed of cohesive sandstone and mudstone layers and some of them have been tilted during translation. Area 3 corresponds to the uphill shoulder of the slide where sedimentation is interpreted to have never stopped.

Displaced and deformed sediments resting above the slide surface

Deformed deposits may rest locally above the slide surface. They are composed of cohesive sandstone and/or mudstone layers translated as horizontally bedded rafts (Fig. 6) or as rafts with beds tilted or gently folded during translation (Fig. 5). Rafts are up to 15 m thick and up to 130 m long. Some layers of small-to medium-bedded sandstones embedded in

mudstones are cut by small normal faults giving a step shape to bedding surfaces (Fig. 8). They look like the closely spaced syn-sedimentary normal faults described by Pickering (1983).

Some thick or very thick beds of debris flow deposits are observed over the slide deposits. Cohesive debris flow deposits (interpreted as mudflows) are composed of mudstone cobbles and blocks embedded in structureless marlstones. Non cohesive debris flow deposits (interpreted as grain flows) are composed of structureless sandstone with numerous clay chips. Only in few cases, slump structures with small folds are observed over the studied area and they are limited to thin slump sheets.

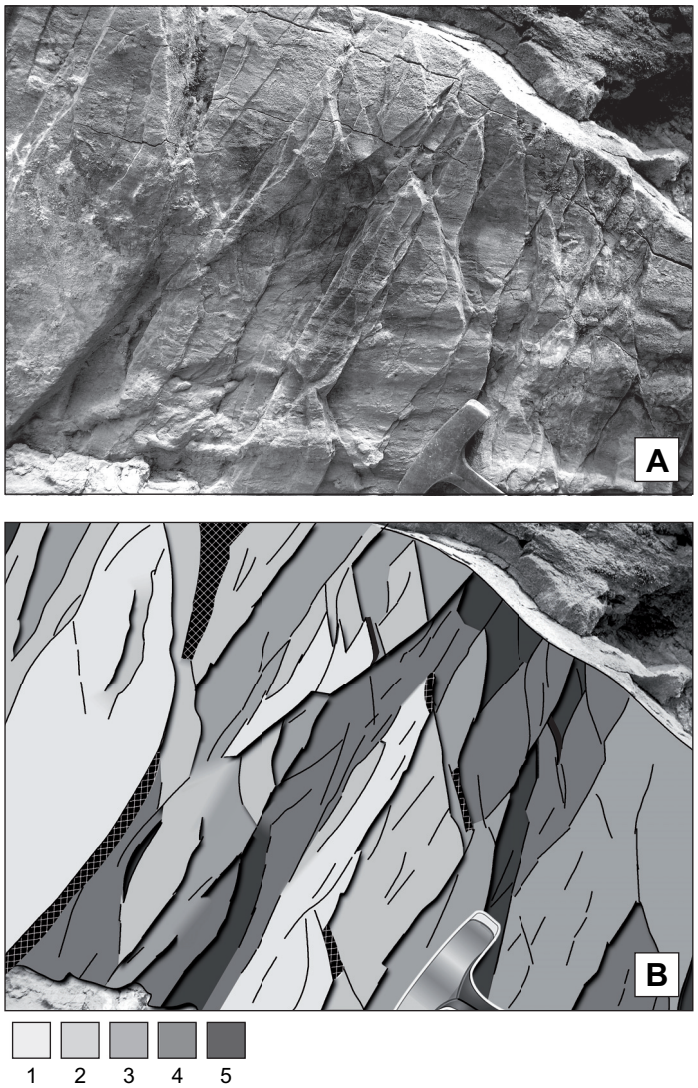

Fig. 8. Soft sediment faulting of a sandstone bed observed in the infill of the S2 surface. A) View of a sandstone bed sole that is cut by numerous small normal faults. B) line drawing highlighting the step-shaped of the same sole. No mineral fibre has been observed on fault planes.

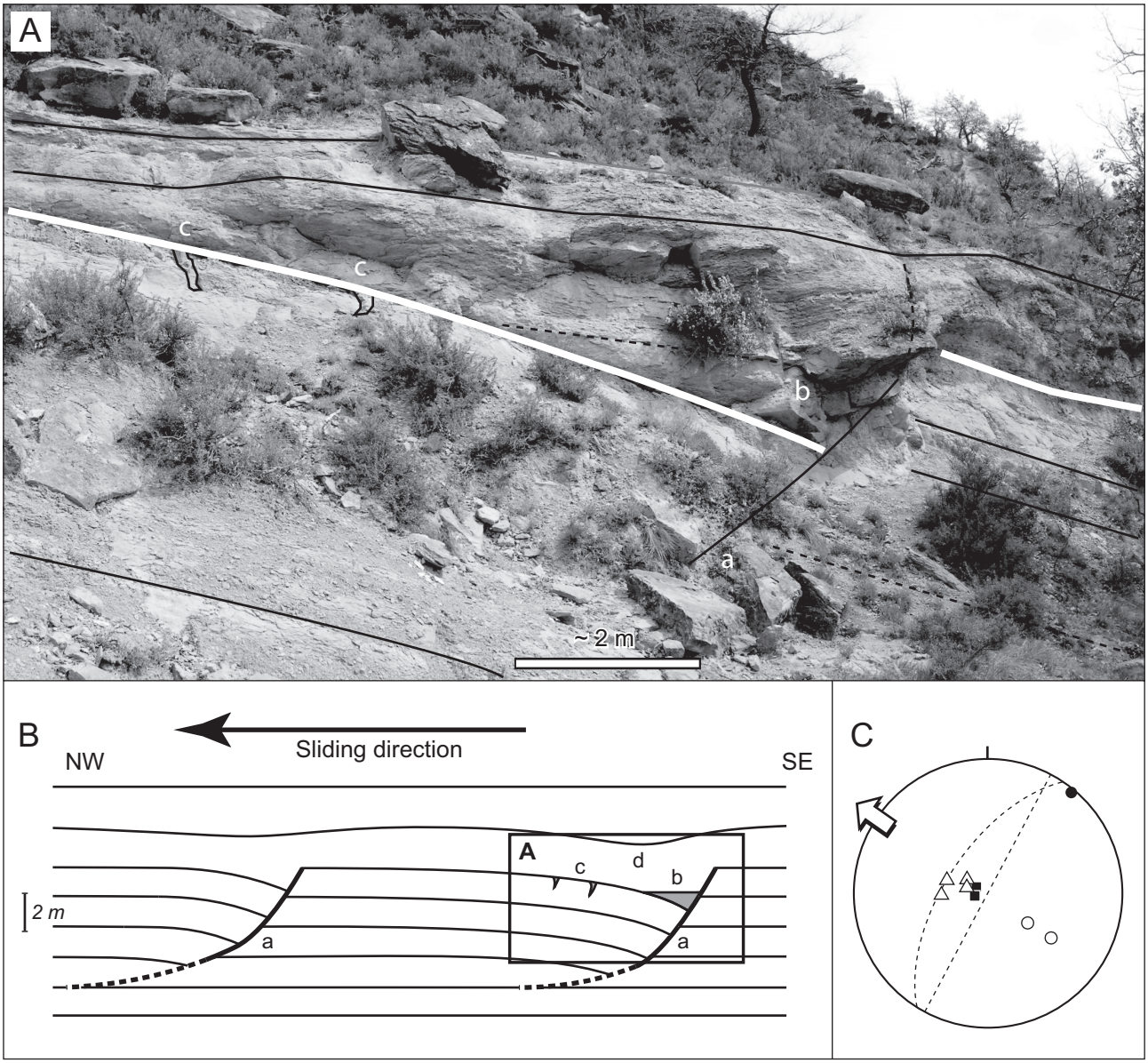

Fig. 9. Soft-sediment normal faults and associated structures affecting the S1 surface (white line) and in-situ layers surface observed on the right bank of the Rio Ena, below point 756 of figures 4 and 11. A) Picture; B) schematic line drawing of a complete roll-over structure composed of (a) soft listric normal fault orientated N40°; (b) horizontal wedge of laminated coarse-grained sandstone with clay chips, fine plant fragments and flute casts at the base, cover both the tilted layers and the fault surfaces over ten metres width, both are orientated N40°; (c) few metres far from the fault, on top of the tilted in-situ layers, thin vertical sandstone dykes have been formed parallel to the fault. They are filled with the same coarse-grained sandstone than the horizontal wedges, the opening of the vertical dykes involves some cohesion of the muddy layers in which they form. (d) laminated fine sandstones and silstones. "b" to "d" are interpreted as a tsunami deposits. C) stereographic projection of fault (open circles), footwall layers (black square), tilted layers (open triangles), vertical dykes (planes) and half graben gutter axis (black dot). The suggested sliding direction points toward the NW.

Deformation features observed below the slide surface

In some downslope areas, normal faults offset the slide surface up to 2 metres (Fig. 9). The in-situ layers and the main slide surface are tilted. Both the tilted layers and the fault surfaces are covered by horizontal wedges made of structureless and coarse-grained sandstone with clay chips and small plants fragments at the bottom and of horizontally laminated fine sandstone to silstone at the top (Fig. 9). They fill small half graben gutters between the fault scarp and the tilted layers. Some flute casts can be observed at the base of the sandstones striking parallel to the fault and the gutter axis. This kind of erosive basal structure can occur in cohesive but not completely lithified muddy sediments.

The top of the tilted layers are broken by synsedimentary vertical dykes. These dykes are parallel to the fault (Fig. 9). Many other dykes have been observed along other sliding surfaces. They all range from 5 to 50 cm width at the top and are up to 2.5 m deep. They are filled by a coarse-grained sandstone similar to the inferred grain flows overlying the sliding surfaces. These dykes seem to be extensive cracks opened by the flexure of the tilted blocks along the outer arc of a roll over structure. The tensile failure of these vertical cracks involved some cohesion of the muddy layers at the time of formation equivalent to mode I rupture (Price, 1966; Engelder, 1987; Price & Cosgrove, 1990).

RESTORATION AND MAPPING OF THE SLIDE SURFACES

Once identified at a point, each of the surfaces has been accurately followed downslope and upslope in the field. In most cases, the distinct surface segments are difficult to link together or to classify in order to restore the geometry of a main surface. The connection of the different segments from facies differences between in-situ layers and the infilling is not always clear because lateral facies variations are significant along the same main surface. In downslope areas, the Quaternary terraces of the Rio Ena partially cover some sliding surfaces. They were thus mapped from panoramic points of view. In upslope areas, the unconformity, the onlap and the fan shape of the infilling have been used. In such cases, the reconstruction of the slide surface geometry was constrained by the geometry of its banks, since it is not possible to connect directly both sides of a sliding scar (Fig. 10). However, this type of reconstruction must be used with care because: (1) a slide is not necessarily rectilinear, as exemplified by numerous present-day submarine slides (McAdoo *et al*., 2000; Lastras *et al*.,

2002; De Blasio *et al*., 2004); (2) a scarp head may be confused with the lateral bank of a slide. Consequently, geometric observations must be interpreted in relation to structural observations indicating the displacement direction. Some small isolated outcrops of elementary slide surfaces have not been mapped and integrated into the 3D model because their complete size and correlations are poorly defined. However detailed observations from these elementary slides can help to understand the triggering mechanisms.

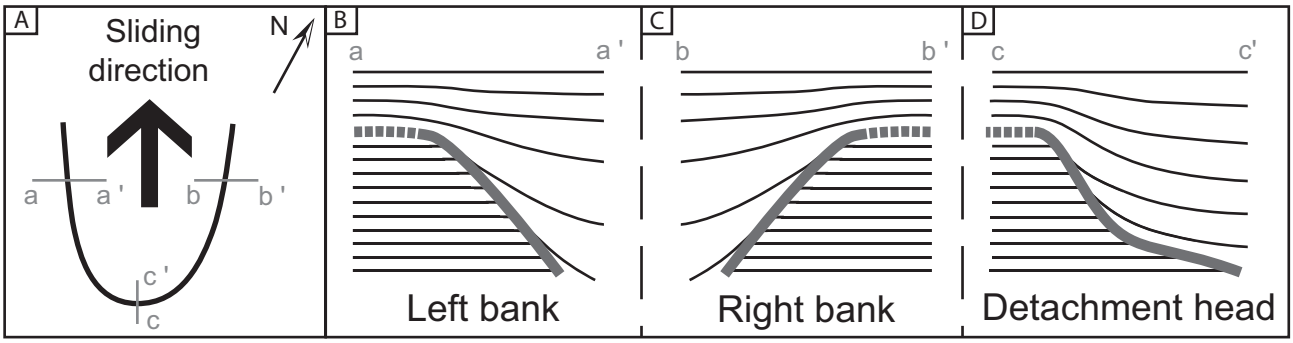

Fig. 10. (A) General shape and orientation of the head scarp discontinuities based on the data shown in figure 14. (B, C and D) Polarity of the unconformity according to its position in the slide. (B) and (C) opposite polarities related to the positions of right banks or left banks of slides have been used to connect the different slide surfaces observed in the Sobrarbe Deltaic Complex. (D) Geometry of the scarp at a slide head.

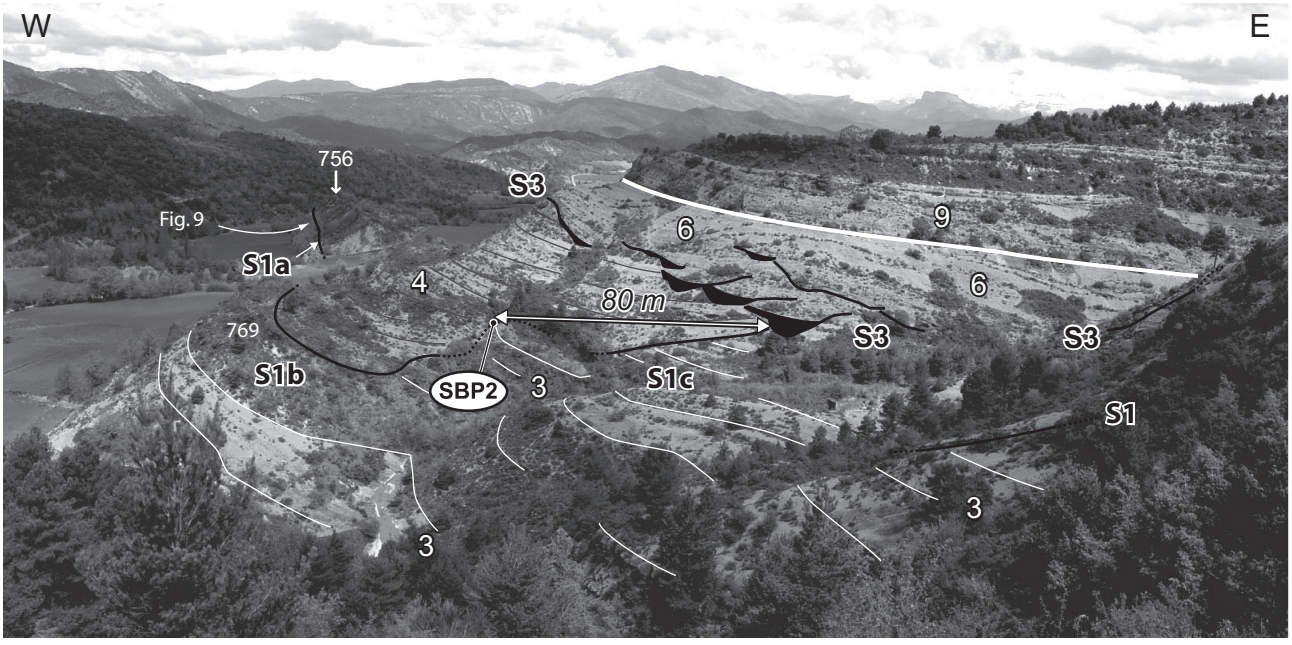

Fig. 11. The S1a to S1c composite slide surface and the S3 erosive surface on right bank of the Barranco El Solano. SBP is the slope breaking point of S1 surface. 3) in-situ layers of the Las Gorgas Composite Sequence; 4) sedimentary infilling of the S1a and S1b scars; 6) the S3 sandy infilling with laminated sandstone lenses (in black) over five minor erosive surfaces that developed successively upward and westward (= Biñas d'Ena sequence deposits); 9) deposits of the Barranco El Solano Composite Sequence above the boundary of the LGCS (white heavy line).

The main slide surfaces of the Sobrarbe delta

Surface S1 can be observed from three segments that are exposed from its upslope part 150 m south of Barranco El Solano to Rio Ena, below point 756 where it disappears under the Quaternary terraces (Figs. 4 and 11). This S1 composite surface cuts up to 170 m of the distal marly deposits of the Las Gorgas Composite Sequence and is interpreted to overlie the top of the Las Gorgas sandstones in the vicinity of Las Gorgas (Fig. 4).

To the NW the deepest segment of surface S1 (S1a) exhibits a low angular unconformity between in-situ and infilling layers and is interpreted as the right bank of the scar. A sliding direction toward the NW is indicated by the N40° orientation of normal faults and clastic vertical dykes (Fig. 9). The first part of the infill is composed of few metres of laminated marls followed by some metres of debris flows deposits with olistoliths and blocks of laminated marls. Both are cut by an elementary slide surface covered by lenticular sandy layers of re-sedimented nummulites. The onlap of the layers to the NE correspond to a right bank deposit while flute casts and the imbrication of the nummulites show a current toward the NW. Such resedimentation of the nummulites suggests a low sea level deposit.

S1b, the middle segment of surface S1, corresponds again to a right bank (Fig. 11). A sliding direction toward the NW is indicated by the extensive synsedimentary deformation of a step-shaped sandstone bed, faults strikes are from N40° to N85°.

To the SE the shallowest S1c segment of surface S1 is still a right bank (Fig. 11). The infill is composed of a basal lag deposit of nummulites covered with mudstone beds.

Surface S2 can be observed over a length of 400 m between Barranco Fuente Mazana (Wadsworth, 1994) and Biñas d'Ena (Fig. 4). This S2 surface cuts the sedimentary infilling or the cover of the S1 surface that represent its own relative substratum. Only the base of the left bank of the basal slide surface is exposed with an angular unconformity of about 15° between in-situ layers and the infilling. The sliding direction was towards the NW, indicated by the orientation of clastic vertical dykes (striking from N7° to N60°) and extensive synsedimentary deformation of step-shaped sandstones with faults striking from N33° to N100° (Fig. 8). This surface could be related to a sliding surface observed 300m to the north, west of Barranco As Peras (Fig. 4). The infill is preserved under the S3 surface and its cover, it is composed by 7 to 8 m of marlstones covered by a ten of metres of silty mudstones (Fig. 12).

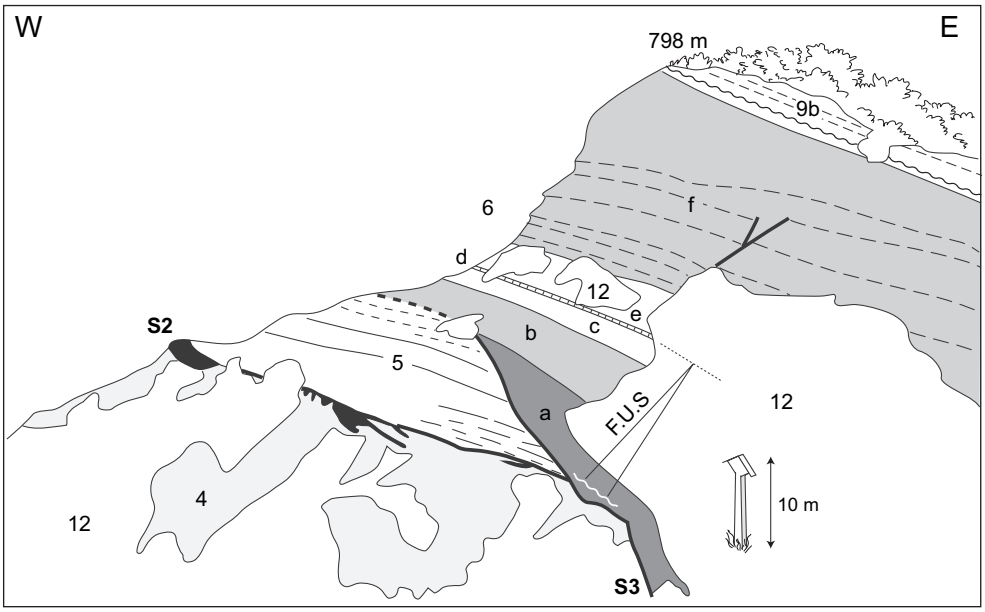

Fig. 12. Picture of the S2 and the S3 slide surfaces on the right bank of the Barranco Mazana. The S2 surface is marked by sandstone bodies: deformed horizontal wedges, small vertical dykes and step-shaped displaced beds. The S3 surface cuts about 10 m high of the infills of S2 (5) and S1 (4), and disappears to the W where in-situ layers and cover are conformable. 4) sedimentary infilling or cover of the S1 scar. 5) sedimentary infilling or cover of the S2 scar. 6) sedimentary infilling and cover of the S3 surface successively composed of (a) sandstones and siltstones, (b) lower siltstones, (c) lower marlstones, (d) limestone bed, (F-US) finning-upward sequence a to d, (e) upper marlstones, (f) upper siltstones and sandstones (= Biñas d'Ena sequence deposits). 9b) fossil rich transgressive base of the Barranco El Solano Composite Sequence.

Surface S3 can be observed on both sides of Barranco El Solano (Figs. 4, 11 and 12) from its head scarp 250 m south of Barranco El Solano (Dreyer *et al*., 1999) to its left bank North of Barranco Mazana (Wadsworth, 1994). This S3 surface corresponds to a 15-m-deep and more than 400-m-wide scar with a general orientation facing to the North. It cuts the siltstones deposits of the Las Gorgas Composite Sequence and the sedimentary infillings and covers of the S1 and S2 surfaces (Fig. 12). No soft sediment deformation was observed along this surface.

High values (up to 45°) of angular unconformity between in-situ sandy layers and infilling layers can be observed at the head of the scar. The base of the upslope scarp is covered by 4 m of re-sedimented deposits: (1) lens-shaped bodies composed of tilted thin-bedded sandstone and mudstone layers; (2) a thick structureless sandstone bed with numerous clay chips.

Other high values of angular unconformity are observed northward along the left bank but re-sedimented deposits are not observed elsewhere along this S3 surface. On the left bank of the Barranco Mazana, the S3 infilling consists of about 10 m of cross-laminated sandstones overlain by horizontally-laminated siltstones ("a" Fig. 12). Infilling deposits overlap the

surface and the cover lies conformably on the top of S2 infilling ("b" Fig. 12). The lower part of this cover is 16 m thick and is composed of a fining-upward sequence (laminated siltstones, laminated silty marls and a 50 cm-thick limestone bed: "b", "c" and "d", respectively, Fig. 12).-

Southward, on the right bank of Barranco El Solano (Fig. 11), the S3 surface is composed of five erosional surfaces that develop successively upward and westward. The sandy infilling of each surface starts with hummocky cross-stratified sandstones.

This S3 surface may have been formed by the erosion resulting from a relative sea level drop, when its infill and cover sedimentation has occurred during the following lowstand and highstand, they both constitute the new described Biñas d'Ena sequence.

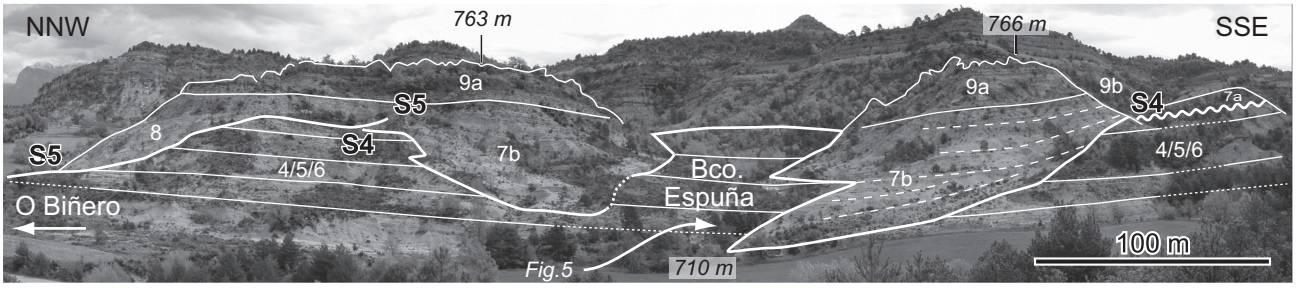

Fig. 13. Panoramic view of the S4 and the S5 slide surfaces on both sides of Barranco Espuña. The S4 Barranco Espuña surface deeply cuts in-situ layers, up to 130 m in the top of the LGCS (S1, S2 infilling and Biñas d'Ena sequence). The scar has been progressively filled by tilted blocks, slumped beds and some debris flow separated by in-situ deposits. (4) and (5) infilling resting above the S1, S2 surfaces; (6) deposits of Biñas d'Ena sequence; 7a) Barranco as Peras sandstone body; 7b) Barranco Espuña re-sedimented and in-situ deposits; 9) Barranco El Solano Composite Sequence deposits; 9a) upper infilling of the S4 and S5 scars; 9b) marlstones and Buil Nummulite banks. The angular unconformity between in-situ and filling layers is from 23 to 34°. On the left, only the upper part of the head scarp and of the infill (8) of the S5 O Binero surface can be observed.

Surface S4 can be observed from Biñas d'Ena to North of Barranco Espuña (Fig. 4). The southern segment S4a lies on both sides of Barranco As Peras where it incises up to 30 m of the marly top of the Biñas d'Ena sequence along 350 m. This segment is covered by the Barranco As Peras sandstone body. As for the S3 surface, the erosive surface and the sandstone body may result from a relative sea level drop and its consecutive lowstand. The northern segments S4b, c and d are exposed on the both sides of Barranco Espuña (Fig. 13). They correspond to the right bank of the sliding surface. South of the Barranco the S4 surface appears as the head scarp of a composite slide surface where the angular unconformity between in-situ and infilling layers is from 23 to 34° (Fig 5). The substratum is deeply incised, up to 130 m both in the base of Barranco el Solano Composite Sequence and at the top of Las Gorgas Composite Sequence (S1, S2 and S3 infilling). The sliding direction can be

interpreted as being toward the NW from the relative positions of its right bank and head scarp. The lower part of the scar has been filled by alternating tilted mudstone beds, cohesive debris flow and in-situ mudstones and marlstones deposits (7b of Figs. 4 and 5). Most of the upper part of the infilling is composed by likely in-situ deposits with an upward progressive increase of the dip values. The highest layers of the infilling (9a of Figs. 4 and 5) exhibit the same dip values as the truncated layers of the substratum. This is an indication that both the substratum and the infilling of S4 have been tilted by the growth of Boltaña anticline after the complete infilling had occurred. The cover of the infill is made of the marly layers of the high sea level of the Barranco el Solano Composite Sequence (9b of Fig. 4). Minor slump are observed elsewhere both in le upper part of the infill and in the marly cover.

Surface S5 can be observed on both sides of the road to Arcusa, from Barranco Espuña to the north of O Binero crest where it cuts the downslope part of S1 and S2, the cover of S3, a part of S4 infilling (Figs. 4 and 13), the Las Gorgas sandstones and the marly beds of the top of the Comaron Composite Sequence (Dreyer *et al*., 1999). The substratum is deeply incised, up to 160 m, and an angular unconformity reduces from 40° in the south to 0° in the north where the S5 surface disappears under Quaternary deposits (Fig. 4). When back-tilted from dip values of the in-situ layers, the slide surface appears to face a NW to N direction (strike measurements of the slide surface are from N58° to N80°). The lower part of the scar has been filled by tilted beds and in-situ mudstones and marlstones. The upper part and the cover of the infilling join the corresponding deposits of surface S4 (9b Fig. 4).

Surface S6 is located north of Fuente Espuña along the road to Santa Maria de Buil (Fig. 4). The incision cuts the top of the in-situ layers up to 25 m in both the Buil Nummulite banks and the top of the underlying marly layers of the Barranco El Solano Composite Sequence (De Federico, 1981) that are separated by a very low angular unconformity observed south of Fuente Espuña. The scarp dip reaches values up to 35° and gradually decreases to zero both upslope and downslope (Fig. 6). The base of the infilling is composed of a large horizontal sandy raft (up to 9 m thick and 130 m long). In the north (10a Fig.6) the raft is made up of horizontal fine sandstone layers that are poorly deformed and segmented by few vertical sandy dykes. In the south the raft thickness reduces, the layering is completely lost and deformation is more important and heterogeneous: the sandstone layer is cut by some vertical sandy dykes or is partially brecciated (10b Fig. 6). At the southern termination of the raft, the scarp base deposits consist of a complex wedge of laminated sandstones and

mudstones slumped layers covered with mud supported sandstone clasts (10c Fig. 6). The southern part of the raft and the slump and breccia deposits are covered by a succession of four horizontal wedges of coarse to medium-grained laminated sandstones. The wedges are about 15 m long and 1.5 to 2.9 m thick (10d Fig. 6). The infilling continues with the last Buil Nummulite banks that overlap the slide surface (10e Fig. 6). The remaining depression (10f and 10g Fig. 6) has been completely filled by about 20 m of laminated marlstones and 2.5 m of structureless marlstones with many small ferruginous nodules (oxidized pyrite). The dip of the slide surface S6 faces towards the W and the overall N-to-S organization of the sandy raft and of the sandy wedges suggest that this outcrop exposes the right bank of a slide that had relocated toward the W-NW direction.

To the North, the upper part of the deposits of the Barranco Solano Composite Sequence is cut by another surface that probably corresponds to the head of the Barranco Rotal slump scar (Dreyer *et al*., 1999). As this scar is mainly located out of the study area, it has not been studied but it is distinguished from the S6 surface in our geological map (S6' of Fig. 4). Both the infilling of the Fuente Espuña and of the Barranco Rotal surfaces were truncated by an upper undifferentiated surface and covered by laminated limestone beds of the last marine levels from the Barranco Solano Composite Sequence and then by the fluvial deposits of the Buil Composite Sequence.

Five out of the six surfaces documented in this paper from the Sobrarbe deltaic complex have been identified on the basis of the angular unconformity between the substratum and the filling layers in the head of the slide (Area 1 in Fig. 7). The directions and dips of the slide surfaces and the angular unconformity between the in-situ layers and the sedimentary infilling have been measured all along the outcrops. A synthetic shape of the slides can be deduced from these measurements (Fig. 14). All the data have been corrected from the dip value of the substratum because most of the tilting of the layers was produced by the growth of the Boltaña anticline after the sediments were deposited. The general shape of the restored data shows that most of the slide surfaces trend about N55° (facing NW), with dip values from 20 to 40° toward the NW. The extreme values indicate N150 directions with dips to the SW and N140 with dips to the NE, they may represent the lateral banks of the slides with dip values up to 30° (Fig. 10A).

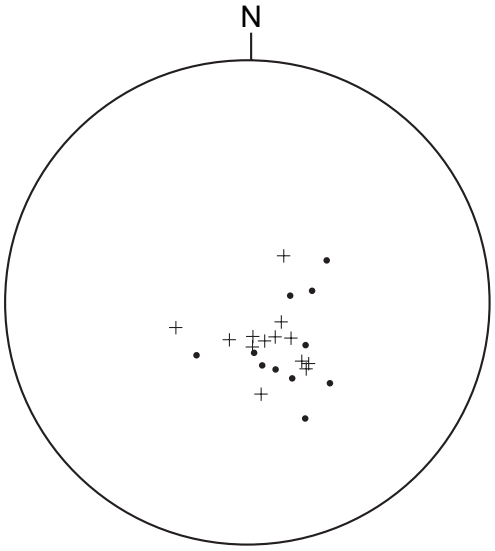

Fig. 14. Measurements of pole of the scarp plane as points and the pole of the first layer of infilling planes as crosses (Wulff, lower hemisphere). All the data have been corrected from the dip value of the substratum. Most of the data are oriented about N55°, with dips values from 20 to 40°. i.e. most of the slides face a NW direction. The extreme values indicate N150 directions with dips to the SW and N140 with dips to the NE, they represent lateral banks of the slides with dip values up to 30°.

3D modelling

The principal aim of this research was to build a 3D geological model in order to better describe the geometry of the slide surfaces through various graphical representations. To improve the field mapping of the surfaces (Fig. 4) and to reconstruct their 3D geometry, accurate topographic data provided the position of each slide surfaces in three dimensions.

High-precision topographic data were measured with a total station LEICA TCR 110. The precision of this measuring device is ± 5 mm over a distance of 500 m, and the vertical precision is within a few centimetres. Two operators are needed to take the measurements. The first one deals with the total station and guides the second operator to the location of the surface being measured. The second operator is on the surface with the reflecting target of the apparatus. Both operator control the accurate position of the surface, one on the outcrop and the other at some distance. The operators communicate by radio throughout the process. The coordinates of 280 points belonging to the six sliding surfaces have been measured in this way within the study area. This methodology results in the build of a 3D architecture of the outcrops including their geometry, and permits the analysis of the topographic data.

A 3D geological database is the representation of geologic units and structures seen as actual volumes following a 3D matrix (x, y, z) at a given time (t) (Dhont *et al*., 2005). Such database is constructed from surface information only: the topography and the outcropping boundaries between the geological units.

The topography is numerically represented from a DEM (Digital Elevation Model) generated by interpolation at 1.25 m ground pixel of 10 m interval contours from a digitized

topographic map at the scale 1:25,000. Both the field mapping of the sliding surfaces and the DEM have been geo-referenced in UTM coordinates and combined.

Each slide surface, identified in the field, corresponds to a mapped geologic contour line represented by a collection of points defined by four variables: the spatial coordinates (x, y, z) and the time (t) corresponding to an isochronous line defining the age of the slide. The composite sequence boundaries and the sedimentary bodies have been drawn onto the DEM from our geologic mapping complemented by aerial orthophotos.

A 3D modeller (Earth Vision) was used to generate the surfaces (2-D grid) passing through the points of each slide surface. The 2-D grids were modified until their intersection with the DEM fitted the mapped contour lines. Each time the input dataset was modified, the entire 3D geologic model was recalculated in a trial and error process i.e., by iteration towards an acceptable solution. Present-day submarine slides (e.g. Canals *et al*., 2004; Haflidason *et al*., 2004; Silva *et al*., 2004) have provided 3D reference shapes that have been used to build the 3D geometry of the slump scars inside the model, where they are not observed. The validation of the resulting 3D geologic model is obtained when there is a close to perfect match between the mapping of the slide surface contours and the intersections of the calculated slide surfaces with the DEM.

The volume of each layer is limited by the slide surfaces and the model boundaries (top, bottom and DEM). Each volume is displayed by one homogeneous color that may represent either the part of the sedimentary infilling preserved over the basal slide surface or the deposit of each regional composite sequence as defined by Dreyer *et al*. (1999). One key sedimentary body was distinguished and referred to as the Las Gorgas sandstones.

The 3D model results from the superimposed succession of eleven coloured volumes (Fig. 15). In stratigraphic order, they correspond to: (1) the last deposit of the Comaron Composite Sequence (CCS); (2) the Las Gorgas sandstone body corresponding to the base of the Las Gorgas Composite Sequence (LGCS); (3) the marly distal part of the LGCS; (4) (5) the deposits resting above the two oldest successive slide surfaces that truncate the LGCS (S1 and S2 surfaces); (6) The deposits of Biñas d'Ena sequence above S3 erosional surface; (7) the infilling of the S4 erosional and slide surfaces; (8) the infilling of the S5 slide surface; (9) the undifferentiated deposits of the Barranco El Solano Composite Sequence (BSCS); (10) the infilling of the S6 and S6' slide surfaces; and (11) the last marine levels of the BSCS and the base of the Buil Composite Sequence (BCS).

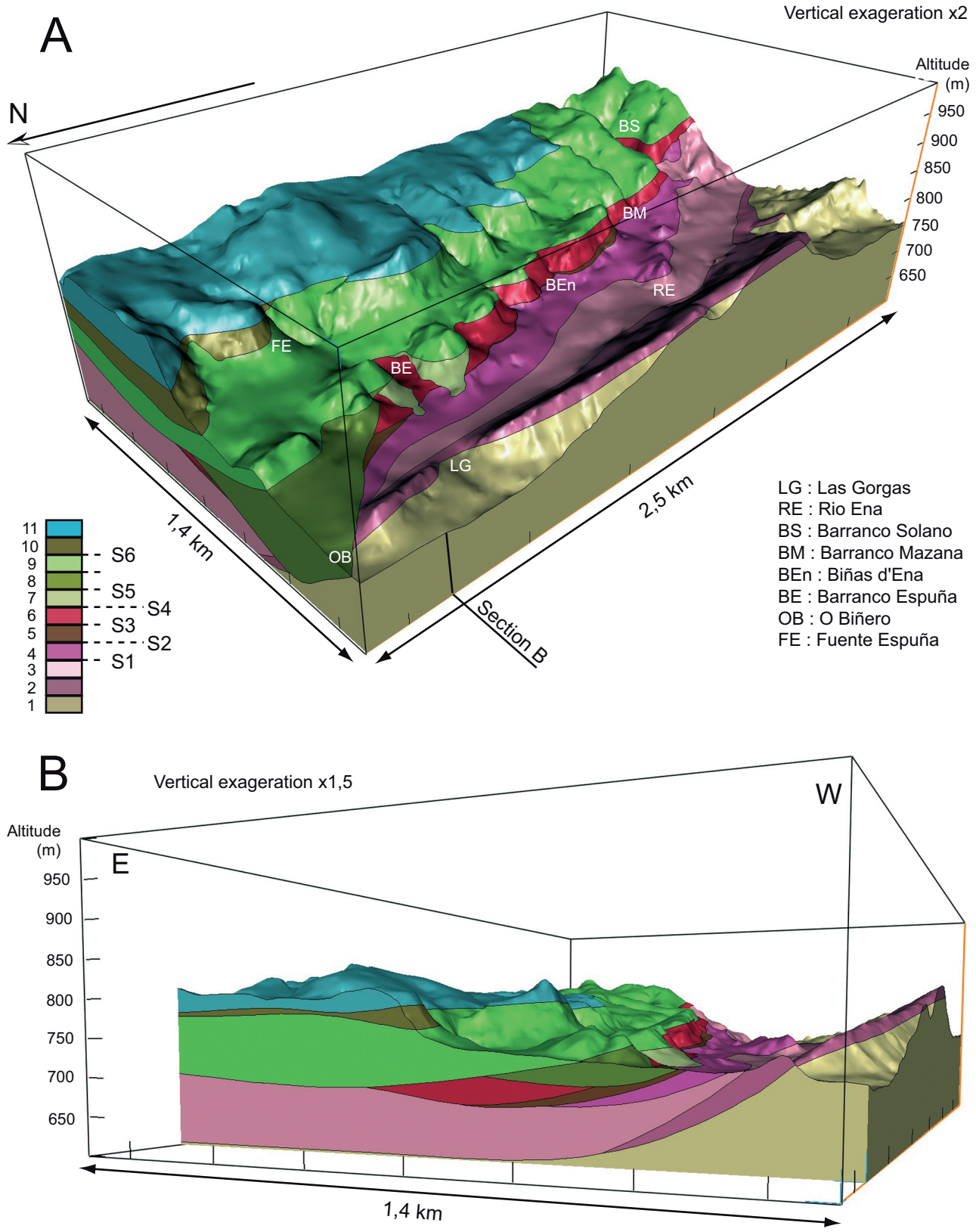

Fig. 15. 3D model constructed with the 3D modeller Earth Vision. A) View of the 3D model with the six slide surfaces and the localization of the places cited in the text. Quaternary deposits have not been included in the model. B) EW vertical section, slides piled up and cut the older infills. In stratigraphic order, numbers correspond to: 1) the last deposit of the Comaron Composite Sequence (CCS); 2) the Las Gorgas sandstone body corresponding to the base of the Las Gorgas Composite Sequence (LGCS); 3) the marly distal part of the LGCS; 4) (5) and (6) the deposits resting above the three first successive slide surfaces that truncate the LGCS (the S1, S2 and S3 surfaces); 7) the first infilling of the S4 slide surface; 8) the first infilling of the S5 slide surface; 9) the deposits of the Barranco El Solano Composite Sequence (BSCS); 10) the infilling of the S6 slide surface; 11) the last marine levels of the BSCS and the base of the Buil Composite Sequence (BCS).

The end-user of the model can examine the 3D model from various aspects (Fig. 15A), can slice it to generate cross-sections (Fig. 15B), or can disassemble it to examine individual slide surface units.

The 3D geometric model provides estimates of the volume of each sedimentary body within the limits of the observed area. From such data, it is then possible to compare the ratio of slide-infilling sediments to bulk in situ deposits. For LGCS the part of the three successive infillings of S1, S2 and S3 represents $32x10^6$ m^3 *i.e.* 12% of the entire deposit volume of the composite sequence. For the BSCS, the corresponding part of S4, S5 and S6 is $15.4x10^6$ m^3 and represents 13% of the volume of the composite sequence. These values for displaced volumes are within the 10-15% of the deposit volume, they are equivalent to the estimation proposed by Dreyer *et al*. (1999). The part of the displaced volumes is of the same amount than those observed in present-day slides (see for example McAdoo *et al*., 2000; Mienert *et al*., 2002; Canals *et al*., 2004; Hühnerbach & Masson, 2004).

INTERPRETATION AND DISCUSSION

The observation of the successive scar surfaces of the Sobrarbe deltaic complex has permit to show the characters of soft sediment deformation along the slide surfaces and has provided information on the sedimentation rate inside a simple slump scar. The progressive development and infill of a composite scar surface has been shown, as well as the successive development of the different slide surfaces of a collapse complex structure. As a result, a conceptual model of the different stages of the slide scar development and infill can be proposed. At last, attention has been carried out to some local data in the way to identify the possible triggering mechanisms responsible for the lutetian Sobrarbe instabilities.

Soft sediment deformation along the slide surface

No mineralization or calcite fibres were observed along the rupture surfaces that cut the substratum beds, indicating that the in-situ layers were not completely lithified at the time of the slide event. Nevertheless, other observations suggest that sediments of the in-situ layers were already sufficiently cohesive to have preserved the marks of bioturbation such as burrows, of erosion structures such as flute casts and of mode I rupture such as vertical cracks.

Both the fine grained sandstones in-situ layers and the nummulites-rich re-sedimented marls of the filling sediments have been mixed together by bioturbation processes across the S6 surface (Fig. 16). At time of failure, the burial depth of the fine grained sandstones of the substratum was about 20 metres. Some flute casts were observed on the S1, S2, S4 and the S6 surfaces where the marlstones have been eroded. The vertical cracks that have been filled with coarse-grained sand were opened in the muddy layers of the substratum of S1 and S2 surfaces. Along S1 surface the burial depth, at time of sliding, had reached about 170 metres. The mode I opening of these extensional cracks requires some cohesion of the sediments in which they form (Price, 1966; Engelder, 1987; Price & Cosgrove, 1990). Because no mineralization has been observed along the rupture surfaces and because the sand has not been completely dissociated, these sandstone layers have been deformed when sediments were soft, moderately cohesive but not completely lithified.

The same grade of consolidation, at time of sliding, is observed in displaced sediments. Some sandstones of the in-situ layers were re-sedimented as rafts embedded in mudstones and translated without tilting. They may be soft-deformed by small-scale normal faults (Fig 8). Sandstone and mudstone layers have been re-sedimented with an increase degree of disorganization from large rafts to grain flow and debris flow layers.

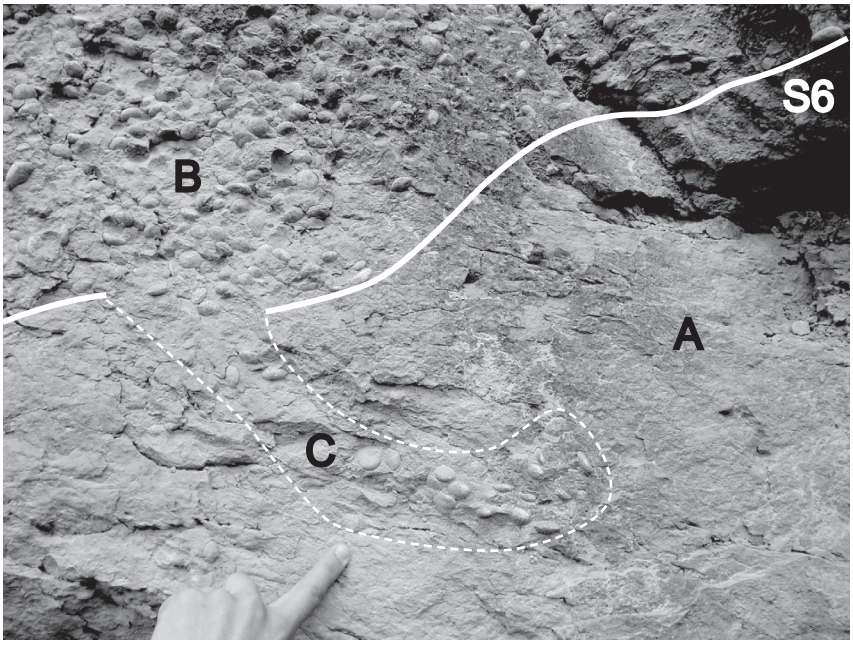

Fig. 16. At Fuente Espuña, the in-situ layers and the infilling sediments have been mixed together by bioturbation processes across the S6 slide surface (outcrop located on Fig. 6). This is a clear indication that the lithification of the in-situ layers was not achieved at the time where sliding occurred. A: Nummulite-free fine grained sandstone (in-situ layers); B: Nummulite-rich re-sedimented marls (infill sediments); C: burrowed sediment across the S6 surface with Nummulites reworked downwards by bioturbation.

Sedimentation rate inside a simple slump scar

Deltaic sedimentation is composed of the succession of many events but when considered over a long period of time it can be seen as an almost continuous process. In the Sobrarbe prodelta, after the mass slide occurred, sedimentation went on and the first layers deposited in the scar successively draped the blocks that rest on the scar surface, these draping layers have onlapped the truncated layers of the scarp and then have draped the scar and its uphill shoulder where no visible unconformity can be observed (Fig. 7). As observed, the thickness of the draping layers increases downslope, in the infilling of the depression (Fig. 7). The available space created by the slide was completely filled while a few metres of continuous sedimentation accumulated on the uphill shoulders of the slides. The depression of Fuente Espuña slump scar (S6 elementary surface) provides an example of marlstone infilling, where about 20 m of sediments correspond to 2 m of in-situ deposits on the uphill shoulder (Fig. 6), not corrected for compaction. The corresponding sedimentation rate is then ~10 times higher in the scar than on the uphill shoulder. Using the rate of 87.5 to 70 cm/1000 years as a mean value for in-situ sediments, and because the scar is filled when two metres of the in-situ sediments are deposited, the required time to completely fill the scar is about 2500 years.

Such high values of sediment accumulation rates in the slump scars can be supposed as being the rule in the Sobrarbe Deltaic complex during late Lutetian period. A fast sediment accumulation rate is one of the factors considered to lead to increase porosity and pore-fluid pressure and to trigger sedimentary instabilities (Mienert *et al*., 2002; Sultan *et al*., 2004).

Progressive development and infill of a composite scar surface

The Barranco Espuña major slide surface (S4) provides a good example of the relationships between a composite slide-surface and the progressive infill of the scar (Fig. 5 and 13). On the left bank of the Barranco Espuña, the S4 surface appears to be composed of three elementary surfaces separated by two slope breaking points (Fig. 5, S4a, S4b and S4c). To the south, the S4b and S4c elementary surfaces cannot be distinguished and the S4 surface appears to be more regular (Fig. 13). The major slide scar infill is composed of alternating sets of apparently in-situ regularly bedded mudstone deposits and displaced sediments such as tilted beds or debris flows. Three elementary slide surfaces are recognized at the base of the displaced sediments. Both the lower and the upper elementary surfaces branch on the S4b and S4c surfaces while the intermediate surface is independent of S4. As a result, the S4 scar

appears to be characterized by three phases of retrogressive sliding (a, b and c) and composed of at least four phases of displaced to in-situ infilling.

The surface S1 (S1a, b and c) show another example of the progressive development of a composite slide surface with the progressive infill of the scar, unfortunately it is largely covered by Quaternary deposits.

Successive development of the different surfaces of a collapse complex structure

The major fossil collapse complex of Barranco El Solano slump (Dreyer et al., 1999) can be subdivided in two collapse complex structures separated by the deposits of the newly described Biñas d'Ena elementary sequence bounded by two regressive surfaces.

The lower collapse complex, Barranco Mazana complex, includes S1 and S2 surfaces. The basal S1 surface is a composite and retrogressive slide surface. The S2 surface cuts the infilling of the S1 scar surface. These oldest scars stack one above the other, the only noticeable shifting is observed in the progressive retrogression of S1a to S1c head scarps.

The Biñas d'Ena elementary sequence starts with the formation of the S3 incision surface due to a relative sea level drop. It is composed of the fining upward sequence already described above S3 surface and the coarsening upward sequence that has followed (Fig. 12). Horizontally, grain size progressively reduces from sandy Barranco O Solano deposits at south to marly Biñas d'Ena deposits at north. This sequence ends with the erosion of the southern segment of S4 surface at Barranco As Peras (Fig. 4). The thickness of the Biñas d'Ena elementary sequence can be estimated at about 75 m.

The upper collapse complex, Barranco Espuña complex, includes S4 and S5 surfaces. The head scarp of the S4 and S5 surfaces shift about 1.5 km to the north of the head scarp of the S1 and S2 surfaces. The S4surface cuts most of the LGCS, down to 130 m deep. The S5 surface cuts more deeply the LGCS and the top of Comaron Composite Sequence, down to 160 m deep.

The northward shift of the upper collapse complex can be related to the relative sea level drops recorded at the boundaries of the Biñas d'Ena elementary sequence. In each collapse complex, the slide surfaces appear to develop retrogressively and to stack successively. Sediment accumulation rates are inferred to be very high in the downward scars. Here, the sediments are poorly compacted and lithified, the porosity is high (Bartetzko & Kopf, 2007). This may be an important contributory factor to explain why minor instabilities preferentially occur in the infilling of composite scars.

At scale of major slides the time of recurrence is defined by the duration of the LGCS and BSCS to the number of slide surfaces. That is about 0.45 Ma to 4 slide surfaces, and this corresponds to one major slide event every 112,500 years. When looking at elementary surface succession, four minor slides have occurred during the formation of both S1 and S4 major slides. That is to say that the recurrence time for minor slides could be about four times shorter than for major slides, i.e. from 25 to 30 thousands years.

Conceptual model for the development of the scars in the Sobrarbe delta

The slide surfaces at the front of the Sobrarbe delta have not been equally preserved. The largest surfaces are composites and have been progressively infilled. They are known from their upslope domains (S4 and S5 surfaces) or from the downslope domains (S1 and S2 surfaces) that are free of re-sedimented deposits resulting from the major slide event. The S6 surface is the only one to exhibit a scar in which the upslope part of such re-sedimented deposits have been preserved at the toe of the scarp. The analysis of the 3D geometry and of the progressive infill has led us to propose a conceptual model for the development of the scars of the Sobrarbe delta (Fig. 17).

Stage 1 is a regressive event that may have developed before the sliding. The occurrence of S6 sliding event at the top of a regressive sequence has been noticed by Dreyer et al. (1999). This stage 1 has been observed along the southern erosive segment of S4 surface where the upper layers of the in-situ deposits have been incised and covered by the As Peras sandstone body before the major slide event occurred. Both incision and sandstone deposits have resulted of a relative sea level drop before the S4 sliding event.

Stage 2 is the major sliding event. The upslope part corresponds to the scarp that is well exposed along S4 surface south of Barranco Espuña (Fig. 13), S5 (Fig. 13) and S6 (fig. 6). The slope of these scarps may reach up to 40° (Fig. 14). Slope gradients progressively reduce and disappear to the downslope parts where they are replaced by a flat bottom that has been deformed by small scale half grabens, normal faults and opened cracks observed along S1 (Fig. 9) and S2 surfaces.

Re-sedimented deposits are observed along the S6 surface, they consist in poorly deformed rafts, the upslope part of which is completely disorganized, showing a wavy roof looking like the half grabens of S1 surface. The rafts rest on the lower part of the scar, at the toe of the 25 m deep scarp while the upper part of the scarp is free of re-sedimented deposits (Fig. 6). Above S5 surface, that cuts up to 150 m, the displaced masses may correspond to the

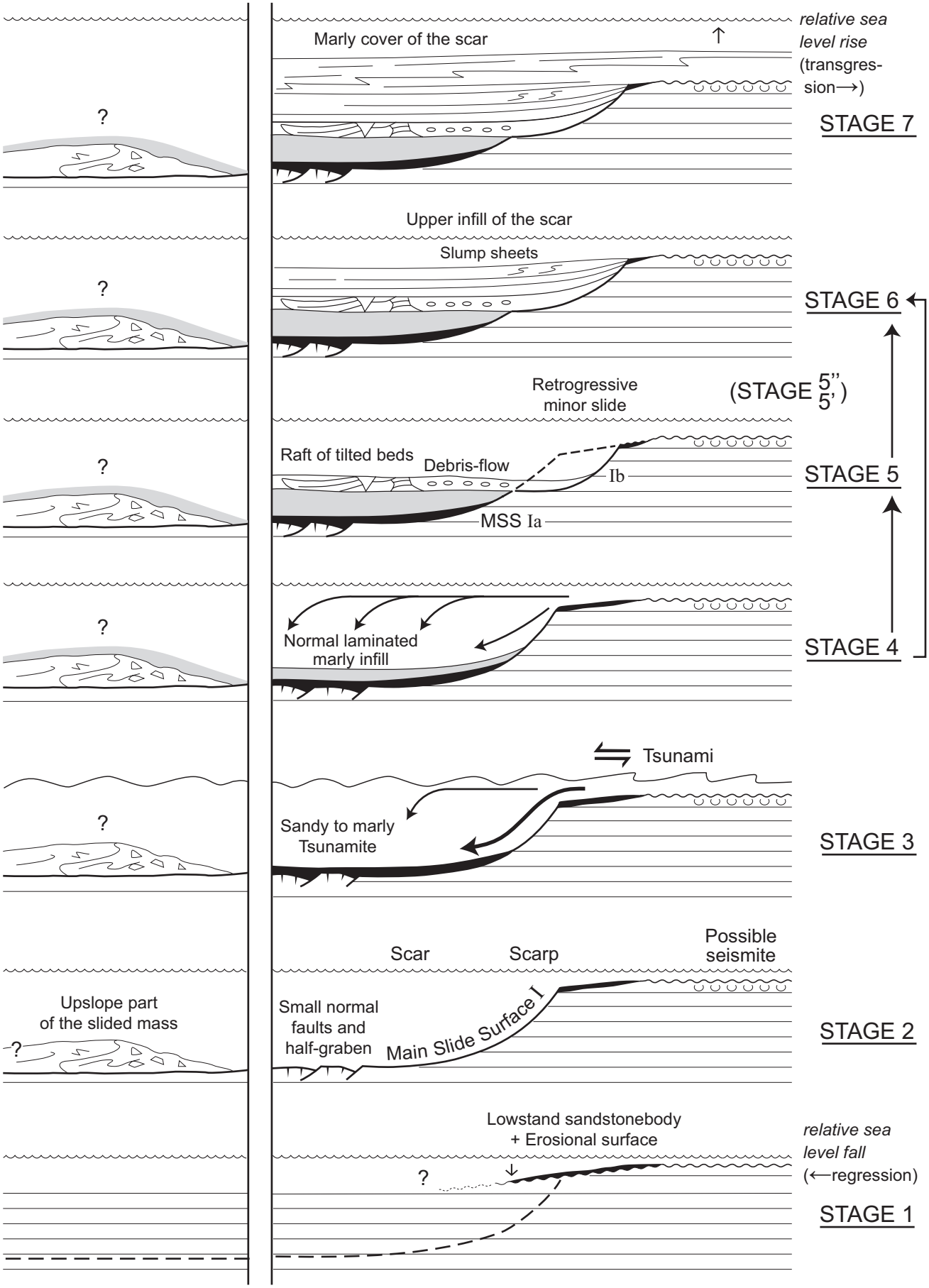
relative sea level rise (transgres-sion→)
Marly cover of the scar
STAGE 7
Upper infill of the scar
Slump sheets
STAGE 6
Retrogressive minor slide
(STAGE 5'' 5')
Raft of tilted beds
Debris-flow
Ib
MSS Ia
STAGE 5
Normal laminated marly infill
STAGE 4
Tsunami
Sandy to marly Tsunamite
STAGE 3
Scar
Scarp
Possible seismite
Upslope part of the slided mass
Small normal faults and half-graben
Main Slide Surface I
STAGE 2
Lowstand sandstonebody + Erosional surface
relative sea level fall (←regression)
STAGE 1
?

Fig. 17 (previous page). Conceptual model of the development of the composite scars of the Sobrarbe delta, not at scale. The seven successive stages are described in the text.

Fig. 18. Large liquefaction pillows observed in silty mudstone layers of the Biñas d'Ena sequence. See location on figure 4. Open and black triangles respectively indicate the lower and the upper erosive limits of the deformed level. These structures are interpreted as a seismite.

re-sedimented deposits that are observed 2000 m far to the north. They consist in 15 m thick mass of disorganized mudstones and sandstones blocks and olistoliths floating in a marly matrix. Displacement of the removed sediments appears to be proportional to the depth of the scar and, of course, to the amount of the displaced volume.

A seismite has been observed in the Biñas d'Ena sequence only. There, between Barranco As Peras and Biñas d'Ena, some 3 or 4 m thick of silty mudstone layers have been hydroplastically deformed (Fig. 18). Below a sharp plane erosive upper surface, they exhibit large mm-size symmetrical pillows probably resulting from an earthquake. Unfortunately the younger slide surface S4 has removed the more distal sediments and the possible relationship with a corresponding slide surface cannot be established any more.

Stage 3 starts immediately after the sliding and can be subdivided in three successive times: (i) the erosive formation of flute marks at the bottom of some half grabens; (ii) the deposition of coarse grained sandstones with clay chips and fine plant fragments in the small half grabens and open cracks; (iii) the deposition of horizontally laminated then structureless fine grained sandstones and mudstones (Fig. 9). This succession records the catastrophic increase of hydrodynamism within the scar followed by its progressive decrease down to the

normal low-energy conditions. This succession probably corresponds to a tsunamite deposit that has followed the sliding.

Stage 4 corresponds to the marly infilling of the scar after the major slide event in the normal conditions of the distal delta front. It is observed above S1 and S6 surfaces (Fig. 6).

Stage 5 is only observed in large scars where retrogressive sliding has occurred. The normal sedimentation is disrupted by either minor inner slides or retrogressive slides. They increase the size of the initial scar as observed on surfaces S1b and S1c (Fig. 13) or S4b and S4c (Fig. 5). Each of the minor slides may be covered by tilted blocks or debris flows such as already described. Minor retrogressive slides have been observed up to three times in S1 and S4 scars.

Stage 6 corresponds to the last infilling time of the scars. In the upslope part of the scar of S4, S5 and S6 surfaces, the scarp surface is overlain by the onlaping strata of the infill until the unconformity has reduced and the last deposits are parallel to the in-situ layers. Nevertheless, the last deposits may be displaced by thin slumps sheets, as observed in S4 and S5 upper part of the infill.

Stage 7 marks the evolution end time with the burial of the scar infill under the high sea level marly cover. This is well illustrated by the marls of the BSCS that overlain S4 and S5 infill.

Triggering mechanisms for Sobrarbe instabilities

High values of sedimentation rates are known to favour instabilities formation at delta front (Nemec et al., 1988). In such conditions, collapses result from both overloading due to sediment accumulation and high pore fluid pressure due to under-compaction of fine grained sediments (Postma, 1983; Gardner et al., 1999; Bartezko and Kopf, 2007). The sedimentation rate in the Sobrarbe delta ranges from 70 to 87.5 cm/1000 years, a high value that makes easier the formation of slides. In the infill of the scars, where the sedimentation rate can be increased ten times, the formation of superimposed slides is all the more easy. In no case the instantaneous overload produced by events such as flood (Klein et al., 1972) or storm waves (Nemec et al., 1988) has been observed in the Sobrarbe.

Relative sea level fall has been proposed as a favourable condition for triggering instabilities (Mutti, 1985; Spence & Tucker, 1997; Dreyer et al., 1999). A pronounced fall in relative sea level has been associated with the slope instability of the S6 and S6' surfaces that is observed at the top of BSCS (Dreyer et al., 1999). Our data show that an older relative sea level drop has preceded the collapse of the Barranco Espuña complex along S4 and S5 slide

surfaces at the top of the Biñas d'Ena sequence. The marly deposits between these two collapse complexes seem to be coeval with the eustatic high sea level of the so-called "Biarritzian" transgression (Dreyer et al., 1999). At the opposite, the older relative sea level fall associated with S1 and S2 surfaces has been related with the tectonic uplift and tilting of the basin floor due to a growing phase of Arcusa anticline (Dreyer et al., 1999). Both the seismite observed in the Biñas d'Ena sequence and the and low angular unconformity that appears between the upper marly level and the lower nummulite banks of BSCS south of Fuente Espuña, along an erosive surface, are other local proofs of the regional syn-sedimentary tectonic activity. The largest part of the relative sea level change could be related to the tectonic uplift, more than to eustatic variations, according to the tectonic control on sedimentation of Ainsa Basin between the main south Pyrenean thrusts (Dreyer et al., 1999; Pickering and Corregidor, 2005).

Apart from Biñas d'Ena, neither classical seismites structures nor sediment liquefaction have been observed in the studied prodelta area. The tectonic activity appears to be responsible for the relative sea level changes but no direct relationship can be established between slides and a possible seismic activity.

CONCLUSIONS

The description of two complex collapse structures in the western part of the Sobrarbe delta reveals five main successive fossil submarine slides. The main result of this work is the identification and characterisation of sedimentary structures associated with these sediment slides.

In the upslope domain, the identification of the head of the scar surfaces is based on the angular unconformity that is visible between the in-situ layers and the first layers of the infilling sediments. Most of the slide scarps trend about N55° with dip values from 20° to 40° toward the NW direction. The deduced sliding movement was toward the NW direction.

In the downslope domain, where the unconformity disappears, slide surfaces are identified by occasionally displaced deposits resting on the sole of the scar, and more generally soft-sediment deformation structures. They are small normal faults that offset the scar surface and the in-situ layers, and that are associated with small extensive cracks along the outer arc in small scale roll-over structures. It is here proposed that such small-scale

associated structures can be used to recognize and trace the sliding surfaces where large displaced deposits are missing. They can also be helpful to assess the sliding and its direction.

The restoration and mapping of the slides has led to a 3D model that provides an important data set showing the topography and the spatial organisation of the six main surfaces. The S1, S2 and S3 surfaces mainly developed in the Las Gorgas Composite Sequence, where they cut and are filled by LGCS sediments. The S4 and S5 surfaces developed in LGCS sediments but they are filled by sediments of the Barranco El Solano Composite Sequence. They show the downward shifting of the unstable area from one sequence to the next, from the LGCS to the BSCS. The S6 surface developed in the Barranco El Solano Composite Sequence.

The S1 and S2 surfaces developed successively to the NW, and the S3 erosional surface developed most probably to the north. Each slide scar developed in a distal part of the Sobrarbe deltaic complex and cut a part of the infilling of the previous slide deposit. The 3D geometric model also provides estimates of the ratio of the slide infilling sediments to the bulk in-situ deposits to be in the order of 12 to 13%. These values are similar to those observed in previous works on the Sobrarbe Delta (Dreyer et al., 1999) and in present-day slides (McAdoo *et al*., 2000; Mienert *et al*., 2002; Canals *et al*., 2004; Hühnerbach & Masson, 2004).

Soft sediment deformation has been recorded along the slide surfaces where the complete lack of mineralization or calcite fibres and the occurrence of bioturbations and flute casts indicate that the sediments were moderately cohesive but not completely lithified at the time of the slide.

The sedimentation rate inside a simple slump scar can be comprised between 7 and 8.75 m/1000 years that is about 10 times higher than the mean rate in the overall area of the Sobrarbe deltaic complex, and some 2500 years are required to fill a 25 m deep scar.

A composite scar surface develops progressively by at least three retrogressive minor slumps surfaces. The infill is composed of alternating displaced sediments and apparently in-situ deposits.

The successive development of the different surfaces of a collapse complex structure is illustrated by the major collapse complex of Barranco El Solano slump (Dreyer et al., 1999). It is subdivided in two collapse complex structures separated by the deposits of the newly described Biñas d'Ena elementary sequence bounded by two regressive surfaces. The northward shift of the upper collapse complex, 1.5 km far from the lower collapse complex, can be related to the relative sea level drops recorded at the boundaries of the Biñas d'Ena

elementary sequence. In each collapse complex, the slide surfaces appear to develop retrogressively and to stack successively. Here, the sediments are poorly compacted with high porosity, that may explain why minor instabilities preferentially occur in the infilling of composite scars.

A conceptual model permits to describe the development of the scars of the Sobrarbe delta from seven stages starting with a regressive event and followed by: i) the major slide event possibly associated with a seismite; ii) deposition of a tsunamite; iii) normal marly infilling; iv) formation of one or more retrogressive minor slides; v) filling-up of the scar; vi) burial of the scar under the high sea level marly cover.

The mechanisms responsible for triggering the Sobrarbe instabilities mainly correspond to three favourable related conditions that are : high values of sedimentation rate; relative sea level falls mainly controlled by tectonic uplift; possible seismic activity.

ACKNOWLEDGEMENTS

This work benefited of the support of the “instabilities” workgroup of the French CNRS-INSU GDR Marges project (2003-2006). We thank all the members of the Instabilities field workshop held in Ainsa (june 30th and july 1rst, 2004) for constructive discussions. We thank Pascal Luxey for help in using Earth Vision 3D modeller and Christiane Cavaré-Hester for the line drawing of the figures. The revised version of the manuscript has benefited of the careful and constructive comments of P. Arbues, M. Moretti, K. T. Pickering and C. Puigdefabregas.

REFERENCES

Allen, J.R.L. (1982) *Sedimentary structures: Their character and physical basis, vol. II*. Elsevier, Amsterdam, 663 pp.

Bartetzko, A. and **Kopf, A.J.** (2007) The relationship of undrained shear strength and porosity with depth in shallow (<50 m) marine sediments. *Sed. Geol.*, **196**, 235-249.

Callot, P., Sempere, T., Odonne, F. and **Robert, E.** (2008) Giant submarine collapse of a carbonate platform at the Turonian-Coniacian transition: The Ayabacas Formation, southern Peru. *Basin Res.*, in press.

Canals, M., Lastras, G., Urgeles, R., Casamor, J.L., Mienert, J., Cattaneo, A., De Batist, M., Haflidason, H., Imbo, Y., Laberg, J.S., Locat, J., Long, D., Longva, O., Masson, D.G., Sultan, N., Trincardi, F. and **Bryn, P.** (2004) Slope failure dynamics and impacts from seafloor and shallow sub-seafloor geophysical data: case studies from the COSTA project. *Mar. Geol.*, **213**, 9-72.

Chapron, E., Beck, C., Pourchet, M. and **Deconinck, J.F.** (1999) 1822 earthquake-triggered homogenite in Lake Le Bourget (NW Alps). *Terra Nova*, **11**, 86-92.

De Blasio, F.V., Elverhøi, A., Issler, D., Harbitz, C.B., Bryn, P. and **Lien, R.** (2004) Flow models of natural debris flows originating from overconsolidated clay materials. *Mar. Geol.*, **213**, 439-455.

De Federico, A. (1981) *La sedimentación de talud en el sector occidental de la cuenca Paleógena de Ainsa*. Ph. D. thesis, Universidad Autónoma de Barcelona, Spain, 272 pp.

Dhont, D., Luxey, P. and **Chorowicz, J.** (2005) 3-D modelling of geologic maps from surface data. *AAPG Bull.*, **89**, 1465-1474.

Dreyer, T., Corregidor, J., Arbues, P. and **Puigdefàbregas, C.** (1999) Architecture of the tectonically influenced Sobrarbe deltaic complex in the Ainsa Basin, northern Spain. *Sed. Geol.*, **127**, 127-169.

Engelder, T. (1987) Joints and shear fractures in rock. In: *Fracture Mechanics of Rock*, (Ed. B.K. Atkinson), pp. 27-69, Academic Press Geology Series.

Field, M.E., Gardner, V., Jennings, A.E. and **Edwards, B.D.** (1982) Earthquake-induced sediment failure on a 0.25° slope, Klamath River delta, California. *Geology*, **10**, 542-546.

Frey Martínez, J., Cartwright, J. and **Hall, B.** (2005) 3D seismic interpretation of slump complexes: examples from the continental margin of Israel. *Basin Res.*, **17**, 83-108.

Frey Martínez, J., Cartwright, J. and **James D.** (2006) Frontally confined versus frontally emergent submarines landslides: a 3D seismic Characterisation. *Mar. Petrol. Geol.*, **23**, 585-604.

Gardner, J.V., Prior, D.B. and **Field, M.E.** (1999) Humboldt Slide - a large shear-dominated retrogressive slope failure. *Mar. Geol.*, **154**, 323-338.

Gonzàlez, J., Schmitz, M., Audemaerd, F., Contreras, R., Mocquet, A., Delgado, J. and **De Santis, F.** (2004) Site effects of the 1997 Cariaco, Venezuela earthquake. *Engineering Geology*, **72**, 143-177.

Gradstein, F.M., Ogg, J.G. and **Smith, A.G.** (2004) *A Geologic Time Scale 2004*. Cambridge University Press, 589 p.

Green, H., Gardner-Tagget, J., Ledbetter, M., Barminski, R., Chase, T., Hicks, K. and **Baxter, C.** (1991) Offshore and onshore liquefaction at Moss Landing spit, central California - Results of the October 17, 1989 Loma Prieta earthquake. *Geology*, **19**, 945-949.

Haflidason, H., Sejrup, H.P., Nygård, A., Mienert, J., Bryn, P., Lien, R., Forsberg, C.F., Berg, K. and **Masson, D.** (2004) The Storegga Slide: architecture, geometry and slide development. *Mar. Geol.*, **213**, 201-234.

Hühnerbach, V. and **Masson, D.G.** (2004) Landslides in the North Atlantic and its adjacent seas: an analysis of their morphology, setting and behaviour. *Mar. Geol.*, **213**, 343-362.

Huvenne, V.A.I., Croker, P.F. and **Henriet, J.P.** (2002) A refreshing 3D view of an ancient collapse and slope failure. *Terra Nova*, **14**, 33-40.

Klein, G.V., Melo, U. and **Della Favera, J.C.** (1972) Subaqueous gravity processes on the front of cretaceous deltas, Recôncavo basin, Brazil. *GSA Bull.*, **83**, 1469-1492.

Lastras, G., Canals, M., Hughes-Clarke, J.E., Moreno, A., De Batist, M., Masson, D.G. and **Cochonat, P.** (2002) Seafloor imagery from the BIG'95 debris flow, western Mediterranean. *Geology*, **30**, 871-874.

Locat, J. and **Lee, H.J.** (2002) Submarine landslides: advances and challenges. *Can. Geotech. J.*, **39**, 193-212.

Loncke, L., Gaullier, V., Bellaiche, G. and **Mascle, J.** (2002) Recent depositional patterns of

the Nile deep-sea fan from echo-character mapping. *AAPG Bull.*, **86**, 7, 1165-1186.

Lucente, C.C. and **Pini, G.A.** (2003) Anatomy and emplacement mechanism of a large submarine slide within a Miocene foredeep in the northern Apennines, Italy: a field perspective. *Am. J. Sci.*, **303**, 565-602.

Mandl, G. and **Crans, W.** (1981) Gravitational gliding in deltas. In: *Thrust and Nappe Tectonics* (Eds K.R. Mc Clay and N.J. Price), *Geol. Soc. London Spec. Publ.*, **9**, 41-54.

McAdoo, B.G., Pratson, L.F. and **Orange, D.L.** (2000) Submarine landslide geomorphology, US continental slope. *Mar. Geol.*, **169**, 103-136.

Martinsen O.J. (1989) Styles of soft-sediment deformation on a Namurian (Carboniferous) delta slope, Western Irish Namurian Basin, Ireland. In : Deltas : Sites and Traps for Fossil Fuels (Eds M.K.G. Whateley & K.T. Pickering), *Geol. Soc. London Spec. Publ.*, **41**, 167-177.

Mello, U.T. and **Pratson, L.F.** (1999) Regional slope stability and slope-failure mechanics from the two-dimensional state of stress in an infinite slope. *Mar. Geol.*, **154**, 339-356.

Mienert, J., Berndt, C., Laberg, J.S. and **Vorren, T.O.** (2002) Slope Instability of Continental Margins. In: *Ocean Margin Systems* (Eds G. Wefer, D. Billet, D. Hebbeln, B.B. Jørgensen, M. Schlüter and T. van Veering), *Springer Verlag*, 179-193.

Moscardelli, L. and **Wood, L.** (2008) New classification system for mass transport complexes in offshore Trinidad. *Basin Res.*, **20**, 73-98.

Mourgues, R. and **Cobbold, P.R.** (2003) Some tectonic consequences of fluid overpressures and seepage forces as demonstrated by sandbox modelling. *Tectonophysics*, **376**, 75-97.

Mulder, T. and **Alexander, J.** (2001) The physical character of subaqueous sedimentary density flows and their deposits. *Sedimentology*, **48**, 269-299.

Mulder, T. and **Cochonat, P.** (1996) Classification of offshore mass movements. *J. Sed. Res.*, **66**, 43-57.

Muñoz, J.A., McClay, K. and **Poblet, J.** (1994) Synchronous extension and contraction in frontal thrust sheet of the Spanish Pyrenees. *Geology*, **22**, 921-924.

Mutti, E. (1985) Turbidite systems and their relations to depositional sequences. In: *Provenance of Arenites* (Ed. G.G. Zuffa), pp. 65-93. NATO Advanced Scientific Institute. D. Reichel, Dordrecht, Holland.

Nemec, W., Steel, R.J., Gjelberg, J., Collinson, J.D., Prestholm, E. and **Oxnevad, I.E.** (1988) Anatomy of collapsed and re-established delta front in Lower Cretaceous of eastern Spitsbergen: gravitational sliding and sedimentation processes. *AAPG Bull.,* **72**, 454-476.

Nichols, R.J. (1995) The liquification and remobilization of sandy sediments. In: *Characterization of Deep Marine Clastic Systems* (Eds A.J. Hartley and D.J. Prosser), *Geol. Soc. London Spec. Publ.*, **94**, 63-76.

Papatheodorou, G. and **Ferentinos, G.** (1997) Submarine and coastal failure triggered by the 1995, Ms = 6.1 R Region earthquake, Gulf of Corinth, Greece. *Oceanographic Literature Review*, 44/8, 281.) *Marine Geology*, **137**, 287-304.

Pickering, K.T. (1983) Small scale syn-sedimentary faults in the UpperJurassic "Boulder Beds". *Scottish Journal of Geology*, **19**, 169-181.

Pickering, K.T. and **Corregidor, J.** (2005) Mass-transport complexes (MTCs) and tectonic control on basin-floor submarine fans, Middle Eocene, south Spanish Pyrenees. *J. Sed. Res*., **75**, 761-783.

Piper, D.J.W., Cochonnat, P. and **Morrison, M.L.** (1999) The sequence of events around the epicentre of the 1929 Grand Banks earthquake: initiation of debris flows and turbidity current inferred from sidescan sonar. *Sedimentology*, **46**, 79-97.

Porebski, S.J. and **Steel, R.J.** (2003) Shelf-margin deltas: their stratigraphic significance and relation to deep-water sands. *Earth-Science Reviews*, **62**, 283-326.

Postma, G. (1983) Water escape structures in the context of a depositional model of a mass flow dominated conglomeratic fan-delta (Abrioja Formation, Pliocene, Almeria Basin, Spain). *Sedimentology*, **30**, 91-103.

Price, N.J. (1966) *Fault and joint development in brittle and semi-brittle rock*. Pergamon Press, New-York, 568 pp.

Price, N.J. and **Cosgrove, J.W.** (1990) *Analysis of geological structures*. Cambridge University Press, 502 pp.

Puigdefàbregas, C., Muñoz, J.A. and **Verges, J.** (1991) Trusting and foreland basin evolution in the southern Pyrenees. In: *Thrust Tectonics* (Ed. K. McClay), pp. 247-254. Chapman and Hall.

Reading, H.G. (1996) *Sedimentary Environments : Processes, Facies and Stratigraphy, 3rd edn*. Blackwell Science, 688 pp.

Remacha, E., Oms, O. and **Gual, G.** (2003) Sand-rich turbidite systems of the Hecho Group from slope to basin plain. Facies, stacking patterns, controlling factors and diagnostic features. Geological field Trip 12, South-Central Pyrenees.

AAPG International Conference and Exhibition, Barcelona, Spain, September 21-24.

Serra-Kiel, J., Hottinger, L., Caus, E., Drobne, K., Ferrandez, C., Jauhri, A.K., Less, G., Pavlovec, R. Pignatti, J., Samso, J.M., Sirel, E., Strougo, A., Tambareau, Y., Tosquella, J. and **Zakrevskaya, E.** (1998) Larger foraminiferal biostratigraphy of the Tethyan Palaeocene and Eocene. *Bull. Soc. géol. France*, **169**, 2, 281-299.

Silva, A.J., Baxter, C.D.P., LaRosa, P.T. and **Bryant, W.R.** (2004) Investigation of mass wasting on the continental slope and rise. *Mar. Geol.*, **203**, 355-366.

Spence, G.H. and **Tucker, M.E.** (1997) Genesis of limestone megabreccias and their significance in carbonate sequence stratigraphic models: a review. *Sed. Geol.*, **112**, 163-193.

Spörli, K.B. and **Rowland, J.V.** (2007) Superposed deformation in turbidites and syn-sedimentary slides of the tectonically active Miocene Waitemata Basin, northern New Zealand. *Basin Res.*, **19**, 199-216.

Sultan, N., Cochonat, P., Canals, M., Cattaneo, A., Dennielou, B., Haflidason, H., Laberg, J.S., Long, D., Mienert, J., Trincardi, F., Urgeles, R., Vorren, T.O. and **Wilson, C.** (2004) Triggering mechanisms of slope instability processes and sediment failures on continental margins: a geotechnical approach. *Mar. Geol.*, **213**, 291-321.

Terzaghi, K. (1943) *Theoretical Soil Mechanics*. Wiley, New York, 510 pp.

Trincardi, F., Cattaneo, A., Correggiari, A. and **Ridente, D.** (2004) Evidence of soft sediment deformation, fluid escape, sediment failure and regional weak layers within the late Quaternary mud deposits of the Adriatic Sea. *Mar. Geol.*, **213**, 91-119.

Vendeville, B.C. and **Gaullier, V.** (2003) Role of pore-fluid pressure and slope angle in triggering submarine mass movements: natural examples and pilot experimental models. In: *Submarine mass movements and their consequences* (Eds J. Locart and J. Mienert), pp. 137-144. Kluwer Academic Publishers, Dordrecht.

Vernhet, E., Heubeck, C., Zhu, M.-Y. and **Zhang J.-M.** (2006) Large-scale slope instability at the southern margin of the Ediacaran Yangtze platform (Hunan province, central China). *Precambrian Res.*, **148**, 32-44.

Wadsworth, J.A. (1994) *Sedimentology and sequence stratigraphy in an oversteepened ramp setting: Sobrarbe formation, Ainsa Basin, Spanish Pyrenees*. Ph. D. thesis, University of Liverpool, 195 pp.

Wilson, C.K., Long, D. and **Bulat, J.** (2004) The morphology, setting and processes of the Afen Slide. *Mar. Geol.*, **213**, 149-167.

I.4. Méthodologie

Dès le départ, il est apparu que cette étude allait nécessiter un important travail de terrain. Il était également clair qu'il ne serait pas possible d'aller partout et de tout voir en détail : les affleurements connus ou supposés de la Formation Ayabacas étant répartis sur plus de 80 000 km^2 (Fig. I.2), dans des régions souvent difficiles d'accès (altitude, qualité des routes inégale). De plus environ quatre jours aller-retour étaient nécessaires pour arriver sur la zone d'étude depuis la capitale Lima. Il fallait donc adopter une méthodologie qui permette d'utiliser au mieux les ressources et le temps disponibles.

I.4.1. Travail bibliographique et analyse des photographies aériennes

Les premiers mois ont consisté à effectuer un travail bibliographique et une analyse des cartes géologiques et surtout des photographies aériennes (à l'échelle 1 / 65 000 environ) de l'ensemble des zones d'affleurement de la formation Ayabacas et d'une partie des zones d'affleurement de la Formation Arcurquina. Ce travail a été effectué en grande partie à l'INGEMMET, à Lima. Les photos aériennes permettent notamment d'apprécier les grandes structures difficilement discernables sur le terrain (Fig. I.16). Ainsi, environ 200 paires de photos aériennes ont été examinées, dont une quarantaine en détail (comme par exemple les figures 8, 10 et 13 de l'article dans *Basin Research*, partie II.2). Pour chaque paire de photos, la surface réellement utile correspond à la zone de chevauchement des deux photos, qui apparaît en relief avec un stéréoscope. C'est un rectangle de 13 x 22,5 cm de côté, ce qui représente en réalité 8,45 x 14,5 km soit ~ 122,5 km^2. L'utilisation des 200 couples stéréoscopiques a donc permis d'examiner relativement rapidement plus de ~ 24 500 km^2 de terrain, et de sélectionner les zones particulièrement déformées où il semblait indispensable d'effectuer une étude sur le terrain. Ce sont généralement ces zones particulièrement déformées qui constituent la quarantaine de couples stéréographiques qui ont été analysées plus en détail. Elles représentent une surface réelle d'environ 5 000 km^2. Bien entendu, l'analyse des seules photographies aériennes a des limites, car elle révèle seulement les structures de taille supérieure à la dizaine de mètres. Ainsi, certains affleurements intéressants pour d'autres raisons que les déformations d'échelle décamétrique (par exemple les affleurements riches en matériaux fluidisés et bréchifiés, comme ceux de Yanaoco, de Cabanillas ou de Cusco-Urubamba ; Fig. I.2) étaient totalement indétectables en photographies aériennes et ont été repérés lors des missions de terrain.

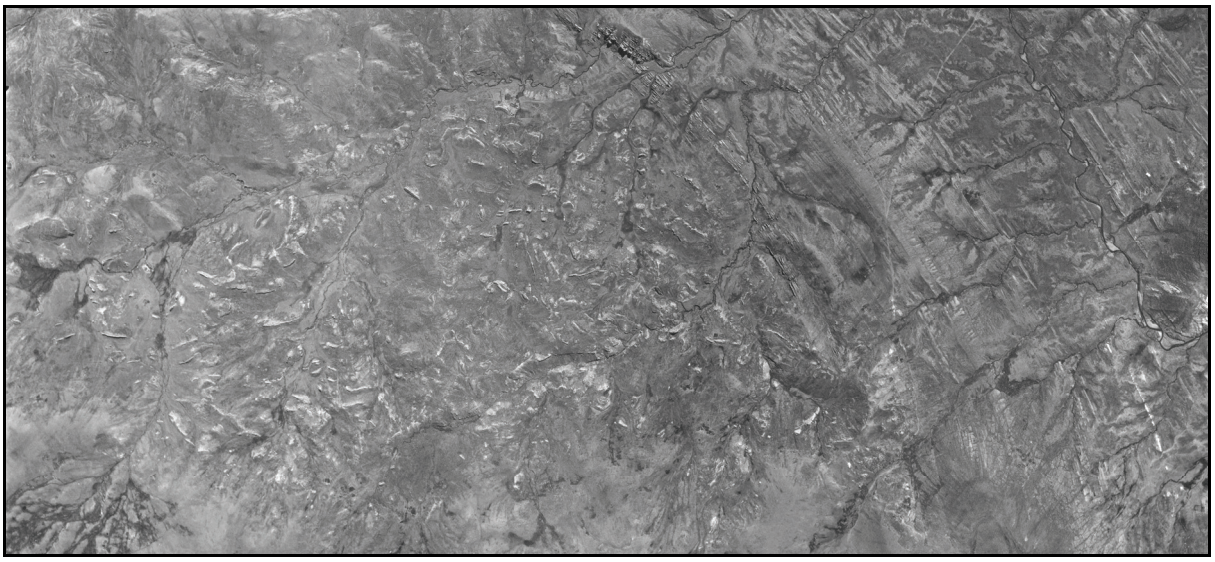

Fig. I.16 : Exemple de photo aérienne avec à gauche la Formation Ayabacas plissée et chaotique et à droite les bancs régulièrement stratifiés du Groupe Puno (Paléocène Supérieur-Eocène Inférieur, voir colonne stratigraphique, Fig. II.1). La surface photographiée ci-dessus est environ de 12,35 x 5,6 km.

Ce travail a permis de cibler des zones qui semblaient particulièrement intéressantes, soit à la lecture des problèmes soulevés et des descriptions faites par les précédents auteurs (*e.g.* Newell, 1949 ; Kalafatovich, 1957; Portugal, 1964, 1974; Audebaud 1967 ; Chanove et al., 1969; Audebaud, 1971a,b; Audebaud et al., 1973; De Jong, 1974; Laubacher, 1978; Klinck et al., 1986; Ellison et al., 1989; Moore, 1993; Jaillard, 1994; Carlotto et al., 1992, 1996; Sempere et al., 2000; Carlotto, 2002), soit au vu des déformations perceptibles en photographies aériennes. L'analyse des photographies aériennes a été, avec le travail de terrain, un outil majeur qui a conduit au découpage de la Formation Ayabacas en six zones de déformations du NE vers le SO (voir chapitre II). Le travail bibliographique a également aidé à préciser les âges du dépôt des carbonates et du collapse de la plateforme (Callot et al., 2007).

I.4.2. Travail de terrain

Sept missions de terrain de deux à trois semaines ont été effectuées en mai, juin, août et septembre 2005, puis en juillet, août et septembre 2006. L'objectif des missions de 2005 était d'avoir une vue d'ensemble des affleurements, point essentiel pour comprendre la Formation Ayabacas en tant que dépôt de transports en masse sous-marins et son organisation. Les missions de 2006 ont porté sur la partie nord de la zone d'étude, qui n'avait pratiquement pas été vue en 2005, et ont permis de se concentrer sur des thématiques particulières : les zones de brèches et de matériaux fluidisés (Cabanillas, Yanaoco, Cusco-Urubamba, Livitaca, Espinar, barrage de Condoroma, Fig. I.2), les zones de déformation à grande échelle (Yura, barrage de

Condoroma près de Tisco, Abancay-Chalhuanca) et les zones de radeaux calcaires très plissés (Juli-Ilave, Sangarara).

Des mesures des axes de plis, des directions et pendages des filons, de l'orientation des blocs et des unités antérieures et postérieures, ont été effectuées dans l'ensemble des affleurements visités. Trois campagnes de mesures systématiques ont été réalisées : la première pour mesurer le pendage de radeaux de matériaux d'âge paléozoïque éparpillés dans le mélange Ayabacas, sur une zone de 3 km^2 située à 15 km au sud de Chucuito ; la seconde pour mesurer l'orientation de radeaux (principalement calcaires et plus rarement de matériaux dérivant de la Formation Huancané, une unité plus ancienne d'âge Jurassique Supérieur) dispersés dans le mélange dans la zone de Pusi ; la dernière campagne systématique de mesures a consisté à relever les axes de plis, et, lorsque c'était possible, les plans axiaux de tous les plis présents dans une vaste zone d'affleurements au sud d'Ilave et de Juli, où les radeaux calcaires plissés sont courants. Les résultats de ces campagnes sont présentés dans la Fig. 5 de l'article dans Basin Research, partie II.2.

Plusieurs coupes ont été levées et sont présentées dans le chapitre II :

- dans la Formation Arcurquina (non déstabilisée) près de Huancané (Fig. I.2) ;
- dans l'épaisse succession calcaire plissée près de Yura (Fig. I.2) ;
- dans des radeaux ou nappes calcaires de la Formation Ayabacas, dans les affleurements suivants (Fig. I.2.) : "Cusco", "Nuñoa", "Nuñoa-Antacalla", "San Anton-Larimayo" (2 coupes), "San Anton-Pacuta" et "Yanaoco" pour la zone amont du collapse ; dans les alentours de "Pusi", "Chucuito" et "Juli" un peu plus en aval.

Ces coupes ont notamment permis de définir une "coupe type" des radeaux/nappes rencontrés dans la Zone 1, qui correspond également à la stratigraphie anté-collapse, et qui a pu être corrélée avec la coupe de la Formation Arcurquina près de Huancané, ainsi qu'avec la coupe de Graf (2002) dans la Formation Miraflores, l'équivalent de la Formation Arcurquina en Bolivie (voir chapitre II).

I.4.3. Analyse de lames minces

Lors des missions de terrain, 159 échantillons ont été prélevés dans la matrice, dans les radeaux et plus rarement dans les formations sous-jacentes. Ils ont permis la réalisation de 102 lames minces dont l'analyse est présentée dans le chapitre III. Ces lames minces et les observations de terrains ont permis de mieux comprendre les mécanismes de genèse de la matrice marno-siliceuse proprement dite, des différents clastes (carbonatés et silico-clastiques) et des grands radeaux calcaires (voir chapitre III).

II.

LA FORMATION AYABACAS : CONTEXTE GEOLOGIQUE REGIONAL, AGE, MORPHOLOGIE, ORGANISATION, FACTEURS DECLENCHANTS DU COLLAPSE

II. La Formation Ayabacas : contexte géologique régional, âge, morphologie, organisation, facteurs déclenchants du collapse.

Ce chapitre, qui présente la Formation Ayabacas en détail, a fait en grande partie l'objet d'une publication en anglais dans la revue *Basin Research*. Il a été divisé en deux parties.

Dans une première partie, après une présentation rapide de la zone d'étude et de l'architecture du bassin (développés dans l'article), la stratigraphie ante-néogène du sud du Pérou est détaillée et les âges du dépôt de la plateforme carbonatée (Formation Arcurquina) et de son collapse sont déterminés. Ce travail a été publié en tant que document supplémentaire en ligne de l'article principal (site internet de l'éditeur). Un résumé en français ainsi que les dessins des huit coupes stratigraphiques ayant servi de support pour tester le modèle chrono-stratigraphique obtenu sont également proposés.

La seconde partie est constituée par l'article proprement dit et expose en détail la morphologie et l'organisation de la Formation Ayabacas, ainsi que les facteurs déclenchants du collapse dont elle résulte. Un résumé étendu en français est inséré ci-dessous.

II.1. Cadre géologique de la Formation Ayabacas

II.1.1. Localisation de la zone d'étude et architecture du bassin

La localisation de la zone d'étude et l'architecture du bassin sont présentées dans la première partie de l'article publié dans *Basin Research*. En voici un résumé en français :

La zone d'étude se situe dans le sud du Pérou, principalement sur l'Altiplano, ainsi que sur la bordure sud-ouest de la Cordillère Orientale et pour quelques affleurements dans la Cordillère Occidentale (Arequipa, Chalhuanca-Abancay, Tisco ; Fig I.2 et Fig. 1 de l'article dans *Basin Research*). La Formation Ayabacas et les unités antérieures se sont déposées dans un bassin d'arrière-arc (*western Peru back-arc basin*, WPBAB), actif au Jurassique et au Crétacé (Jaillard et al., 1995). Ce bassin s'est développé dans un contexte tectonique en extension et s'approfondissait à l'ouest, où la subsidence était nettement plus importante qu'à l'est (Myers, 1974 ; Jaillard, 1994). Les faciès et les épaisseurs des dépôts du WPBAB ont notamment été contrôlés par deux importants systèmes structuraux (Sempere, 1995; Sempere et al., 2002a,b, 2004b,c; Pino et al., 2004) : au nord-est (Fig. 1 de l'article dans *Basin Research*) le système de faille Urcos-Ayaviri-Copacabana-Coniri (abrévié par l'acronyme

SFUACC en espagnol), une limite majeure affectant toute la lithosphère (Carlier et al., 2005) ; plus au sud-ouest (Fig. 1 de l'article dans *Basin Research*), le corridor structural Cusco-Lagunillas-Laraqueri-Abaroa (abrévié par l'acronyme CECLLA en espagnol), un large système structural séparant deux domaines qui se sont comportés très différemment au moins du Jurassique au Cénozoïque, notamment avec une subsidence forte et des environnements de dépôts plus profonds au sud-ouest (Sempere *et al*., 2002b, 2004b). Ces structures ont également joué un rôle important lors du collapse de la Formation Ayabacas, ce que nous montrerons par la suite.

II.1.2. Stratigraphie régionale et âge de la Formation Ayabacas

Résumé étendu en français du document supplémentaire en ligne de l'article publié dans *Basin Research* :

La stratigraphie du sud du Pérou a été récemment redéfinie par Sempere et al. (2004a) et Sigé et al. (2004) dans la région du Lac Titicaca. Elle peut généralement être corrélée avec d'autres régions du Pérou et de Bolivie et s'organise de la façon suivante (Fig. II.1) :

- Une succession de couches (généralement des schistes noirs alternant avec des grès et des pélites) d'âge Ordovicien à Dévonien, pouvant atteindre 6 km d'épaisseur, affleure parfois dans la Cordillère Orientale et très localement sur l'Altiplano et dans la région d'Arequipa. Elles forment une partie du segment "Palaeozoic" de la Fig. II.1.
- Dans de rares zones de l'Altiplano et de la Cordillère Orientale se trouvent aussi des grès et des schistes du Mississippien (0-1.5 km d'épaisseur) ainsi que des calcaires du Pennsylvanien et du Permien (0-1.5 km d'épaisseur). Ils forment également une partie du segment "Palaeozoic" de la Fig. II.1.
- Le Groupe Mitu (principalement Trias, 0-2 km d'épaisseur) s'est déposé en grabens dans un système de rift et affleure dans certaines parties de l'Altiplano et de la Cordillère Orientale.
- Le groupe Mitu est recouvert en discordance par des grès fluvio-éoliens de la Formation Quilcapunco (≤ 400 m d'épaisseur), elle-même recouverte localement par des marnes et des calcaires marins noirs (Sipín Formation, 0-40 m d'épaisseur, Lias et/ou Dogger inférieur). Au sud-ouest du CECLLA, dans les régions de Lagunillas et d'Arequipa, cet intervalle est composé de calcaires marins (≤ 400 m d'épaisseur, Lias à Bajocien inférieur).
- Une surface d'érosion s'observe au sommet des formations Quilcapunco ou Sipín et elle est suivie par des pélites rouges (principalement) de la Formation Muni puis par une unité fluvio-éolienne grano- et strato-croissante, la Formation Huancané (300 m d'épaisseur,

Jurassique moyen et supérieur). Cet ensemble est corrélé au sud-ouest du CECLLA (région d'Arequipa) par le Groupe Yura (formations Puente, Cachíos, Labra, Gramadal, Hualhuani, et Murco *p.p.*, 4 km d'épaisseur, Bajocien supérieur à Crétacé inférieur), qui enregistre une progradation vers le sud-ouest de dépôts silicoclastiques.

- Au cours du Crétacé inférieur, des déformations ont affecté le bassin du sud Pérou, en particulier le long du SFUACC (Sempere et al., 2002b, 2004b). Elles ont causé des surrections avec pour conséquence une érosion partielle et parfois complète des dépôts mésozoïques. Cette surface d'érosion est "onlapée" au Crétacé moyen par des dépôts transgressifs qui progradent du SO vers le NE. Dans la région d'Arequipa, les dépôts transgressifs commencent par le sommet de la Formation Murco puis continuent par ~250 m de calcaires de la Formation Arcurquina. Dans l'Altiplano, la série stratigraphique transgressive du Crétacé inférieur à moyen est constituée des formations Angostura (conglomérats et grès affleurant dans certaines zones), Murco (principalement pélites rouges) et Arcurquina (calcaires marins, régulièrement stratifiés, strato-croissants, gris à noirs, riches en matière organique). Dans la région de Cusco, la Formation Murco est corrélée avec la Formation Maras (Carlotto et al., 1996), constituée de pélites rouges et de masses évaporitiques.
- La Formation Ayabacas est une unité chaotique, remarquablement déformée, qui remanie les dépôts antérieurs. Bien que les formations Arcurquina et Ayabacas occupent les mêmes positions stratigraphiques – au-dessus de la Formation Murco et sous la Formation Vilquechico –, elles doivent être formellement distinguées puisque la Formation Arcurquina s'est déposée en bancs réguliers sur une plate-forme carbonatée, tandis que la Formation Ayabacas résulte du remaniement de la Formation Arcurquina et des unités antérieures. Leurs dépôts ne sont donc pas contemporains et ne découlent pas des mêmes processus.
- Le groupe Vilquechico (Coniacien-Paléocène inférieur) scelle et postdate la Formation Ayabacas et ses déformations particulières. Il se compose généralement de pélites rouges et vertes entrecoupées de barres de grès. Dans la région d'Arequipa, il est corrélé avec la Formation Ashua (Cruz, 2002).
- Enfin, entre ~60 et ~30 Ma, se dépose dans un grand bassin d'avant-pays une série de plus de 5 km d'épaisseur (le Groupe Puno), grano- et strato-croissante, dont la base est dominée par des pélites rouges (Formation Muñani, Paléocène supérieur – Eocène inférieur). Dans la région d'Arequipa, la Formation Huanca (≤ 2 km d'épaisseur ; Cruz, 2002) est corrélée avec le Groupe Puno, mais elle a été partiellement érodée et est incomplète.

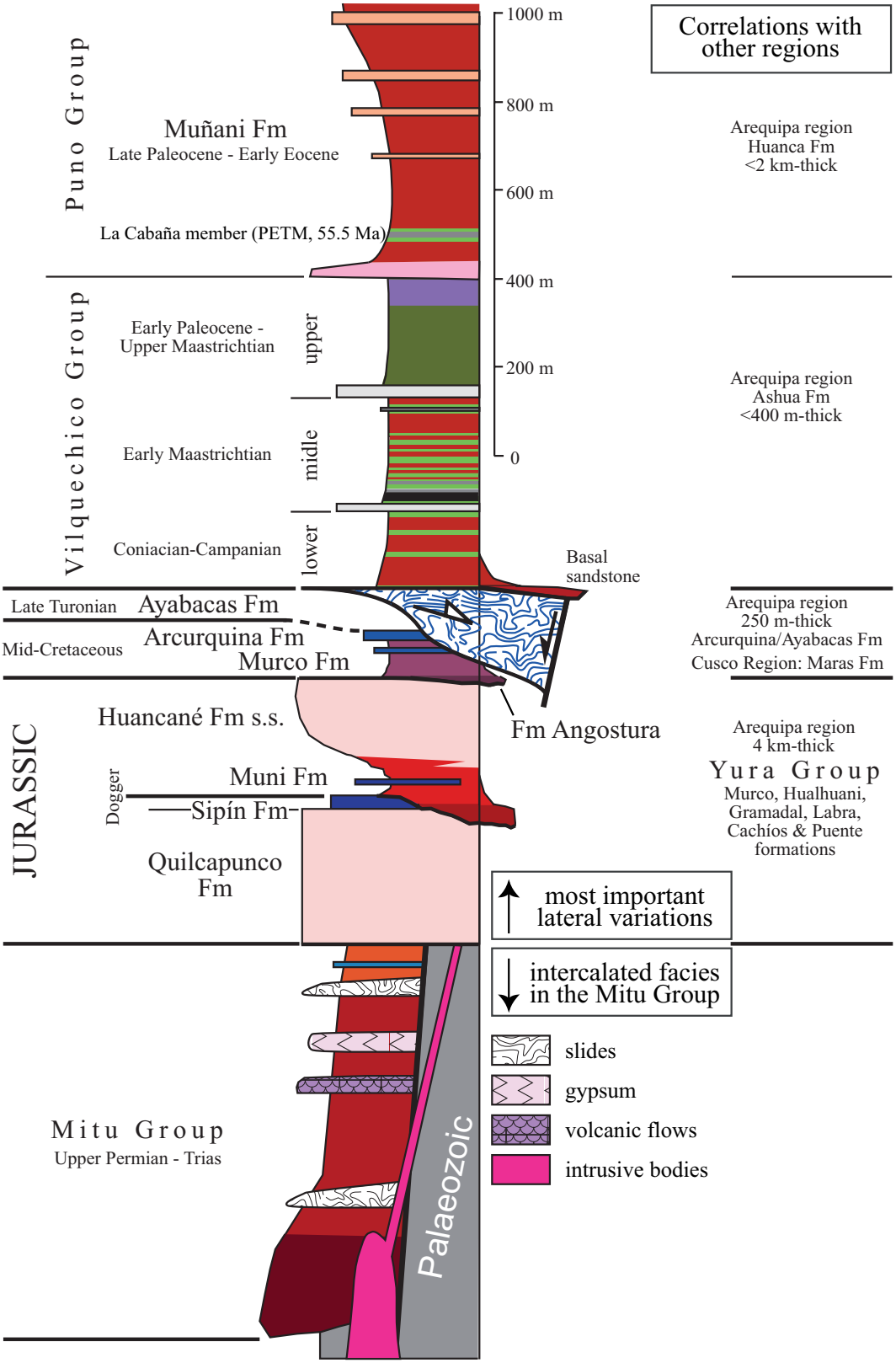

Fig. II.1 *: colonne stratigraphique des unités de la région du lac Titicaca, du Mésozoïque au Paléogène. Les corrélations avec d'autres régions de la zone d'étude sont spécifiées dans la colonne de droite. Les épaisseurs sont approximatives et sujettes à d'importantes variations latérales. Les couleurs sont évocatrices des couleurs réelles, à l'exception du bleu qui représente les calcaires. PETM = Paleocene-Eocene Thermal Maximum. Adapté d'après Sempere et al. (2004a).*

Remarquablement, les unités mésozoïques du sud du Pérou antérieures au collapse Ayabacas se sont déposées dans un bassin principalement marin s'approfondissant vers l'ouest, tandis que les unités postérieures se sont déposées dans un bassin presque exclusivement continental et limité au sud-ouest par des reliefs positifs, apparemment de nature volcanique. Cela souligne un changement dramatique et définitif des conditions de dépôts dans le bassin du sud du Pérou au moment du collapse Ayabacas.

L'âge de la Formation Ayabacas a été déterminé en considérant l'âge de la plus jeune unité remaniée (*i.e.* la Formation Arcurquina) et l'âge le plus ancien de la formation sus-jacente (*i.e.* la Formation Vilquechico). Les équivalents de ces formations dans la région d'Arequipa, dans le centre et le nord du Pérou, ainsi qu'en Bolivie, ont également été pris en compte. Dans l'équivalent bolivien de la Formation Arcurquina, l'événement anoxique océanique 2 (*Oceanic Anoxic Event 2* ; OAE-2) a été constaté (Graf, 2002 ; Graf et al., 2003). La position exacte de cet événement dans la série et sa reconnaissance dans des blocs de la Formation Arcurquina remaniés lors du collapse est discutée et permet de proposer un âge pour les derniers dépôts de la Formation Arcurquina précédant le collapse.

La synthèse de ces données permet de proposer la séquence d'événements suivante :

- Lors d'une première transgression entre l'Albien inférieur et l'Albien supérieur (~108,5 - ~102 Ma), des calcaires de la Formation Arcurquina sont déposés dans la partie ouest du bassin, jusqu'au SFUACC (Fig. 1 de l'article dans *Basin Research*).
- Après un hiatus de ~7 Ma, une deuxième transgression se produit entre le Cénomanien supérieur et le Turonien supérieur (~95 - ~90 Ma). Celle-ci est enregistrée au-delà du SFUACC dans la partie est du bassin, et atteint même la Bolivie centrale (Sempere, 1994, 1995 ; Fig. 1 de l'article dans *Basin Research*), déposant de nouveaux calcaires de la Formation Arcurquina.
- Le collapse Ayabacas se produit à la fin du deuxième épisode transgressif, aux environs de la limite Turonien-Coniacien (~91-89 Ma) et remanie une partie de la Formation Arcurquina et des formations antérieures.

Le modèle stratigraphique proposé pour la Formation Arcurquina à l'est du SFUACC a été testé en calculant un taux de sédimentation moyen à partir de huit coupes levées dans des radeaux de calcaires (Fig. II.2), puis en utilisant ce taux de sédimentation moyen pour déterminer l'âge de la base et du sommet du niveau interprété comme étant l'intervalle OAE-2. La bonne adéquation entre le résultat obtenu (Table 1) et les données les plus récentes de la

littérature permet de valider le modèle proposé et d'avancer un âge Turonien pour la partie supérieure de la Formation Arcurquina.

Supplementary online material to **"Giant submarine collapse of a carbonate platform at the Turonian-Coniacian transition: The Ayabacas Formation, southern Peru"** (P. Callot, T. Sempere, F. Odonne, E. Robert). *Basin Research*.

THE AYABACAS FORMATION IN ITS STRATIGRAPHIC SETTING

Detailed stratigraphy of southern Peru

The Mesozoic stratigraphy of southern Peru has suffered for decades from serious discrepancies between authors (Newell, 1949; Portugal, 1964, 1974; Audebaud, 1967, 1971; Audebaud *et al*., 1973; De Jong, 1974; Laubacher, 1978; Klinck *et al*., 1986; Laubacher & Marocco, 1990; Jaillard, 1995) and from the belief that deposition had occurred in two independent basins, the Putina basin in part of the Altiplano and the Arequipa basin southwest of the latter. Due to this situation, the entire region was restudied in the late 1990s and both areas were shown to belong to only one sub-basin, namely the southern portion of the WPBAB. A new stratigraphy was defined and successfully tested (Sempere *et al*., 2004a; Sigé *et al*., 2004). In the study area, continental to shallow-marine facies were deposited in the northeast and deeper water facies in the southwest and west.

Pre-Neogene sedimentary strata in southern Peru are distributed into the following stratigraphic sets, which can generally be correlated to other regions of Peru and Bolivia (Fig. 3 in main text) (Benavides-Cáceres, 1962; Laubacher, 1978; Vicente, 1981; Jaillard & Arnaud-Vanneau, 1993; Sempere *et al*., 2002a, 2004a):

• A >6 km-thick sedimentary succession of Ordovician to Devonian age crops out in the Cordillera Oriental and very locally in the Altiplano and Arequipa region (part of the "Palaeozoic" section in Fig. 3 of the main text). It mainly consists of dark shales intercalated with generally subordinate siltsones and sandstones.

• Mississippian sandstones and shales (Ambo Group, 0-1.5 km-thick) and Pennsylvanian-Permian limestones (Tarma-Copacabana Group, 0-1.5 km-thick) are preserved in limited areas of the Altiplano and Cordillera Oriental (part of the "Palaeozoic" section in Fig. 3 of the main text).

• The Mitu Group (mainly Triassic, 0-2 km-thick) accumulated in a continental rift system, and crops out only in specific areas, mainly in the Cordillera Oriental and Altiplano.

• Whitish fluvio-eolian sandstones (Quilcapunco Formation, ≤ 400 m-thick) unconformably overlie the Mitu or the Palaeozoic, and are locally overlain by marine, black limestones and marls of Liassic and/or early Dogger age (Sipín Formation, 0-40 m-thick). Southwest of the CECLLA system, in the Lagunillas and Arequipa areas, the entire interval is represented by up to 500 m of Liassic to Early Bajocian marine limestones.

• The Muni Formation is dominated by red mudstones, overlies the two previous units with an erosional and/or weathering discontinuity, and grades into a thickening- and coarsening-upward fluvio-eolian unit (Huancané Formation *s.s.*), forming a continental prograding set of Middle and Late Jurassic age. This ~300 m-thick continental set grades, southwest of the CECLLA system, into the Late Bajocian-Early Cretaceous, ≥ 4 km-thick, Yura Group (Puente, Cachíos, Labra, Gramadal, Hualhuani, and Murco *p.p.*), which records progradation of marine siliciclastic depositional systems toward the southwest.

• Some deformation affected the southern Peruvian basin at some time in the Early Cretaceous (and, possibly, Late Jurassic), in particular along the SFUACC system (Sempere *et al.*, 2002b, 2004b). This deformation produced local uplifts that led to partial to complete erosion of the Mesozoic succession, locally down to the Paleozoic basement. The resulting erosional surface was subsequently onlapped by the mid-Cretaceous transgression.

• In the Arequipa area, the major mid-Cretaceous transgression is mainly recorded by the ~250 m-thick Arcurquina Formation (but was initiated with the upper Murco Formation). In the Altiplano, a ~100 m-thick transgressive stratigraphic set of late Early to middle Cretaceous age is formed by the Angostura (conglomerates and sandstones, occurring in specific areas), Murco (mainly red mudstones and siltstones) and Arcurquina (marine, regularly-bedded, thickening-upward, grey to black, organic-rich micritic limestones; see below) formations, and onlaps a regional unconformity. Contacts between these units are gradational. Interstratified red mudstones and thin, grey to black limestones are typical of the rapid Murco-Arcurquina transition, as in the Arequipa area. In the Cusco area, the continental set formed by the Angostura and Murco formations is represented by the local Maras Formation (Carlotto *et al.*, 1996), which mainly consists of red mudstones and silstones, and evaporite masses (mainly gypsum; halite also occurs).

• The Ayabacas Formation, the object of this paper, consists of an extraordinarily deformed, chaotic unit reworking previous deposits and rocks. Although the Ayabacas and Arcurquina formations occupy the same stratigraphic position — overlying the Murco Formation and

underlying the Vilquechico Group and equivalent units —, they must be formally distinguished since the Arcurquina was deposited in regular beds in a stable carbonate platform, whereas the Ayabacas resulted from the reworking of the Arcurquina and previous units: their deposition was therefore neither contemporaneous nor driven by similar processes. Due to these markedly different depositional processes, they display distinct characteristics, which are obvious in the field.

• The Vilquechico Group (Late Campanian-Early Paleocene, ~700 m-thick) post-dates the Ayabacas Formation and its typical deformation. Its equivalent in the Arequipa area is the ≤ 400 m-thick Ashua Formation (Cruz, 2002; see below). A Coniacian ammonite from the Ashua Formation (see below) testifies that the Ayabacas-Ashua contact represents an interruption of the stratigraphic record of little time duration, if any. In contrast, the Ayabacas-Vilquechico contact, more to the north, apparently marks a ~5 Myr-long hiatus, during which some erosion must have occurred (Sempere *et al*., 2002a, 2004a). However, the preservation of stromatolites at the very top of the Arcurquina Formation, east of Huancané, suggests that this hiatus may have been much shorter at least locally.

• The Puno Group forms a ≥ 5 km-thick, thickening- and coarsening-upward, reddish succession that was deposited in a large foreland-type basin between ~60 and ~30 Ma, its lower part being dominated by red mudstones (Muñani Fm, Late Paleocene-Early Eocene). In the Arequipa area, the ≤ 2 km-thick Huanca Formation (Cruz, 2002) is the equivalent of the Puno Group but is likely to be incomplete due to partial erosion.

It is noteworthy that, prior to the Ayabacas collapse, the Mesozoic units of southern Peru were deposited in a largely marine basin that deepened to the west. In contrast, the units younger than the Ayabacas Formation were deposited in an almost exclusively continental basin that was bounded to the southwest by topographic highs, apparently volcanic in nature. In particular, the Arcurquina Formation (and equivalent deposits) mostly consists of marine limestones, whereas the Lower Vilquechico Formation (and equivalents) is dominated by abundant red mudstones that testify of a continental or near-continental environment. In the Central Andean domain, away from the coast, true marine deposits are extremely rare afterwards. The Ayabacas Formation was thus deposited at the time when the south Peruvian basin underwent a dramatic and permanent change from marine to continental conditions.

Age of the Ayabacas Formation

The age of the Ayabacas Formation is bracketed by the youngest age yielded by the

youngest reworked unit, namely the Arcurquina Formation (and its Bolivian and north Peruvian equivalents), and by the oldest age yielded by the overlying units, i.e. the Vilquechico Group and Ashua Formation (and equivalents).

Age of the Arcurquina Formation northeast of the SFUACC fault system

In the Lake Titicaca region, just southwest of the SFUACC fault system (Ayabacas, Pusi and Puno areas), the Ayabacas Formation is generally >100 m-thick and reworks limestones bearing late Early Albian to Late Cenomanian fossils. In contrast, the Arcurquina Formation is <35 m-thick and has only yielded fossils of Late Cenomanian age (see discussion hereafter) in the area located northeast of the SFUACC (Huancané area and western to central Bolivia).

Northeast of the SFUACC system in Peru, the Arcurquina Formation, where preserved, is generally <25 m-thick and crops out at Huatasane (10 m) and from Huancané (23 m) to the Bolivian border (Figs. 1, 2 in main text). In Bolivia, two units, generally <35 m-thick, are equivalent to the Arcurquina Formation: the Matilde Formation north of Lake Titicaca and the Miraflores Formation in central Bolivia. The Miraflores Formation yielded the ammonite *Neolobites kummeli* Benavides-Cáceres, 1956 (Branisa, 1968), now considered as synonym of the Late Cenomanian *N. vibrayeanus* (d'Orbigny, 1841) (Kennedy & Juignet, 1981; Wiese & Schulze, 2005). Graf (2002) and Graf *et al*. (2003) described a 33 m-thick section near Mina Matilde, ~90 km southeast of Huancané (Fig. 3 in main text). These authors identified the purportedly Late Cenomanian planktonic foraminiferum *Asterohedbergella asterospinosa* Hamaoui (1965) at several levels in the organic-rich lower half of this section, in agreement with other paleontological data from other parts of the basin (see below). On the basis of this Late Cenomanian age, $\delta^{13}C$ data, facies, and biostratigraphic correlations, they assigned most of this portion of the section to the Oceanic Anoxic Event 2 (OAE-2), and, because the termination of OAE-2 is now considered to mark the Cenomanian-Turonian boundary (93.5 Ma; Ogg *et al*., 2004), the upper half of the Arcurquina Formation at Mina Matilde should implicitly be of Turonian age. However, attribution of as much as ~14 m of this section to the OAE-2 interval is questionable given the shallow depositional environment and low subsidence (see section below), whereas *Asterohedbergella asterospinosa* has been shown to also occur in the Turonian (Abdallah et al., 2000).

We accept Graf *et al*.'s (2003) identification of OAE-2 in this area, but propose that it is likely to be restricted to one of two conspicuous calcareous shale intervals known in most of this domain (Fig. 4 in main text), which we denominate 'Nuñoa-1' and 'Nuñoa-2' intervals. Between them, the Nuñoa-1 interval is particularly rich in organic matter, as revealed by its

dominantly black coloration and high degree of subsequent *per descensum* bioturbation. We test this hypothesis below.

Age of the Arcurquina Formation southwest of the SFUACC fault system

Southwest of the SFUACC system, limestone blocks of the Arcurquina Formation reworked in the Ayabacas Formation yielded Albian and Cenomanian fossils (Lissón, 1924; Boit, 1926; Lissón & Boit, 1942; Cooke, 1949; Newell, 1949; Kalafatovich, 1957): the oldest age, *viz*. the late Early Albian, is recorded by the ammonite *Glottoceras* sp. (previously assigned to the genus *Knemiceras*; Robert *et al.*, 2002), and the echinid *Heteraster texanus* (Roemer, 1849) (Ayabacas locality); the Middle Albian is recorded by the ammonite *Oxytropidoceras* (*Oxytropidoceras*) *peruvianum* (von Buch, 1839) (early Middle Albian; Robert, 2002; Robert *et al.*, 2002) and the echinid *Coenholectypus planatus* (Roemer, 1849) (Ayabacas locality); the echinid *Orthopsis titicacana* Cooke, 1949, common in the Pusi and Puno areas, and the coral *Epistreptophyllum* aff. *budaensis* (Wells *in* Newell, 1949) indicate a Cenomanian age (possibly Early Cenomanian; Cooke, 1949; Wells *in* Newell, 1949); the Late Cenomanian is characterised by the ammonite *Neolobites vibrayeanus* from 4 km northeast of Cusco and 13 km north of Ayabacas.

Age of the Arcurquina Formation in the Arequipa area

We have determined that the Yura section, 200 km southwest of the Ayabacas locality and 40 km northwest of the city of Arequipa, displays both the Arcurquina and Ayabacas formations. The first is ~275 m-thick and makes up most of the limestone succession there, whereas the second is only ~25 m-thick. Diagnostic fossils (Benavides-Cáceres, 1962) were found in the Arcurquina Formation, which consists of two members. The lower Arcurquina member is characterised in its lower part by the common occurrence of *Ostrea minos* (Coquand, 1869), which is found associated with *Glottoceras raimondii* (Lissón, 1908) in northern Peru (Chúlec Formation, late Early Albian; Robert, 2002; Robert et al., 2002); its upper part is dated by the echinid *Coenholectypus planatus*, considered to range from the latest Early Albian to earliest Late Albian. The lower Arcurquina thus spans the late Early Albian - Middle Albian interval (102-108.5 Ma; Hardenbol *et al*., 1998). In contrast, the upper Arcurquina member has only yielded *Neolobites* sp. (Middle to Late Cenomanian). Diagnostic fossils from the two intervals are only ~30 m apart, revealing that the two members are separated by a chronologic hiatus of ~7 Myr (between at least ~102 and ~95 Ma). We found no evidence of a post-Albian, pre-Late Cenomanian protracted, major emersion or alteration in the outcropping uppermost part of the lower member, although a mudcracked and silicified

surface is indeed locally observed at the top of this unit.

Age of the Vilquechico Group and equivalent units

The Vilquechico Group of the Lake Titicaca region places constraints on the minimum age of the Ayabacas Formation. It consists of three formations, referred to as the Lower, Middle, and Upper Vilquechico formations (Jaillard *et al*., 1993), which correlate with dated Bolivian units (Sempere *et al*., 2004a; Sigé *et al.*, 2004). In the Arequipa region, this time interval is represented by the Ashua Formation (Cruz, 2002).

The Lower Vilquechico Formation generally overlies the Ayabacas Formation and consists of dominantly red mudstones (Jaillard *et al*., 1993; Sigé *et al*., 2004). Northeast of the SFUACC fault system, the Lower Vilquechico Formation generally consists at its base of a 5-30 m-thick sandstone member, which comprises poorly bedded, red argillaceous sandstones distributed in beds several m-thick (Fig. 6 in main text). This irregular member grades upward into the Lower Vilquechico typical mudstones. The Lower Vilquechico Formation is equivalent to the set formed by the Coniacian? Aroifilla and Santonian-Campanian Chaunaca formations of Bolivia (Sempere *et al*., 1997, 2004a).

In particular, the Aroifilla Formation is highly variable in thickness and mainly consists of orange-red mudstones, subordinate fine-grained red to green laminated sandstones, and evaporites, which include gypsum beds and ≤ 50 m-thick stratabound bodies. Coarse sandstones or conglomerates (including mafic volcanic clasts) are locally present at the base of the unit. Basaltic flows intercalate in the lower part of the formation at several localities of central Bolivia (one yielded an apparent age of 85.1 Ma; Evernden *et al*., 1977; McBride *et al*., 1983), and <30 cm-thick tuffaceous beds are known in a few western sections. The Aroifilla was deposited in a distal alluvial to salt-lacustrine (playa-lake) environment. Its high thickness variability has been interpreted to reflect syndepositional normal faulting (Sempere, 1994).

The Ashua Formation of the Arequipa region sharply overlies the Ayabacas Formation and shares a number of characteristics with the Aroifilla Formation of Bolivia. It dominantly consists of red mudstones and includes ≤ 4 m-thick gypsum bodies, ≤ 15 m-thick volcaniclastic conglomerates and sandstones, and ≤ 10 m-thick limestone beds (Cruz, 2002). One of these limestones yielded an ammonite initially determined as *Tissotia steinmanni* (Lissón, 1908) (Hosttas, 1967). However, a recent reappraisal of the palaeontological bibliography (Hyatt, 1903; Lissón, 1908; Knechtel *et al*., 1947; Benavides-Cáceres, 1956) by one of us (E.R., unpublished) leads us to consider that this species must be assigned to the

genus *Paratissotia* Hyatt, 1903, instead of *Tissotia* Douvillé, 1890. *Paratissotia steinmanni* was thought to indicate the Santonian Lenticeras baltai Zone (Benavides-Cáceres, 1956; Vicente, 1981), but revision by one of us (E.R., unpublished) of the faunal association of this zone, as listed by Benavides-Cáceres (1956), makes us challenge this chronostratigraphic position. Although no precise stratigraphic data are available for the specimen mentioned by Hosttas (1967), the stratigraphic distribution of *Paratissotia* is commonly considered as Coniacian (Wright *et al*., 1996). *P. steinmanni* must therefore be recognised to indicate the Coniacian, without more precisions, until more informative new material is collected. This datum strictly constrains the Ayabacas Formation to be older than the end of the Coniacian (~86 Ma).

The red-bed basin where the Ashua, Aroifilla and lower Vilquechico formations were deposited was thus episodically connected to the sea, possibly through the volcanic arc, in the Arequipa region. No younger marine connections are documented in this area.

Northern Peru counterparts

Thicknesses and reconstructed depositional depths in the WPBAB show an overall increase from southern Peru northwards. Much of the relevant information relative to the mid-Cretaceous stratigraphy and evolution of central and northern Peru is mainly found in Jaillard (1986, 1987, 1990, 1992, 1994), Jaillard & Sempere (1991), and Jaillard & Soler (1996).

A first major transgression started in the middle Early Albian (~110 Ma; Hardenbol *et al*., 1998) with ammonite-bearing marine mudstones and sandstones. The first massive limestones are represented by the Chúlec Formation of late Early Albian age (Robert *et al*., 2002a,b), and a >2 km-thick succession of limestones and marls was deposited until the Late Turonian. The west-Peruvian carbonate platform was affected by a relative regression during the Late Albian-Middle Cenomanian interval (102-95 Ma, ~7 Myr). In the entire west-Peruvian basin, a major transgression was initiated in the latest Middle Cenomanian (~95 Ma) and culminated in the Early Turonian (~92.5 Ma). Carbonate-dominated sedimentation continued until the Late Turonian. In northern Peru, the Turonian limestones are sharply overlain by ~300 m of reddish to brown mudstones and fine sandstones, Early Coniacian to Middle Campanian in age, which were deposited in marine to non-marine environments and are thought to reflect the onset of aerial erosion in western areas throughout the Central Andes (Jaillard, 1994; Sempere, 1994). As indicated by the respective ammonite faunas, the sharp change from carbonates to reddish mudstones thus occurred approximately at the Turonian-Coniacian boundary (~89 Ma).

Discussion: Age of the Ayabacas Formation

The chronologic constraints available from southern Peru only indicate that deposition of the Ayabacas Formation occurred between the earliest Late Cenomanian and latest Coniacian. Recognition of the OAE-2 event in the lower and/or middle part of the west-Bolivian equivalent of the Arcurquina Formation (Graf, 2002) however strongly suggests that its upper part is Turonian in age, although diagnostic Turonian fossils have not been reported yet.

The data from southern Peru presented above are quite consistent with the better constrained evolution of central and northern Peru. The two major transgressions known in the north, respectively starting in the middle to late Early Albian (~110 Ma) and in the latest Middle Cenomanian (~95 Ma) are recognised southwest of the SFUACC system (Fig. 1 in main text) and recorded by the late Early and Middle Albian, and Late Cenomanian, faunas found in limestones reworked in the Ayabacas Formation and in the Yura section. The ~7 Myr-long hiatus observed in the Arequipa area is apparently correlative to the Late Albian - Middle Cenomanian regression (~102-95 Ma) documented in northern Peru. The Arcurquina Formation of southern Peru was thus mainly deposited during two distinct transgressive-highstand intervals.

Unlike the Albian transgression, which is only recorded southwest of the SFUACC fault system, the worldwide Late Cenomanian transgression flooded the area northeast of it, reaching central Bolivia (Sempere, 1994, 1995; Fig. 1 in main text).

In northern as in southern Peru, termination of the carbonate platform and subsequent deposition of dominantly reddish mudstones record a major sedimentary upheaval. This first-order change occurred near the Turonian-Coniacian boundary in northern Peru and, consistently with the regional constraints, it is reasonable to propose that this change took place at about the same time in southern Peru. Because the Ayabacas Formation coincides with this change, post-dating the termination of the carbonate platform and pre-dating the onset of red mudstone deposition, the Ayabacas collapse is likely to have also occurred near the Turonian-Coniacian boundary (~89 Ma).

Testing the chronostratigraphic model

The chronostratigraphy proposed above for the Arcurquina Formation northeast of the SFUACC can be tested by calculating a mean compacted sedimentation rate for each of the 8 measured sections and, on this basis, deriving mean ages for the initiation and termination of the Nuñoa-1 and Nuñoa-2 intervals, one of which is supposed to be the local correlative of OAE-2 (Table 1). As stated above, and using Ogg *et al.*'s (2004) chronostratigraphy, we

assume that deposition of the Arcurquina Formation in this area started at ~94.7 Ma (latest Middle Cenomanian or basal Late Cenomanian) and ended at ~89.3 Ma (Turonian-Coniacian transition). We find that, in southern Peru, compacted depositional rates varied between 2.7 and 4.3 m/Myr northeast of the SFUACC system. Assuming a constant rate at each locality, we calculate the mean ages for initiation and termination of the Nuñoa-1 deposition as 94.1 ± 0.2 and 93.6 ± 0.2 Ma, respectively; and, for Nuñoa-2, as 93.2 ± 0.35 and 92.6 ± 0.35 Ma, respectively. Based on these results, we calculate that deposition of the Nuñoa-1 and Nuñoa-2 intervals respectively lasted 0.5 ± 0.4 and 0.6 ± 0.7 Myr.

Section	Total thickness (m)	Sed rate (m/Myr)	Position lower level 1 (m)	Position upper level 1 (m)	Age lower level 1 (Ma)	Age upper level 1 (Ma)	Duration Nunõa-1 (Myr)	Position lower level 2 (m)	Position upper level 2 (m)	Age lower 2 (Ma)	Age upper 2 (Ma)	Duration Nunõa-2 (Myr)	Duration Nunõa-1+2 (Myr)
San Antón - Pacuta	14.7	2.7	1.7	nd	94.08	nd	nd	nd	5.7	nd	92.60	nd	1.48
San Antón - Coñejuno	15.8	2.9	1.4	nd	94.23	nd	nd	nd	5.4	nd	92.85	nd	1.38
Yanaoco	20.7	3.8	2.6	5.1	94.03	93.37	0.66	6.9	8.9	92.9	92.37	0.53	1.66
Nuñoa	20.8	3.9	2.9	5.2	93.95	93.35	0.60	8,0	10.8	92.62	91.89	0.73	2.07
Cusco	20.5	3.8	2.3	3.75	94.10	93.71	0.38	4.7	6.7	93.46	92.93	0.53	1.17
Huancané	23.2	4.3	1.2	4.4	94.43	93.68	0.75	5.1	8.9	93.51	92.62	0.89	1.81
Larimayo 1	18.0	3.3	2.8	3.6	93.86	93.62	0.24	4.5	6.4	93.35	92.78	0.57	1.09
Larimayo 2	18.0	3.3	1.9	3,0	94.14	93.8	0.33	4.4	5.8	93.38	92.96	0.42	1.18
Average	**18.96**	**3.49**			**94.10**	**93.59**	**0.51**			**93.20**	**92.62**	**0.61**	**1.48**
Standard deviation	2.85	0.52			0.17	0.19				0.36	0.35		0.34
Result			Duration **Nuñoa 1** = **0.51 ± 0.36** Myr					Duration **Nuñoa 2** = **0.61 ± 0.71** Myr					

Table 1. Calculation of the ages and durations of Nuñoa-1 and Nuñoa-2 intervals, using 8 complete sections of Zone 1 limestone rafts from San Antón, Yanaoco (~8 km WSW of Huancané), Nuñoa, Cusco, Huancané and Larimayo (~9 km NNW of San Antón), deposited between the base of the Late Cenomanian and the Turonian-Coniacian boundary (respectively 94.71 and 89.27 Ma in Jarvis *et al*., 2006). The thickness of each section is divided by the duration of the depositional interval, 5.44 Myr, to estimate each compacted sedimentation rate (Sed. rate). The ages of the base and top of the Nuñoa-1 and Nuñoa-2 intervals are estimated by assuming that sedimentation rates were constant at each site and thus that they are proportional to their stratigraphic position above the base of the section; nd = no data.

Values relative to the Nuñoa-1 interval agree fairly with available data concerning OAE-2, which was initiated at 94.0 ± 0.2 Ma (Caron *et al*., 1999), 94.09 Ma (Sageman *et al*., 2006), or 94.21 Ma (Mitchell *et al*., 2008), terminated at 93.5 ± 0.2 (Caron *et al*., 1999) or 93.5 ± 0.8 Ma (Ogg *et al*., 2004), and is estimated to have lasted 0.5 ± 0.4 Myr (Caron *et al*., 1999), between 0.1 and 0.7 Myr (Wright *et al*., 2003), between 0.56 and 0.89 Myr (Sageman *et al*., 2006), or ~0.7 Myr (Wendler *et al*., 2007). Such a good agreement strongly suggests that our proposed chronostratigraphy is consistent, and that the organic-rich Nuñoa-1 interval does

represent OAE-2 in southern Peru. The overlying portion of the Arcurquina Formation must therefore be considered to be of Turonian age.

In the Arequipa area, the Early-Middle Albian and Late Cenomanian-Turonian intervals are ~135 and ~165 m-thick, respectively, from which mean compacted depositional rates of ~20 and ~28 m/Myr are deduced. These values imply that subsidence was higher by one order of magnitude in the Arequipa area than northeast of the SFUACC, as suggested by the overall deeper and thicker facies in the former.

References

ABDALLAH, H., SASSI, S., MEISTER, C. & SOUISSI, R. (2000) Stratigraphie séquentielle et paléogéographie à la limite Cénomanien-Turonien dans la région de Gafsa-Chotts (Tunisie centrale). *Cretaceous Research*, **21**, 35-106.

AUDEBAUD, E. (1967) Etude géologique de la région de Sicuani et Ocongate (Cordillère Orientale du Sud Péruvien). Thèse de 3ème cycle, Université de Grenoble, 60 p.

AUDEBAUD, E. (1971) Mise au point sur la stratigraphie et la tectonique des calcaires Cénomaniens du Sud-Est péruvien (formation Ayavacas). *Comptes rendus de l'Académie des Sciences, série D*, **272**, 1059-1062.

AUDEBAUD, E., CAPDEVILA, R., DALMAYRAC, B., DEBELMAS, J., LAUBACHER, G., LEFEVRE, C., MAROCCO, R., MARTINEZ, C., MATTAUER, M., MEGARD, F., PAREDES, J. & TOMASI, P. (1973) Les traits géologiques essentiels des Andes Centrales (Pérou-Bolivie). *Revue de géographie physique et de géologie dynamique*, **15**, 73-114.

BENAVIDES-CACERES, V. (1956) Cretaceous system in northern Peru. *Bulletin of the American Museum of Natural History*, **108**, 353-494.

BENAVIDES-CÁCERES, V. (1962) Estratigrafía pre-Terciaria de la región de Arequipa. *Boletín de la Sociedad Geológica del Perú*, **38**, 5-45.

BOIT, B. (1926) Dos Neolobites. *Boletín de la Sociedad Geológica del Perú*, **2**, 39-40.

BRANISA, L. (1968) Hallazgo del amonite *Neolobites* en la Caliza Miraflores y de huellas de dinosaurios en la Formación El Molino y su significado para la determinación de la edad del "Grupo Puca". *Boletín del Instituto Boliviano del Petróleo*, **8**, 16-28.

von BUCH, L. (1839) Pétrifications recueillies en Amérique par M. Alexandre de Humboldt et par M. Charles Degenhardt. Imprimerie de l'Académie Royale des Sciences, Berlin, 22 p.

CARLOTTO, V., GIL, W., CÁRDENAS, J. & CHÁVEZ, R. (1996) Geología de los cuadrángulos de Urubamba y Calca hojas 27-r y 27-s. *Boletín INGEMMET*, **65**, serie A, Carta Geológica Nacional, 245 p.

CARON, M., ROBASZYNSKI, F., AMEDRO, F., BAUDIN, F., DECONINCK, J.-F., HOCHULI, P.A., VON SALIS-PERCH NIELSEN, K. & TRIBOVILLARD, N. (1999) Estimation de la durée de l'événement anoxique global au passage Cénomanien/Turonien; approche cyclostratigraphique dans la formation Bahloul en Tunisie centrale. *Bulletin de la Société Géologique de France*, **170**, 145-160.

COOKE, C.W. (1949) Two Cretaceous echinoids from Peru. *Journal of Paleontology*, **23**, 84-86.

COQUAND, H. (1869) Monographie du genre Ostrea. Terrain crétacé. H. Seven Ed., Marseille, France, 215 p.

CRUZ, M. (2002) Estratigrafía y evolución tectono-sedimentaria de los depósitos sin-orogénicos del cuadrángulo de Huambo: Las formaciones Ashua y Huanca, departamento de Arequipa. Tesis de la Universidad Nacional San Agustín de Arequipa, 127 p.

DE JONG, K.A. (1974) Melange (Olistostrome) near Lago Titicaca, Peru. *AAPG Bull.*, **58**, 729-741.

DOUVILLÉ, H. (1890) Sur la classification des Cératites de la Craie. *Bulletin de la Société Géologique de France,* série 3, **18**, 275-292.

EVERNDEN, J.F., KRIZ, S. & CHERRONI, C. (1977) Potassium-argon ages of some Bolivian rocks. *Economic Geology*, **72**, 1042-1061.

GRAF, A.A. (2002) Le Cénomanien supérieur en Bolivie: Etude sédimentologique et stratigraphique de la Formation Matilde-Miraflores. Travail de diplôme, Université de Fribourg, Suisse.

GRAF, A.A., STRASSER, A. & CARON, M. (2003) OAE-2 equivalent (Upper Cenomanian) recorded in Bolivian shallow-water sediments. *Abstract 11th Swiss Sed. Meeting, Fribourg*, 39-40.

HAMAOUI, M. (1965) Type Sections of Cretaceous Formations in the Jerusalem - Bet-Shemesh Area. II. Biostratigraphy. *Geological Survey of Israel, Stratigraphic Section*, **1**, 27-39.

HARDENBOL, J., THIERRY, J., FARLEY, M.B., JACQUIN, T., DE GRACIANSKY, P.-C. & VAIL, P.R. (1998) Mesozoic and Cenozoic sequence chronostratigraphic framework of European basins, chart 1. In: *Mesozoic and Cenozoic sequence stratigraphy of European basins* (Ed. by P.-C. de Graciansky, J. Hardenbol, T. Jacquin & P.R. Vail), *SEPM Special Publication*, **60**, 363-364.

HOSTTAS, J. (1967) Estudio geológico del túnel terminal entre Huambo y Querque. Tesis de la Universidad Nacional San Agustín de Arequipa, 107 p.

HYATT, A. (1903) Pseudoceratites of the Cretaceous. *Monographs of the United States Geological Survey*, **44**, 352 p.

JAILLARD, E. (1986) La sédimentation crétacée dans les Andes du Pérou central: exemple de la formation Jumasha (Albien moyen-supérieur à Turonien supérieur) dans la région d'Oyón (Département de Lima). *Géodynamique*, **1**, 97-108.

JAILLARD, E. (1987) Sedimentary evolution of an active margin during middle and Upper Cretaceous times: the north Peruvian margin from late Aptian up to Senonian. *International Journal of Earth Sciences* (*Geologische Rundschau*), **76**, 677-697.

JAILLARD, E. (1990) Evolución de la margen andina en el norte del Perú desde el Aptiano superior hasta el Senoniano. *Boletín de la Sociedad Geológica del Perú*, **81**, 3-13.

JAILLARD, E. (1992) La fase peruana (Cretáceo superior) en la margen peruana. *Boletín de la Sociedad Geológica del Perú*, **83**, 81-87.

JAILLARD, E. (1994) Kimmeridgian to Paleocene tectonic and geodynamic evolution of the Peruvian (and Ecuadorian) margin. In: *Cretaceous tectonics of the Andes* (Ed. by J.A. Salfity), pp. 101-167. Earth Evolution Sciences Monograph Series, Vieweg Publications, Wiesbaden.

JAILLARD, E. (1995) La sedimentación Albiana – Turoniana en el Sur del Perú (Arequipa – Puno – Putina). *Sociedad Geológica del Perú*, *Volumen Jubilar Alberto Benavides*, 135-157.

JAILLARD, E. & SEMPERE, T. (1991) Las secuencias sedimentarias de la Formación Miraflores y su significado cronoestratigráfico. *Revista técnica de YPFB*, **12**, 257-264.

JAILLARD, E. & ARNAUD-VANNEAU, A. (1993) The Cenomanian – Turonian transition on the Peruvian margin. *Cretaceous Research*, **14**, 585-605.

JAILLARD, E. & SOLER, P. (1996) Cretaceous to early Paleogene tectonic evolution of the northern Central Andes (0-18°S) and its relations to geodynamics. *Tectonophysics*, **259**, 41-53.

JAILLARD, E., CAPPETTA, H., ELLENBERGER, P., FEIST, M., GRAMBAST-FESSARD, N., LEFRANC, J.-P. & SIGE, B. (1993) The Late Cretaceous Vilquechico Group of southern Peru. Sedimentology, paleontology, biostratigraphy, correlations. *Cretaceous Research*, **14**, 623-661.

JARVIS, I., GALE, A.S., JENKYNS, H.C. & PEARCE, M.A. (2006) Secular variation in Late Cretaceous carbon isotopes: a new δ13C carbonate reference curve for the Cenomanian–Campanian (99.6–70.6 Ma). *Geological Magazine*, **143**, 561-608.

KALAFATOVICH, V. (1957) Edad de las calizas de la Formación Yuncaypata, Cuzco. *Boletín de la Sociedad Geológica del Perú*, **32**, 127-139.

KENNEDY, W.J. & JUIGNET, P. (1981) Upper Cenomanian Ammonites from the Environs of Saumur, and the Provenance of the Types of *Ammonites vibrayeanus* and *Ammonites geslinianus*. *Cretaceous Research*, **2**, 19-49.

KLINCK, B.A., ELLISON, R.A. & HAWKINS M.P. (1986) The geology of the Cordillera Occidental and Altiplano west of Lake Titicaca,

southern Peru. *Preliminary report*, INGEMMET, Lima, Peru, 353 p.

KNECHTEL, M.M., RICHARDS, E.F. & RATHBUN, M.V. (1947) Mesozoic fossils of the Peruvian Andes. *The John Hopkins University studies in geology*, **15**, 150 p.

LAUBACHER, G. (1978) Géologie des Andes péruviennes: Géologie de la Cordillère Orientale et de l'Altiplano au nord et nord-ouest du lac Titicaca (Pérou). *Travaux et Documents de l'ORSTOM*, **95**, 219 p.

LAUBACHER, G. & MAROCCO, R. (1990) La cuenca cretácica del Altiplano peruano: Litoestratigrafía e interpretación secuencial. *Boletín de la Sociedad Geológica del Perú*, **81**, 33-46.

LISSÓN, C. (1908) *Contribución al conocimiento sobre algunos ammonites del Perú*. 4th Congreso Cientifico Latino-Americano, Tipografia del Perú, 22 p.

LISSÓN, C. (1924) *Edad de los fósiles peruanos y distribución de sus depósitos*. 3rd edition, Lima, 226 p.

LISSÓN, C. & BOIT, B. (1942) *Edad de los fósiles peruanos y distribución de sus depósitos*. 4th edition, Lima, 320 p.

McBRIDE, S.L., ROBERTSON, R.C.R., CLARK, A.H. & FARRAR, E. (1983) Magmatic and metallogenetic episodes in the northern tin belt, Cordillera Real, Bolivia. *Geologische Rundschau*, **72**, 685-713.

MITCHELL, R.N., BICE, D.M., MONTANARI, A., CLEAVELAND, L.C., CHRISTIANSON, K.T., COCCIONI, R. & HINNOV, L.A. (2008) Oceanic anoxic cycles? Orbital prelude to the Bonarelli Level (OAE 2). *Earth and Planetary Science Letters*, **267**, 1-16.

NEWELL, N.D. (1949) Geology of the Lake Titicaca region, Peru and Bolivia. *Geological Society of America Memoir*, **36**, 111 p.

OGG, J.G., AGTERBERG, F.P. & GRADSTEIN, F.M. (2004) The Cretaceous Period. In: *A Geologic Time Scale 2004* (Ed. by F.M. Gradstein, J.G. Ogg & A.G. Smith), pp. 344-383. Cambridge University Press, Cambridge.

d'ORBIGNY, A. (1840-42) Paléontologie française: Terrains crétacés. I. Céphalopodes. Masson Ed., Paris, 1-120 (1840), 121-430 (1841), 431-662 (1842).

PORTUGAL, J. (1964) Geology of the Puno-Santa Lucia area, Department of Puno, Peru. Unpublished PhD Thesis, University of Cincinnati, 141 p.

PORTUGAL, J. (1974) Mesozoic and Cenozoic stratigraphy and tectonic events of Puno-Santa Lucia area, Department of Puno, Peru. *AAPG Bull.*, **58**, 982-999.

ROBERT, E. (2002) La transgression albienne dans le Bassin Andin (Pérou) : biostratigraphie, paléontologie et stratigraphie séquentielle. *Strata*, **38**, 380 p.

ROBERT, E., BULOT, L.G., JAILLARD, E. & PEYBERNÈS, B. (2002) Proposition d'une nouvelle biozonation par ammonites de l'Albien du Bassin andin (Pérou). *C. R. Palevol*, **1**, 1-9.

ROBERT, E., JAILLARD, E., PEYBERNÈS, B. & BULOT, L.G. (2002) La transgresión albiana en la Cuenca Andina (Perú Central - Ecuador): modelo general y diacrónismo de los depósitos marinos. *Boletín de la Sociedad Geológica del Perú*, **94**, 25-30.

ROEMER, C.F. (1849) Mit besonderer Rücksicht auf deutsche Auswanderung und die physischen Verhältnisse des Landes nach eigener Beobachtung geschildert; mit einem naturwissenschaftlichen Anhänge, und einer topographisch-geognostichen Karte von Texas. Bonn, 464 p.

SAGEMAN, B.B., MEYERS, S.R. & ARTHUR, M.A. (2006) Orbital time scale and new C-isotope record for Cenomanian-Turonian boundary stratotype. *Geology*, **34**, 125-128.

SEMPERE, T. (1994) Kimmeridgian? to Paleocene tectonic evolution of Bolivia. In *Cretaceous tectonics in the Andes* (Ed. by J.A. Salfity), pp. 168-212. Earth Evolution Sciences Monograph Series, Vieweg Publications, Wiesbaden.

SEMPERE, T. (1995) Phanerozoic evolution of Bolivia and adjacent regions. In *Petroleum Basins of South America*, A.J. Tankard, R. Suárez & H.J. Welsink (eds.), *American Association of Petroleum Geologists Memoir* **62**, 207-230.

SEMPERE, T., BUTLER, R.F., RICHARDS, D.R., MARSHALL, L.G., SHARP, W. & SWISHER III, C.C. (1997) Stratigraphy and chronology of Late Cretaceous - Early Paleogene strata in Bolivia and northwest Argentina. *Geological Society of America Bulletin*, **109**, 709-727.

SEMPERE, T., CARLIER, G., SOLER, P., FORNARI, M., CARLOTTO, V., JACAY, J., ARISPE, O., NÉRAUDEAU, D., CARDENAS, J.,

ROSAS, S. & JIMÉNEZ, N. (2002a) Late Permian - Middle Jurassic lithospheric thinning in Peru and Bolivia, and its bearing on Andean-age tectonics. *Tectonophysics*, **345**, 153-181.

SEMPERE, T., JACAY, J., FORNARI, M., ROPERCH, P., ACOSTA, H., BEDOYA, C., CERPA, L., FLORES, A., HUSSON, L., IBARRA, I., LATORRE, O., MAMANI, M., MEZA, P., ODONNE, F., OROS, Y., PINO, A., & RODRÍGUEZ, R. (2002b) Lithospheric-scale transcurrent fault systems in Andean southern Peru. Extended abstract, *V International Symposium on Andean Geodynamics*, Toulouse, 601-604.

SEMPERE, T., ACOSTA, H. & CARLOTTO, V. (2004a) Estratigrafía del Mesozoico y Paleógeno al Norte del Lago Titicaca. *Publicación Especial Sociedad Geológica del Perú*, **5**, 81-103.

SEMPERE, T., JACAY, J., CARLOTTO, V., MARTÍNEZ, W., BEDOYA, C., FORNARI, M., ROPERCH, P., ACOSTA, H., ACOSTA, J., CERPA, L., FLORES, A., IBARRA, I., LATORRE, O., MAMANI, M., MEZA, P., ODONNE, F., ORÓS, Y., PINO, A. & RODRÍGUEZ, R. (2004b) Sistemas transcurrentes de escala litosférica en el Sur del Perú. *Publicación Especial Sociedad Geológica del Perú*, **5**, 105-110.

SIGÉ, B., SEMPERE, T., BUTLER, R.F., MARSHALL, L.G. & CROCHET, J.-Y. (2004) Age and stratigraphic reassessment of the fossil-bearing Laguna Umayo red mudstone unit, SE Peru, from regional stratigraphy, fossil record, and paleomagnetism. *Geobios*, **37**, 771-794.

VICENTE, J.-C. (1981) Elementos de la estratigrafia Mesozoica sur-peruana. *Comité Sudamericano del Jurásico y Cretácico: Cuencas sedimentarias del Jurásico y Cretácico de América del Sur*, Buenos Aires, **1**, 319-351.

WENDLER, J., KUSS, J. & STEIN, R. (2007) Late Cenomanian carbon isotope stratigraphy of the Levant carbonate platform (Central Jordan): Cyclic patterns and correlations. *Geophysical Research Abstracts*, **9**, EGU2007-A-11163.

WIESE, F. & SCHULZE, F. (2005) The upper Cenomanian (Cretaceous) ammonite *Neolobites vibrayeanus* (d'Orbigny, 1841) in the Middle East: taxonomic and palaeoecologic remarks. *Cretaceous Research*, **26**, 930-946.

WRIGHT, C.W., CALLOMAN, J.H. & HOWARTH, M.K. (1996) Treatise on Invertebrate Paleontology. Part L. Mollusca 4 revised, Cephalopoda, Cretaceous Ammonoidea. *The Geological Society of America and University of Kansas Press*, 362 p.

WRIGHT, J.D., CRAMER, B.S., MILLER, K.G. & KATZ, M.E. (2003) Orbital Cycles, Climate, and Diagenesis Mimic Methane Releases: Results from a High Resolution Study of OAE-2, New Jersey Coastal Plain. *Eos Trans. AGU*, **84 (46)**, Jt. Assem. Suppl., Abstract PP42D-03.

Fig. II.2 *(pages suivantes) : dessin des huit sections levées dans les radeaux calcaires de la Formation Ayabacas à l'est du SFUACC (A à G) et dans la Formation Arcurquina à Huancané (H). Remarquer les correspondances entre les huit coupes dans lesquelles 5 niveaux se reconnaissent. Les niveaux Nuñoa 1 (correspondant à OAE-2) et Nuñoa 2 (voir texte et figure 4 de l'article de Basin Research) sont représentés en grisé.* **B** *= bioturbation, le nombre de B indiquant le degré de bioturbation ;* **FC** *= fragments coquillers ;* **F** *= fossiles ;* **OC** *= organismes constructeurs ;* **Str** *= stromatolithes ;* ***m*** *= coloration marron marquée ;* ***r*** *= coloration rouge ou rosée. La hauteur de chaque section est indiquée en haut à droite.*

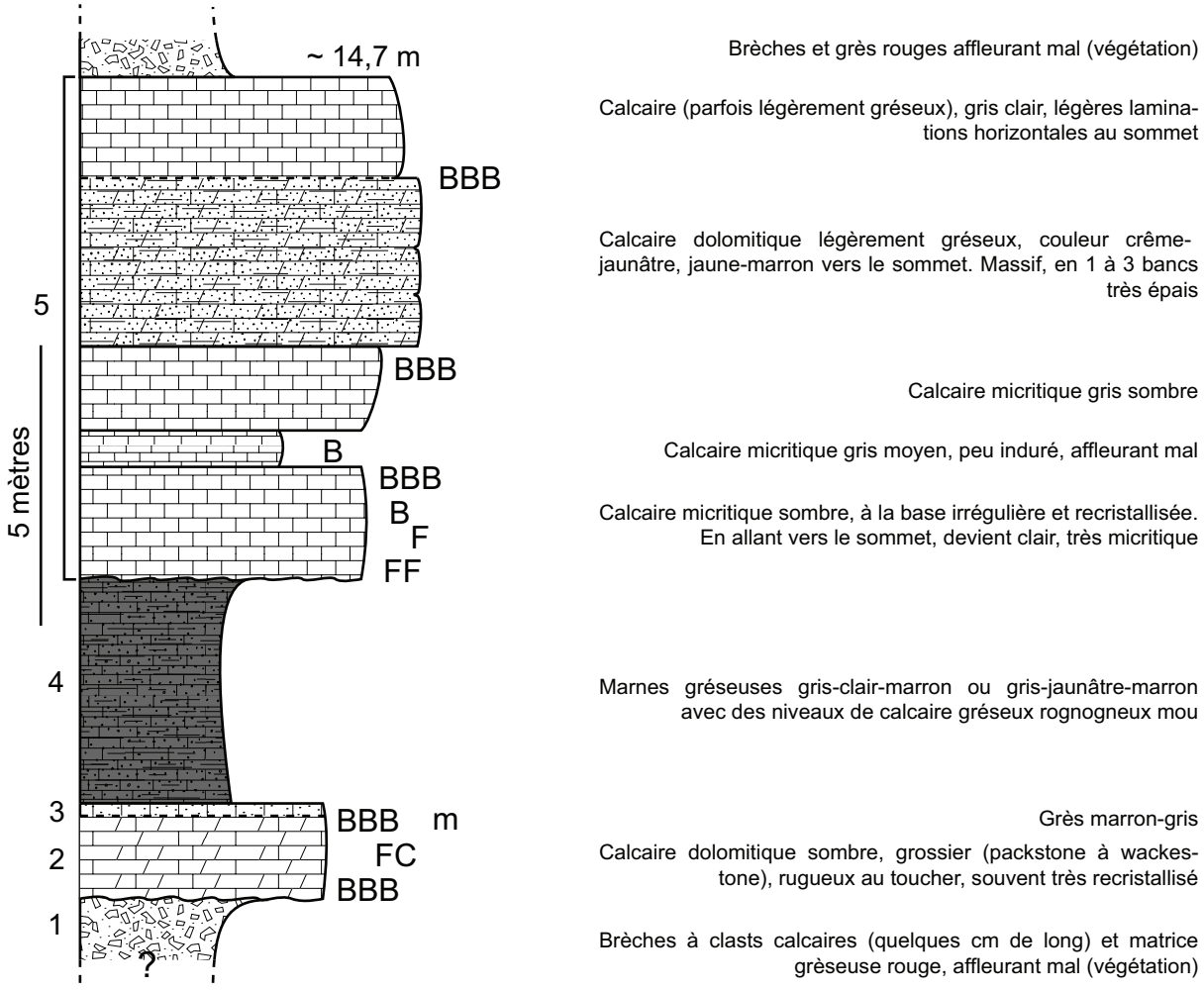

Fig. II.2.A *: section de San Antón Pacuta. UTM 0354775 – 8383476 – 3963 m, Zone 19L.*

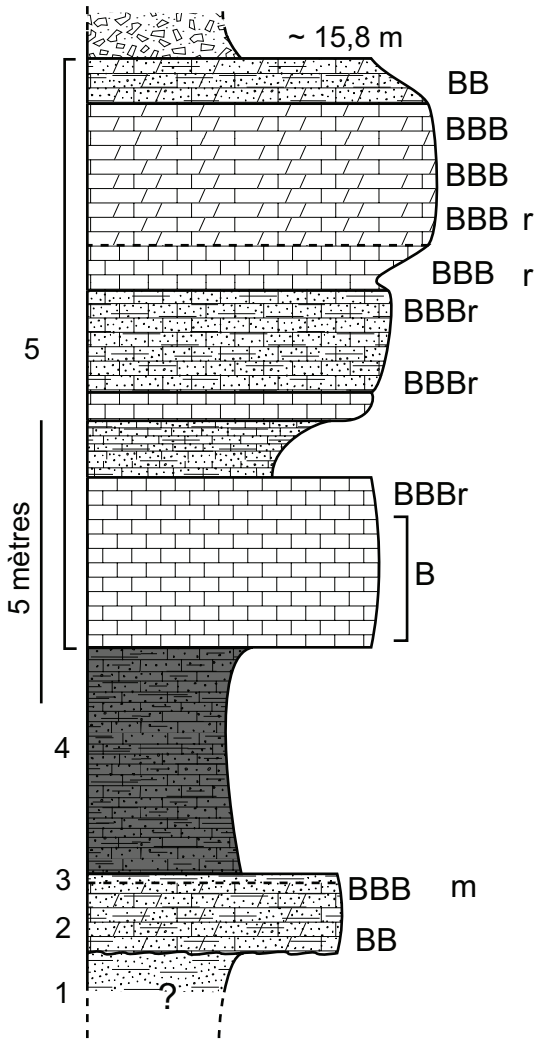

Brèches (hydroplastiques) à clasts calcaires (marron-jaune-gris-rose) et matrice gréseuse rouge, affleurant mal (végétation)

Calcaire gréseux gris clair ou jaunâtre (de plus en plus vers le sommet), en petits bancs affleurants mal

Calcaire micritique rosâtre-violacé devenant gris clair, plus induré et dolomitique en allant vers le sommet

Calcaire micritique rouge-rosé-violacé

Calcaire gréseux gris sombre (patine et cassure). Rosé à la base, plus clair au sommet

Calcaire micritique très sombre

Calcaire gréseux affleurant mal, jaunâtre, devenant gris clair et moins gréseux en allant vers le sommet

Calcaire massif gris clair à la patine patine se remarquant dans le paysage. Calcaire très micritique gris sombre à la base devenant gris clair au sommet (grosses bioturbations rouge)

Marnes gréseuses affleurant mal, de couleur variable: gris-jaunâtre-marron, plus ou moins foncées

Calcaire très gréseux, gris-marron-jaunâtre, affleurant mal

Calcaire dolomitique sombre, grossier, rugueux au toucher, souvent très recristallisé

Grès rouge, affleurant très mal (végétation)

***Fig. II.2.B** : section de San Antón Coñejuno. UTM 0352465 – 8390190 – 3991 m, Zone 19L.*

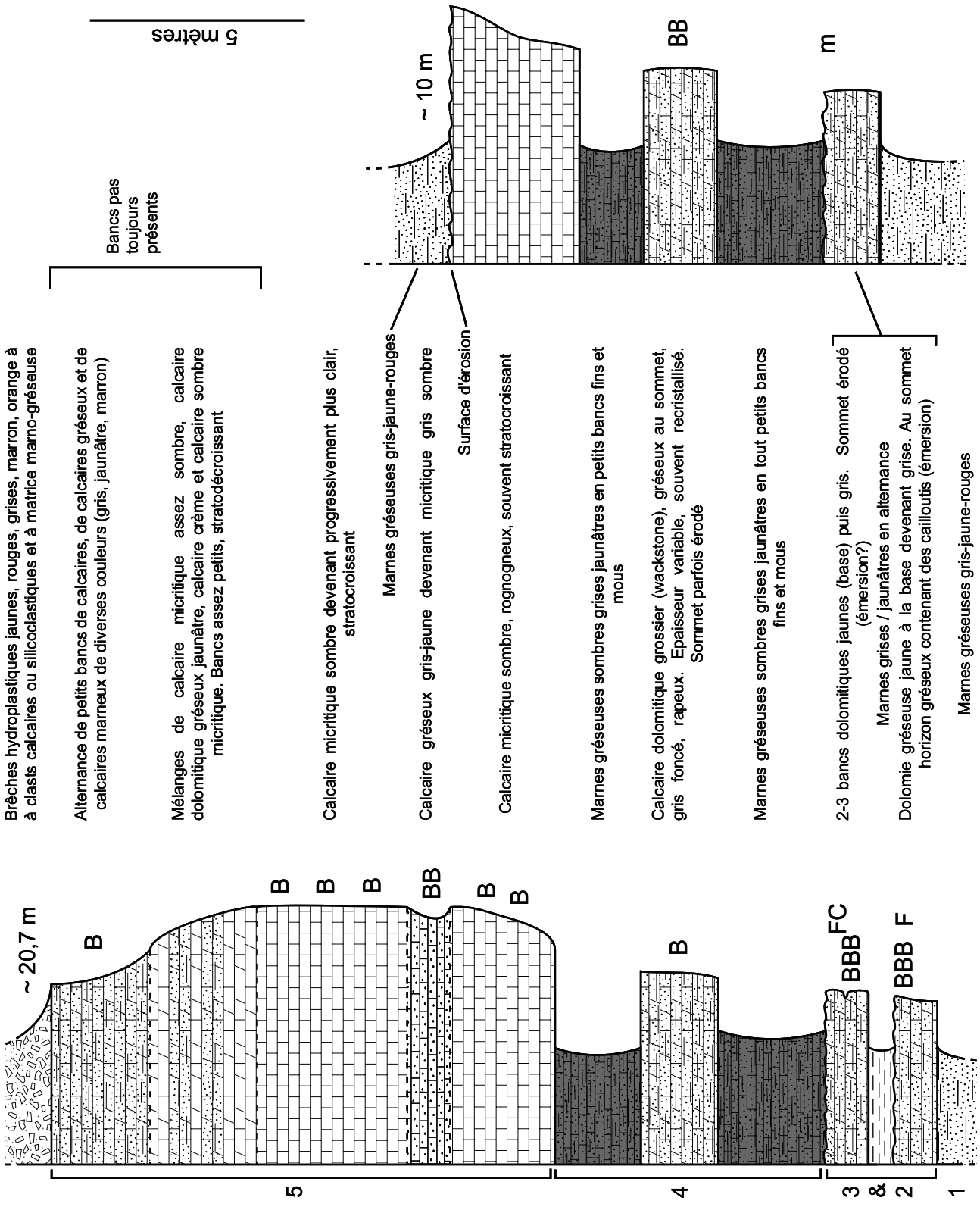

***Fig. II.2.C** : sections de Yanaoco. UTM 0411075 – 8316180 – 3858 m, Zone 19L. La section de gauche correspond à un raft complet, celle de droite à un autre raft du mélange dont le sommet a été érodé.*

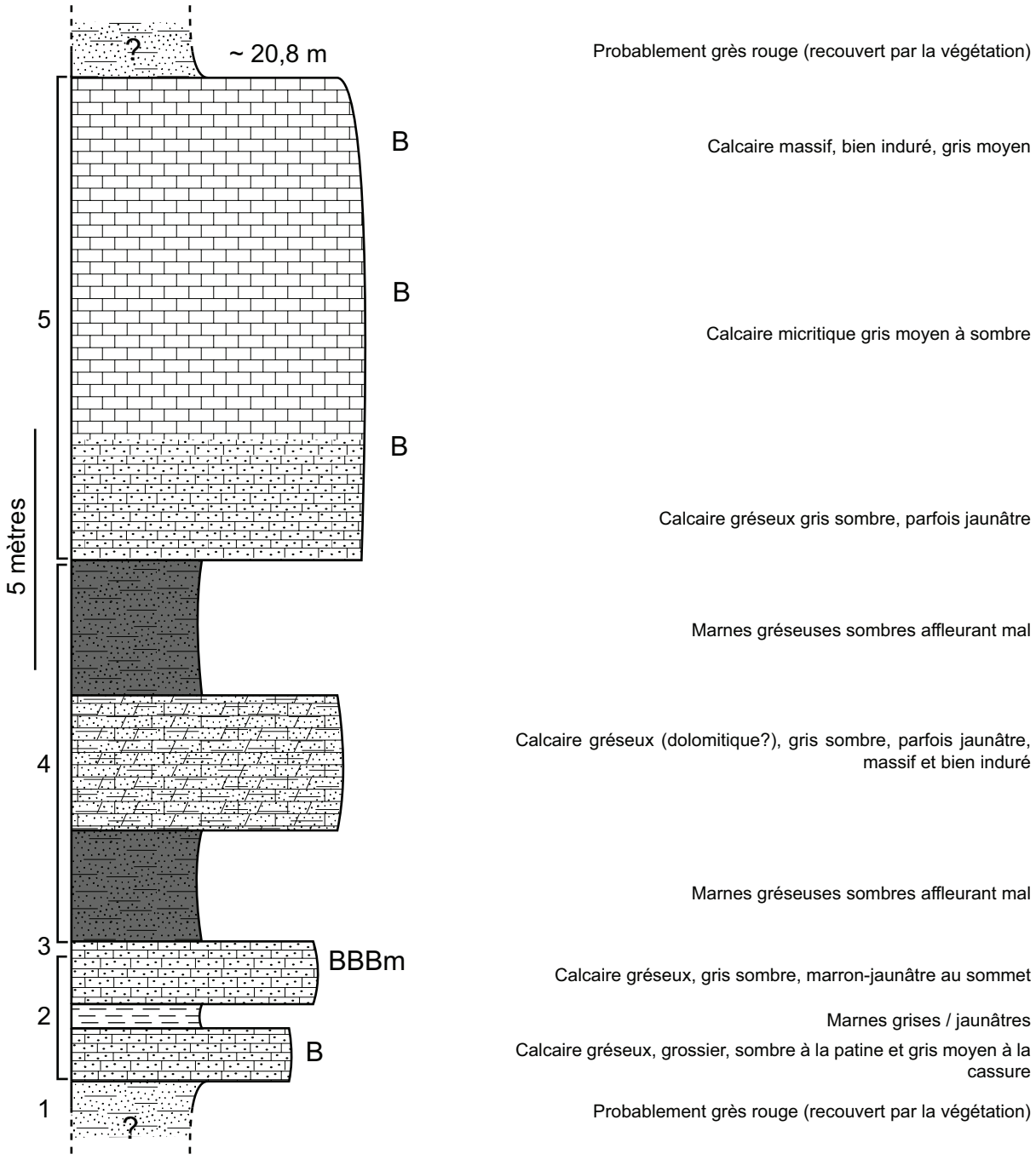

Fig. II.2.D *: section de Nuñoa. UTM 0314620 – 8411370 – 4210 m, Zone 19L.*

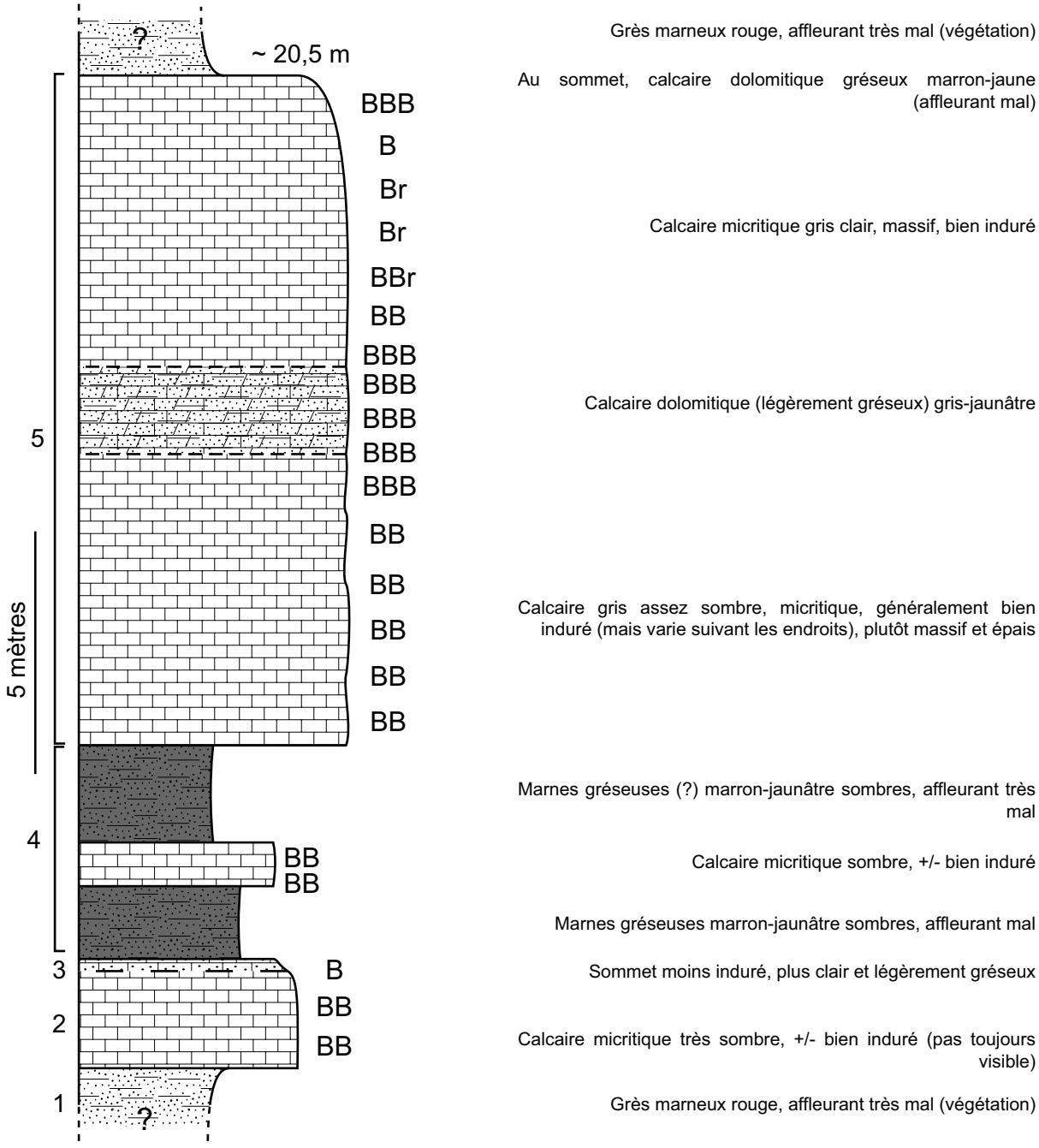

***Fig. II.2.E** : section de Cusco. UTM 0179555 – 8507210 – 3790 m, Zone 18L.*

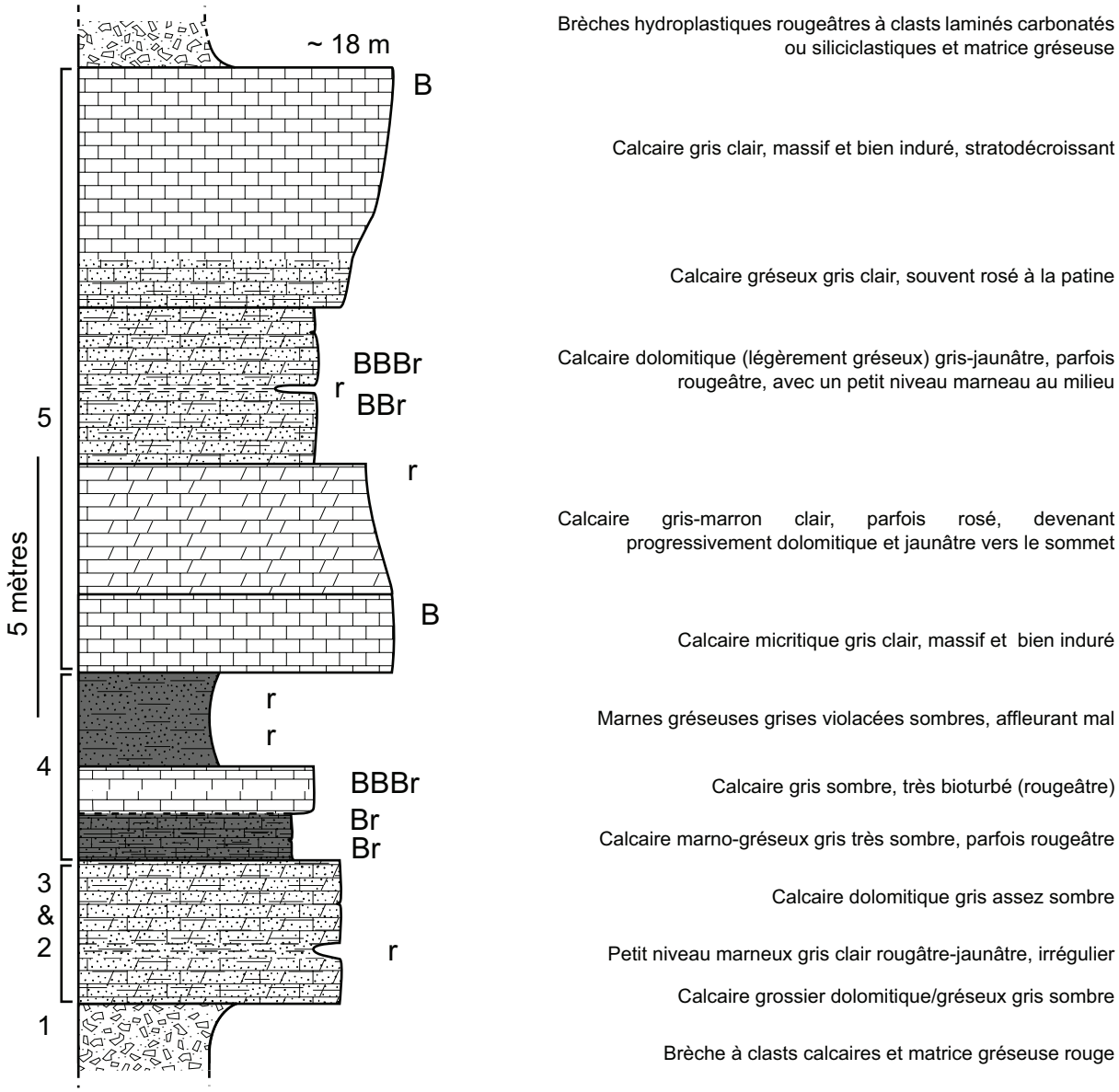

***Fig. II.2.F** : section d'un des radeaux de Larimayo (voir Fig. 6 de l'article dans Basin Research), au NNW de San Antón. UTM 0355160 – 8396670 – 4090 m, Zone 19L.*

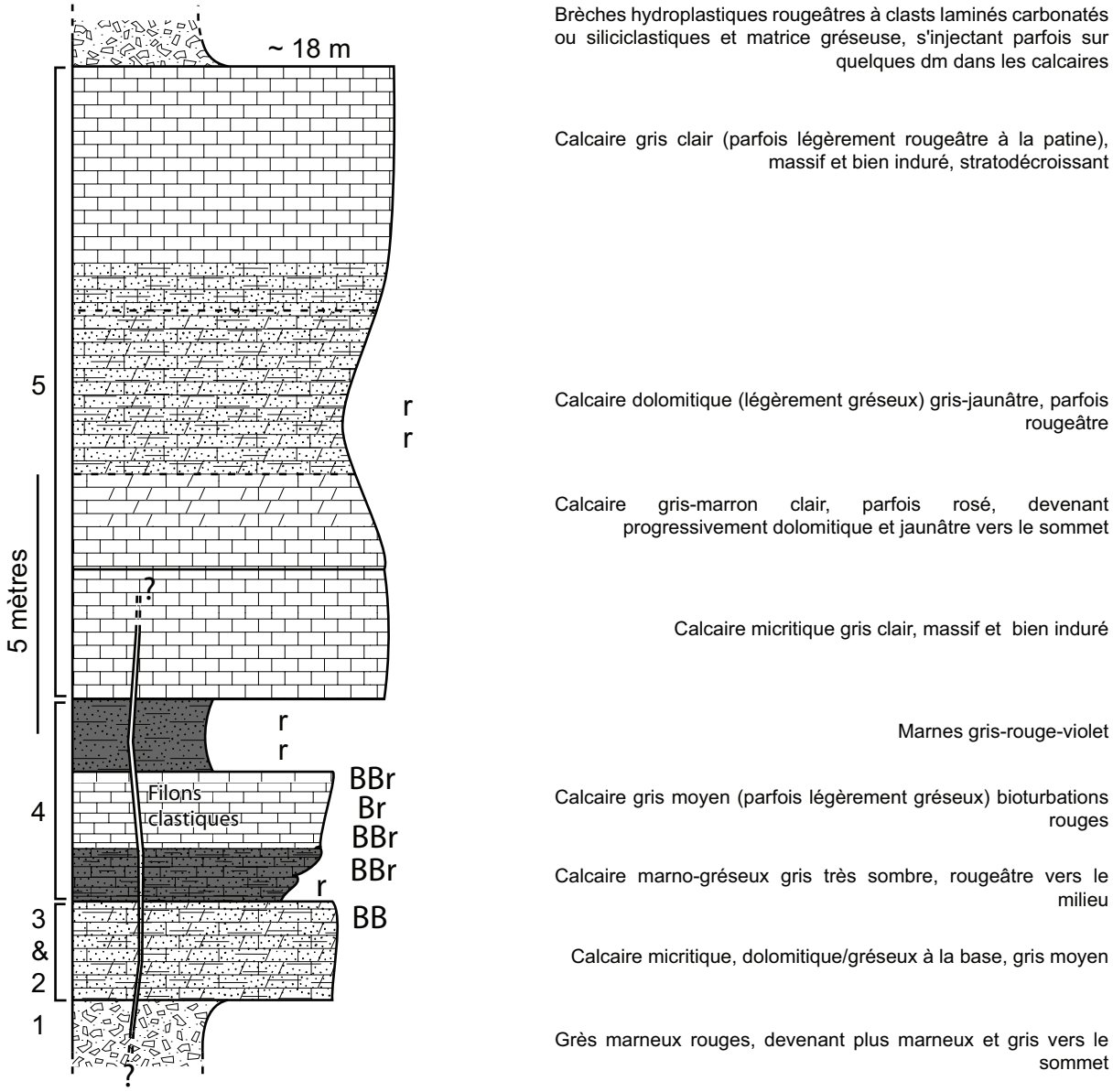

***Fig. II.2.G** : section d'un des radeaux de Larimayo (voir Fig. 6 de l'article dans Basin Research), au NNW de San Antón. UTM 0355290 – 8396550 – 4150 m, Zone 19L.*

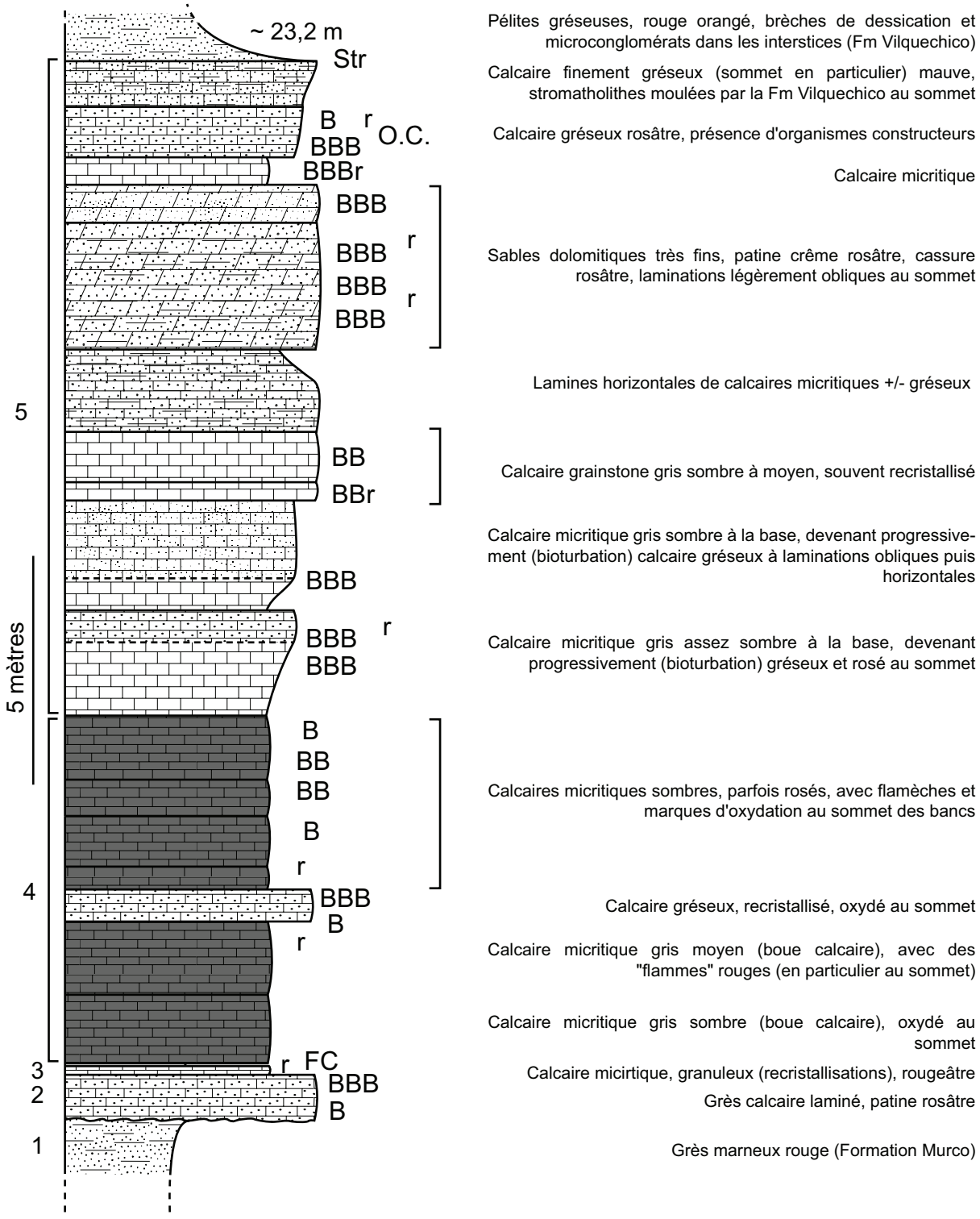

Fig. II.2.H *: section de la Formation Arcurquina (dépôts de la plate-forme non déstabilisée), levée à l'est de Huancané. UTM 0421470 – 8316600 – 3888 m, Zone 19L.*

II.2. Morphologie, organisation et facteurs déclenchants du collapse

Résumé étendu en français de l'article 2 : "Giant submarine collapse of a carbonate platform at the Turonian-Coniacian transition : The Ayabacas Formation, southern Peru". *Basin Research*, sous presse.

La Formation Ayabacas est une unité extraordinairement déformée qui affleure irrégulièrement sur plus de 60 000 km^2 dans les cordillères et l'Altiplano du sud du Pérou. La majeure partie des affleurements se trouvent au sud et à l'est du lac Titicaca ainsi que sur l'Altiplano et la bordure est de la Cordillère Orientale en allant vers Cusco. La densité d'affleurements décroît notablement en allant vers le SW (Fig. I.2). Les déformations qui affectent la Formation Ayabacas contrastent fortement avec les formations sous- et sus-jacentes, peu perturbées. Les interprétations proposées par les précédents auteurs pour expliquer ces déformations sont variées et contradictoires : déformations tectoniques orogéniques, processus gravitationnels subaériens, et glissements sous-marins. Plusieurs arguments présentés dans cet article favorisent l'hypothèse d'un collapse sous-marin géant aux alentours de la limite Turonien-Coniacien (~91-89 Ma) de la plate-forme carbonatée mise en place au Crétacé moyen dans le bassin d'arrière arc de l'ouest du Pérou (WPBAB).

Le collapse s'est naturellement produit vers les zones les plus profondes du bassin, *i.e.* vers le sud-ouest. Il s'organise du nord-est au sud-ouest en six zones sur la base des faciès de déformation, une septième zone au nord-est (Zone 0) correspondant aux dépôts non déstabilisés de la Formation Arcurquina. Les zones 1 à 3 présentent une fragmentation progressive et croissante du NE au SW et sont composées de nappes et de radeaux calcaires flottant dans une matrice de matériaux pélitiques généralement rougeâtres, carbonatés et siliciclastiques. Au contraire les zones 4 et 5 sont exclusivement carbonatées, consistant en un empilement de masses calcaires qui forment des systèmes de plis et de chevauchements sédimentaires (*"sedimentary thrust and fold system" sensu* Frey-Martínez et al., 2006). La taille et la continuité des masses calcaires sont croissantes jusqu'à la Zone 6.

Dans la Zone 1 les blocs calcaires présentent généralement la même stratigraphie interne (Fig. II.2) et sont peu épais (généralement inférieurs à 20 m), mais se caractérisent par une importante extension latérale, de 40 mètres pour les radeaux à plusieurs kilomètres pour les nappes. La Formation Ayabacas est constituée par l'empilement de ces radeaux ou nappes calcaires, parfois fortement plissés et séparés par des brèches et la matrice pélitique rougeâtre.

La Zone 2 se caractérise par des radeaux assez similaires à ceux de la Zone 1, bien qu'un peu plus épais, plus fragmentés et généralement très plissés. La continuité latérale est moins nette, bien que des nappes fragmentées en rafts consécutifs peuvent être suivies sur quelques kilomètres en photographies aériennes. La partie centrale de la Zone 2 est également caractérisée par la présence dans le mélange de grands blocs massifs (jusqu'à plusieurs centaines de mètres de long et plusieurs dizaines de mètres d'épaisseur) d'unités antérieures (Formation Huancané, roches paléozoïques) qui se rencontrent principalement au voisinage du SFUACC. Ces radeaux rigides et non plissés étaient lithifiés au moment du collapse et sont interprétés comme résultant d'une érosion catastrophique suite à l'exposition de ces anciennes unités par le jeu du SFUACC.

La Zone 3 est la plus chaotique. Comparés à la Zone 2, les radeaux calcaires sont généralement plus épais (30-40 m d'épaisseur), moins plissés, mais plus fragmentés et avec une très faible continuité latérale, quasiment inexistante y compris en photographies aériennes. L'abondante matrice entourant les radeaux calcaires se caractérise par d'impressionnantes brèches sédimentaires et des figures de déformations de matériaux non consolidés, notamment dans les affleurements au sud-ouest de Cabanillas.

Dans la Zone 4, les affleurements sont rares et localisés principalement dans le corridor du CECLLA. La Formation Ayabacas consiste en un empilement de radeaux calcaires dont certains bancs sont bréchifiés. Ces radeaux sont séparés par des brèches, elles aussi presque exclusivement carbonatées, les abondantes pélites rouges des Zones 1 à 3 deviennent extrêmement rares. Une partie de la matrice des brèches et certains clastes sont constitués de calcite.

La Zone 5 consiste en un mélange chaotique de grands radeaux et nappes carbonatés (jusqu'à plus d'un kilomètre de long plus de 100 mètres d'épaisseur), qui n'a été bien observé qu'au SE de Tisco. Les masses sont constituées de niveaux bien stratifiés, de bancs bréchifiés et/ou d'une association des deux. Des plis affectent certaines masses dans leur ensemble, ou certains radeaux à l'intérieur d'une masse calcaire. Certaines masses ou parties des masses sont peu déformées, suggérant qu'elles étaient plus rigides et lithifiés au moment du collapse.

La Zone 6 affleure seulement dans deux régions : au NW de Yura (principalement) et au N de Chalhuanca. Dans les deux cas la série calcaire est épaisse (> 300 m), la base semble régulièrement déformée et seule la partie supérieure semble affectée par des déplacements de matériaux. Dans la région de Yura (mais pas dans celle de Chalhuanca), l'ensemble de la série carbonatée est plissé en grands anticlinaux et synclinaux asymétriques (> 500 m de large) qui n'affectent ni le substratum sous-jacent ni les unités postérieures. Des variations d'épaisseurs

des couches sont observées dans les 25-40 derniers mètres de la série, les bancs étant amincis au niveau des charnières anticlinales et fortement épaissis dans les charnières synclinales dans lesquelles les sédiments se sont accumulés (constitués de calcaires généralement lithifiés et de marnes ductiles). Ces plis gravitationnels sont interprétés comme étant synsédimentaires des derniers dépôts carbonatés et contemporains du collapse.

Des failles normales ont découpé le substratum de la Formation Ayabacas en blocs basculés dans la partie supérieure du collapse (Zone 1 à 3). Quelques excellents affleurements (Cabanillas, San Anton) montrent que ces failles sont contemporaines du collapse et que les matériaux de la Formation Ayabacas ont glissé le long des pentes alors créées. Des blocs lithifiés de 10-100 m de côté associés à certaines de ces failles normales synchrones du collapse se rencontrent dans le mélange. Les grands blocs lithifiés provenant d'unités du Crétacé inférieur ou même du Paléozoique, observés dans le mélange de part et d'autre du SFUACC, indiquent également que le rejet cumulé du SFUACC a dépassé 400 m pendant la relativement courte période du collapse pour mettre à l'affleurement ces formations anciennes. A certaines périodes, l'escarpement a été important, au moins égal à l'épaisseur de certains blocs, *i.e.* jusqu'à 100 m de haut. L'élément déclencheur du collapse est cette importante activité tectonique en extension et ses conséquences : création de pentes avec dépassement de l'angle limite de repos des sédiments (*oversteepening*) et donc très probablement sismicité. Des indications d'augmentation de la pression de fluide interstitiel ou de contrastes de lithification existent, mais ces phénomènes ont seulement facilité les glissements et ne peuvent être considérés comme le principal facteur déclenchant. L'hypothèse d'une rupture provoquée par la chute relative du niveau marin, parfois avancée comme facteur déclenchant, a été écartée car aucun collapse ne s'est produit dans le WPBAB lors de la régression marine à la fin de l'Albien.

Entre la section nord (Cusco-Abancay-Chalhuanca) et la section sud (Huancané-Juliaca-Santa Lucía-Lagunillas-Yura) du collapse, il existe une différence notable de taille (120 km au nord ; 200 km au sud) et de faciès (faciès proximaux pauvres en calcaires et riches en pélites et évaporites au nord ; faciès proximaux riches en calcaires et absence d'évaporites au sud), qui ne peut être expliquée seulement par un raccourcissement plus important lors de l'orogénèse andine. Cette différence est expliquée par la coalescence du SFUACC et du CECLLA au nord, entraînant un escarpement probablement plus prononcé au moment du collapse et favorisant le glissement de la plate-forme carbonatée. Dans la région de Cusco, la présence de masses évaporitiques sous les dépôts carbonatés de la Formation Arcurquina a

également pu faciliter le glissement de cette dernière. Ces deux éléments pourraient expliquer la rareté de masses calcaires dans le nord de la zone d'étude, la Formation Arcurquina étant massivement transportée et désintégrée vers l'aval.

Les dimensions du collapse sont importantes : la surface affectée est estimée à au moins 80 000 m^2, l'épaisseur des dépôts variant de 0 m (dans les zones de départ au NE) à plus de 500 m (au SW), ce qui implique un volume de sédiments déplacés évalué à plus de 10 000 km^3. Ces dimensions sont du même ordre de grandeur que celles des grands glissements sous-marins actuels et font du collapse Ayabacas le plus grand glissement sous-marin fossile actuellement connu.

Basin Research (2008) doi: 10.1111/j.1365-2117.2008.00358.x

Giant submarine collapse of a carbonate platform at the Turonian–Coniacian transition: The Ayabacas Formation, southern Peru

Pierre Callot,* Thierry Sempere,* Francis Odonne* and Emmanuel Robert†

**LMTG, Université de Toulouse, CNRS, IRD, OMP, Edouard Belin, Toulouse France*
†*OSUG, Université Joseph Fourier, Institut Dolomieu, Grenoble cedex, France*

ABSTRACT

The Ayabacas Formation of southern Peru is an impressive unit formed by the giant submarine collapse of the mid-Cretaceous carbonate platform of the western Peru back-arc basin (WPBAB), near the Turonian–Coniacian transition (~90–89 Ma). It extends along the southwestern edge of the Cordillera Oriental and throughout the Altiplano and Cordillera Occidental over $> 80\,000\,km^2$ in map view, and represents a volume of displaced sediments of $> 10\,000\,km^3$. The collapse occurred down the basin slope, i.e. toward the SW. Six zones are characterised on the basis of deformational facies, and a seventh corresponds to the northeastern 'stable' area (Zone 0). Zones 1–3 display increasing fragmentation from NE to SW, and are composed of limestone rafts and sheets embedded in a matrix of mainly red, partly calcareous and locally sandy, mudstones to siltstones. In contrast, in Zones 4 and 5 the unit consists only of displaced and stacked limestone masses forming a 'sedimentary thrust and fold system', with sizes increasing to the southwest. In Zone 6, the upper part of the limestone succession consists of rafts and sheets stacked over the regularly bedded lower part. The triggering of this extremely large mass wasting clearly ensued from slope creation, oversteepening and seismicity produced by extensional tectonic activity, as demonstrated by the observation of synsedimentary normal faults and related thickness variations. Other factors, such as pore pressure increases or lithification contrasts probably facilitated sliding. The key role of tectonics is strengthened by the specific relationships between the basin and collapse histories and two major fault systems that cross the study area. The Ayabacas collapse occurred at a turning point in the Central Andean evolution. Before the event, the back-arc basin had been essentially marine and deepened to the west, with little volcanic activity taking place at the arc. After the event, the back-arc was occupied by continental to near-continental environments, and was bounded to the southwest by a massive volcanic arc shedding debris and tuffs into the basin.

INTRODUCTION

Mass-wasting processes are recognised as a major mechanism of sediment redistribution over continental margins, but how they are triggered is incompletely understood. Most giant submarine landslides have been described from the Recent on the basis of bathymetric and geophysical data (e.g. Collot *et al.*, 2001; Huvenne *et al.*, 2002; Haflidason *et al.*, 2004, 2005; Frey-Martínez *et al.*, 2005, 2006) but ancient examples of such phenomena are scarce (Martinsen & Bakken, 1990; Steen & Andresen, 1997; Payros *et al.*, 1999; Graziano, 2001; Floquet & Hennuy, 2003; Lucente & Pini, 2003; Vernhet *et al.*, 2006; Spörli & Rowland, 2007) and their anatomy has been rarely described at scales > 100 km.

Correspondence: Pierre Callot, LMTG, Université de Toulouse, CNRS, IRD, OMP, 14 av. Edouard Belin, F-31400 Toulouse France. E-mail: callot@lmtg.obs-mip.fr.

This paper deals with the Ayabacas Formation of southern Peru, an interesting rock unit that has received a puzzling variety of interpretations. Here, we confirm one of these by demonstrating that the unit was formed by the giant submarine collapse, at the Turonian-Coniacian transition, of a carbonate platform that had developed in the Andean back-arc basin during the Albian-Turonian interval. The unit mostly consists of millimetric to kilometric size limestone fragments and can therefore be described as a limestone megabreccia (*sensu* Spence & Tucker, 1997). In the northeastern half of the study area, these fragments are enclosed in reddish siltstones and mudstones reworked from the underlying stratigraphic unit, and rock fragments from older units also occur; only limestones are involved in the southwestern half.

The Ayabacas Formation forms a single mass-wasting body, which displays noteworthy internal facies variations. It irregularly crops out over $> 60\,000\,km^2$ and is inferred to extend over more than $80\,000\,km^2$. Its thickness varies

from 0 to $\geq$ 500 m, and its volume is estimated to be $>10\,000\,km^3$ ($>10^{13}\,m^3$). Although it is formed by a number of coalescent landslides, these can be clearly distinguished only in some cases. No undisturbed strata divide the Ayabacas Formation into subordinate sliding units. The Ayabacas collapse is $\geq$ 500 km in width and >100 m in average thickness, and when compared with the published dimensions of mass-wasting bodies it plots at the far end of Lucente & Pini's (2003) compilation diagram. The Ayabacas thus appears as the most extensive ancient submarine mass-wasting body currently known, and one of the thickest. Its extension and thickness are of the same magnitude as the largest and thickest recent bodies described to date, e.g. the Storegga Slide (Haflidason *et al*., 2004, 2005), the Bjørnøyrenna Slide (Vorren & Laberg, 2001), the Cape Fear Slide (Popenoe *et al*., 1993), the Saharan Debris Flow (Gee *et al*., 1999), the Israel Slump Complexes (Frey-Martínez *et al*., 2005) or the Orotava-Icod-Tino Avalanche (Wynn *et al*., 2000). Here, we focus on the age and anatomy of the Ayabacas Formation, and on the cause(s) of the collapse.

Absolute stratigraphic ages mentioned in this paper are taken from Hardenbol *et al*.'s (1998) chart unless specified otherwise. We use the abbreviation Ma (*mega-annum*) for a point in time, and Myr (millions of years) for a duration of time.

THE AYABACAS FORMATION IN ITS GEOLOGICAL SETTING

Location of the study area and basin architecture

The study area extends in southern Peru, along the southwestern rim of the Cordillera Oriental and throughout the Altiplano and Cordillera Occidental, including the Arequipa area (Figs 1 and 2). The number and extension of Ayabacas Formation outcrops decrease markedly toward the west-southwest due to an increasing cover of Neogene volcanic rocks and other deposits. No mid-Cretaceous limestone unit has been mapped so far immediately west and south of the study area.

The study area includes a few important Andean-age structural systems that have also controlled a number of depositional characteristics of the pre-orogenic accumulations, such as facies and thicknesses (Sempere, 1995; Sempere *et al*., 2002a, b, 2004b, c; Pino *et al*., 2004). In particular, Mesozoic subsidence has constantly been lower, and depositional environments shallower, northeast of the Urcos-Ayaviri-Copacabana-Coniri fault system (abbreviated as SFUACC in Spanish; Fig. 1), a major lithospheric boundary (Carlier *et al*., 2005) that has behaved as a mainly sinistral fault system during the Andean orogeny (Sempere *et al*., 2002b, 2004b; Sempere & Jacay, 2006, 2007). The Cusco-Lagunillas-Laraqueri-Abaroa structural corridor (abbreviated as CECLLA in Spanish; Fig. 1) is a broad structural system which separates two domains that behaved very distinctly during the Cenozoic and at least the Jurassic, more subsidence and a much deeper depositional environment being recorded west of the CECLLA (Sempere *et al*., 2002b, 2004b). We provide evidence below that the SFUACC and CECLLA fault systems played a significant role during the Ayabacas collapse as they separate domains characterised by different facies distribution, subsidence, and depositional processes.

The Ayabacas Formation and underlying units were deposited in the southern region of the western Peru back-arc basin (WPBAB), which was active in the Jurassic and Cretaceous (Jaillard *et al*., 1995). This basin had developed in an extensional tectonic context and deepened overall to the west. Subsidence was greatly enhanced in the mid-Cretaceous, starting in the Early Albian, as a consequence of the western WPBAB evolution toward a state of marginal basin in central Peru, due to considerable lithospheric thinning there (Casma sub-basin; Atherton & Webb, 1989; Atherton, 1990; Jaillard, 1994; and references therein). Myers (1974) proposed that the accumulation of >2 km of eastward-tapering carbonates and marls during the Early Albian-Turonian interval ($\sim$109–89 Ma) east of the Casma sub-basin implied significant subsidence, which must have been facilitated by the ongoing lithospheric thinning. The edge of the continental domain, along which the Albian-Turonian carbonate platform developed, thus technically behaved as a kind of passive margin in relation to the much deeper Casma sub-basin to the west. To the south ($\sim$13–15°S), 1–2 km of calc-alkaline basalts and basaltic andesites interbedded with locally bituminous Albian marine strata were deposited in the southern extension of the WPBAB, which was narrowing in a southeastward direction (Atherton & Aguirre, 1992; Jaillard, 1994). A 'passive margin' setting similar to that in central Peru can thus be proposed for the carbonate platform in southern Peru, although lithospheric thinning was much less intense in this region.

Stratigraphy of southern Peru

The Mesozoic stratigraphy of southern Peru is summarised in Fig. 3 (see supplementary documentation online for details). Before the Ayabacas collapse, the Mesozoic units of southern Peru were deposited in a largely marine basin, with continental to shallow-marine facies in the northeast, and deeper water facies in the southwest and west. In contrast, the units younger than the Ayabacas Formation were deposited in an almost exclusively continental basin that was bounded to the southwest by topographic highs, apparently volcanic in nature. In particular, the Arcurquina Formation (and equivalent deposits) mostly consists of marine limestones, whereas the Lower Vilquechico Formation (and equivalents) is dominated by abundant red mudstones that testify to a continental or near-continental environment (Jaillard, 1995). In the Central Andean domain, away from the coast, true marine deposits are extremely rare afterwards. The Ayabacas Formation was thus deposited at the time when

 Basin Research, 10.1111/j.1365-2117.2008.00358.x

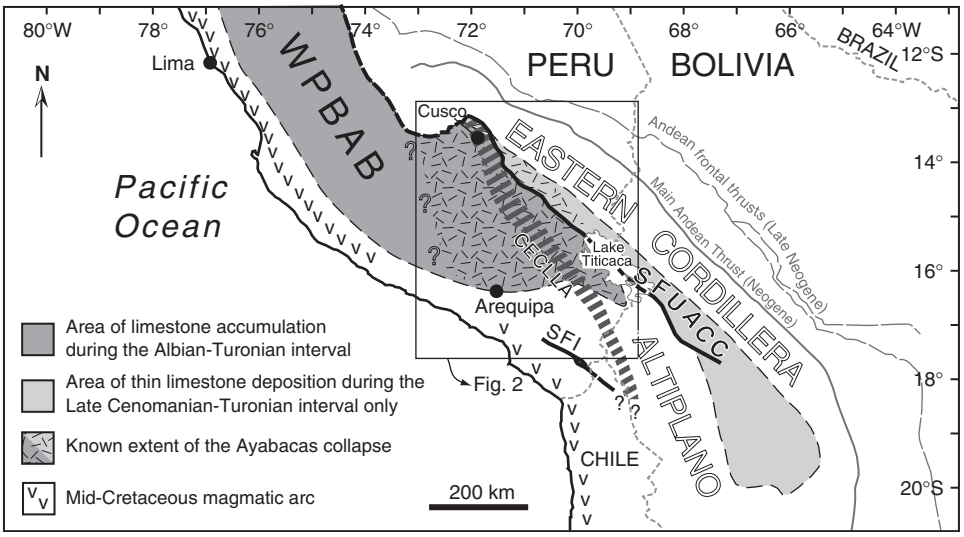

Fig. 1. Map of southern Peru and adjacent regions with elements relevant for Albian to Turonian times. Both shaded areas belong to the western Peru back-arc basin (WPBAB) which accumulated mostly limestones during this time interval. The Early and Middle Albian transgression is only recorded in the main basin (darker shading); the Late Cenomanian–Turonian transgression flooded this main basin and also the sub-basin located northeast of the SFUACC system (lighter shading). The Ayabacas collapse (irregular dashes) developed in the northwesternmost segment of this sub-basin, and in the southwestern part of the main basin. A magmatic arc was active along the present-day coastal belt, but, before the Coniacian, the region south of Arequipa was apparently devoid of volcanic activity as only plutons are recorded there. CECCLA, SFUACC: see text; SFI = Incapuquio fault system (Spanish abbreviation). Adapted from Jaillard & Sempere (1991), Jaillard & Arnaud-Vanneau (1993), Jaillard (1994), Sempere (1994), Jaillard *et al.* (1995), Sempere (1995), Sempere *et al.* (2002b, 2004b).

the south Peruvian basin underwent a dramatic and permanent change from marine to continental conditions.

Some units are particularly relevant to the Ayabacas issue:

- The Paleozoic basement is Ordovician to Devonian in age and mainly consists of dark shales intercalated with generally subordinate siltsones and sandstones.
- The Middle Jurassic Muni Formation (red mudstones and subordinate sandstones) grades into the Late Jurassic Huancané Formation s.s. (dominantly quartzose sandstones of fluvio-eolian origin), these two units forming a continental sedimentary system prograding toward the southwest.
- Some deformation affected the southern Peruvian basin at some time in the Early Cretaceous (and, possibly, Late Jurassic), in particular along the SFUACC system (Sempere *et al.*, 2002b, 2004b). This deformation produced local uplifts that led to partial to complete erosion of the Mesozoic succession, locally down to the Paleozoic basement. The resulting erosional surface was subsequently onlapped by the major mid-Cretaceous transgression. In the Arequipa area, this transgression is mainly recorded by the ~250 m-thick Arcurquina Formation. In the Altiplano, the ~100 m-thick transgressive stratigraphic set of late Early to middle Cretaceous age is formed by the Angostura (conglomerates and sandstones, occurring in specific areas), Murco (mainly red mudstones and siltstones) and Arcurquina (marine, regularly bedded, thickening-upward, grey to black, organic-rich micritic limestones; see section 'Age of the Ayabacas formation') formations, and onlaps the mentioned regional unconformity. Contacts between these units are gradational. Interstratified red mudstones and thin, grey to black limestones are typical of the rapid Murco-Arcurquina transition, as in the Arequipa area. In the Cusco area, the continental set formed by the Angostura and Murco formations is represented by the local Maras Formation (Carlotto *et al.*, 1996), which mainly consists of red mudstones and silstones, and evaporite masses (mainly gypsum; halite also occurs).
- The Ayabacas Formation, the object of this paper, consists of an extraordinarily deformed, chaotic unit reworking previous deposits and rocks. Although the Ayabacas and Arcurquina formations dominantly consist of limestones and occupy the same stratigraphic position, overlying the Murco Formation and underlying the Vilquechico Group and equivalent units, they must be formally distinguished since the Arcurquina was deposited in regular beds in a stable carbonate platform, whereas the Ayabacas resulted from the reworking of the Arcurquina and previous units: their deposition was therefore neither contemporaneous nor driven by similar processes. Owing to these markedly different depositional processes, they display distinct characteristics, which are obvious in the field.
- The Vilquechico Group (Late Campanian-Early Paleocene, ~700 m thick) post-dates the Ayabacas Formation and its typical deformation. Its equivalent in the Arequipa area is the $\leq$ 400 m-thick Ashua Formation (Cruz, 2002). A Coniacian ammonite from the Ashua Formation testifies that the Ayabacas-Ashua contact represents an interruption of the stratigraphic record of little time duration, if any. In contrast, the

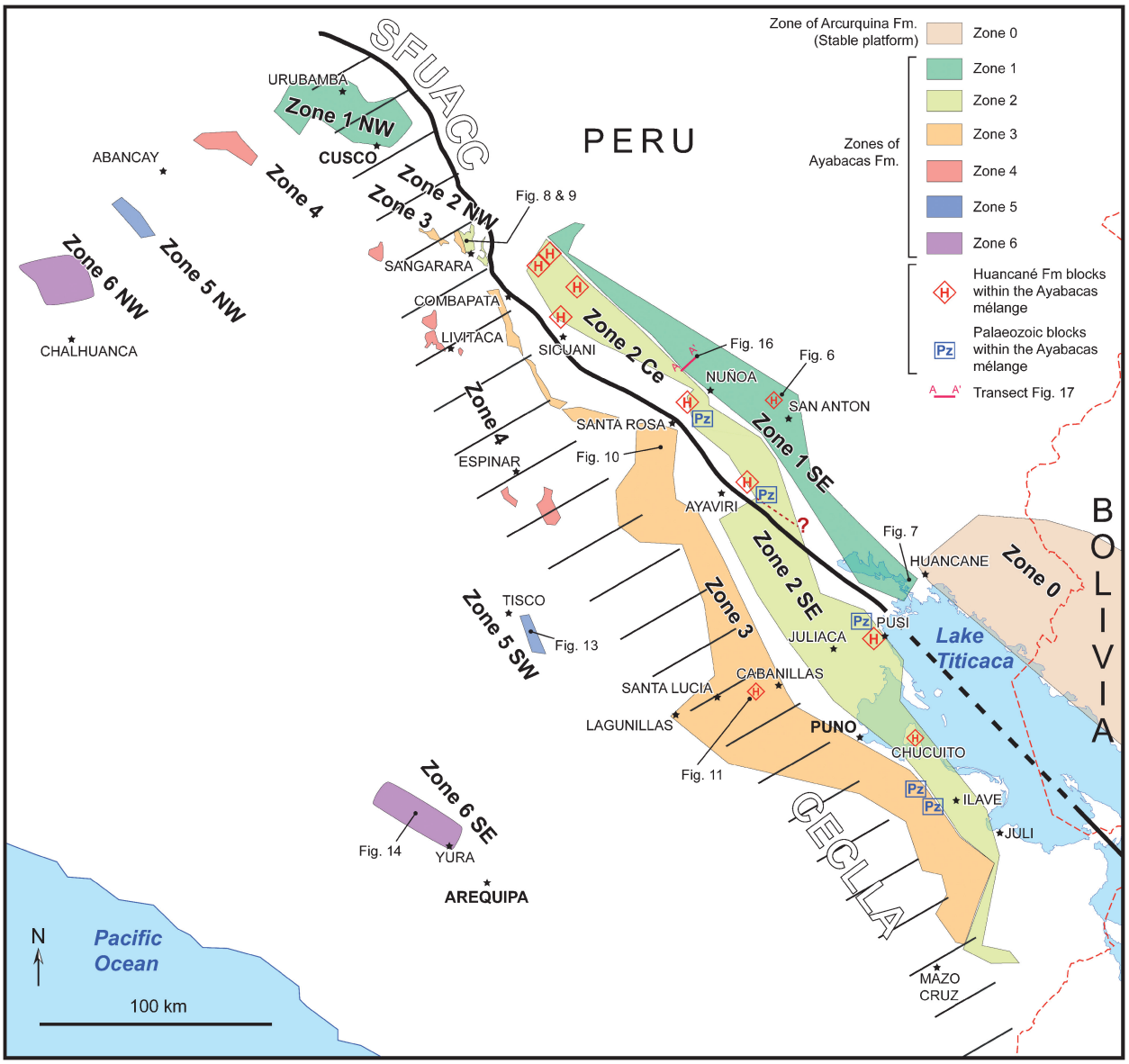

Fig. 2. Distribution of main deformational facies in the Ayabacas Formation, localities cited in text, and location of the SFUACC and CECLLA fault systems. According to deformational facies, outcrops of the Ayabacas Formation are distributed into six zones, numbered 1–6 (see details in the text). Zone 0 is formed by the Arcurquina Formation, i.e. the deposits of the stable carbonate platform. Pz and H indicate sites where massive blocks respectively derived from the Palaeozoic and Huancané Formation occur within the mélange; these sites are located near the SFUACC fault system, or near local normal faults (San Antón and Cabanillas). Note the NW–SE variations in zone width, in particular between northern (Cusco–Abancay–Chalhuanca) and southern (Huancané–Juliaca–Santa Lucía–Lagunillas–Yura) transects; see details in the text.

Ayabacas-Vilquechico contact, more to the north, apparently marks a ~5 Myr-long hiatus, during which some erosion must have occurred (Sempere *et al.*, 2002a, 2004a). However, the preservation of stromatolites at the very top of the Arcurquina Formation, east of Huancané, suggests that this hiatus may have been much shorter at least locally.

Stratigraphic and depositional characteristics of the Ayabacas formation

The Ayabacas Formation typically lacks internal stratification and presents a highly disrupted to chaotic aspect, in marked contrast with the underlying and overlying units. Its thickness is irregular but generally increases from a few metres in the northeasternmost sections, where it can be locally lacking, to $\geq$ 500 m in the west and southwest.

The Ayabacas mainly consists of mm- to km-size fragments of regularly stratified and/or folded limestones, mostly or entirely reworked from the Arcurquina Formation, and enclosed in a largely red-siltstone 'matrix' reminiscent of the Murco deposits (given their similar facies, presence of fragments of the Sipín limestones and involvement of Muni red siltstones cannot be excluded). Particularly significant is the frequent local occurrence of

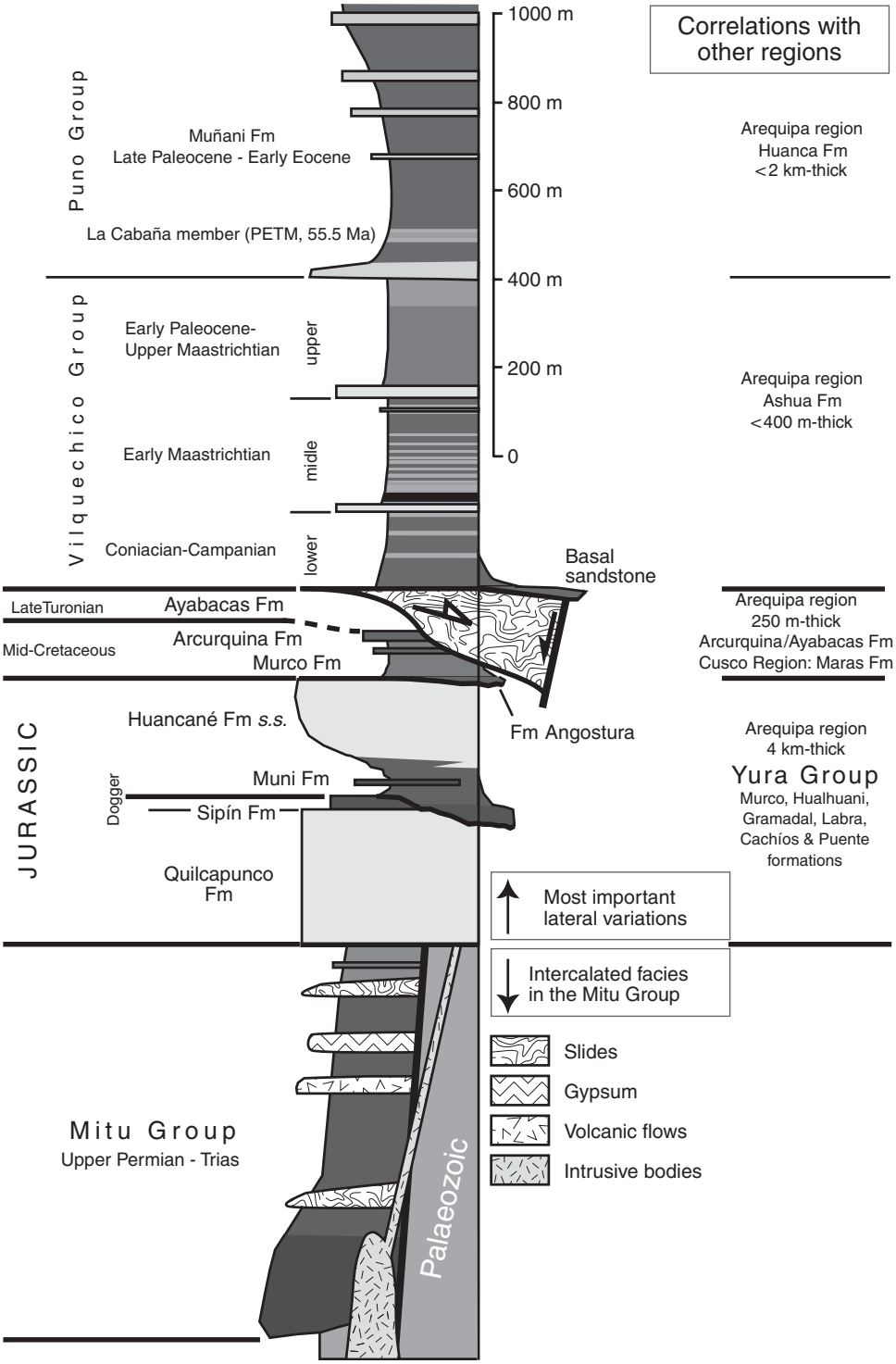

Fig. 3. Generalised Palaeozoic to Paleogene stratigraphic column in the Lake Titicaca region. Correlations with other areas are specified on the right. Thicknesses are approximate and subject to lateral variations. PETM = Paleocene-Eocene Thermal Maximum. Adapted from Sempere *et al.* (2004a).

fluidised sediments and breccias within the 'matrix'. In northeastern areas, lithified blocks of Huancané sandstones and Paleozoic shales are, respectively, commonly and locally observed. In specific areas, cm- to dm-size clasts of typical Mitu volcanic conglomerates are also found.

We underline that no undisturbed marine limestone strata occur either within or at the top of the Ayabacas Formation, which is directly overlain by reddish strata of mainly continental origin.

Age of the Ayabacas formation

A regional synthesis of the available information concerning the units that predate and postdate the Ayabacas Formation indicate that the collapse occurred near the Turonian-Coniacian transition, i.e. at ~90–89 Ma (see supplementary documentation online, and Callot *et al.*, 2007).

The Arcurquina Formation was deposited during two transgressive periods, which are also recorded in the more

subsident northern Peruvian part of the WPBAB. The first transgression and highstand lasted from the middle Early to the late Middle Albian (~110–102 Ma; Hardenbol *et al.*, 1998). The Late Albian–Middle Cenomanian interval (~102–95 Ma, ~7 Myr) was characterised by a relative regression. The second transgression was initiated in the latest Middle Cenomanian (~95 Ma) and highstand lasted until the Late Turonian (~90–89 Ma). Only the second transgression reached areas northeast of the SFUACC system, where compacted depositional rates varied between 2.7 and 4.3 m Myr^{-1}, whereas in the Arequipa area they were ~20 m Myr^{-1} for the Early–Middle Albian interval, and ~28 m Myr^{-1} for the Late Cenomanian–Turonian interval. This contrast implies that subsidence was higher by one order of magnitude in the Arequipa area than northeast of the SFUACC, as suggested by the overall deeper and thicker facies in the former. Our chronostratigraphy confirms the recognition of the OAE-2 event in the lower part of the Arcurquina Formation in westernmost Bolivia (Graf, 2002; Graf *et al.*, 2003) and nearby Peru, where it is represented by an organic-rich mudstone layer referred to as the 'Nuñoa-1' level (Fig. 4; and supplementary documentation online).

The Vilquechico Group and Ashua Formation sharply postdate the Ayabacas collapse in the Lake Titicaca and Arequipa regions, respectively. These deposits dominantly consist of red mudstones and span the Coniacian–Paleocene interval (Jaillard *et al.*, 1993; Sigé *et al.*, 2004). A similar stratigraphic contrast is known in northern Peru, where the Turonian limestones are sharply overlain by ~300 m of reddish to brown mudstones and fine sandstones that were deposited in marine to non-marine environments from the Early Coniacian to the Middle Campanian. This noteworthy discontinuity is thought to reflect the onset of aerial erosion in western areas throughout the Central Andes (Jaillard, 1994; Sempere, 1994). As indicated by ammonite faunas in northern Peru, this sharp change from carbonates to reddish mudstones occurred approximately at the Turonian–Coniacian transition. Because the Ayabacas Formation post-dates the termination of the carbonate platform and pre-dates the onset of red mudstone deposition, it coincides with this change. The Ayabacas collapse is thus likely to have also occurred near the Turonian–Coniacian transition (~90–89 Ma).

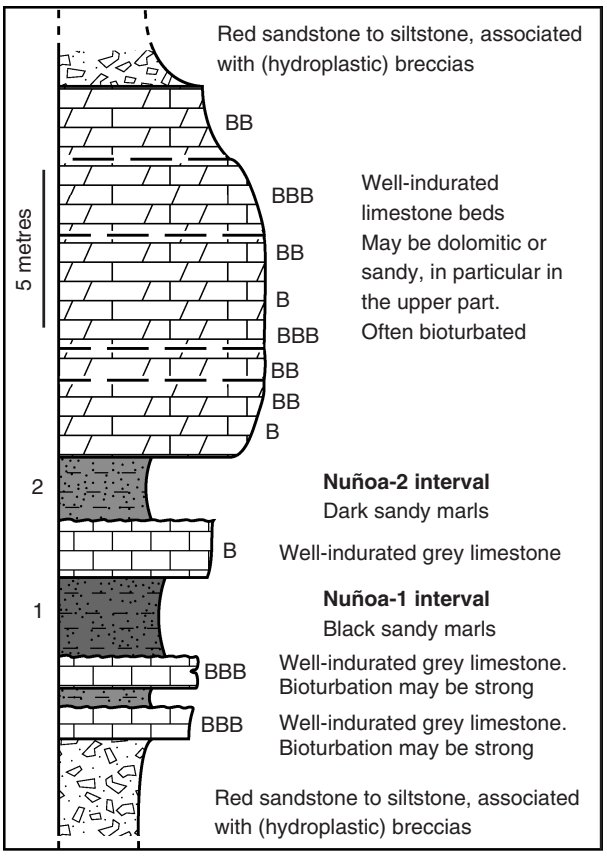

Fig. 4. Standard section of limestone blocks in Zone 1. Stratigraphic sections from San Antón (Pacuta and Coñejuno), Yanaoco, Nuñoa (Antacalla), Larimayo 1 and 2, and Cusco, are shown. Thicknesses are used in Table 1 (see supplementary documentation online). Nuñoa-1 and Nuñoa-2 mudstone levels may include limestone fragments derived from the brecciated base of the overlying limestone bed. Minor lateral facies variations occur: the three beds underlying the Nuñoa-1 interval cannot be distinguished everywhere; the limestone bed between the Nuñoa-1 and Nuñoa-2 intervals is locally missing (e.g. in San Antón).

ONE DISRUPTED UNIT, A VARIETY OF INTERPRETATIONS

Previous descriptions of the Ayabacas Formation, and conflicting interpretations

This intriguing unit was first described as the Ayavacas [*sic*] Formation by Cabrera La Rosa & Petersen (1936) from the outcrops near the namesake village located ~10 km northeast of Juliaca; spelling was later corrected to Ayabacas by Sempere *et al.* (2000) to be in conformity with the official local toponymy. The first studies were mainly limited to the area formed by the Pirín, Ayabacas and Pusi localities, due to the existence of a small oil field. Because Rassmuss (1935) and, more precisely, Cabrera La Rosa & Petersen (1936), authors have wondered about the amazing peculiarities of these deeply disturbed limestones (Heim, 1947; Newell, 1949; Kalafatovich, 1957; Portugal, 1964, 1974; Audebaud & Laubacher, 1969; Chanove *et al.*, 1969; Audebaud, 1970, 1971a, b; Audebaud & Debelmas, 1971; Audebaud *et al.*, 1973; De Jong, 1974; Laubacher, 1978; Green & Wernicke, 1986; Klinck *et al.*, 1986; Ellison *et al.*, 1989; Moore, 1993; Carlotto *et al.*, 1992, 1996; Jaillard, 1994; Sempere *et al.*, 2000; Carlotto, 2002). Newell (1949) eloquently described these peculiarities, highlighting that the unit is intricately folded and faulted, in extreme disorder, in so far that it may form a nondescript mass of red shales and large limestone blocks; complex masses of deformed limestone are locally violently disturbed; beds may form intricate isoclinal to recumbent folds, and locally they '*are oriented in every conceivable position with numerous duplications of the same strata in every hillside*'. Newell (1949) also described

 Basin Research, 10.1111/j.1365-2117.2008.00358.x

fragments of older units involved in the Ayabacas Formation, and emphasised that the formation displays a '*very characteristic*' deformation that contrasts with the underlying and overlying units.

However, although descriptions of the Ayabacas Formation have been generally similar, interpretations have divided between tectonic and gravitational processes, and, among the latter, between subaerial and submarine sliding (discussed below).

Compressional tectonic interpretations, and why they are untenable

The first work concerning the Ayabacas Formation was produced by Rassmuss (1935), who described the limestone unit as a chaotic formation and suggested a tectonic explanation for its disrupted aspect. Heim (1947) and Newell (1949) both observed multiple repetitions of stratified limestone blocks and interpreted them as the result of Andean tectonics. Audebaud (1967) wondered whether early mass sliding might have been partly responsible for the deformation, but considered that the deformation was mainly of tectonic origin (Audebaud & Laubacher, 1969; Audebaud, 1970, 1971a, b; Audebaud & Debelmas, 1971; Audebaud *et al*., 1973), locally complicated by early karstification (producing the noteworthy breccias mentioned below), gypsum diapirs, and hypovolcanic intrusions (Audebaud, 1971a). In the Pirín area (SW of Pusi), Chanove *et al*. (1969) interpreted the Ayabacas Formation as a piling-up of tectonic nappes.

The observed deformation has however a markedly 'soft' aspect and is hardly compatible with tectonic processes. Tectonic thrusting and folding would have produced typical features, such as slickenslides and striated faults, oriented tectonic breccias, cleavage, and/or pervasive calcite veining. But all of these elements are missing. Away from Andean structures, faults in limestone blocks neither display calcite slickenslides nor are they striated. Limestone blocks are piled up without signs of tectonic thrusting, as noted by Heim (1947) and Portugal (1964, 1974). Limbs of recumbent folds are generally unthinned (Portugal, 1964, 1974), suggesting a low overlying load during folding (Audebaud, 1967). Contrary to what is expected in the case of tectonic phenomena, orientations of folds and faults in the Ayabacas Formation are usually extremely variable at each locality (Fig. 5a).

It is also noteworthy that the grade of deformation in the Ayabacas Formation decreases toward the Eastern Cordillera, i.e. in the direction of increasing Andean deformation. Andean folding and faulting has very generally developed at much larger scales than the Ayabacas deformation. As underlined above, the Ayabacas Formation contrasts greatly with the underlying and overlying units, which have similar bedding attitudes at each locality and have generally been only tilted by Andean deformation at the outcrop scale. Furthermore, in all visited localities, the basal and top contacts of the Ayabacas Formation are evidently stratigraphic, not tectonic.

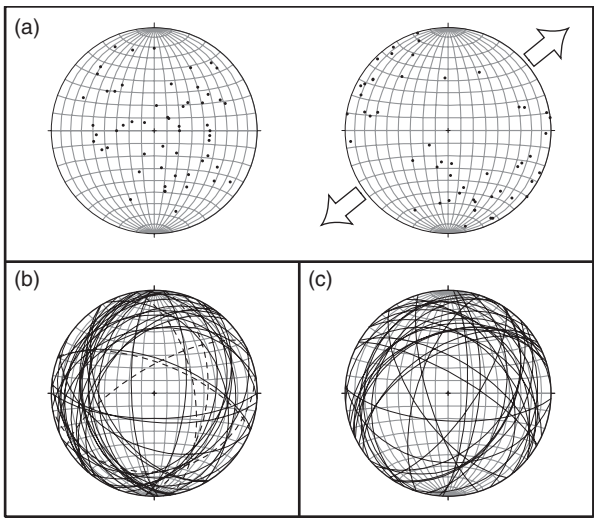

Fig. 5. Schmidt stereonets (lower hemisphere) of data from Zones 2 and 3. (a) Fold axes in rafts ($N = 52$) in the Ilave-Juli (left), corrected (right) for tectonic tilting (using underlying and/or overlying units). Scattering is evident before correction, implying that deformation was not produced by orogenic shortening. A ~NW–SE preferential orientation becomes apparent after correction, suggesting sliding occurred to the NE or SW. (b) Bedding attitudes of rafts (solid lines, $N = 35$) and Huancané blocks (dashed lines, $N = 5$) dispersed in the mélange in the Pusi area, where Chanove *et al*. (1969) interpreted the unit as resulting from the piling up of tectonic nappes. Their random distribution is not compatible with orogenic tectonics. (c) Bedding attitudes of Palaeozoic rafts in the Ayabacas mélange, from a ~3 km^2 area ~15 km south of Chucuito ($N = 34$); their random distribution confirms they are elements in a sedimentary mélange, and not the result of tectonic deformation.

All these observations are compelling evidence against any idea that the Ayabacas deformation results from large-scale Andean tectonic deformation.

Subaerial gravity sliding: also untenable

De Jong (1974) published interesting descriptions of the Ayabacas Formation in the Puno-Juliaca area and rightfully criticised Newell's (1949) and Chanove *et al*.'s (1969) tectonic interpretations. However, he favoured that the unit resulted from subaerial sliding in the mid-Cretaceous, drawing a comparison with the Amargosa Chaos in Death Valley, western USA. Laubacher (1978) discussed the diverse interpretations published at that time, and concluded that both Chanove *et al*.'s (1969) and De Jong's (1974) interpretations were warranted. Klinck *et al*. (1986) and Ellison *et al*. (1989) also favored subaerial gravity sliding, but of Late Neogene age.

Green & Wernicke (1986) and Moore (1993) claimed that the Ayabacas Formation was a continental collapse produced in the Late Miocene by large-magnitude crustal extension, caused by the gravitational spreading of the overthickened Andean crust. They mapped low-angle detachments at the base of the Ayabacas Formation, and estimated that they accomodated 10s of kilometers of extension. They agreed with De Jong's (1974) observations

of similarities between the Ayabacas Formation and the Amargosa Chaos.

A subaerial sliding interpretation is precluded, however, by the abundance of plastic, soft-deformation features, hydroplastic breccias and fluidised sediment facies. The fact that the Ayabacas deformation is regionally postdated by Late Cretaceous strata precludes any Neogene process as its cause. Interpretations by Klinck *et al.* (1986), Green & Wernicke (1986), Ellison *et al.* (1989), and Moore (1993) are contradicted by the fact that the base of the Ayabacas Formation is clearly not a tectonic contact, at any locality visited by us.

It is interesting that the Ayabacas could be interpreted as the product of contractional tectonics by some authors and of extensional tectonics by others. In particular, the same area of Pirín (southwest of Pusi) has been mapped as a piling-up of contractional nappes by Chanove *et al.* (1969) and as structured by low-angle normal faults, interpreted to express ≥ 5 km of extension, by Green & Wernicke (1986) and Moore (1993). In addition to the fact that key characteristics have been overlooked, such contrasts in interpretations are intriguing.

Evidence for submarine sliding

Cabrera La Rosa & Petersen (1936) were the first to precisely describe the Ayabacas Formation. In particular, they noted that generation of its typical limestone breccias could not be explained by any tectonic deformation, and proposed instead that submarine sedimentary processes were responsible for their facies and the overall disruption displayed by the unit. Although the notion of submarine mass wasting was largely ignored at that time, these authors reached conclusions close to modern models, understanding that limestone strata had been fragmented before their lithification and that brecciation had occurred 'on the sea bottom', probably due, in their mind, to a tsunami-triggered instability.

Portugal (1964, 1974) was the first to clearly identify, in the Puno-Santa Lucia area, that the Ayabacas Formation was the result of submarine mass wasting, toward the southwest, necessarily on a slope, and that sliding had possibly been facilitated by the underlying red mudstones; among other features, he emphasised that the chaotic distribution of limestone blocks was evidence that they had moved independently from one another, and that deformation preserved unthinned limbs and produced no cleavage.

In the Cusco area, Carlotto *et al.* (1992, 1996) re-interpreted the intriguing disruption displayed by Kalafatovich's (1957) Yuncaypata Formation as a result of synsedimentary deformation, and identified this unit as the local expression of the Ayabacas Formation. The peculiarities and size of this formation in southern Peru were underlined by Sempere *et al.* (2000), who recognised again that the unit, best described as a limestone megabreccia, resulted from submarine sliding.

In the northeastern half of the study area (Zones 1–3 as defined below), the Ayabacas Formation generally has a chaotic appearance (Fig. 5b). The limestones are highly disturbed, folded, disrupted, fragmented and brecciated (e.g. Newell's (1949) description above). When folded, limestone strata yielded plastically, and are deformed without cleavage. Other evidence of soft-deformation includes: slumps, fluidised sediments, hydroplastic breccias, clastic and/or mud dykes. Limestone blocks are often chaotically distributed, and have clearly moved independently from one another. All these characteristics are strongly indicative of gravitational submarine deformation, especially as shown by 3D seismic images of recent landslides (e.g. Collot *et al.*, 2001; Huvenne *et al.*, 2002; Frey-Martínez *et al.*, 2005, 2006), and confirm the interpretation of the Ayabacas Formation as a giant submarine mass-wasting body.

ORGANISATION OF THE AYABACAS COLLAPSE INTO DEPOSITIONAL ZONES

Distribution of deformation facies characterises depositional zones

Restriction of previous studies to limited areas has obviously hampered accurate and precise interpretations of the intriguing Ayabacas deformation. Here we attempt to understand the collapse as a whole, i.e. over its entire known extension. Such a large-scale vision of the basin consolidates the interpretation of the Ayabacas Formation as the collapse of a major part of the regional Albian-Turonian carbonate platform.

The Arcurquina Formation, which marks the parts of the platform that were not destabilised, mainly occurs in the eastern part of the basin. The Ayabacas Formation characteristically occurs in all localities WSW of this area. Six different zones are characterised on the basis of the deformational facies exhibited by the Ayabacas Formation (Fig. 2), and a seventh corresponds to the northeastern 'stable' area. Facies evolve progressively from Zones 1 to 3, and from Zones 4 to 5. In contrast, sharp facies differences separate Zone 3 from Zone 4, whereas Zone 5 is somewhat distinct from Zone 6 in some aspects.

Zone 0: Northeastern, undisturbed part of the platform

In Peru, the Arcurquina Formation is entirely preserved northeast of Lake Titicaca (Figs 1 and 2), where it is < 25 m-thick and overlies the red mudstones and siltstones of the Murco Formation. The Arcurquina Formation displays lagoonal to supratidal facies; bioturbation is often intense in the former. East of Huancané, the very top of the unit exhibits numerous stromatolites which have been buried by the overlying red mudstones (Lower Vilquechico Formation). This unit is neither fragmented nor folded and there is no indication of soft-sediment deformation, testifying to the stability of this part of the basin during the Ayabacas collapse.

 Basin Research, 10.1111/j.1365-2117.2008.00358.x

Zone 1: Gravitational sliding, folding and thrusting of rafts and sheets

Zone 1 is entirely located northeast of the SFUACC. In this zone, the Ayabacas Formation displays synsedimentary deformation of diverse intensity. It consists of a mélange of limestone blocks and a mainly red, partly calcareous and locally sandy, mudstone to siltstone matrix, sometimes turning to yellow near the limestone masses. The unit is very variable in thickness: locally, the Vilquechico Group directly overlies the Huancané Formation and the Ayabacas and Murco formations are totally absent; in other areas, the Ayabacas Formation consists of a chaos of limestone rafts and folded strata floating in the red matrix, whose thickness can be over several hundreds of metres.

In Zone 1, the unit mainly consists of limestone sheets or rafts 'floating' in the red matrix. These sheets and rafts are generally $\leq$ 20 m-thick, fairly reflecting the depositional thickness before the collapse when compared with Zone 0, and clearly exhibit the same internal stratigraphy (Fig. 4). Although relatively thin, the sheets display a fair to excellent lateral continuity, ranging from 40 m (raft-type end-member) to over several kilometres (sheet-type end-member, as observed in aerial photography). These limestone rafts can overlap each other and form stacks of two or more elements separated by breccias and red marly siltsones (Fig. 6). Some rafts are strongly folded; folds are generally asymmetric and recumbent, rarely with thinned limbs, and without any cleavage (Portugal, 1964, 1974; Audebaud, 1967; De Jong, 1974; Sempere *et al.*, 2000). Although a large-scale organisation is generally evident in aerial photographs, the folds are chaotically organised at the outcrop scale. Orientation of fold axes is variable, but folds are generally NE- or SW-vergent, indicating that sliding occurred in opposite directions. Along with evidence for synsedimentary normal faulting, this suggests that opposite slopes were locally created by tectonic tilting of the substratum.

The base of the standard stratigraphic section (Fig. 4) of these rafts and sheets consists of two (or sometimes three) 0.5–3 m-thick lithified limestone beds that display incipient hard-grounds at their tops. These limestones are separated by two to three darker and marlier beds (the Nuñoa-1 and Nuñoa-2 intervals, and a lower, similar, ~0,5 m-thick bed; see supplementary documentation online for details) that may include limestone fragments derived from the brecciated base of the overlying limestone; this brecciation apparently developed at the interface between the two lithologies through injection of the unlithified mudstones into the already partly lithified limestones. An 8–14 m-thick set of limestone beds forms the upper part of the section and is often highly bioturbated. Bioturbation affects all beds, with among-block vertical and lateral variations, but ranges from very intense to nearly absent.

Other breccias, generally hydroplastic in origin, are frequently observed at the bases and tops of rafts and sheets (they are particularly well-exposed at Yanaoco, ~8 km WSW of Huancané, with abundant fluidised sediments, and randomly oriented clastic and/or mud dykes). In good outcrops, the matrix that usually separates rafts and sheets

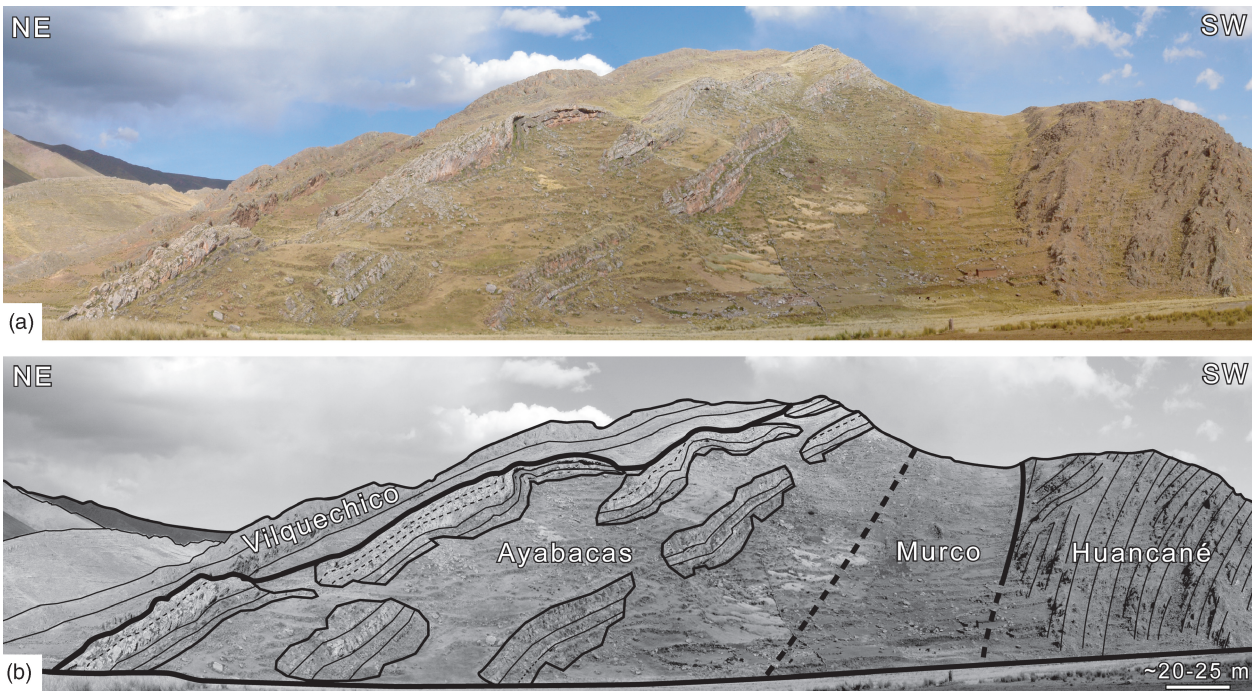

Fig. 6. (a) Deformation typical of Zone 1 near Larimayo (~9 km NNW of San Antón, UTM 0354876–8396892–4081 m, Zone 19L). Limestone rafts (interpretative outline highlighted in (b) 'float' in a matrix of siltstones and hydroplastic breccias and overlap each other with some gentle folding. Stratigraphic sections from each raft (Fig. 4) are identical. The Ayabacas Formation is underlain by the Huancané Formation (SW) and overlain by the Vilquechico Formation (NE), which includes here its basal sandstone member (Fig. 3); both units have been only tilted by Andean tectonics, very unlike the Ayabacas Formation.

appears itself as a breccia of red to locally yellow marly siltstones, and includes clearly fluidised sediments (Fig. 7). Clasts are of mm- to m-size and somewhat heterogeneous in nature, usually from surrounding limestone blocks; reddish and yellowish sandstones are also found. Clastic and mud dykes partly or completely intersect some limestone blocks, and others commonly cut across breccias within the matrix.

Two sub-zones, one limestone-rich and the other limestone-poor, are respectively distinguished in the SE (from Huancané to Sicuani) and NW (Cusco-Urubamba area) parts of Zone 1 (Fig. 2). The NW part of Zone 1 displays a peculiar large-scale facies characterised by sporadic (either isolated or concentrated in limited areas), chaotic limestone blocks dispersed within large stretches covered by the Maras Formation, which is the local equivalent of the Murco Formation and consists of red calcareous siltstones and subordinate gypsum and halite bodies. The presence of evaporites beneath thin carbonate deposits is likely to have favoured sliding, and facilitated larger displacements of limestone sheets, rafts and blocks during the collapse (Vendeville & Cobbold, 1987; Demercian *et al.*, 1993; Spathopoulos, 1996; Brun & Fort, 2004; Gradmann *et al.*, 2005). The sporadic occurrence, and thus rarity, of limestone blocks in this area is explained by their massive removal toward the SW, due to a regional facilitation and enhancement of sliding by the evaporite horizons that underlay the carbonate platform.

Zone 2: Chaotic melange of commonly strongly folded rafts

Zone 2 forms a strip running from the southern (Juli, Ilave) and western (Pusi, Juliaca) shores of Lake Titicaca, to Sangarara through Santa Lucía and Sicuani. Three sub-zones are distinguished, respectiveley in the SE, centre (sub-zone 2Ce), and NW (Fig. 2). Sub-zones 2SE and 2NW are located southwest of the SFUACC system and exhibit very similar facies; in contrast, sub-zone 2Ce is located northeast of the SFUACC and displays somewhat different facies. No sharp boundary separates the adjacent zones 1 and 2; the change in deformational facies is transitional, in particular between Zone 1 in the northeast and sub-zones 2SE and 2NW in the southwest. In the three sub-zones, and in particular in sub-zone 2Ce, the Ayabacas Formation is on the whole thicker than in Zone 1. Its thickness varies generally rapidly, from locally 0 m to >400 m.

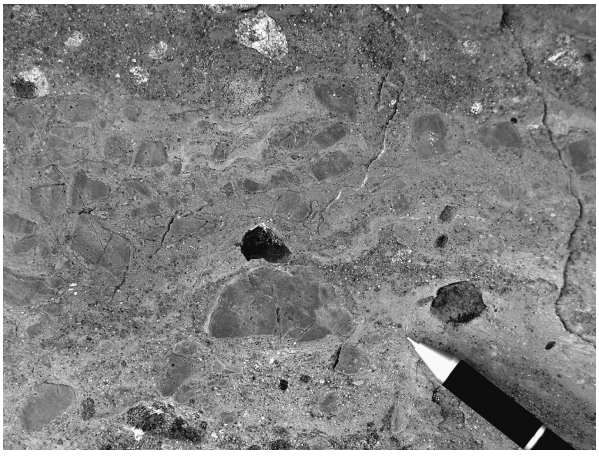

Fig. 7. Fluidised sediments in Zone 1, near Yanaoco ($\sim$8 km WSW of Huancané). Real size of the picture is $\sim 14 \times 10.5$ cm. Note the cm-sized limestone clasts, tilted and floating in a fluidised matrix of marly–sandy sediments.

Limestone rafts are similar to those in Zone 1, but sheets are less common. They are thicker, generally about 20–30 m, suggesting that subsidence had been higher in their source area during initial deposition of the Arcurquina Formation. The limestones are often very bioturbated, in particular at their stratigraphic top. A majority of rafts in sub-zones 2NW and 2SE exhibit a somewhat similar internal stratigraphy, albeit less markedly than in Zone 1. The internal stratigraphy of rafts usually differs from that recorded in Zone 1 in that limestone beds are thicker and more frequently separated by marly interbeds. As in Zone 1, rafts are wrapped in a red calcareous siltstone to mudstone matrix. Hydroplastic breccias are also found, although less commonly than in Zones 1 and 3.

In sub-zones 2SE and 2NW, limestone rafts (and sheets) are more folded and fragmented than in Zone 1 (Figs 8 and 9). However, their lateral continuity remains significant, and is generally over a few hundreds of metres. Sheets appear to have been fragmented into discontinuous successions of rafts that can generally be followed over a few kilometres in aerial photographs (Fig. 8). Outcrops are also locally particularly chaotic and fragmented, notably near Uyuccasa (E of Mazo Cruz) at the southeastern end of the zone, and near Sangarara in the northwestern end of the zone.

Deformational facies in sub-zones 2SE and 2NW closely resemble that in Zone 1. The similitude of facies and the presence of recumbent folds with a majority of ENE and WSW vergences suggest that these sub-zones behaved similarly to Zone 1 during the collapse. We thus assume that a sliding mechanism in two opposite directions was also active in Zone 2, pointing to the creation of local opposite slopes by tectonic tilting of the substratum.

Sub-zone 2Ce, i.e. the part of Zone 2 located northeast of the SFUACC, is characterised by the occurrence of large and massive blocks of older units (Huancané Formation, Palaeozoic rocks) within the Ayabacas mélange, in association with the usual limestone rafts. These blocks are locally abundant, and such concentrations of displaced older units have no known equivalent in any other part of the study area. They are variable in size, but on the whole clearly larger and thicker than limestone rafts in sub-zones 2SE and 2NW, exceeding 100 s of m in length and 10 s of m in thickness. They form rigid rafts that are generally much more massive than the limestone rafts; unlike the limestone rafts, they are not affected by folding, although they locally exhibit incipient bending. They must therefore have been already fully lithified at the time of collapse. Internal cross-stratification in sandstone rafts shows that

 Basin Research, 10.1111/j.1365-2117.2008.00358.x

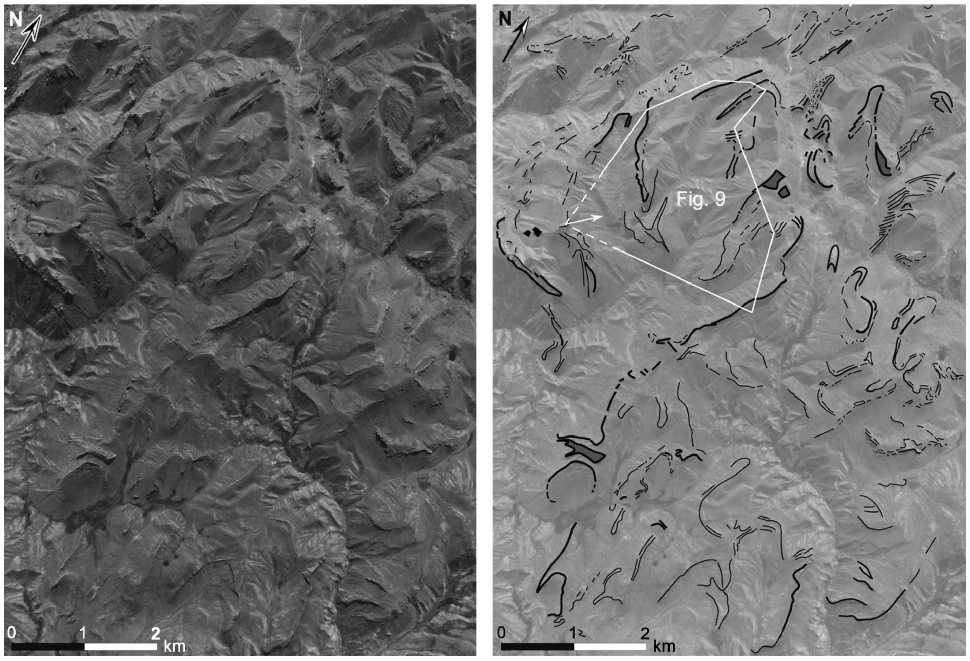

Fig. 8. Aerial photo of Zone 2 typical large-scale facies north of Sangarara, and interpretative outline of its folded rafts. Sheets, although folded and fragmented into rafts, can still be recognised (see text).

some of them are upside down. Their distribution is chaotic to the point that clear orientations appear neither in the field (Fig. 5c) nor in aerial photographs. The only exception is provided, in some of these rafts, by a regularly spaced and regularly oriented fracturation that developed at a ~30–40° angle with the raft sole, revealing the sense of displacement of the rigid mass.

The abundance and huge size of Early Cretaceous-Jurassic and Paleozoic olistolites in sub-zone 2Ce imply that these older units were being exposed to catastrophic erosion, down to the Paleozoic basement, in a nearby area. This could only be achieved by the creation and subsequent collapse of a major fault scarp in the vicinity of sub-zone 2Ce.

Zone 3: Chaotic mélange of more fragmented limestone blocks

Deformational facies in Zone 2 transitionally grade into those in Zone 3, to the point that they are often difficult to distinguish, particularly in the southeast. Here, the Ayabacas Formation generally consists of a mix of limestone blocks, 10–100 s of m in size, enclosed in a matrix of red mudstone and siltstone including a large amount of fluidised sediments and hydroplastic breccias. Good outcrops are found north of Mazo Cruz; south of Ilave and Puno; in the Cabanillas-Santa Lucía-Lagunillas area; south of Santa Rosa, Sicuani and Combapata; and in the Sangarara area. The thickness of the unit is difficult to measure due to the fact that its stratigraphic base and/or top are rarely exposed, and due to the gentle relief in this area. Thickness is however estimated to be approximately 500 m, and appears variable as in other zones.

Maximum stratigraphic thickness of limestone blocks increases in Zone 3 to reach 30–40 m, but blocks can also be ~20–25 m-thick as in Zone 2. However, blocks are much more fragmented, and rarely display significant lateral continuity. At Cabanillas a ~25 cm-thick stromatolitic bed locally duplicated by minor thrusts during the sliding is observed in the lowermost part of the unit, below the main wasting body, indicating that facies deposited in a supratidal environment during the early stage of transgression were here involved in the collapse. Folded blocks are rare, in contrast with Zone 2 (Figs 10 and 11). Although blocks are generally roughly oriented ENE-WSW, some outcrop areas are strongly disorganized (for example SW of Juli-Ilave, as shown by the disparate orientation of the fold axes in Fig. 5a).

Zone 3 is particularly rich in sedimentary breccias, the abundance of which varies in all outcrops. The breccias consist of a mix of red and yellow marly and sandy mudstones to siltstones, locally fluidised, and heterogeneous angular clasts derived from the Murco and Arcurquina formations, and less frequently from the Angostura Formation; all facies known in the Arcurquina Formation are represented; cm- to dm-size rounded clasts of the Triassic Mitu Group occur in breccias 13 km west of Santa Rosa. Limestone clasts are of mm- to m-size, but grade into stratified blocks that can be up to 10–100 s of m in size. Breccia clast shapes often indicate that they were produced by fracturing under an isotropic state of stress (Cosgrove, 1995). Some outcrops reveal that injection of fluidised breccia into a more lithified block locally split the limestone and fragmented it into clasts that were incorporated into the breccia.

The outcrops along the Cabanillas-Santa Lucía road are impressively rich in breccias. They are clearly associated here with a series of normal faults affecting the substratum (including here the Angostura Formation). They exhibit heterogeneous masses mixed with sedimentary breccias, on the whole up to 100 m-thick (but the top does not crop out). These masses are derived from the

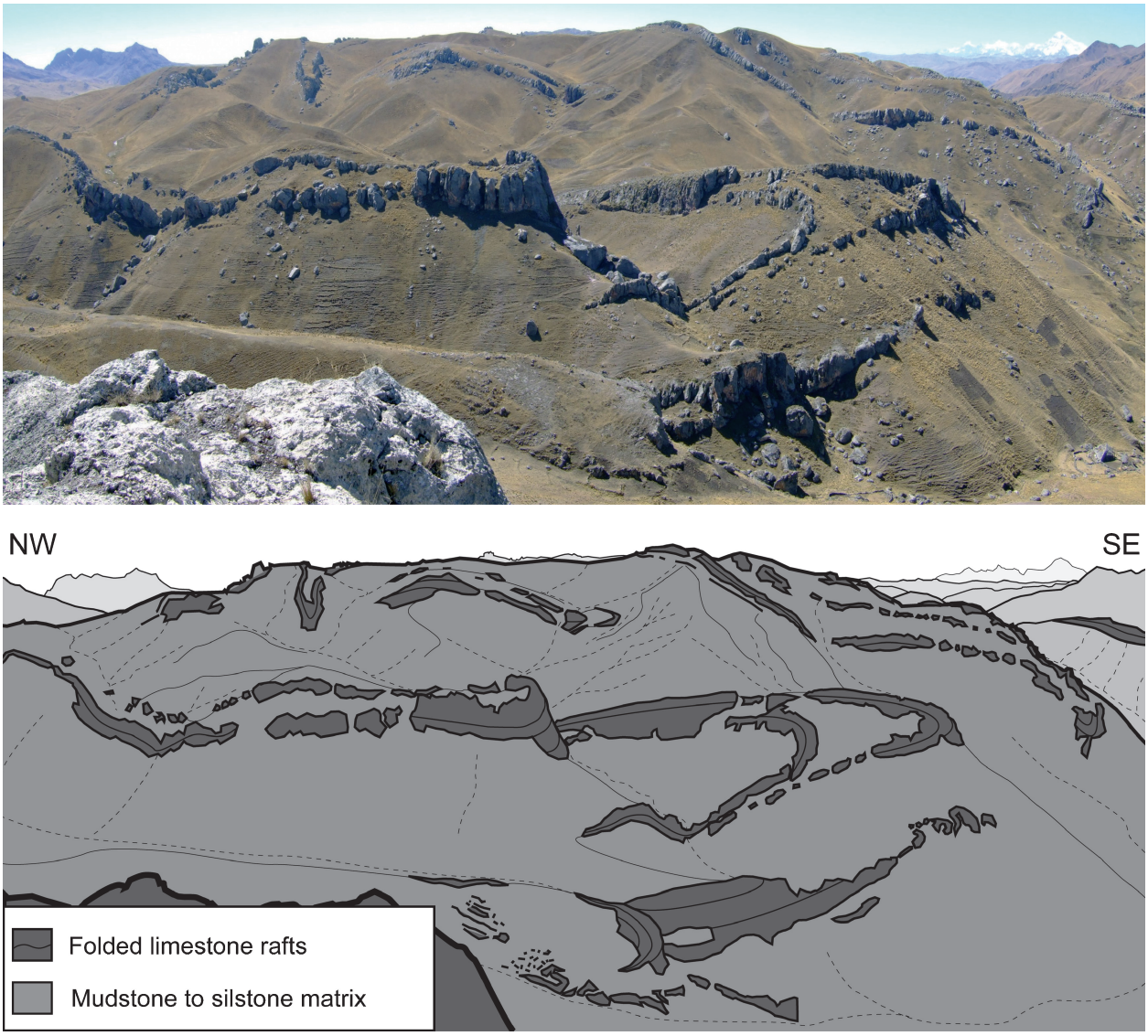

Fig. 9. Field view (looking towards N40) of the Ayabacas Formation in area depicted in Fig. 8 (Zone 2, north of Sangarara, UTM Zone 19L 0215394/8461415, 4377 m elevation). Shaded areas highlight fragmented and plastically folded limestone rafts. This Zone 2 outcrop is somewhat atypical in that the rafts are relatively thin (~20 m).

Arcurquina Formation, and less frequently from the Angostura Formation.

Zone 4: Rafts associated with stratabound breccias

The Ayabacas Formation crops out rather poorly in Zone 4, mainly around Yauri (Espinar) and Livitaca, and, badly, NE of Abancay (Fig. 2). Zone 4 is located ~15–20 km southwest of Zone 3, mainly within the CECLLA structural corridor, and exhibits a number of markedly distinct features. Owing to the gentle relief and to extensive covering by younger rocks, outcrops generally have a limited extent, making difficult to define characteristic deformational facies, as well as a precise measurement of its thickness (estimated to be at least a few 100s of meters).

In marked contrast with Zones 1–3, red mudstones to siltstones are extremely rare in the Ayabacas Formation of Zone 4. The unit almost exclusively consists of < 40 m-thick stacked stratified limestone rafts separated by, and including, limestone breccias (Fig. 12). The only observable features are these stacked rafts, as well as recumbent folds and slumps. Their horizontal dimensions generally vary between 1 and 500 m. At a larger scale, the unit appears less chaotic than in previous zones due to the absence of red mudstones (limestone blocks do not stand out in relief) and because the rafts are more regularly piled up.

At Livitaca, many beds within these rafts consist of breccias. In all of Zone 4, the matrix of these breccias is calcareous, not argillaceous (in contrast with previous zones), and their clasts are almost exclusively composed of limestones (displaying different facies), limestones with calcite veins, and calcite. As usual in the Ayabacas Formation, clast size varies considerably, from < 1 mm to several metres. As in previous zones, their shapes indicate that

 Basin Research, 10.1111/j.1365-2117.2008.00358.x

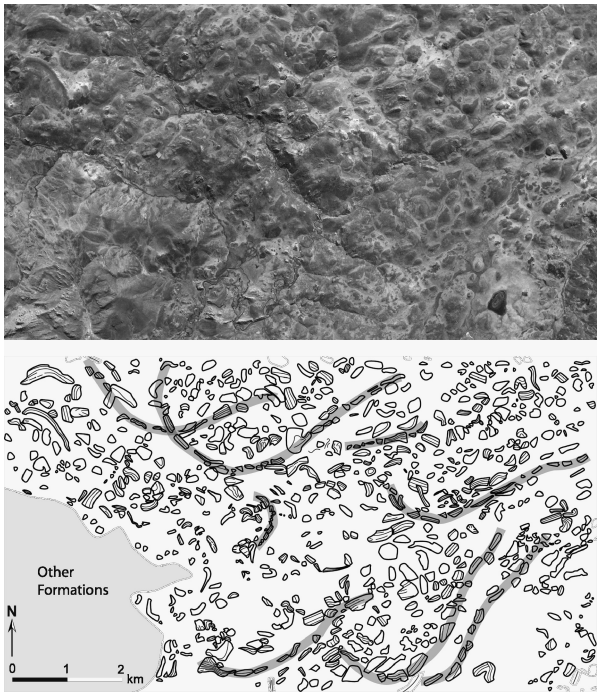

Fig. 10. Aerial photo in Zone 3 SW of Santa Rosa and interpretative outline of rafts and possible slide lobes. Raft thicknesses and fragmentation is higher than in Fig. 8 (Zone 2). There is almost no organisation, although some ~SW-ward slide lobes may be detected (highlighted in light grey). This view markedly resembles Huvenne *et al.*'s (2002) Fig. 3.

they were initially fractured by hydrostatic stress. Some breccias or parts of breccias were clearly fluidised and locally even show fluid motion (e.g. in Fig. 12).

In contrast with Zone 3, the breccias locally include clasts of calcite and of calcite-veined limestones. In some limestone rafts, fluidised-sediment dykes may cut calcite veins. These observations demonstrate that calcite veining developed quite early in the diagenesis, before the Ayabacas collapse.

Zone 5: Chaotic mélange of very large rafts and sheets

This zone is defined by two main outcrop areas: SW of Abancay, and around the pass ~14 km SE of Tisco (7 km WSW of the Condoroma dam at Lago del Colca) in the Western Cordillera (Fig. 2). In Zone 5, the Ayabacas Formation consists of a > 500 m-thick mélange of km-size stratified limestone masses that amalgamate smaller sheets and rafts. This mélange is particularly impressive near Lago del Colca (Fig. 13). This zone can be described as a 'sedimentary thrust and fold system' (*sensu* Frey-Martínez *et al.*, 2006; see also Lewis, 1971; Varnes, 1978; Martinsen, 1989; Frey-Martínez *et al.*, 2005).

Limestone is nearly the only lithology, as in Zone 4. Limestone masses consist of well-stratified strata, brecciated beds, and/or associations of both; lateral transitions between well-stratified and brecciated beds are commonly observed. Stromatolitic beds 0.1–1 m in thickness are observed in association with brecciated beds, again indicating that facies deposited in a supratidal environment were involved in the collapse as far as Zone 5. The masses reach 2–4 km in length and < 1 km in width, but their internal characteristics are not uniform over large distances; smaller bodies, ~100 m in size, are also found. Stratigraphic thickness of the masses generally exceeds several 10 s of m and can reach 100 m. The well-stratified masses are gently to strongly folded. Folds can affect the entire mass or only some rafts within it. Some portions of the masses are undeformed, implying that they were more lithified and rigid at the time of collapse. Despite bedding continuity, variations in folding geometry and in the degree of brecciation are generally observed within each mass.

The masses appear to have moved somewhat independently during the collapse. The larger however display a dominant NNW-SSE orientation in map view (e.g. Fig. 13), which suggests that they slid toward the WSW or ENE. A km-size mass forms a WSW-vergent recumbent fold, indicating motion in this direction. In agreement with the data from other zones, a general motion of masses toward the WSW is deduced in Zone 5. Collecting more data is made impossible by the paucity of outcrops in this zone.

Zone 6: Burial of autochthonous limestones by stacking of rafts and sheets, and gravitational folding

Zone 6 crops out in two relatively small areas: northwest of Yura in the Arequipa region, and north of Chalhuanca in the NW region. In both areas, the limestone succession is thick and generally devoid of mudstone intercalations, and apparently includes both the Arcurquina and Ayabacas formations.

Most observations were obtained in the Yura area, where outcrops are better. Here the lower part of this succession is ≥ 130 m-thick and displays regular beds of even thickness. The ≤ 135 m-thick upper part exhibits signs of destabilisation, with a somewhat increasing-upward degree of deformation; this deformation, however, is minor over the first ~100 m as strata appear essentially regular, and this part of the succession is regarded as the upper Arcurquina Fomation in order to keep the stratigraphic nomenclature simple. In contrast, the ~25–40 m-thick topmost part of this upper succession includes rafts, piled-up slides, slumps, and commonly display boudinage structures, and is therefore described as the local Ayabacas Formation.

In the Arequipa area, the deformation is furthermore marked by large, > 500 m-wide, asymmetrical to overturned WSW-vergent anticlines and related synclines (Fig. 14), which fold the entire limestone succession but neither the Jurassic-Early Cretaceous substratum nor younger strata. These folds formed shortly after termination of limestone deposition, i.e. at the time of the Ayabacas collapse, and, because they do not 'root' into underlying units, they must have been similarly produced by gravitational deformation. Furthermore, in this folded

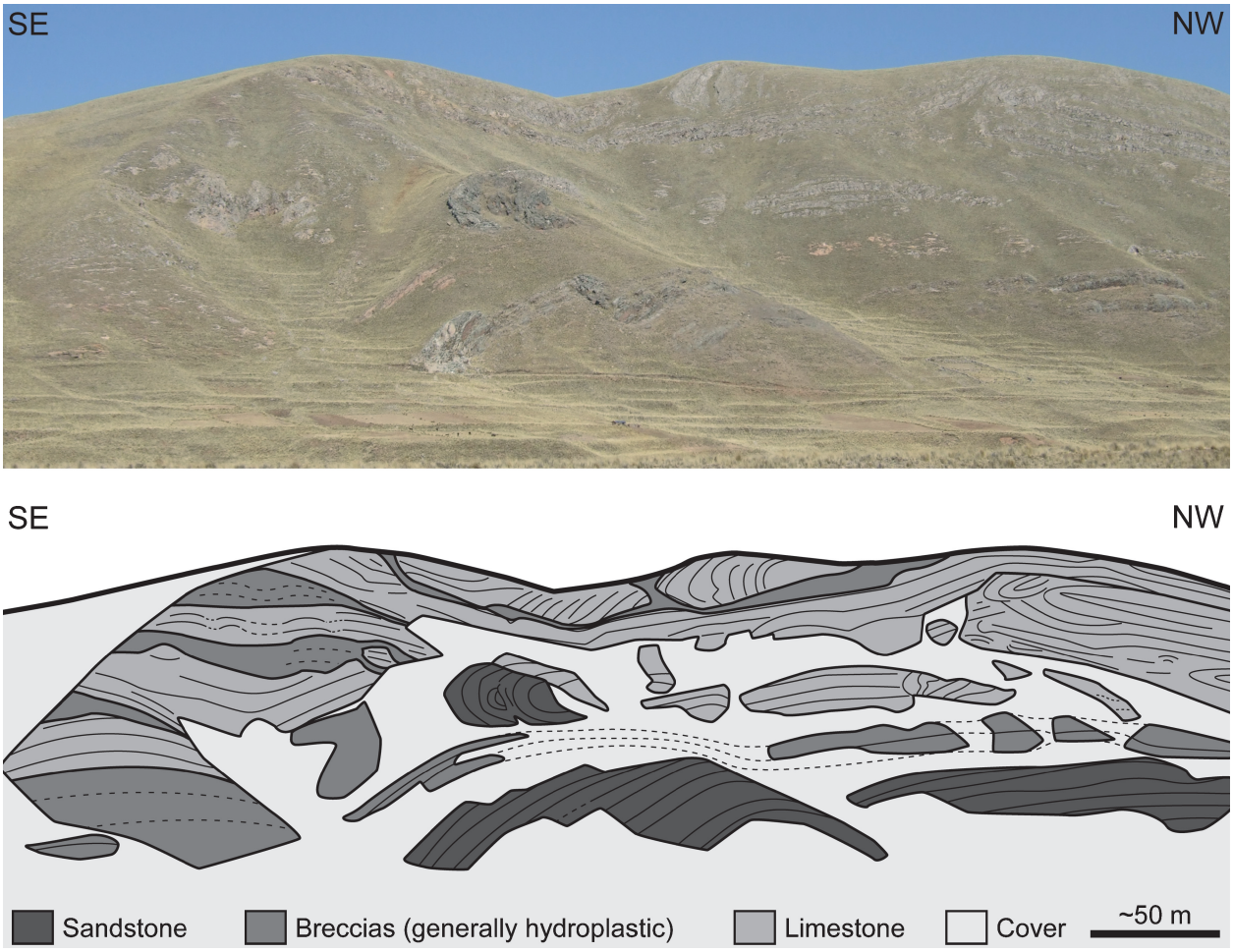

Fig. 11. Field view of the Ayabacas Formation in Zone 3, south of the Cabanillas–Santa Lucía road (UTM Zone 19L 0343000/8267000, 4000 m elevation), and interpretative outline. The unit consists of a mixture of limestone rafts (light grey) and a few lithified sandstone-conglomerate blocks derived from the Angostura Formation (dark grey; see Fig. 3) within a matrix mainly composed of hydroplastic breccias and fluidised marly siltstones (medium grey). It is likely that syndepositional normal faults, as those known elsewhere in this area (see text), were responsible for exposing the Angostura Formation at scarps and causing blocks to slide.

section northwest of Yura, the upper stratigraphic sets that consist of 'cobbly marls' are thicker (up to ~15, ~30, and ~40 m-thick, respectively, for beds 30, 33 and 35) in the synclinal depressions, and much thinner (~1 m, ~0.5 m, and ~1 m, respectively) in the anticlinal crests (Fig. 14), whereas the underlying and immediately overlying limestone beds do not show any variation in thickness. Thickness variations across the folds are clearly restricted to the 'cobbly marl' lithology, which appears as a mix of plastically crushed, smooth-shaped fragments of limestone beds in a marly matrix (Fig. 15); many limestone 'cobbles' exhibit flattening parallel to the bedding plane and stretching perpendicular to the anticlinal axis. These observations strongly suggest that the 'cobbly marl' beds were relatively unlithified at the time of deformation and that during folding they underwent a dominantly plastic flow that redistributed their mass gravitationally, producing thickening in the synclinal axes from thinning in the anticlinal axes, in marked contrast with the limestone beds, which were folded concentrically because they were already lithified at that time. It is also noteworthy that the upper ~25–40 m of the Ayabacas Formation are made up by plastically deformed limestone beds and rafts (Fig. 14c), that testify that these were partially unlithified at the time of deformation, in contrast with the underlying limestones. As lithification is delayed in marls relative to limestones (cementation of carbonates is much faster than that of argillaceous sediments; Müller, 1967; Bathurst, 1971; Bryant *et al.*, 1974), the simplest interpretation is that folding developed at a time when the most recent limestones, over the upper 25 m, and marls, down to a depth of ~135 m, were only partly lithified.

The limbs of these gravitational folds are locally affected by normal and reverse synsedimentary faults that cut bedding over 10 s of cm to a few m. These faults generally agree with a downslope movement along the fold limbs (i.e. ENE-vergent reverse fault and WSW-vergent normal fault in the short limbs; WSW-vergent inverse fault and ENE-vergent normal fault in the long limbs). NNW- and ENE-trending minor synsedimentary normal faults have also been locally observed by Jaillard (1994) in the upper part of the limestone succession.

 Basin Research, 10.1111/j.1365-2117.2008.00358.x

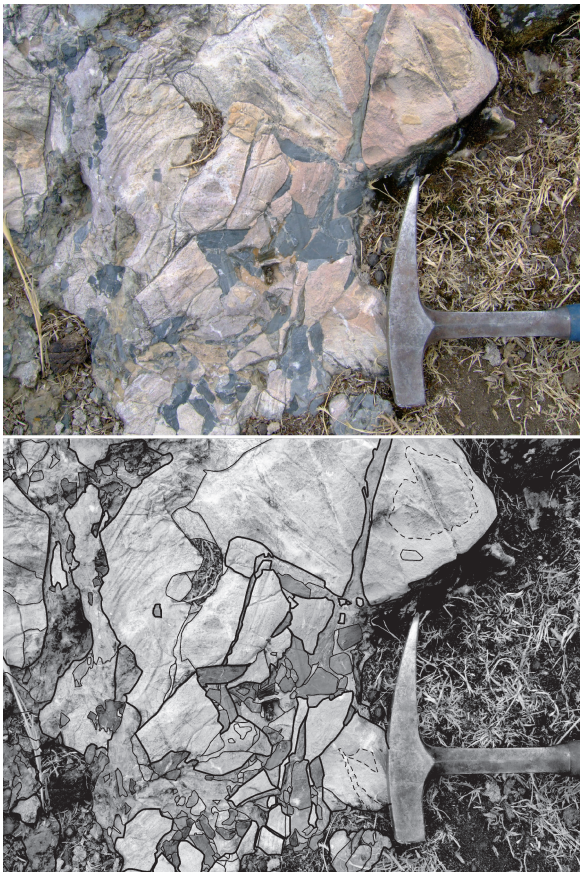

Fig. 12. Detail of a brecciated limestone bed in Zone 4. All clasts and the matrix are calcareous. The fluidised sediment (e.g. the little clastic dyke top-left of the hammer, and the matrix) locally displays fluid motion. Calcite veins are limited to some clasts and thus veining developed before the breccia formation. Size of the hammer head is ~17 cm.

We favor that gravitational folding of the Albian-Cenomanian limestone succession slowly developed during the Ayabacas collapse but that the emerging anticlines did not yield catastrophically, except for the upper few 10 s of m which developed more typical Ayabacas deformational facies. It is likely that the same process led to varying degrees of disruption in other areas, whereas it was 'frozen' in the Yura area. The recumbent folds and stratified masses observed at Lago del Colca (~100 km NNE of Yura; Zone 5) probably represent more evolved states initially produced by similar gravitational folding, but in this case reaching mass thrusting and km-scale disruption.

SYNSEDIMENTARY NORMAL FAULTING AND BLOCK TILTING

In areas where the Ayabacas Formation is thick and the underlying and/or overlying strata do not crop out, it is not always possible to securely separate deformation due to the collapse from the possible local effects of Andean tectonics. A few excellent outcrops in Zones 1 and 3, however, provide evidence that the Ayabacas collapse was accompanied by block faulting and tilting of the underlying rocks.

Syn-collapse normal faulting

A geological cross-section ~15 km northeast of Nuñoa (Zone 1) shows several normal faults affecting the Ayabacas substratum. The Antacalla outcrop is particularly significant (Fig. 16): a W-dipping normal fault offsets the Huancané Formation more than 100 m, is accompanied by a marked thickness variation of the Ayabacas Formation (from < 1 m in the footwall to > 100 m in the hangingwall), and is post-dated by the basal sandstone beds of the Vilquechico Group and younger units. East of the fault, a NE-vergent recumbent fold occurs in the Ayabacas mélange and is interpreted to have been produced by sliding on the tilted surface of the local substratum.

Near Cabanillas (Zone 3), the pre-Ayabacas substratum has been shaped into tilted blocks by a number of normal faults oriented ~N130–N180 that affect the Angostura Formation and below. These faults are post-dated by hydroplastic breccias within the Ayabacas Formation; however, these breccias do exhibit some gentle plastic deformation above the faults, but no fracturing, indicating they were emplaced during faulting.

Asymmetrical thickness variations as a signature of normal faulting

In Zone 1, the thickness of the Ayabacas Formation generally increases gradually from a minimum near a fault to a maximum near the next fault. On the contrary, it varies sharply across such faults, regardless of whether these are post-dated by the Vilquechico Group or not. Because of the evidence of synsedimentary normal faulting in this Zone, our interpretation is that these characteristic asymmetrical thickness variations were produced by block faulting and tilting, the minimum thicknesses corrresponding to the elevated part of a tilted block, i.e. on the footwall of the fault, whereas the maximum thickness was accumulated at the foot of the normal faults (Fig. 17b).

In Zone 1 (e.g. near San Antón – Coñejuno), sharp boundaries between a thick and a thin Ayabacas often coincide with ~NNW-trending reverse faults that dip strongly to the ENE or WSW. It is noteworthy that a thick Ayabacas systematically occurs in the hangingwalls, and a thin Ayabacas in the footwalls, pointing to a link between sedimentary accumulation and the existence of these faults; such geometries, however, are contrary to what would be expected in the case of synsedimentary reverse faults, and instead strongly suggest that the observed reverse faults developed as Andean-age reactivations of former normal faults dipping the same way, in agreement with the observation of non-inverted normal faults in the same zone (Fig. 17).

Extensional faulting and tilting of the substratum was synchronous with sliding

At least Zones 1 and 3 thus provide evidence that the substratum of the Ayabacas Formation was normal-faulted and tilted (some faults in Zone 1 undergoing inversion during the Andean orogeny; e.g. Fig. 17). Normal faults were

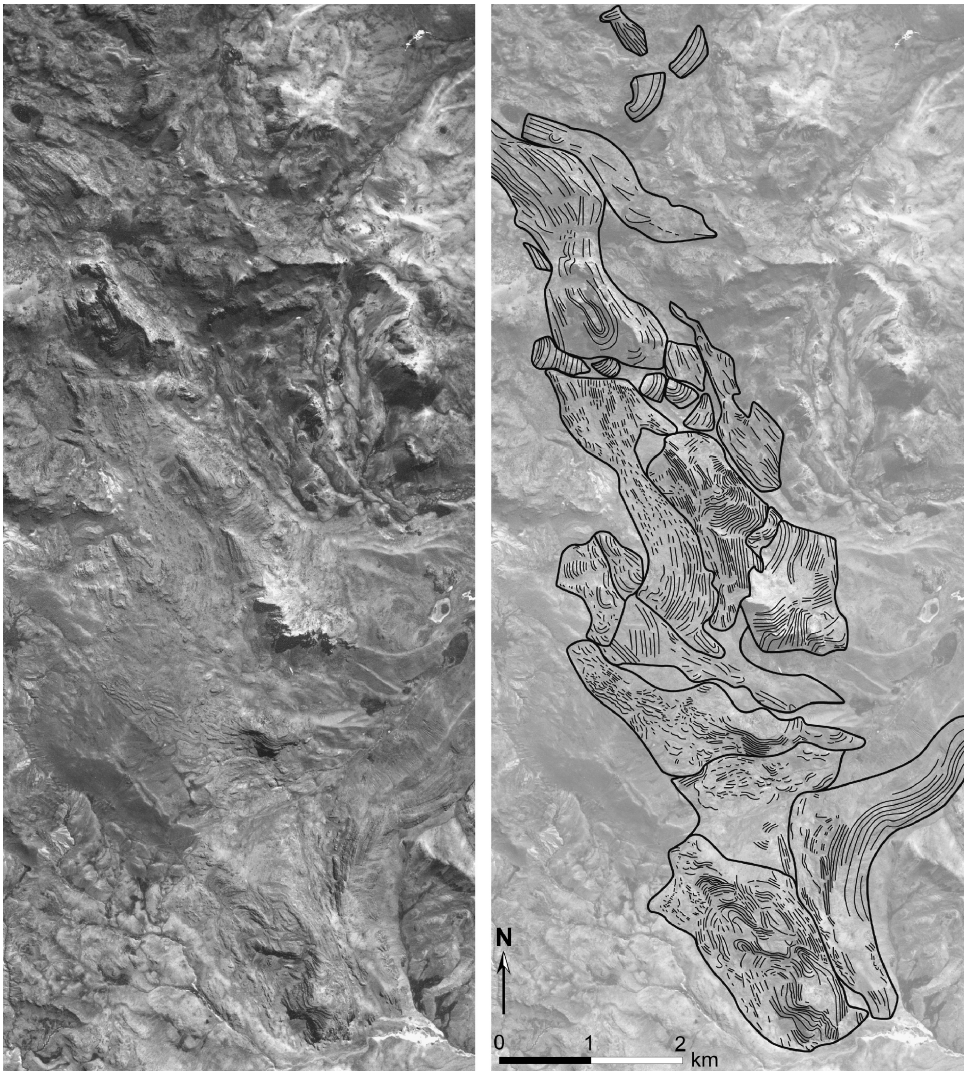

Fig 13. Aerial photo of the road pass ~14 km SE of Tisco (Zone 5), and interpretative outline. The outcrop consists of km-size limestone masses, some of them forming recumbent folds (with ~WSW trend). The masses are not homogenous, consisting of a mixture of sheets and rafts that include well-stratified and brecciated beds in lateral transition (see section 'Zone 5: Chaotic mélange of very large rafts and sheets' in text).

generally NW-trending and associated with down-to-the-NE tilting of substratum blocks, making gravity sliding of mudstones and limestones of the Murco and Arcurquina formations possible both NE-ward above the tilted surface and SW-ward along the fault scarps (Fig. 17). Evidence also exists that both normal faults and sliding were post-dated by the Vilquechico Formation (e.g. Fig. 16). In Zone 2, no clear evidence of normal faulting and tilting has been found so far, but this may be due to a lack of favourable outcrops. A similar association of normal faults, tilted blocks, and large-scale sliding has been described offshore New Zealand by Collot *et al*. (2001).

Measurements of fold axes and vergences are commonly considered to provide indications on sliding directions when they are sufficiently numerous and distributed over a sufficiently large area (Lajoie, 1972; Woodcock, 1979; Strachan & Alsop, 2006). Gravitational folds in the Ayabacas limestones are commonly distributed into outcrop sets displaying opposite NE and SW trends, indicating that at a large scale slides developed in these two main directions. Furthermore, observations are highly suggestive that NE-ward sliding developed at smaller scales and SW-ward sliding at larger scales. The first are interpreted to result from local tilting of the pre-Ayabacas surface down to the NE in association with SW-dipping faults, whereas the second are likely to represent sliding toward the greater basin in agreement with the more regional slopes generated by these faults. Based on the vergence of overturned folds, Portugal (1964, 1974) recognised in Zone 3 that sliding motion was dominantly toward the SW. The other synsedimentary structures (clastic dykes, palaeodirectional indications in the breccias) observed in the study area generally agree with the reconstructed NE and SW directions of sliding.

Block faulting and tilting of the substratum during the Ayabacas collapse is in agreement with the fact that the western Peru back-arc basin (WPBAB) developed in a dominantly extensional context until at least the end of the Turonian (see above). Northeast of the SFUACC, some

 Basin Research, 10.1111/j.1365-2117.2008.00358.x

normal faults underwent inversion when Andean-age shortening developed in the Eastern Cordillera (similar to faults described by Bond & McClay, 1995). Normal faults were not inverted in the Cabanillas area, i.e. southwest of the SFUACC where Andean shortening has been weak or absent (Sempere & Jacay, 2006, 2007).

Catastrophic erosion along fault scarps

Large blocks of lithified sandstones derived from the Angostura and/or Huancané formations, and others from older units, down to the Palaeozoic basement, occasionally occur chaotically in areas of high thickness [at various places in Zone 2 (see Fig. 2)]. These blocks are up to 100 s of m in length and width, and up to several 10 s of m in stratigraphic thickness. The occurrence of such large blocks implies that the pre-Ayabacas units were exposed to catastrophic erosion. We suggest that this was made possible by creation of significant fault scarps. These particular facies rich in older blocks are therefore interpreted to have accumulated at the foot of such scarps, from which they were removed catastrophically. Huancané blocks 10–100 m in size are indeed observed in association with the small syn-sedimentary normal faults in zones 1SE (near San Antón) and 3 [near Cabanillas (e.g. Fig. 11)]. However, the localities where the largest blocks are observed closely follow the SFUACC fault system (Fig. 2), strongly suggesting that this major, old, subvertical structure (Carlier *et al.*, 2005) came to form a significant scarp during the Ayabacas collapse. Normal faulting being documented in Zones 1SE and 3 in association with the collapse, it is likely that the SFUACC scarp was also created by normal fauting. Taking into account the stratigraphic thicknesses known in the area, and the caveat that the Paleozoic basement had been locally uplifted in the Early Cretaceous, this fault scarp is estimated to have been at some time at least ~100 m high, in order to enable catastrophic erosion of basement blocks. It is likely that this scarp was created by accumulated offsets along the SFUACC.

In contrast with Zone 2, where blocks derived from the Huancané Formation commonly occur, Huancané clasts of only cm–dm size are observed in Zone 3 and only at some localities; this implies that some Huancané blocks underwent pervasive desintegration during collapse of the SFUACC scarp and acquired an impetus sufficient to transport large fragments several km away from this scarp. Near Santa Rosa and Cabanillas, clasts of volcanic conglomerates typical of the Mitu Group are observed, likewise suggesting that the Mitu Group had been exhumed in some fault scarp located in the local upslope area.

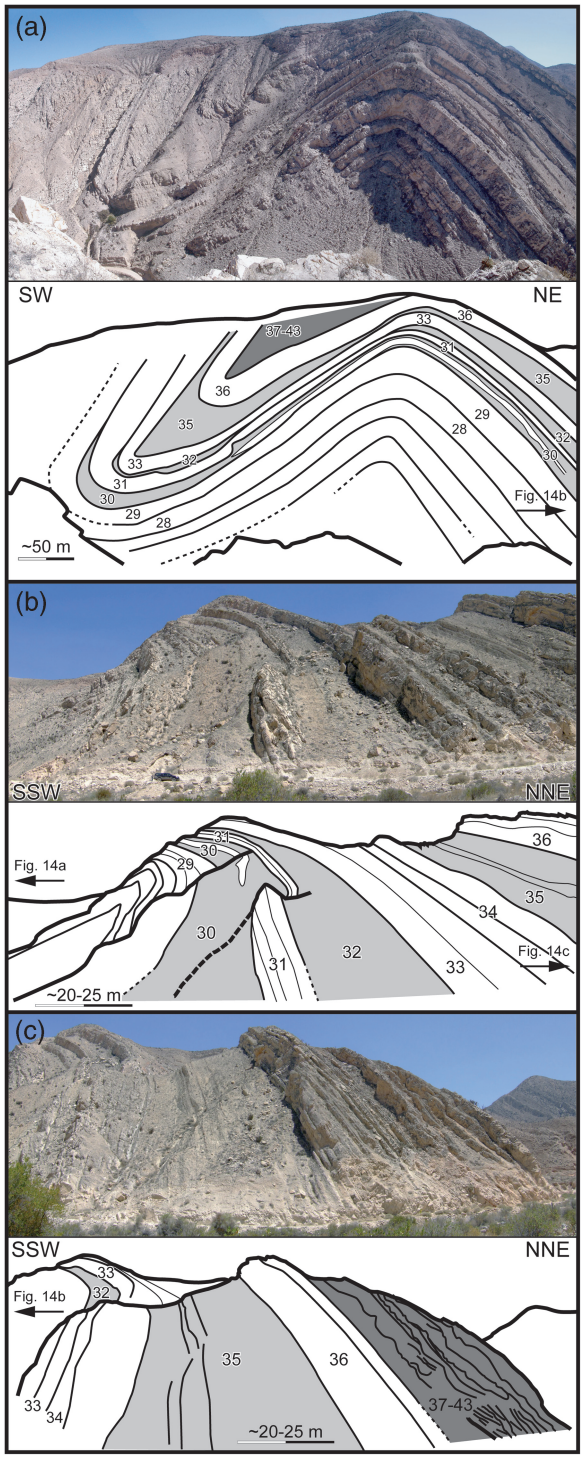

Fig 14. Photographs and interpretative outlines of the same asymmetrical fold 20 km NW of Yura (Zone 6), taken from different points of view from SW to NE (a to c). Bed numbers are those used by Benavides-Cáceres (1962). Vergence is to the WSW (underlying and overlying units evidence that Andean deformation has tilted the local section down to the NE). The 'cobbly marl' beds (no. 30, 32 and 35, in grey in the line drawings; see also Fig. 15) are clearly thicker in the synclinal depressions and much thinner in the anticlinal crests. Older beds (29 and below) do not display such thickness variations, whereas limestone beds 31, 33 and 36 are hardly affected. Beds 29 and below are typical of the Arcurquina Formation; although they display minor deformation, beds 30–36 are sufficiently regular to be also assigned to the Arcurquina Formation. In contrast, deformation in the topmost part of the succession (beds 37–43 in dark grey) is much more pronounced, due to sliding of unlithified marls and limestone rafts and slumps, typical of the Ayabacas Formation.

DISCUSSION

Anatomy of the Ayabacas mass-wasting body

Deformational facies vary across the six zones recognised in the basin, depending on the involved lithologies and pre-collapse thicknesses and lithification states. Across Zones 1–3, from NE to SW, strata deposited in the mid-Cretaceous carbonate platform were progressively and increasingly fragmented. Thicknesses of the limestone rafts and of the entire collapse increase, respectively, from ~20 to ≤ 40m, and from ~40 to > 300 m. The average shape of the limestone elements evolve from relatively unfolded, ~20 m-thick, km-size sheets in Zone 1, to folded sheets fragmented into rafts in Zone 2 and more fragmented, chaotically arranged rafts in Zone 3. Mid-Cretaceous deposits were removed, locally completely, from areas where slides originated, as in the uplifted parts of tilted blocks (e.g. Fig. 16). In contrast, relatively thick Ayabacas deposits accumulated in downwarped areas (as already suggested by Portugal, 1964, 1974) such as those in the hangingwalls of normal faults. Zones 1–3 thus exhibit a characteristic downslope fragmentation of the collapsed material.

In contrast with Zones 1–3, the average size and continuity of limestone masses increase from Zones 4–6. In Zones 4 and 5, the Ayabacas deposits are thick (commonly > 500 m) and result from the stacking of limestone rafts and sheets, whose average size increases from east to west, as in a 'sedimentary thrust and fold system' (*sensu* Frey-Martínez *et al.*, 2006). In Zone 6, the upper part of the limestone succession consists of stacked rafts and sheets characteristic of the Ayabacas Formation, whereas the lower part consists of the regularly bedded Arcurquina Formation. Thus, no sliding occurred during at least the first part of the depositional interval, dismissing the hypothesis that the carbonate platform would have been repeatedly affected by mass-wasting processes, and instead confirms that the Ayabacas collapse represents a unique event that occurred at the end of the platform history. In the Yura area, gravitational folds represent a 'frozen stage' of the 'sedimentary thrust and fold systems' observed in Zone 5, complete sliding having probably been hampered by the high viscosity imposed by a more advanced state of lithification. More generally, it seems reasonable to propose that lithification progressed at a quicker pace in the western areas, because these lay deeper in the Arcurquina basin and were reached earlier by the transgressions. Higher viscosity and cohesiveness in the west are likely to have prevented the local Arcurquina limestones from being involved in the Ayabacas collapse. We therefore expect the Ayabacas-related structures to die out into the WPBAB west of the study area.

The deformational facies and anatomy of the Ayabacas body furthermore refute an origin by compressional tectonics. The organisation of the collapse into six deformational facies zones, plus one undisturbed zone in the northeast, closely parallels the architecture of the mid-Cretaceous marine basin but is clearly unrelated to the Andean-age deformation distribution and styles, in particular in the northeast. It is revealing that the Ayabacas disruption is maximum in Zone 3, where Andean shortening

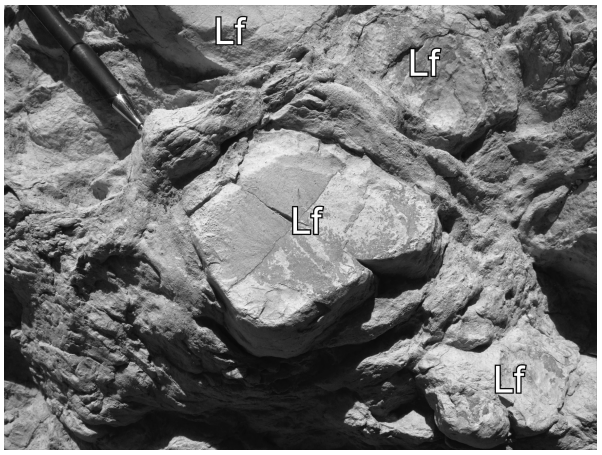

Fig. 15. Illustration of the 'cobbly marl' lithology, characterised by smooth-shaped limestone fragments (Lf) surrounded by a marly matrix. The visible part of the pen is ~4 cm.

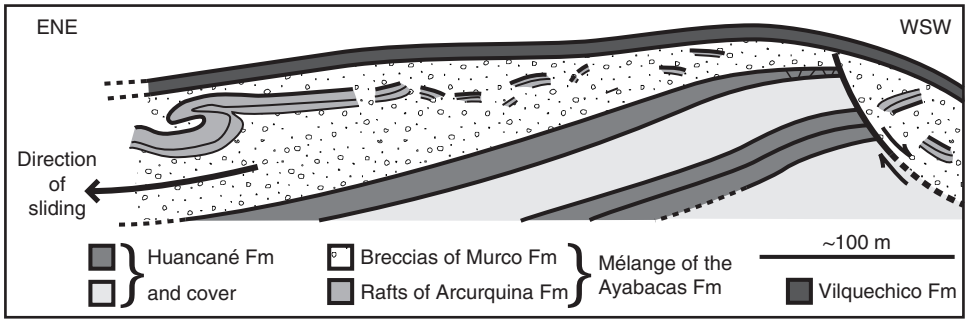

Fig. 16. Line drawing of the Antacalla outcrop (UTM Zone 19L: 0317728/8405150, 4120 m elevation; see also Sempere *et al.* 2000). The normal fault affects both the Huancané and Ayabacas formations, but is post-dated by the sandstone basal member of the Vilquechico Formation (see Fig. 3). The attitude of the Vilquechico Fm nevertheless appears gently controlled by the existence of the buried fault scarp. The Ayabacas is thick in the hanging-wall. In the footwall, the Huancané Formation is tilted down to the NE and its top is fractured close to the fault (black lines). Limestone blocks occur SW of the fault, but are absent just NE of it and progressively appear NE-wards, where one of them displays soft, NE-vergent folding, indicating that sliding occurred in this direction.

 Basin Research, 10.1111/j.1365-2117.2008.00358.x

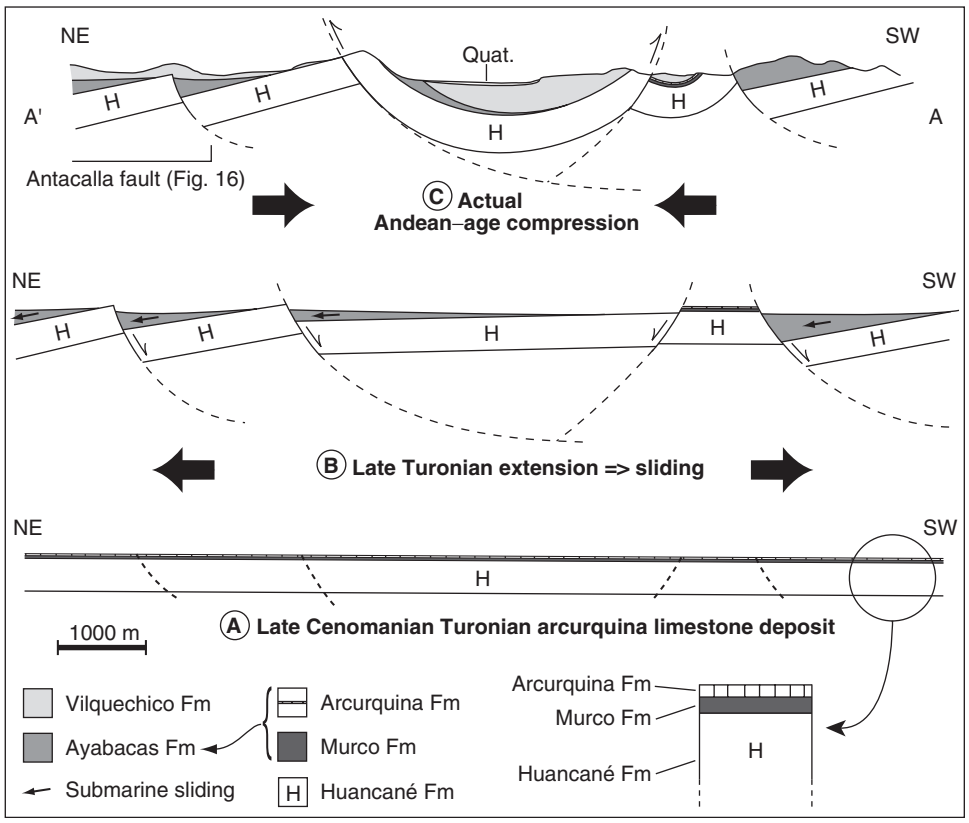

Fig. 17. Present (C) and reconstructed (B, A) sections near Nuñoa (Zone 1). (a) Deposition of the Arcurquina limestones during the Late Cenomanian-Turonian tectonic quiescence. (b) Intense extensional tectonics at the Turonian-Coniacian transition (~90–89 Ma); the pre-Ayabacas substratum is shaped into tilted blocks by ~NW-trending normal faults; the Arcurquina and Murco formations collapse on the created, oversteepening slopes to form the Ayabacas Formation, which is very thin or absent in the origination areas of the slides and very thick (up to > 100 s of m) in the hanging-wall of the normal faults. (c) During the Andean-age shortening of the Eastern Cordillera, some normal faults undergo inversion; others, as the Antacalla fault (Fig. 16), do not, making clear that the normal faulting and Ayabacas deformation are post-dated by the Vilquechico Formation.

was weak or absent (Sempere & Jacay, 2006, 2007), whereas it is minimum in Zone 1 to non-existent in Zone 0, i.e. close to the Eastern Cordillera where Andean shortening was maximum.

What triggered the Ayabacas collapse?

Submarine slides are widely viewed to result from a variety of short-term triggering mechanisms such as oversteepening of the depositional surface, increase in pore pressure, seismic loading, storm-wave loading, rapid sediment accumulation and under-consolidation, gas charging, gas hydrate dissociation, low tides, seepage, diapirism, glacial loading and volcanic island processes (Locat & Lee, 2002; Mienert *et al*., 2002; Sultan *et al*., 2004). Factors such as slope angle, mass-movement history and unloading, may be insufficient to initiate failures but can favour them, and therefore constitute long-term, 'slow' triggers. Sea-level changes have also been proposed as a potentially favourable factor for slope failure (Spence & Tucker, 1997).

Increase in pore pressure and differences in lithification rate (Nichols, 1995; Spence & Tucker, 1997; Mourgues & Cobbold, 2003; Vendeville & Gaullier, 2003) were indeed likely to be present at the time of the Ayabacas collapse, and to have facilitated sliding, but they quite probably existed also during the entire deposition of the Arcurquina limestones and yet no sliding is recorded before the Ayabacas event: therefore they cannot be invoked as a triggering factor for the collapse. At the end of the Early-Middle Albian transgression, sediment characteristics in the western part of the basin (Arequipa region) must have been similar to those that later preceded the Ayabacas collapse more to the northeast: the water-laden Murco siltstones and sandstones were underlying partly lithified Arcurquina limestones, probably generating some excess pore pressure, but, although this potential sliding sole was present throughout the deposition of the carbonate platform, sliding did not occur in any part of the basin until the Ayabacas event.

Absence of slides interstratified in the Arcurquina Formation, where this unit is preserved (Zones 6 and 0), dismisses relative sea-level fall or rise as triggering factors because neither the Early Albian and Late Cenomanian transgressions, nor the Late Albian regression, had any noticeable effect on the stability of the southern Peruvian carbonate platform. The Ayabacas event, however, apparently occurred during a marked global regression that was abruptly initiated in the late Middle Turonian (~91 Ma)

and slowly terminated near the Turonian–Coniacian boundary (~89 Ma) (Hardenbol *et al.*, 1998). However, a triggering role of this ~91 Ma sharp sea-level fall appears unlikely because its age apparently disagrees with the ammonite record from northern Peru, which documents that carbonate sedimentation continued into the Late Turonian (Jaillard, 1990, 1994), and with our own chronostratigraphic model (see above and supplementary documentation online). Furthermore, the global sea-level was dominantly high again during the Senonian, whereas the Ayabacas collapse was immediately followed by nearly exclusively continental sedimentation in the southern Peruvian basin. The collapse in fact coincided with other, non-eustatic, geological phenomena in southern Peru, an intriguing observation that should provide valuable insights into this triggering mechanism.

One main clue lies in the striking association of the Ayabacas collapse with extensional tectonic activity, as demonstrated by synsedimentary normal faults and related thickness variations. As documented in outcrops, normal faulting produced tilting of the substratum as well as scarps, and thus created seismicity and slopes on which sliding of the Arcurquina and earlier strata was enabled. The nearly constant thickness and standard internal stratigraphy of the limestone rafts and/or sheets within each zone (as observed in Zones 1–3, and therefore also inferred to be true in Zones 4–6) suggest that the bottom of the basin had been remarkably flat before the Ayabacas collapse, confirming that slopes had to be created in order to make the mass-wasting process possible. In the Late Albian–Early Cenomanian limestone succession of northern Peru, slumps, breccias, and large clastic dykes, likewise occur in association with synsedimentary normal faulting (Jaillard, 1994). Such associations between extensional tectonics and sedimentary sliding in the WPBAB, at different times, strongly suggest that the triggering of mass wasting in this carbonate platform ensued from slope creation and seismicity produced by extensional tectonic activity, and that other factors, such as pore pressure increases or lithification contrasts, only facilitated sliding.

The relationship between regional extensional tectonic activity and the Ayabacas collapse is strengthened by the occurrence of some peculiar features in the vicinity of the two major fault systems that cross the study area (SFUACC, CECLLA; Figs 1 and 2). During the Cenozoic and in particular the Central Andean orogeny, these two ancient fault systems have had significant tectonic activity, and have been the loci of considerable magma emplacement, revealing that they represent major crustal to lithospheric heterogeneities (Sempere *et al.*, 2002b, 2004b; Carlier *et al.*, 2005, for the SFUACC). Although synsedimentary normal faults and related thickness variations were observed in Zones 1 and 3, thanks to outcrops providing spectacular exposures, there is evidence that the SFUACC and CECLLA were activated during the Ayabacas collapse.

The SFUACC had had some syndepositional activity during the mid-Cretaceous carbonate sedimentation (Arcurquina depositional interval) as it formed the northeastern boundary of the depositional area during the Early and Middle Albian transgression and highstand. This barrier was overflowed by the Late Cenomanian-Turonian trangression and highstand, but subsidence and water depth apparently remained much lower northeast of the SFUACC. During the Ayabacas collapse, older rock units, down to the Paleozoic, were exposed along $\geq$ 100 m-high, southwest-facing scarps formed by the SFUACC activity; giant blocks of these lithified units were catastrophically removed as these scarps collapsed and slid down to the southwest, and their fragments were transported away in the same general direction. The occurrence of large blocks along the northeast fringe of the SFUACC (Fig. 2) documents that some of them underwent little transport and remained stuck in the slope. It is likely that the smaller normal faulting documented in Zone 1, i.e. a few km northeast of the SFUACC, developed in relation to major normal faulting along the SFUACC. Occurrence of blocks of Paleozoic shales southwest of this fault system (i.e. in its downwarped side) reflects that the Paleozoic basement had been locally uplifted in the Early Cretaceous, rather than implying that its cumulated vertical offset was $>$ 400 m during the Ayabacas collapse, which seems unlikely. Given the relative shortness of the event, even a 100 m throw is by itself suggestive of a considerable tectonic upheaval in the region.

Activity of the CECLLA system during the Ayabacas collapse is inferred from the sharp facies differences between Zones 3 and 4, which are respectively located east of, and within, this broad fault system. Whereas in Zones 1–3 the mass-wasting body abundantly involved red siltstones derived from the Murco Formation, it only reworked Arcurquina limestones in Zones 4–6, where the Murco Formation was not involved in the collapse. This contrast indicates that, from the CECLLA system to the west, the Murco Formation was located below the sole of the collapse, whereas it lay well above it east of the CECLLA. This geometry suggests that the domain within and west of the CECLLA was structurally downwarped when the collapse was initiated, and it is likely that this resulted from normal faulting along and within this broad fault system. Respective estimated thicknesses of the involved units suggest that vertical offsets within the CECLLA must have been $<$ 100 m, as they did not form scarps where pre-Arcurquina units could be exposed (unlike what occurred along the SFUACC system), but sufficient enough to downwarp the pre-Arcurquina units to a position where they could be preserved from involvement into the collapse. This was possibly due to the broad, diffuse character of the CECLLA structural system (Fig. 1).

Facies zones distinguished in the Ayabacas Formation vary laterally in map view. The northern Cusco–Abancay–Chalhuanca transect is 120 km-long, clearly shorter than the 200 km-long southern Huancané–Juliaca–Santa Lucía–Lagunillas–Yura transect (Fig. 2), a difference that cannot be explained by a higher Andean-age shortening in the north but rather reflects the different position of

 Basin Research, 10.1111/j.1365-2117.2008.00358.x

these transects relative to the SFUACC and CECLLA. Furthermore, this asymmetry is matched by differences in the deformational facies of the Ayabacas collapse. Southern deposits are limestone-rich along a ~100 km-long transect across Zones 1–3 and their matrix consists exclusively of mudstones to siltstones. From there the width of the set formed by these three zones progressively decreases northwards, down to ~30 km in the Cusco-Urubamba area, which was mapped as a whole as Zone 1NW because facies typical of Zones 2 and 3 could not be recognised; here the Ayabacas Formation presents an atypical limestone-poor facies, its abundant matrix includes voluminous gypsum masses, but its limestone rafts exhibit pre-collapse stratigraphic thickness and facies similar to those in Zone 1SE.

This northern area is likely to have behaved in a particular manner because the SFUACC coalesces with the CECLLA in this area (Figs 1 and 2), suggesting that more pronounced scarps and cumulated relief were created here during the event, enhancing the regional slope and significantly favouring collapse of the local platform. Limestone rafts and sheets disintegrated downslope and were massively transported toward the southwest, explaining the limestone-poor facies observed in this area, which would have resulted from a differential transport of the denser limestone blocks in this direction. The thick stacking of exclusively limestone sheets observed in Zones 4–6 in the same transect is in agreement with this idea. Sliding would have been furthermore facilitated by the abundance of gypsum and halite in the Maras (= Murco) Formation, which provided a weaker sole for the collapse.

The Ayabacas event of southern Peru correlates well with the also extensional Vilcapujio event inferred in central Bolivia (Sempere, 1994) on the basis of (1) rapid thickness variations limited to the Coniacian? Aroifilla Formation (interpreted to result from synsedimentary normal faulting) and (2) local partial to total erosion of the Bolivian equivalent of the Arcurquina Formation (which otherwise testifies to a tectonically quiescent Cenomanian-Turonian period). Extensional tectonics thus appear to have abruptly developed near the Turonian-Coniacian transition over a large Central Andean region, at least from central Bolivia to southern Peru. The duration of this extensional deformation is poorly constrained in Peru, but the case of the Bolivian Aroifilla Formation suggests it possibly lasted some Myr.

CONCLUSION

The mid-Cretaceous carbonate platform of southern Peru was brutally disrupted and terminated by a giant collapse at about the Turonian-Coniacian transition (~90–89 Ma). The resulting mass-wasting body was very large, $> 80\,000\,km^2$ in map view and $> 10\,000\,km^3$ in volume. It now forms the Ayabacas Formation, which is organised into six deformational zones from NE to SW. The observed directions of sliding and of material disintegration are consistent and indicate that the platform regionally collapsed toward the southwest, i.e. down the general slope of the pre-Senonian basin. Consistently, most part of the shallow and little subsident sub-basin located northeast of the SFUACC system was not affected by the collapse and remained stable.

The Ayabacas Formation unequivocally appears to be the result of a major submarine mass redistribution, which was triggered by significant slope creation and subsequent oversteepening abruptly forced at that time by extensional tectonic activity. The key role of tectonics in triggering mass movement has often been underlined (e.g. Spence & Tucker, 1997; Payros *et al*., 1999; Graziano, 2001; Mienert *et al*., 2002; Floquet & Hennuy, 2003; Canals *et al*., 2004). Seismicity may have been significant, in particular in the vicinity of the two major fault systems (SFUACC and CECLLA) where large lithified blocks from underlying units were involved in the collapse. Increase in pore pressure and differences in lithification rates facilitated the slides but cannot be considered as the main triggering factor.

The Ayabacas Formation records the only sedimentary collapse that disrupted the mid-Cretaceous marine succession of southern Peru. It thus represents a unique and peculiar event in the history of the regional Andean margin and back-arc. Although it is likely that the collapse resulted from several sliding episodes, the Ayabacas Formation is neither intercalated with, nor post-dated by, limestone strata similar to those involved in it. The collapse was submarine and yet abruptly terminated the carbonate platform evolution. It must therefore have taken place during a limited time span, and can technically be considered as one event.

It seems highly meaningful that the Ayabacas event occurred at a turning point in the Central Andean evolution, namely when the south Peruvian back-arc basin underwent a dramatic and permanent change from marine to continental conditions. Before the event, this basin had been essentially marine since the Early Jurassic and deepened to the west. After the event, the back-arc was bounded to the southwest by topographic highs, apparently volcanic in nature, and occupied by continental to near-continental environments. This regional association of extraordinary events, including a significant reactivation of arc volcanism, is likely to shed considerable light on the regional Andean evolution and will be dealt with elsewhere.

ACKNOWLEDGEMENTS

This work was funded by the Institut de Recherche pour le Développement (IRD), and the GDR 'Marges'. We thank the Instituto Geológico Minero y Metalúrgico de Peru (INGEMMET) for helpful collaboration and orientation in Lima. We are especially grateful to the IRD office in Peru and its director Pierre Soler. Special thanks to José Berrospi for invaluable help and efficiency during field work, and to C. Lézin and B. Andreu (LMTG, Toulouse) for fruitful discussions. This paper was improved by constructive comments from Joe Cartwright and an anonymous reviewer.

REFERENCES

Atherton, M.P. (1990) The coastal batholith of Peru: the product of rapid recycling of "new" crust formed within rifted continental margin. *Geol. J.*, **25**, 337–349.

Atherton, M.P. & Webb, S. (1989) Volcanic facies, structure, and geochemistry of the marginal basin rocks of central Peru. *J. South Am. Earth Sci.*, **2**, 241–261.

Atherton, M.P. & Aguirre, L. (1992) Thermal and geotectonic setting of Cretaceous volcanic rocks near Ica, Peru, in relation to Andean crustal thinning. *J. South Am. Earth Sci.*, **5**, 47–69.

Audebaud, E. (1967) Etude géologique de la région de Sicuani et Ocongate (Cordillère Orientale du Sud Péruvien). Thèse de 3ème cycle, Université de Grenoble, 60 p.

Audebaud, E. (1970) Premières observations sur la tectonique tangentielle polyphasée des terrains secondaires de la Cordillère Orientale du Sud-Est péruvien. *C. R. Acad. Sci., Sér. D*, **270**, 3190–3193.

Audebaud, E. (1971a) Mise au point sur la stratigraphie et la tectonique des calcaires Cénomaniens du Sud-Est péruvien (formation Ayavacas). *C. R. Acad. Sci., Sér. D*, **272**, 1059–1062.

Audebaud, E. (1971b) Photogéologie de reconnaissance et difficultés d'interprétation dans une zone à structure complexe (Cordillère Orientale du Sud du Pérou : hameau Hanchipacha, nord de Sicuani). *Photo-interprétation*, **5**, fascicule 3, Technip, Paris, 15–21.

Audebaud, E., Capdevila, R., Dalmayrac, B., Debelmas, J., Laubacher, G., Lefevre, C., Marocco, R., Martinez, C., Mattauer, M., Megard, F., Paredes, J. & Tomasi, P. (1973) Les traits géologiques essentiels des Andes Centrales (Pérou-Bolivie). *Rev. Géograph. Phys. Géol. Dynam.*, **15**, 73–114.

Audebaud, E. & Debelmas, J. (1971) Tectonique polyphasée et morphotectonique des terrains Crétacés dans la Cordillère Orientale du Sud péruvien. Etude d'une structure caractéristique. *Cahiers ORSTOM, Sér. Géol.*, **3**, 59–66.

Audebaud, E. & Laubacher, G. (1969) Présence du Tertiaire plissé (groupe Puno) dans la Cordillère Orientale du sud du Pérou. *C. R. Acad. Sci., Sér. D*, **269**, 2301–2304.

Bathurst, R.G.C. (1971) Carbonate sediments and their diagenesis. *Developments in Sedimentology*, **12**. Elsevier, Amsterdam, 620 p.

Benavides-Cáceres, V. (1962) Estratigrafía pre-Terciaria de la región de Arequipa. *Bol. Soc. Geol. Perú*, **38**, 5–45.

Bond, R.M.G. & McClay, K.R. (1995) Inversion of a Lower Cretaceous extensional basin, south central Pyrenees, Spain. In: *Basin Inversion* (Ed. by J.G. Buchanan & P.G. Buchanan), *Spec. Pfubl. Geol. Soc. London*, **88**, 415–431.

Brun, J.-P. & Fort, X. (2004) Compressional salt tectonics (Angolan margin). *Tectonophysics*, **382**, 129–150.

Bryant, W.R., Deflacke, A.P. & Trabant, P.K. (1974) Consolidation of marine clays and carbonates. In: *Deep Sea Sediments; Physical and Mechanical Properties; Determination of Mechanical Properties in Marine Sediments* (Marine Science, **2**, 209–244. Plenum, New York.

Cabrera La Rosa, A. & Petersen, G. (1936) Reconocimiento geológico de los Yacimientos Petrolíferos del Departamento de Puno. *Bol. Cuerpo Ingenieros de Minas del Perú*, **115**, 100 p.

Callot, P., Sempere, T., Odonne, F. & Robert, E. (2007) The Mid-Cretaceous carbonate platform of southern Peru collapsed at the Turonian-Coniacian transition. 4th European Meeting on the Palaeontology and Stratigraphy of Latin America (EMPSLA). Cuadernos del Museo Geominero, Instituto Geológico y Minero de España, Madrid, **8**, 75–80.

Canals, M., Lastras, G., Urgeles, R., Casamor, J.L., Mienert, J., Cattaneo, A., De Batist, M., Haflidason, H., Imbo, Y., Laberg, J.S., Locat, J., Long, D., Longva, O., Masson, D.G., Sultan, N., Trincardi, F. & Bryn, P. (2004) Slope failure dynamics and impacts from seafloor and shallow sub-seafloor geophysical data: case studies from the COSTA project. *Mar. Geol.*, **213**, 9–72.

Carlier, G., Lorand, J.P., Liégeois, J.P., Fornari, M., Soler, P., Carlotto, V. & Cárdenas, J. (2005) Potassic-ultrapotassic mafic rocks delineate two lithospheric mantle blocks beneath the southern Peruvian Altiplano. *Geology*, **33**, 601–604.

Carlotto, V. (2002) Evolution andine et raccourcissement au niveau de Cusco (13–16°S) Pérou. Thèse de Doctorat Université Joseph Fourier, Grenoble. *Géologie Alpine, Mémoire Hors Série*, **39**, 203 p.

Carlotto, V., Gil, W., Cárdenas, J. & Chávez, R. (1996) Geología de los cuadrángulos de Urubamba y Calca hojas 27-r y 27-s. Boletín INGEMMET, **65**, serie A, Carta Geológica Nacional, 245 p.

Carlotto, V., Jaillard, E. & Mascle, G. (1992) Relación entre sedimentación, paleogeografía y tectónica en la región de Cusco (Sur del Perú) entre el Jurásico Superior-Paleoceno. *Bol. Soc. Geol. Perú*, **83**, 1–20.

Chanove, G., Mattauer, M. & Mégard, F. (1969) Précisions sur la tectonique tangentielle des terrains secondaires du massif de Pirin (Nord-Ouest du lac Titicaca, Pérou). *C. R. Acad. Sci., Sér. D*, **268**, 1698–1701.

Collot, J., Lewis, K., Lamarche, G. & Lallemand, S. (2001) The giant Ruatoria debris avalanche on the northern Hikurangi margin, New Zealand: result of oblique seamount subduction. *J. Geophys. Res. (B9)*, **106**, 19271–19298.

Cosgrove, J.W. (1995) The expression of hydraulic fracturing in rocks and sediments. In: *Fractography: Fracture Topography as a Tool in Fracture Mechanics and Stress Analysis* (Ed. by M.S. Ameen), *Spec. Publ. Geol. Soc. London*, **92**, 187–196.

Cruz, M. (2002) Estratigrafía y evolución tectono-sedimentaria de los depósitos sin-orogénicos del cuadrángulo de Huambo: Las formaciones Ashua y Huanca, departamento de Arequipa. Tesis de la Universidad Nacional San Agustín de Arequipa, 127 p.

De Jong, K.A. (1974) Melange (Olistostrome) near Lago Titicaca, Peru. *AAPG Bull.*, **58**, 729–741.

Demercian, S., Szatmari, P. & Cobbold, P.R. (1993) Style and pattern of salt diapirs due to thin-skinned gravitational gliding, Campos and Santos basins, offshore Brazil. *Tectonophysics*, **228**, 393–433.

Ellison, R.A., Klinck, B.A. & Hawkins, M.P. (1989) Deformation events in Andean orogenic cycle in the Altiplano and Western Cordillera, southern Peru. *J. South Am Earth Sci.*, **2**, 263–276.

Floquet, M. & Hennuy, J. (2003) Evolutionary gravity flow deposits in the Middle Turonian – Early Coniacian southern Provence Basin (SE France): origins and depositional processes. In: *Submarine Mass Movements and their Consequences* (Ed. by J. Locat & J. Mienert), pp. 417–424. Kluwer Academic Publishers, Dordrecht (the Netherlands).

Frey-Martínez, J., Cartwright, J. & Hall, B. (2005) 3D seismic interpretation of slump complexes: examples from the continental margin of Israel. *Basin Res.*, **17**, 83–108.

Frey-Martínez, J., Cartwright, J. & James, D. (2006) Frontally confined versus frontally emergent submarine landslides: a 3D seismic characterisation. *Mar. Petrol. Geol.*, **23**, 585–604.

Gee, M.J.R., Masson, D.G, Watts, A.B. & Allen, P.A. (1999) The Saharan debris flow: an insight into the mechanics of long runout submarine debris flows. *Sedimentology*, **46**, 317–335.

Gradmann, S., Hübscher, C., Ben-Avraham, Z., Gajewski, D. & Netzeband, G. (2005) Salt tectonics off northern Israel. *Mar. Petrol. Geol.*, **22**, 597–611.

Graf, A.A. (2002) Le Cénomanien supérieur en Bolivie: Etude sédimentologique et stratigraphique de la Formation Matilde-Miraflores. Travail de diplôme, Université de Fribourg, Suisse.

Graf, A.A., Strasser, A. & Caron, M. (2003) OAE-2 equivalent (Upper Cenomanian) recorded in Bolivian shallow-water sediments. Abstract 11th Swiss Sed. Meeting, Fribourg, 39–40.

Graziano, R. (2001) The Cretaceous megabreccias of the Gargano Promontory (Apulia, southern Italy): their stratigraphic and genetic meaning in the evolutionary framework of the Apulia Carbonate Platform. *Terra Nova*, **13**, 110–116.

Green, A. & Wernicke, B. (1986) Possible large-magnitude Neogene extension on the southern Peruvian Altiplano: implications for the dynamics of mountain building. *Eos Trans. AGU*, **67**(44), Jt. Assem. Suppl., Abstract T52C-02.

Haflidason, H., Lien, R., Sejrup, H.P., Forsberg, C.F. & Bryn, P. (2005) The dating and morphometry of the Storegga Slide. *Mar. Petrol. Geol.*, **22**, 123–136.

Haflidason, H., Sejrup, H.P., Nygård, A., Mienert, J., Bryn, P., Lien, R., Forsberg, C.F., Berg, K. & Masson, D. (2004) The Storegga Slide: architecture, geometry and slide development. *Mar. Geol.*, **213**, 201–234.

Hardenbol, J., Thierry, J., Farley, M.B., Jacquin, T., De Graciansky, P.-C. & Vail, P.R. (1998) Mesozoic and Cenozoic sequence chronostratigraphic framework of European basins, chart 1. In: *Mesozoic and Cenozoic Sequence Stratigraphy of European Basins* (Ed. by P.-C. de Graciansky, J. Hardenbol, T. Jacquin & P.R. Vail), *SEPM Spec. Publ.*, **60**, 363–364.

Heim, A. (1947) Estudios tectónicos en la región del campo petrolífero de Pirín, lado NW del Lago Titicaca. Boletín Oficial de la Dirección de Minas y Petróleo (Ministerio de Fomento), Año XXVI, **79**, 47 p.

Huvenne, V.A.I., Croker, P.F. & Henriet, J.P. (2002) A refreshing 3D view of an ancient collapse and slope failure. *Terra Nova*, **14**, 33–40.

Jaillard, E. (1990) Evolución de la margen andina en el norte del Perú desde el Aptiano superior hasta el Senoniano. *Bol. Soc. Geol. Perú*, **81**, 3–13.

Jaillard, E. (1994) Kimmeridgian to Paleocene tectonic and geodynamic evolution of the Peruvian (and Ecuadorian) margin. In: *Cretaceous Tectonics of the Andes* (Ed. by J.A. Salfity), pp. 101–167. Earth Evolution Sciences Monograph Series, Vieweg Publications, Wiesbaden.

Jaillard, E. (1995) La sedimentación Albiana–Turoniana en el Sur del Perú (Arequipa–Puno–Putina). *Soc. Geol. Perú, Vol. Jubilar Alberto Benavides*, 135–157.

Jaillard, E. & Arnaud-Vanneau, A. (1993) The Cenomanian–Turonian transition on the Peruvian margin. *Cretaceous Res.*, **14**, 585–605.

Jaillard, E., Cappetta, H., Ellenberger, P., Feist, M., Grambast-Fessard, N., Lefranc, J.-P. & Sige, B. (1993) The Late Cretaceous Vilquechico Group of southern Peru. Sedimentology, paleontology, biostratigraphy, correlations. *Cretaceous Res.*, **14**, 623–661.

Jaillard, E. & Sempere, T. (1991) Las secuencias sedimentarias de la Formación Miraflores y su significado cronoestratigráfico. *Rev. Tëcn. YPFB*, **12**, 257–264.

Jaillard, E., Sempere, T., Soler, P., Carlier, G. & Marocco, R. (1995) The role of Tethys in the evolution of the northern Andes between Late Permian and Late Eocene times. In: *The Ocean Basins and Margins, Volume 8: The Tethys Ocean* (Ed. by A.E.M. Nairn, L.-E. Ricou, B. Vrielynck & J. Dercourt), pp. 463–492. Plenum Press, New York.

Kalafatovich, V. (1957) Edad de las calizas de la Formación Yuncaypata, Cuzco. *Bol. Soc. Geol. Perú*, **32**, 127–139.

Klinck, B.A., Ellison, R.A. & Hawkins, M.P. (1986) The geology of the Cordillera Occidental and Altiplano west of Lake Titicaca, southern Peru. Preliminary report, INGEMMET, Lima, Peru, 353 p.

Lajoie, J. (1972) Slump fold axis orientations: an indication of paleoslope? *J. Sedimen. Petrol.*, **42**, 584–586.

Laubacher, G. (1978) Géologie des Andes péruviennes: Géologie de la Cordillère Orientale et de l'Altiplano au nord et nord-ouest du lac Titicaca (Pérou). Travaux et Documents de l'ORSTOM, **95**, 219 p.

Lewis, K.B. (1971) Slumping on a continental slope inclined at 1–4°. *Sedimentology*, **16**, 97–110.

Locat, J. & Lee, H.J. (2002) Submarine landslides: advances and challenges. *Can. Geotech. J.*, **39**, 193–212.

Lucente, C.C. & Pini, G.A. (2003) Anatomy and emplacement mechanism of a large submarine slide within a Miocene foredeep in the Northern Apennines, Italy: a field perspective. *Am. J. Sci.*, **303**, 565–602.

Martinsen, O.J. (1989) Styles of soft-sediment deformation on a Namurian (Carboniferous) delta slope, western Irish Namurian Basin, Ireland. In: *Deltas: Sites and Traps for Fossil Fuels* (Ed. by M.K.G. Whateley & K.T. Pickering), *Spec. Publ. Geol. Soc. London*, **41**, 167–177.

Martinsen, O.J. & Bakken, B. (1990) Extensional and compressional zones in slumps and slides in the Namurian of County Clare, Ireland. *J. Geol. Soc. London*, **147**, 153–164.

Mienert, J., Berndt, C., Laberg, J.S. & Vorren, T.O. (2002) Slope Instability of Continental Margins. In: *Ocean Margin Systems* (Ed. by G. Wefer, D. Billet, D. Hebbeln, B.B. Jørgensen, M. Schlüter & T. van Veering), pp. 179–193. SpringerVerlag, Berlin.

Moore, A. (1993) Neogene crustal extension in the southern Peruvian Altiplano: Implications for the dynamics of mountain building. Unpublished PhD Thesis, Harvard University, 279 p.

Mourgues, R. & Cobbold, P.R. (2003) Some tectonic consequences of fluid overpressures and seepage forces as demonstrated by sandbox modelling. *Tectonophysics*, **376**, 75–97.

Müller, G. (1967) Diagenesis in argillaceous sediments. In: *Diagenesis in Sediments* (Ed. by G. Larsen & G.V. Chilingar), *Developments in Sedimentology*, **8**, 127–177. Elsevier, Amsterdam.

Myers, J.S. (1974) Cretaceous stratigraphy and structure, western Andes of Peru between latitudes 10° and 10°30′S. *Am. Assoc. Petrol. Geol. Bull.*, **58**, 474–487.

Newell, N.D. (1949) Geology of the Lake Titicaca region, Peru and Bolivia. *Geol. Soc. Am. Memoir*, **36**, 111 p.

Nichols, R.J. (1995) The liquification and remobilization of sandy sediments. In: *Characterization of Deep Marine Clastic Systems* (Ed. by A.J. Hartley & D.J. Prosser), *Spec. Publ. Geol. Soc. London*, **94**, 63–76.

Payros, A., Pujalte, V. & Orue-Etxebarria, X. (1999) The South Pyrenean Eocene carbonate megabreccias revisited: new interpretation based on evidence from the Pamplona Basin. *Sediment. Geol.*, **125**, 165–194.

Pino, A., Sempere, T., Jacay, J. & Fornari, M. (2004) Estratigrafía, paleografía y paleotectónica del intervalo Paleozoico

Superior – Cretáceo inferior en el área de Mal Paso – Palca (Tacna). *Publ. Especial Soc. Geol. Perú*, **5**, 15–44.

Popenoe, P., Schmuck, E.A. & Dillon, W.P. (1993) The Cape Fear Landslide; slope failure associated with salt diapirism and gas hydrate decomposition. In: *Submarine Landslides; Selected Studies in the U.S. Exclusive Economic Zone* (Ed. by W.C. Schwab, H.J. Lee & D.C. Twichell), pp. 40–53. U.S. Geological Survey Bulletin.

Portugal, J. (1964) Geology of the Puno-Santa Lucia area, Department of Puno, Peru. Unpublished PhD Thesis, University of Cincinnati, 141 p.

Portugal, J. (1974) Mesozoic and Cenozoic stratigraphy and tectonic events of Puno-Santa Lucia area, Department of Puno, Peru. *AAPG Bull.*, **58**, 982–999.

Rassmuss, J.E. (1935) Informe sobre la región petrolífera de Puno. *Bol. Dir. Minas y Petróleo Ministerio Fomento del Perú, año 15*, **45**, 85–105.

Sempere, T. (1994) Kimmeridgian? to Paleocene tectonic evolution of Bolivia. In: *Cretaceous Tectonics in the Andes* (Ed. by J.A. Salfity), pp. 168–212 Earth Evolution Sciences Monograph Series, Vieweg Publications, Wiesbaden.

Sempere, T. (1995) Phanerozoic evolution of Bolivia and adjacent regions. In: *Petroleum Basins of South America* (Ed. by A.J. Tankard, R. Suárez & H.J. Welsink), *American Association of Petroleum Geologists Memoir* **62**, 207–230.

Sempere, T., Acosta, H. & Carlotto, V. (2004a) Estratigrafía del Mesozoico y Paleógeno al Norte del Lago Titicaca. *Publ. Especial Soc. Geol. Perú*, **5**, 81–103.

Sempere, T., Carlier, G., Soler, P., Fornari, M., Carlotto, V., Jacay, J., Arispe, O., Néraudeau, D., Cardenas, J., Rosas, S. & Jiménez, N. (2002a) Late permian–middle Jurassic lithospheric thinning in Peru and Bolivia, and its bearing on Andean-age tectonics. *Tectonophysics*, **345**, 153–181.

Sempere, T. & Jacay, J. (2006) Estructura tectónica del sur del Perú (antearco, arco, y Altiplano suroccidental). Extended abstract, *XIII Congreso Peruano de Geología*, Lima, 324–327.

Sempere, T. & Jacay, J. (2007) Synorogenic extensional tectonics in the forearc, arc and southwest Altiplano of southern Peru. *Eos Trans. AGU*, **88 (23)**, Jt. Assem. Suppl., Abstract U51B-04.

Sempere, T., Jacay, J., Carrillo, M.-A., Gómez, P., Odonne, F. & Biraben, V. (2000) Características y génesis de la Formación Ayabacas (Departamentos de Puno y Cusco). *Bol. Soc. Geol. Perú*, **90**, 69–76.

Sempere, T., Jacay, J., Carlotto, V., Martínez, W., Bedoya, C., Fornari, M., Roperch, P., Acosta, H., Acosta, J., Cerpa, L., Flores, A., Ibarra, I., Latorre, O., Mamani, M., Meza, P., Odonne, F., Orós, Y., Pino, A. & Rodríguez, R. (2004b) Sistemas transcurrentes de escala litosférica en el Sur del Perú. *Publ. Especial Soc. Geol. Perú*, **5**, 105–110.

Sempere, T., Jacay, J., Fornari, M., Roperch, P., Acosta, H., Bedoya, C., Cerpa, L., Flores, A., Husson, L., Ibarra, I., Latorre, O., Mamani, M., Meza, P., Odonne, F., Oros, Y., Pino, A. & Rodríguez, R. (2002b) Lithospheric-scale transcurrent fault systems in Andean southern Peru. Extended abstract, *V International Symposium on Andean Geodynamics*, Toulouse, 601–604.

Sempere, T., Jacay, J., Pino, A., Bertrand, H., Carlotto, V., Fornari, M., García, R., Jiménez, M., Marzoli, A., Meyer, C.A., Rosas, S. & Soler, P. (2004c) Estiramiento litosférico del Paleozoico Superior al Cretáceo Medio en el Perú y Bolivia. *Publ. Especial Soc. Geol. Perú*, **5**, 45–79.

Sigé, B., Sempere, T., Butler, R.F., Marshall, L.G. & Crochet, J.-Y. (2004) Age and stratigraphic reassessment of the fossil-bearing Laguna Umayo red mudstone unit, SE Peru, from regional stratigraphy, fossil record, and paleomagnetism. *Geobios*, **37**, 771–794.

Spathopoulos, F. (1996) An insight on salt tectonics in the Angola Basin, South Atlantic. In: *Salt Tectonics* (Ed. by G.I. Aslop, D.J. Blundell & I. Davison), *Spec. Publ. Geol. Soc. London*, **92**, 187–196.

Spence, G.H. & Tucker, M.E. (1997) Genesis of limestone megabreccias and their significance in carbonate sequence stratigraphic models: a review. *Sediment. Geol.*, **112**, 163–193.

Spörli, K.B. & Rowland, J.V. (2007) Superposed deformation in turbidites and syn-sedimentary slides of the tectonically active Miocene Waitemata Basin, northern New Zealand. *Basin Res.*, **19**, 199–216.

Steen, Ø. & Andresen, A. (1997) Deformational structures associated with gravitational block gliding: examples from sedimentary olistoliths in the Kalvåg Melange, western Norway. *Am. J. Sci.*, **297**, 56–97.

Strachan, J.L. & Alsop, G.I. (2006) Slump folds as estimators of palaeoslope: a case study from the Fisherstreet Slump of County Clare, Ireland. *Basin Res.*, **18**, 451–470.

Sultan, N., Cochonat, P., Canals, M., Cattaneo, A., Dennielou, B., Haflidason, H., Laberg, J.S., Long, D., Mienert, J., Trincardi, F., Urgeles, R., Vorren, T.O. & Wilson, C. (2004) Triggering mechanisms of slope instability processes and sediment failures on continental margins: a geotechnical approach. *Marine Geol.*, **213**, 29–321.

Varnes, D.J. (1978) Slope movement types and processes. In: *Landslides-Analysis and Control. Special Report* (Ed. by R.L. Shuster & R.J. Krizek). **176** (pp. 11–33. National Academy of Sciences, Washington.

Vendeville, B. & Cobbold, P.R. (1987) Glissements gravitaires synsédimentaires et failles normales listriques: modèles expérimentaux. *C. R. Acad. Sci., Sér. II*, **305**, 1313–1319.

Vendeville, B. & Gaullier, V. (2003) Role of pore-fluid pressure and slope angle in triggering submarine mass movements: natural examples and pilot experimental models. In: *Submarine Mass Movements and their Consequences* (Ed. by J. Locat & J. Mienert), pp. 137–144. Kluwer Academic Publishers, Dordrecht (the Netherlands).

Vernhet, E., Heubeck, C., Zhu, M.-Y. & Zhang, J.-M. (2006) Large-scale slope instability at the southern margin of the Ediacaran Yangtze platform (Hunan province, central China). *Precambrian Res.*, **148**, 32–44.

Vorren, T.O. & Laberg, J.S. (2001) Late Quaternary sedimentary processes and environment on the Norwegian-Greenland Sea continental margins. In: *Sedimentary Environments Offshore Norway – Palaeozoic to Recent* (Ed. by O.J. Martinsen & T. Dreyer), pp. 451–456. Elsevier, Amsterdam.

Woodcock, N.H. (1979) The use of slump structures as paleoslope orientation estimators. *Sedimentology*, **26**, 83–99.

Wynn, R.B., Masson, D.G., Stow, D.A. & Weaver, P.P. (2000) The Northwest African slope apron: a modern analogue for deep-water systems with complex sea floor topography. *Mar. Petrol. Geol.*, **17**, 253–265.

Manuscript received 10 July 2007; Manuscript accepted 10 March 08.

Supplementary material

The following supplementary material is available for this article:

Table S1. Table of abbreviations used in the paper.

Appendix S1. Detailed documentation about the stratigraphy of southern Peru and the data and discussion relative to the age of the Ayabacas collapse.

This material is available as part of the online article from: http://www.blackwell-synergy.com/doi/abs/10.1111/j.1365-2117.2008.00358.x

(This link will take you to the article abstract).

Please note: Blackwell Publishing are not responsible for the content or functionality of any supplementary materials supplied by the authors. Any queries (other than missing material) should be directed to the corresponding author for the article.

Supplementary online material to **"Giant submarine collapse of a carbonate platform at the Turonian-Coniacian transition: The Ayabacas Formation, southern Peru" (**P. Callot, T. Sempere, F. Odonne, E. Robert). Basin Research.

TABLE OF ABBREVIATIONS

CECLLA: Spanish abbreviation for Cusco-Lagunillas-Laraqueri-Abaroa structural corridor.

i.e.: *id est* ("that is").

e.g.: *exempli gratia* ("for example").

Fm: Formation.

Ma: mega-annum, for a point in time.

Myr: millions of years, for a duration of time.

OAE-2: Oceanic Anoxic Event 2.

PETM: Paleocene-Eocene Thermal Maximum.

p.p.: *pro parte* ("in part")

sensu: "in the sense of"

SFI: Spanish abbreviation for Incapuquio fault system.

SFUACC: Spanish abbreviation for Urcos-Ayaviri-Copacabana-Coniri fault system.

s.s.: *sensu stricto* ("in the stricter sense").

sp.: species.

viz: *videlicet* ("namely").

WPBAB: Western Peru back-arc basin.

III.

ORGANISATION SPATIALE DES FACIES DE RESEDIMENTATION, SEMELLE DE GLISSEMENT ET GENESE DES STRUCTURES DU COLLAPSE

III. Organisation spatiale des faciès de resédimentation, semelle de glissement et genèse des structures du collapse.

Ce chapitre s'intéresse aux faciès des matériaux redistribués (brèches, matériaux liquifiés, filons sédimentaires, déformations plastiques) dans la Formation Ayabacas et explique leur mise en place. Il est également souligné l'effet d'une semelle de glissement (*sliding sole*) qui a permis le déplacement des masses calcaires et de grands blocs des formations antérieures. Ce travail a fait l'objet d'une publication soumise à la revue *Sedimentary Geology*.

III.1. Causes and consequences of liquification and soft-sediment deformation in a limestone megabreccia: A case study from the Ayabacas giant collapse, southern Peru

Article soumis à *Sedimentary Geology*. Résumé étendu en français de l'article 3 :

Les dépôts de la Formation Ayabacas consistent en une mégabrèche, organisée du NE au SO en relation avec deux systèmes de failles majeurs (le SFUACC et le CECLLA). Des faciès de remobilisation des sédiments (tels que bréchification, liquification, filons sédimentaires, déformation plastique des sédiments) sont décrits et définissent quatre types de faciès de resédimentation. Les trois premiers, qui présentent une matrice siliciclastique et carbonatée, se rencontrent dans les parties amont du collapse (au NE du CECLLA), tandis que le quatrième type de faciès comporte seulement des matériaux carbonatés et affleure plus en aval, dans le corridor du CECLLA et à l'ouest de celui-ci.

Le faciès de Type-1 se rencontre principalement dans la zone de Cusco-Urubamba et se caractérise par des filons sédimentaires de plusieurs mètres de long et ~10-20 cm d'épaisseur expulsant vers le haut des matériaux rouges dérivant de la Formation Murco. Ces filons se rétrécissent vers le haut jusqu'à disparaître dans les radeaux calcaires plus lithifiés.

Le faciès de Type-2 affleure notamment à Yanaoco et au sud de la route reliant Cabanillas à Santa-Lucia. Dans ce faciès, de grandes quantités de matériaux issus des formations Murco et Arcurquina ont été remobilisés, déformés plastiquement et/ou liquifiés (présence de filons sédimentaires). Les radeaux calcaires flottent dans un mélange de matériaux, constitués de la matrice *s.s.* et de clastes anguleux de taille millimétrique à pluridécimétrique. Ces clastes sont généralement carbonatés (dérivant de la Formation Arcurquina) ou moins souvent

siliciclastiques (dérivant de la Formation Murco). La matrice *s.s.* est silico-marneuse, constituée de matériaux liquifiés dérivant des formations Murco et Ayabacas.

Le faciès de Type-3 est très semblable au faciès de Type-2, mais se distingue de ce dernier par la présence de clastes arrondis, de 1-20 cm de diamètre, issus de la Formation Mitu (Permo-Trias). Il affleure localement, principalement au sud de Santa Rosa.

Ces trois premiers faciès se caractérisent également par des déformations et des faciès bréchiques quelle que soit l'échelle d'observation : à l'échelle kilométrique en photographies aériennes, à l'échelle de la centaine de mètres jusqu'au centimètre à l'affleurement, ou encore à l'échelle du centimètre et du millimètre en lames minces. En conséquence la Formation Ayabacas se définit comme une brèche multi-échelle ou "fractale", au contraire des brèches tectoniques localisées dans les zones de faille. Les matériaux resédimentés de ces parties amont étaient enclins à se déformer plastiquement et à se liquifier, leur permettant de fonctionner comme une semelle de glissement qui a facilité la migration de radeaux calcaires et de blocs lithifiés des formations antérieures.

Les affleurements du faciès Type-4 partagent les caractères suivants : (i) le matériel est presque exclusivement calcaire, les matériaux silicoclastiques dérivés de la Formation Murco ne s'observent pas dans les dépôts du collapse ; (ii) les clastes calcaires anguleux sont omniprésents ; (iii) les bancs bréchifiés alternent avec des bancs régulièrement stratifiés ; (iv) chaque niveau bréchifié est constitué de clastes de deux ou trois faciès calcaires différents dérivant des bancs sus- et/ou sous-jacents ; (v) les clastes sont presque toujours en contact dans les brèches ; (vi) l'espace entre les clastes est faible et généralement comblé par de la boue carbonatée, de la calcite ou un mélange des deux. Des slumps et des radeaux calcaires de 10 à 100 mètres de long sont parfois observés.

Les sédiments de la Formation Murco, enfouis plus profondément, étaient déjà lithifiés, plus difficilement déformables, et n'ont pas été entraînés dans le collapse. En conséquence la semelle de glissement très ductile, qui s'est comportée comme une couche lubrifiante plus en amont, n'existe plus ici, ce qui est également suggéré par la fragmentation et la désorganisation décroissante des dépôts du collapse à partir du CECLLA vers l'aval.

Les matériaux impliqués dans la Formation Ayabacas présentaient différents degrés de lithification avant le collapse. Du NE au SW une augmentation du degré de lithification résulte d'un âge de dépôt plus ancien ainsi que d'une subsidence et d'un enfouissement plus important à l'ouest du bassin d'arrière-arc, notamment en relation avec l'activité du CECLLA et les deux transgressions marines (Albien inférieur - Albien Supérieur et Cénomanien

supérieur - Turonien supérieur). Dans les zones amont du collapse (au NE du CECLLA), d'importantes variations du degré de lithification des matériaux semblent avoir existé verticalement dans la pile sédimentaire peu avant le collapse : à la base (i) se trouvaient des pélites et des grès fins argileux lithifés de la Formation Murco, devenant progressivement en remontant dans la série (ii) moins cimentés, riches en eau et donc potentiellement liquifiables et remobilisables. Ils sont recouverts entre le CECLLA et le SFUACC par (iii) des calcaires cimentés de quelques mètres d'épaisseur, au plus, déposés lors de la première transgression puis, (iv) par 20-30 m (épaisseur moyenne des radeaux calcaires) de carbonates cohésifs mais pas totalement lithifiés et enfin (v) par une boue carbonatée récemment déposée.

Les calcaires cimentés à la base de la Formation Arcurquina ont ainsi formé un couvercle imperméable, empêchant l'expulsion des fluides piégés dans la Formation Murco sous-jacente. Bien que le collapse soit déclenché par l'activation de failles normales et la création de pentes, l'étendue et l'intensité du collapse ont probablement été augmentées par la présence de ces matériaux non cimentés et saturés en eau, qui ont joué le rôle de semelle de glissement. La fracturation, la fragmentation et l'ablation des matériaux de la couche indurée de calcaire ont également généré les clastes calcaires de toutes tailles rencontrés dans le mélange.

Dans la partie sud du collapse (transect Huancané-Juliaca-Santa Lucia-Lagunillas-Yura), la surface de décollement se situe dans la Formation Murco entre la tête du collapse et le CECLLA, puis à l'interface entre les formations Murco et Arcurquina entre le CECLLA et le pied du collapse. Là, dans la région de Yura, de grands plis affectant toute la pile sédimentaire carbonatée (mais ni les formations antérieures ni les postérieures) amortissent le collapse, qui semble avoir été bloqué par un seuil topographique probablement dû à l'arc magmatique. Le glissement serait donc frontalement confiné (*frontally confined slide* ; Frey-Martínez et al., 2006).

Dans la partie nord du collapse (transect Cusco-Abancay Chalhuanca), la surface de décollement est, comme au sud, localisée dans la Formation Murco jusqu'au CECLLA, mais semble ensuite se situer dans la succession carbonatée plus en aval. La coalescence du SFUACC et du CECLLA suggère qu'ici l'enfouissement de la Formation Murco et de la base de la Formation Arcurquina a été significatif, préservant ces matériaux du collapse. Le pied du collapse n'a pas été précisément observé dans la partie nord, mais l'absence de structures de compression similaires à celles de la région de Yura suggère que la partie nord du collapse n'a pas été bloquée dans la région de Chalhuanca et a pu s'écouler plus librement.

Causes and consequences of liquification and soft-sediment deformation in a limestone megabreccia: A case study from the Ayabacas giant collapse, southern Peru

Pierre Callot*, Francis Odonne and Thierry Sempere

LMTG, Université de Toulouse, CNRS, IRD, OMP, 14 av. Edouard Belin, F-31400 Toulouse France [callot@lmtg.obs-mip.fr, odonne@lmtg.obs-mip.fr, sempere@lmtg.obs-mip.fr]

* corresponding author

Abstract

In the back-arc basin of southern Peru, the bulk of the mid-Cretaceous carbonate platform collapsed near the Turonian-Coniacian boundary (~90-89 Ma), due to slope creation and resulting oversteepening. The resulting mass-wasting deposits, namely the Ayabacas Formation, consist of a megabreccia which is organised from NE to SW in relation with two major fault systems. Facies of sediment reworking (such as brecciation, liquification, sedimentary dykes and soft-sediment deformation) are described and define four types of resedimentation facies.

In the northeastern part of the study area, deposits mainly consist of a mix of very heterometric clasts (millimetric to kilometric in size), mainly carbonated but also sandy-marly in nature, floating in sandy-marly matrix that exhibit features of liquification (sedimentary dykes and flows) and plastic deformations. Here, resedimentation facies are characterized by deformations and a brecciated facies at each observation scale (from aerial photographs to thin sections) and are therefore defined as fractal or multi-scale breccias. Some clasts and large amounts of the matrix were derived from the underlying clay-rich sandstones of the Murco Formation. These materials were prone to liquification and plastic deformation, allowing them to act as a sliding sole that facilitated the slides and the downslope movement of large limestone rafts.

In the southwestern part of the study area, only limestone breccias are observed, in alternation with well-stratified levels. The sliding sole of plastically deformable siliciclastic sediments that previously acted as a lubricating layer was not present here, as materials were more deeply burried.

Variations in the lithification degree of materials are inferred to have existed before the collapse from northeast to southwest and also in the sedimentary succession in the northeastern part. In particular, limestones were well-cemented at the base of the carbonated

succession and formed a cap that prevented water to escape from the underlying siliciclastic materials. Such a succession allowed the formation of limestone clasts and of a sliding sole constituted by water-saturated siliciclastic materials.

In the southern part of the study area, the sliding surface was located within the Murco Formation in the upper part of the collapse and just above the Murco Formation downslope. The collapse was frontally confined as it was blocked downslope by a topographic high that folded the whole limestone succession. In the northern part of the study area, the sliding surface was also within the Murco Formation in the upper part, but is observed within the limestone succession downslope, due to a higher subsidence that buried more deeply the sediments. The compressional structure affecting the limestone succession in the south are not observed there, suggesting that the toe of the collapse was not blocked here.

Keywords: fossil submarine slides; sedimentary instabilities; slope instabilities; soft sediment deformation; megabreccia; Turonian Coniacian boundary; Ayabacas Formation.

1) Introduction

Submarine mass movements are recognized as a major mechanism of sediment redistribution over continental margins (Mienert et al., 2002; Canals et al., 2004) and both present-day and fossil submarine landslides are assiduously studied to understand instability processes. On the basis of bathymetric and geophysical data or, less often, core analysis, several studies in the last decade have dealt with the characteristics, morphology and triggering mechanisms of recent large-scale submarine landslides (*e.g.*, Mulder & Cochonat, 1996; Gee et al., 1999; McAdoo et al., 2000; Wynn et al., 2000; Collot et al., 2001; Mulder & Alexander, 2001; Vorren and Laberg, 2001; Huvenne et al., 2002; Canals et al., 2004; Haflidason et al., 2004, 2005; Wilson et al., 2004; Frey-Martínez et al., 2005, 2006; Moscardelli and Wood, 2008; Tripsanas et al., 2008; Henrich et al., 2008). Studies of ancient examples of such phenomena are less common and dimensions of the slide bodies rarely exceed >100 km (*e.g.*, Martinsen and Bakken, 1990; Hine et al., 1992; George et al., 1995; Steen and Andresen, 1997; Payros et al., 1999; Graziano, 2001; Drzewiecki and Simó, 2002; Lucente and Pini, 2003; Floquet and Hennuy, 2003; Alonso et al., 2006; Vernhet et al., 2006; Spörli and Rowland, 2007). When compared to present-day submarine landslides, fossil slides provide detailed informations on internal structures and facies as well as deformation and depositional processes (Naylor, 1981; Lucente and Pini, 2003; Strachan, 2008) that are difficult to obtain in present-day mass-transport deposits.

In southern Peru, most of the mid-Cretaceous carbonate platform collapsed near the Turonian-Coniacian boundary. The resulting deposits constitute the Ayabacas Formation, a prime example of very large fossil mass-transport deposits (Callot et al., 2008). It consists of an impressive unit of mm- to km-size limestone fragments and so described as a limestone megabreccia (*sensu* Spence and Tucker, 1997). Its deposits deriving from different processes (*e.g.* sliding, slumping, debris flow, rafts within a sandy-muddy matrix, brecciation), the Ayabacas collapse can also be defined as a mass-wasting deposit (*sensu* Lucente and Pini, 2003, 2008). The triggering of this extremely large mass wasting ensued from slope creation, oversteepening and seismicity produced by extensional tectonic activity (Callot et al., 2008), but large amount of sedimentary breccias and liquified sediments within the mélange strongly suggests that a *sliding sole* has greatly facilitated the formation of the submarine slides in the proximal part of the collapsed area. The presence of a lubricating layer of mud has been proposed in some present-day submarine slide, *e.g.* in the Storegga Slide (De Blasio et al., 2004). In the present study, it has been possible to examine the spatial evolution of deformational facies and structures at a wide range of scales (micrometric to multi-kilometric). This analysis provides information about their generation in relation with fault systems and explains their role in the collapse.

2) Geological setting

2.1. Location of the Ayabacas Formation and basin architecture

The study area is located in southern Peru and extends along the southwestern rim of the Eastern Cordillera and throughout the Altiplano and Western Cordillera, including the Arequipa area (Fig. 1). The Ayabacas Formation and underlying units were deposited in the southern region of the western Peru back-arc basin (WPBAB, Fig. 1), which was active in the Jurassic and Cretaceous (Jaillard et al., 1995). The basin, subsident from Early Albian to Turonian times, had developed in an extensional tectonic context and deepened overall to the west (Jaillard, 1994). The number and extension of Ayabacas Formation outcrops decrease markedly toward the west-southwest due to an increase of Neogene volcanic cover and other deposits. No mid-Cretaceous limestone unit has been mapped so far immediately west and south of the study area.

The study area includes two important Andean-age structural systems that have also controlled a number of depositional characteristics of the pre-orogenic accumulations, such as facies and thicknesses (Sempere, 1995; Sempere et al., 2002a,b, 2004b,c; Pino et al., 2004).

First, the Urcos-Ayaviri-Copacabana-Coniri fault system (abbreviated as SFUACC in Spanish; Fig. 1) has played an important role in the triggering of the Ayabacas collapse and in the control of its morphology (Callot et al., 2008). The SFUACC is a major lithospheric boundary (Carlier et al., 2005) that has mainly behaved as a sinistral fault system during the Andean orogeny (Sempere et al., 2002b, 2004b; Sempere and Jacay, 2006, 2007). Second, the Cusco-Lagunillas-Laraqueri-Abaroa structural corridor (abbreviated as CECLLA in Spanish; Fig. 1) is a broad structural system which separates two domains that behaved very distinctly during at least the Cenozoic, Cretaceous and Jurassic, more subsidence and a much deeper depositional environment being recorded west of the CECLLA (Sempere et al., 2002b, 2004b, Callot et al., 2008).

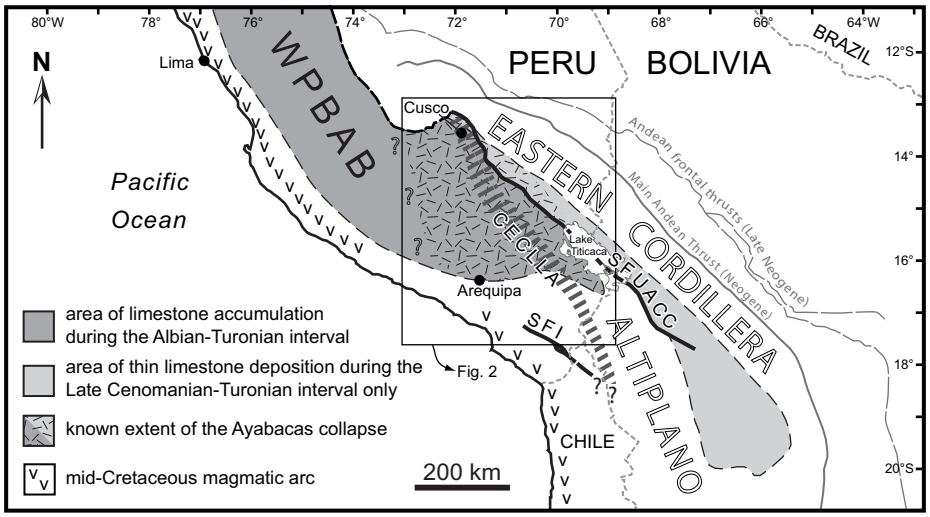

Fig. 1. Map of southern Peru and adjacent regions with elements relevant for Albian to Turonian times. Both shaded areas belong to the western Peru back-arc basin (WPBAB) and accumulated mostly limestones during this time interval. The Early and Middle Albian transgression is only recorded west of the SFUACC system in the main basin (darker shading); the Late Cenomanian - Turonian transgression flooded this main basin and also the sub-basin located northeast of the SFUACC system (lighter shading). The Ayabacas collapse (irregular dashes) developed in the northwesternmost segment of this sub-basin, and in the southwestern part of the main basin. A magmatic arc was active along the present-day coastal belt, but, prior to the Coniacian, the south of Peru was apparently devoid of volcanic activity as only plutons are recorded at the west and south of Arequipa. CECCLA, SFUACC: see text (section 1.1); SFI = Incapuquio fault system (Spanish abbreviation). Adapted from Jaillard and Sempere (1991), Jaillard and Arnaud-Vanneau (1993), Jaillard (1994), Sempere (1994), Jaillard et al. (1995), Sempere (1995), Sempere et al. (2002b, 2004b), Callot et al. (2008).

2.2. Stratigraphic summary of the study area

Absolute stratigraphic ages mentioned in this paper are taken from Ogg et al.'s (2004) chart. The abbreviation Ma (*mega-annum*) is used for a point in time, and Myr (millions of years) for a duration of time.

The stratigraphy of the study area was updated by Sempere et al. (2004a) and Sigé et al. (2004) and is detailed in Callot et al. (2007, 2008). The Upper Jurassic to Upper Cretaceous stratigraphy of the Lake Titicaca region can be briefly described as follows:

- Fluvio-aeolian sandstones described as the Huancané Formation were deposited during the Late Jurassic and earliest Cretaceous. Some gentle deformation affected the southern Peruvian basin at some time in the Early Cretaceous and produced local uplifts that led to partial to complete erosion of the previous Mesozoic accumulations, locally down to the mid-Paleozoic basement.
- The resulting erosional surface was subsequently onlapped by continental and overlying marine deposits:

  - The Angostura and Murco formations grade horizontally and vertically into one another, and consist respectively of conglomerates to sandstones, and of red siltstones to mudstones with subordinate sandstones. The Angostura Formation occurs at the base of this transgressive set, but only in specific areas, whereas the Murco Formation was deposited over the entire region.

  - This Early Cretaceous continental set was overlain by marine, regularly-bedded, thickening-upward, grey to black, organic-rich micritic limestones (Arcurquina Formation, Early Albian to Late Turonian southwest of the SFUACC fault system, and Late Cenomanian to Late Turonian northeast of it; Callot et al., 2008). These limestones were deposited in an extensive carbonate platform, mostly during two transgressions and subsequent highstands (Early Albian — Late Albian, ~108.5 - ~102 Ma; Late Cenomanian — Late Turonian, ~95 - ~90 Ma) (Fig. 1). In the Cusco area, the local equivalent of the Murco Formation consists of red mudstones and silstones, and evaporite masses (mainly gypsum; halite also occurs), and is described as the Maras Formation (Carlotto et al., 1996).
- The Ayabacas Formation consists of a particularly disturbed and chaotic unit, which results from the collapse of the Arcurquina carbonate platform (Callot et al., 2008). It mainly reworks deposits from the Arcurquina Formation and parts of the Murco (Maras) Formation; fragments of older units (down to Paleozoic rocks) are also found within the mélange in specific areas. The breccias and liquified sediments dealt with in this paper occur in the Ayabacas Formation. The collapse occurred near the Turonian-Coniacian boundary or in the latest Turonian (~91-89 Ma; Callot et al., 2008; Sempere et al., submitted).
- The Ayabacas Formation and its characteristic deformation are overlain by the Vilquechico Group (and equivalent units) of Coniacian to Paleocene age (Jaillard et al., 1993;

Sigé et al., 2004). The lower formation of the Vilquechico Group consists of dominantly red mudstones and argillaceous sandstones (Jaillard, 1995); gypsum bodies and coarse sandstones (at the base of the unit) are locally present, as well as Coniacian ammonite-bearing limestones in the equivalent Ashua Formation of the Arequipa area (Cruz, 2002).

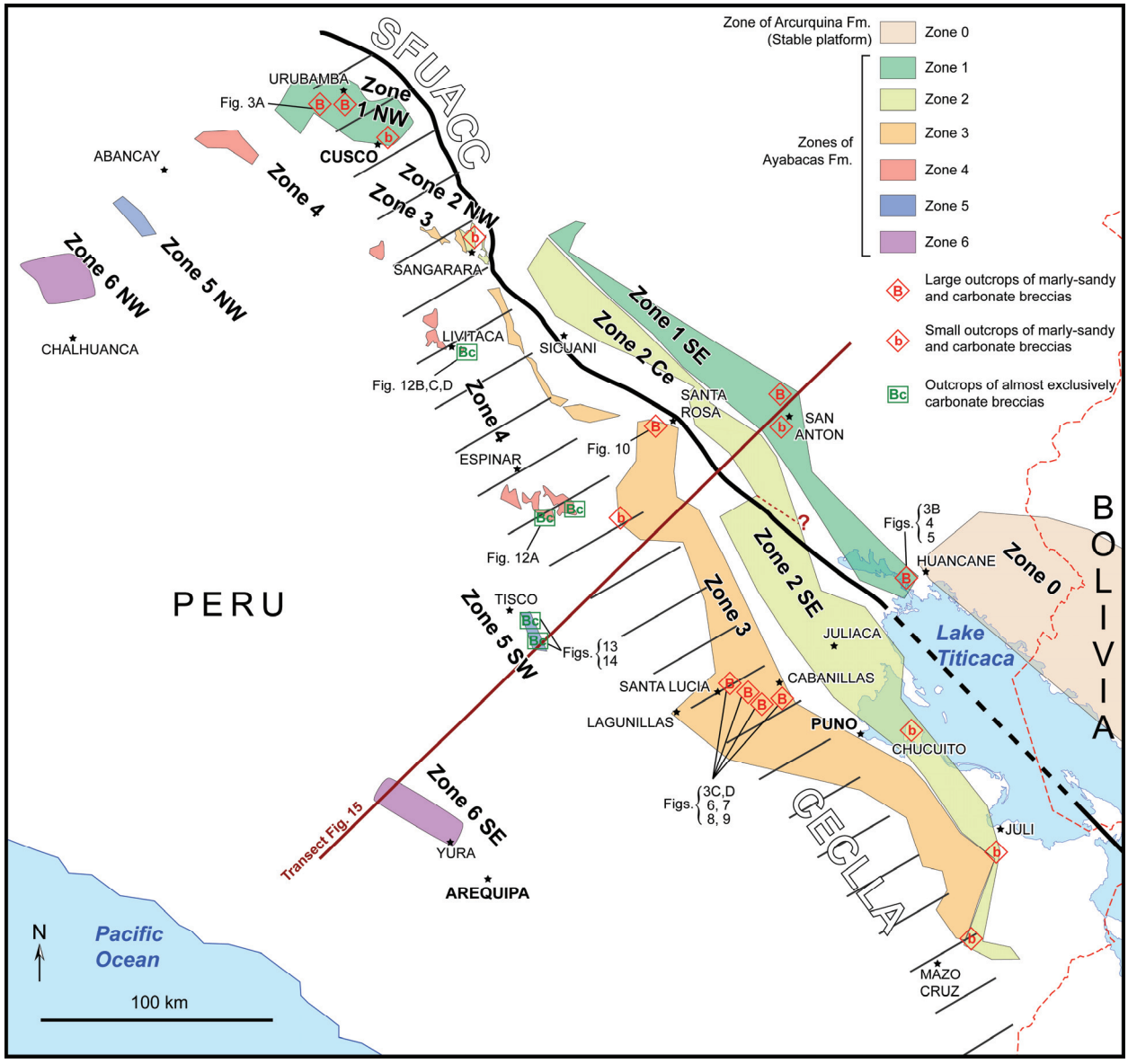

Fig. 2. Main deformational facies in the Ayabacas Formation, localities cited in text, location of the SFUACC and CECLLA fault systems and of the outcrops where breccias and fluidized sediments are abounding. According to deformational facies, outcrops of the Ayabacas Formation have been distributed into six zones by Callot et al. (2008). Zone 0 is formed to the Arcurquina Formation, i.e. the deposits of the stable carbonate platform. In zones 1 to 3 the three most significant outcrops for breccias and fluidized sediments are south of the Cabanillas-Santa Lucía road (~UTM zone 19L 0343000/8267000, 4000 m elevation), at Yanaoco (~8 km WSW of Huancané, UTM zone 19L 0411000/8316220, 3850 m elevation) and NW of Pancarhualla (~13.25 km WSW of Urubamba, UTM zone 18L 0807700/8514490, 3610 m elevation). In zones 4 and 5 the breccias, almost exclusively carbonated, are mainly found southeast of Livitaca (UTM zone 19L 0215660/8413000, 3750 m elevation), Espinar (in particular around UTM zone 19L 0250960/8343000, 4100 m elevation) and Tisco (~UTM zone 19L 0248220/8292770, 4800 m elevation). Breccias are not found in any part of Zone 6 or in the undestabilized Zone 0.

2.3. The Ayabacas Formation

The Ayabacas Formation consists of an extraordinarily deformed, highly disrupted, chaotic unit that reworks previous deposits and rocks (Cabrera and Petersen, 1936; Portugal, 1964, 1974; Sempere et al., 2000; Callot et al., 2008). It typically lacks regular stratification, in marked contrast with the underlying and overlying units. No undisturbed marine limestone strata occur either within or at the top of the Ayabacas Formation, which is directly overlain by reddish strata of mainly continental origin (Vilquechico Group and equivalent units). In contrast, the Arcurquina Formation was deposited as regular strata, as is evident from the rafts and sheets included in the collapse and from outcrops in the preserved sectors of the platform, *i.e.* those that were not involved in the collapse (mainly the eastern part of the basin).

The Ayabacas Formation irregularly crops out over 60,000 km² and is inferred to extend over >80,000 km². As its thickness varies from 0 to ≥500 m, its volume is estimated to be >10,000 km^3 (>10^{13} m^3). Given its dimensions, the Ayabacas appears as the most extensive ancient submarine mass wasting body currently known, and one of the thickest, when compared to the published dimensions of mass-wasting bodies plotted by Lucente and Pini (2003). Its extension and thickness are of the same magnitude as the largest and thickest recent bodies described to date, *e.g.* the Storegga Slide (Haflidason et al., 2004, 2005), the Bjørnøyrenna Slide (Vorren and Laberg, 2001), the Cape Fear Slide (Popenoe et al., 1993), the Saharan Debris Flow (Gee et al., 1999), the Israel Slump Complexes (Frey-Martínez et al., 2005) or the Orotava-Icod-Tino Avalanche (Wynn et al., 2000). It is organized in six zones characterized on the basis of deformational facies and a seventh corresponds to the northeastern "stable" area, *i.e.* the preserved Arcurquina Formation (Fig. 2; Callot et al., 2008). It mainly includes mm- to km-size limestone fragments reworked from the underlying Arcurquina Formation. In the northeastern half of the study area (Zones 1 to 3), these fragments are enclosed in a "matrix" of reddish mudstones and siltstones reworked from the Murco Formation, *i.e.* the unit underlying the Arcurquina Formation. Only limestones are documented in the southwest (Zones 4 to 6). In northeastern areas, lithified blocks of Jurassic sandstones and even Paleozoic shales are sometimes observed embedded in the Ayabacas Formation. Particularly significant is the common occurrence of liquified sediments and breccias within the "matrix", implying a submarine collapse process (Fig. 2). The Ayabacas Formation thus forms a single mass-wasting body that displays noteworthy internal facies variations.

The collapse was mainly triggered by a significant extensional tectonic activity, as demonstrated by synsedimentary normal faults and related thickness variations in the Ayabacas Formation. The collapse coincided with the abrupt end of the regional carbonate platform and termination of extensive limestone deposition: after the collapse deposits in the backarc were almost exclusively continental or volcanic in nature. Extension created seismicity and slopes on which sliding of the Arcurquina and earlier strata was enabled (Callot et al., 2008). Slidings might have been favoured and/or enhanced by other factors: in particular a potential *sliding sole*, constituted by the partially unlithified Murco, was present throughout the carbonate platform. Remains of this sole, mainly composed of mudstone to siltstone, are found within all the NE part of the sliding area (and absent from zones 4 to 6, Fig. 2), where it constitutes a significant part of the mélange, in particular of the breccias.

3) Resedimentation facies in the Ayabacas Formation

Following Nichols (1995), the terms liquification, fluidization and liquefaction are used in this paper. Sediment liquification describes any process that transforms a sediment into a liquid-like state (Allen, 1982), including: (1) fluidization when it results from pore fluid movement; (2) liquefaction when caused by the agitation of grains during cyclic shear stress; and (3) shear liquification which results from the movement of grains during the application of a shear stress across the sediment. The three phenomena occurred during the Ayabacas collapse. However, because it is generally difficult to distinguish between fluidization and liquefaction, the term liquification is mostly used hereafter.

The matrix surrounding the limestone rafts in the Ayabacas Formation displays peculiar facies of sediment reworking, such as brecciation and liquification. The lack of classical tectonic features, such as slickenslides and striated faults, oriented tectonic breccias, cleavage, and/or pervasive calcite veining, shows that these facies result from soft-sediment deformation processes. The breccias were previously considered as the product of early karstification (Audebaud, 1971; Audebaud et al., 1973) or subaerial sliding (De Jong, 1974), but such mechanism would have taken place after lithification whereas many features show evidence of soft-sediment deformation (Callot et al., 2008). Onasch and Kahle (2002) highlighted a similar confusion in Silurian carbonates where breccias resulting from seismites were previously attributed to karstification (Carman, 1927; Sparling, 1970) or karst collapse (Johnson, 1974).

Due to the Cenozoic and vegetation covers, the best observations were provided by a few particularly good outcrops described below. Four types of resedimentation facies were observed throughout the region in which the Ayabacas Formation is known (Fig. 2). The first three of them involve a siliciclastic matrix, whereas the fourth type consists only of limestone material, in marked difference with the former.

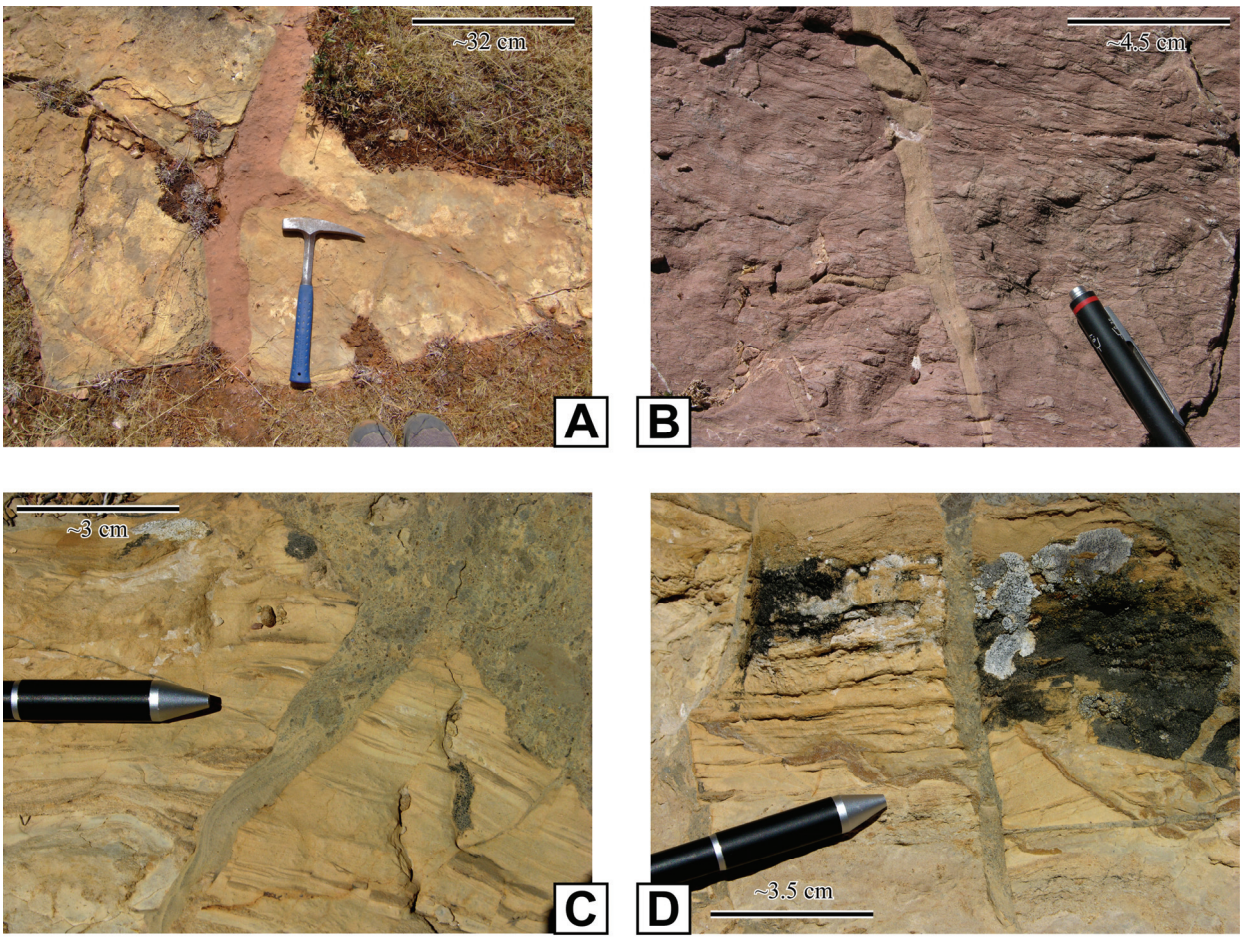

Fig. 3. Photos of sedimentary dykes in Zone 1 (Pancarhualla outcrop, A; Yanaoco outcrop, B) and in Zone 3 (Cabanillas outcrop, C and D). Dyke in A is injected from the bottom to the top, whereas dykes in B, C and D are filled in from the top to the bottom. In D also occur horizontal dykes that display the injection of liquified sediments in the fractures of more lithified rocks. Such injections have probably facilitated the fragmentation of lithified sediments and the formation of clasts.

3.1. Eastern resedimentation facies: breccias and liquified sediment

3.1.1. Type-1 facies: The Pancarhualla outcrops (Cusco-Urubamba area)

This outcrop area is located ~13 km WSW of Urubamba in the Cusco region (Fig. 2). Here the Ayabacas Formation displays a peculiar large-scale facies characterized by sporadic, chaotic limestone blocks included in a material adscribed to the Maras Formation, which covers extensive stretches. The Maras Formation, the local equivalent of the Murco

Formation (Carlotto et al., 1996), consists of red calcareous siltstones and subordinate gypsum and halite bodies. Breccias and fluidized sediments crop out at the base of a few isolated limestone rafts confined in the Maras/Murco Formation.

The base of the Ayabacas Formation consists of red mudstones to siltstones, which probably were a part of the Maras Formation before the collapse. In thin sections its facies is quite heterogeneous but generally appears as ~25-30% of small (<50 μm in size), angular quartz grains floating in a marly matrix. It also contains rare, large (~100-200 μm), rounded quartz grains (apparently aeolian in origin), as well as some oxides in some areas. They are covered by a yellow marly to progressively grey calcareous material, usually without any quartz grain and commonly dolomitized and oxide-rich in its lower part. Porosity of the materials increases from bottom to top. This level is crossed by red clastic dykes (Fig. 3A). Field and thin-section observations show that dykes originated in the red level at the base: both facies are identical, but porosity is higher in the clastic dykes. Dykes are ~10-20 cm-wide and vertical in the lower part and get progressively thinner and of variable orientation up to disappear ~10 m upwards in the massive grey limestone. At the base they sometimes contain angular and solid clasts floating in the matrix. Most of these clasts are elements of the first red level, but some yellow elements deriving from the upper level are also observed.

Type-1 facies are thus characterized by extensive plurimetric clastic dykes expulsing upwards red liquified sediment from the Murco Formation into the more lithified limestone raft, where they progressively die out. Brecciation and clasts are scarce, most often present in the largest part of the dykes. Type-1 facies may also appear north of San Antón and very locally in some Cabanillas outcrops.

3.1.2. Type-2 facies: the Yanaoco and Cabanillas outcrops

Cabanillas and Yanaoco respectively provide the first and second most significant outcrops regarding brecciation and liquification facies. These outcrops are similar despite the fact that the Cabanillas outcrops are located ~85 km southwest of Yanaoco, in a more distal area when referred to the collapse anatomy. The Yanaoco outcrop is located ~8 km WSW of Huancané (Fig. 2) and was previously mentioned by Sempere et al. (2000). It constitutes one of the most proximal outcrops of the Ayabacas Formation, since the limestones cropping out at the nearby locality of Huancané were not involved in the collapse (Callot et al., 2008). Located south of the road between Cabanillas and Santa Lucia, the Cabanillas large and significant area of outcrops displays limestone rafts floating in a particularly well-exposed matrix with illustrative liquification and/or brecciation facies.

3.1.2.1. Yanaoco

In the Yanaoco outcrop, the Ayabacas Formation is ~75 m-thick and displays a local succession. There is no clear boundary between the red mudstones to sandstones of the Murco Formation *s.s.* and the base of the Ayabacas Formation, which consists of ~25 m-thick unit including small (20-30 m-long) and scattered limestone olistolites within a marly-sandy matrix. This zone of small limestone olistolites is overlain by a large raft (>100 m-long and 20 m-thick). Then a fully fluidized and brecciated zone (~30 m-thick) of marly-sandy sediments is present, and finally a mix of numerous small limestone olistolites and marly-sandy matrix occur in the topmost metres of the unit. Such a succession is local and cannot be considered as some "Ayabacas Sequence".

In thin sections, sandstones of the Murco Formation are almost exclusively constituted by two quartz grain families and some opaque minerals (~5-10%). About 80% of quartz grains are small (~50-200 µm) and quite angular, others are large (~400-1000 µm), very well rounded, probably aeolian. Contacts between quartz are generally sutured, indicating a high degree of compaction. The contact between the Murco and Ayabacas formations is blurry due to the facies similarity of *in situ* and reworked red silty to sandy material below and above the base of the slide; in thin sections, the basal portion of the Ayabacas Formation presents a sandy facies characterized by a carbonate cement and a lesser compaction when compared to that observed in the typical Murco Formation.

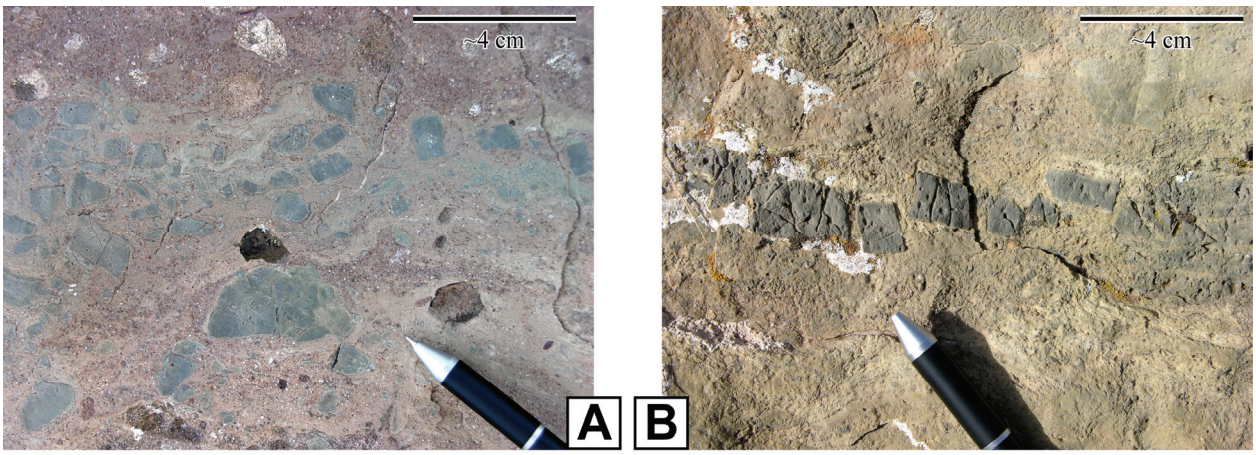

Fig. 4. Mix of sediments from the Ayabacas Formation surrounding the large rafts in the Yanaoco outcrop (Zone 1, Type-2 resedimentation facies). Note the cm-sized limestone clasts, tilted and well-cemented at the time of the collapse. They are floating in marly-sandy sediments that were plastically deformed and thus probably liquified.

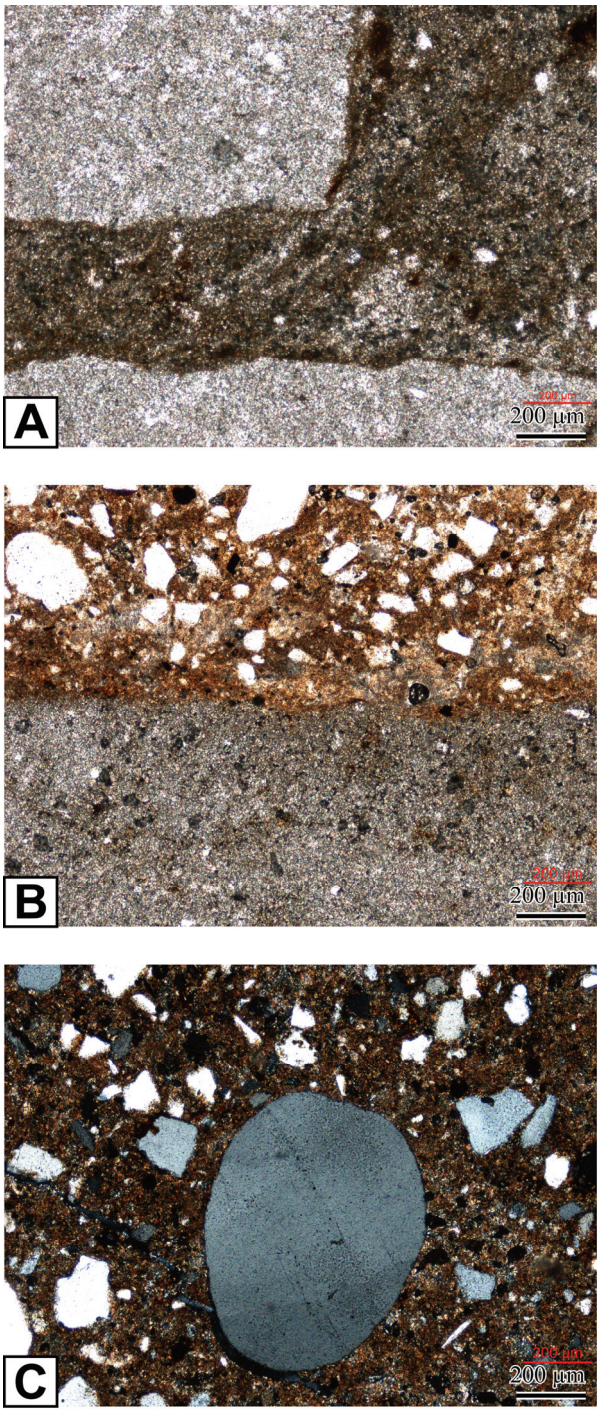

Fig. 5. Thin sections (1.72 mm x 1.29 mm) of samples from Yanaoco displaying the matrix characteristics of the Type-2 resedimented structure. A: limestone clasts are light coloured, the marly matrix is dark coloured and display evidence of plastic deformation. B: Contact between the sandy-marly matrix (top) and a limestone clast (bottom). No mineralization appears between the clast and the matrix. C: The sandy-marly matrix of the Ayabacas Formation displaying the two families of quartz grains of the Murco Formation (large, rounded, aeolian quartz grain and small, angular quartz grains).

In the Ayabacas Formation the matrix surrounding large (> 10 m) limestone rafts and olistolites is also a mix of marly-sandy sediments and sandy or carbonated angular clasts, generally matrix-supported (see section 3.1.4 below). The formation can be described as a megabreccia (*sensu* Spence and Tucker, 1997) composed of very heterometric (mm to km in size), matrix-supported, angular clasts (generally carbonated, less often siliciclastic or marly) within a marly-sandy matrix. Sediments of the matrix often present evident marks of liquification, such as sedimentary dykes (Fig. 3B), fluid movements and plastic deformations

(Fig. 4). Dykes must be defined as "sedimentary dykes" rather than clastic dykes (Montenat et al., 2007) since they are most often filled by partly calcareous material. They are small (~1-3 cm-thick, ~30-100 cm-long) and the infilling material is derived from the top or bottom. They represent injection of over-pressured fluidized material through more lithified strata. Carbonate sediment is generally lithified earlier than siliciclastic deposits, which often exhibit features of liquification and plastic deformation (*e.g.* Fig. 4). In the liquified matrix, Murco quartz grains of the two families are found in thin sections, sometimes scattered and floating in a generally carbonated and clayey matrix (Fig. 5), sometimes aggregated in clusters of quartz grains with sutured contacts.

Large differences in compaction are observed, from the well-compacted sandstones at the base of the Murco Formation to the less compacted matrix at the base of the Ayabacas Formation, and finally to a few zones where high-porosity material exist. In the matrix it is common to observe a low-compacted part (with quartz grains in marly cement) or well-compacted sandstone (with sutured contacts). These well-compacted parts within the matrix could correspond to lithified clasts of the Murco Formation involved into the collapse.

3.1.2.2. Cabanillas

The Cabanillas outcrops are much more diversified and larger than the Yanaoco outcrop. The Ayabacas Formation reaches at least 300 m in thickness (the topmost part is also lacking here) and is composed of limestone blocks and rafts (different from those of Yanaoco, thicker and more fragmented; Callot et al., 2008) embedded in a matrix. The Ayabacas is underlain by well-stratified strata consisting of conglomerates, sandstones and quartzites (Angostura Formation; see section 2.2 above) and this substratum is shaped into tilted blocks by ~NW-trending normal faults. The Murco Formation is generally not observed in its typical stratigraphic position: although its base may appear undisturbed, most of the formation is reworked in the matrix of the Ayabacas Formation as red and yellow material and brecciated clasts. At some localities, the Murco Formation *s.s.* was completely reworked and the Ayabacas Formation directly overlies the Angostura Formation. Remains of the Murco Formation *s.s.* and/or the lowermost Ayabacas Formation are commonly lacerated over ~10-20 m by numerous, brown, oxide-rich, centimetric veins, clearly subsequent to earlier deformations and resulting from later compaction, diagenesis and/or hydrothermal circulations. As observed at Yanaoco, variations in compaction are observed, between a highly compacted Angostura Formation with sutured quartz grain boundaries at the base whereas quartz grains float in a marly mud in the Ayabacas matrix above. Lithified blocks

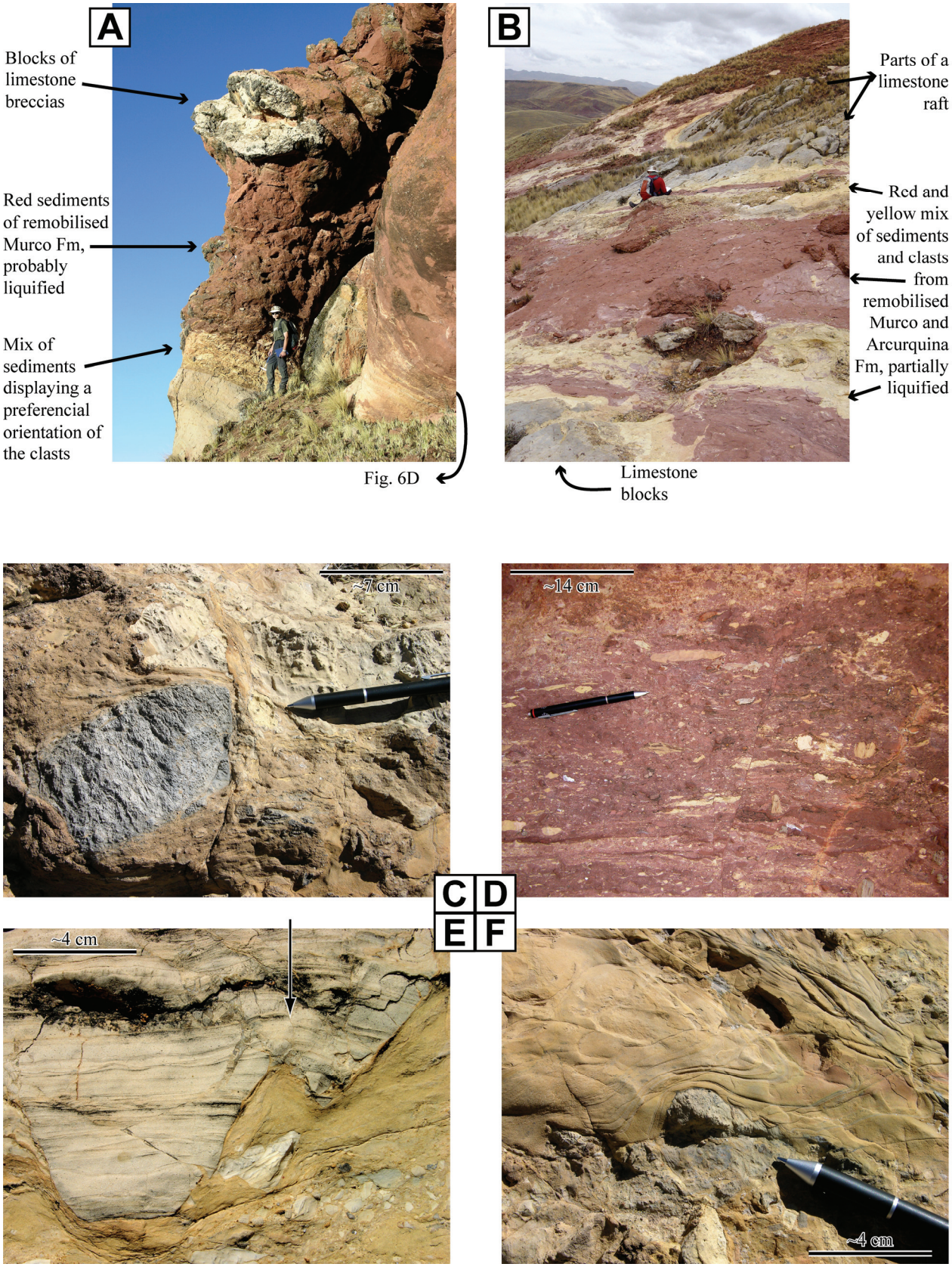

Fig. 6. Liquified sediments and breccias of the matrix surrounding large rafts in the Cabanillas area (Zone 3, Type-2 resedimentation facies). A: Overview of the collapse matrix at the base of the Ayabacas Formation. Red sediments are similar to the Murco Formation but, as a difference, also contain carbonate and clay. Other elements indicate that the Murco Formation has been partially liquified and involved into the collapse: sediments were plastically mixed, clasts are oriented at the base and allochtonous blocks of limestone breccias occur. B: Overview of the collapse matrix near the top of the outcrop. Sediments of the matrix still display characteristics of the Murco Formation unevenly enriched in carbonate and clay and plastically deformed. C:

Detail of the matrix. Note the evidence of liquefied sediments and the occurrence of clasts different in nature (one limestone clast well-rounded, grey-coloured at the left of the pen; above, one angular, fractured by the fluid, yellow-beige-coloured, marly clast; above the pen, two other marly clasts, angular and beige-coloured; at the point of the pen, a little, angular, yellow-coloured, marly-sandy clasts). D: Detail of Fig. 5 A, where lithified limestone clasts have been oriented in the horizontal plane. Some yellow sandy-marly clasts, less lithified, are also oriented and were plastically deformed. E and F: Liquified sediments mould the shape of the more lithified clasts. In E the clasts are fractured but it seems that the fluid pressure also deform them (below the arrow).

(~50 m in size) of the Angostura Formation are locally involved into the mélange (see Fig. 10 in Callot et al., 2008) but such well-compacted elements are only observed as large blocks (>10 m in size). As at Yanaoco, the smaller clasts (centimetric to decimetric in size, siliciclastic or carbonated) are derived from the Murco and Arcurquina formations. The proportion of carbonate clasts is higher than at Yanaoco. Clasts are also more diversified in nature: different sandstones, marls and limestones are commonly found over a few meters of outcrop (*e.g.* Fig. 6C). The resulting deposits range from clast-supported to matrix-supported breccias, with very heterometric (mm to km in size) clasts (see section 3.1.4 below).

Both field and thin-section observations indicate that large amounts of sediment were subjected to liquification, plastic deformation and soft-sediment deformation. In the field, these deformations are marked by sedimentary dykes (Fig. 3C,D), deformed and/or oriented clasts (Fig. 6D), blocks or clasts moulded by sediment (Fig. 6). In thin sections, small clasts (Fig. 7F) or aggregates of grains (Fig. 7C,E) are also plastically deformed and/or oriented. Furthermore, quartz grains and micas locally display preferential orientations (Fig. 7D,E), and thus a fluidal texture. The matrix in which large rafts and blocks are included consists of a mixture of sediments that were partly fragmented into small clasts but also largely liquified (Fig. 6A,B), and thus must have behaved as a fluid.

The liquified matrix was injected into the more lithified limestone rafts according to two processes (Fig. 8). The first one consists of an injection due to pressure at the base of rafts, which caused its brecciation: liquified sediment vertically broke up some beds and was injected into the weakest areas, in particular horizontally into stratification planes (Fig. 8B). This process explains the occurrence of numerous limestone clasts of diverse sizes in the matrix (Figs. 6 and 9). The second process corresponds to a downward flow of the liquified matrix into limestone rafts from their top. It is documented by markers of fluid movements from top to bottom and by the occurrence of continuous beds at the base of such rafts, *i.e.* that are not disrupted by these liquified materials (Fig. 8A). This phenomenon is likely to have been caused by fracturation and mutually independent motion of the limestone rafts (Portugal, 1964, 1974), in contrast with the first process, where the excess of pressure was the main factor of fluid injection and brecciation.

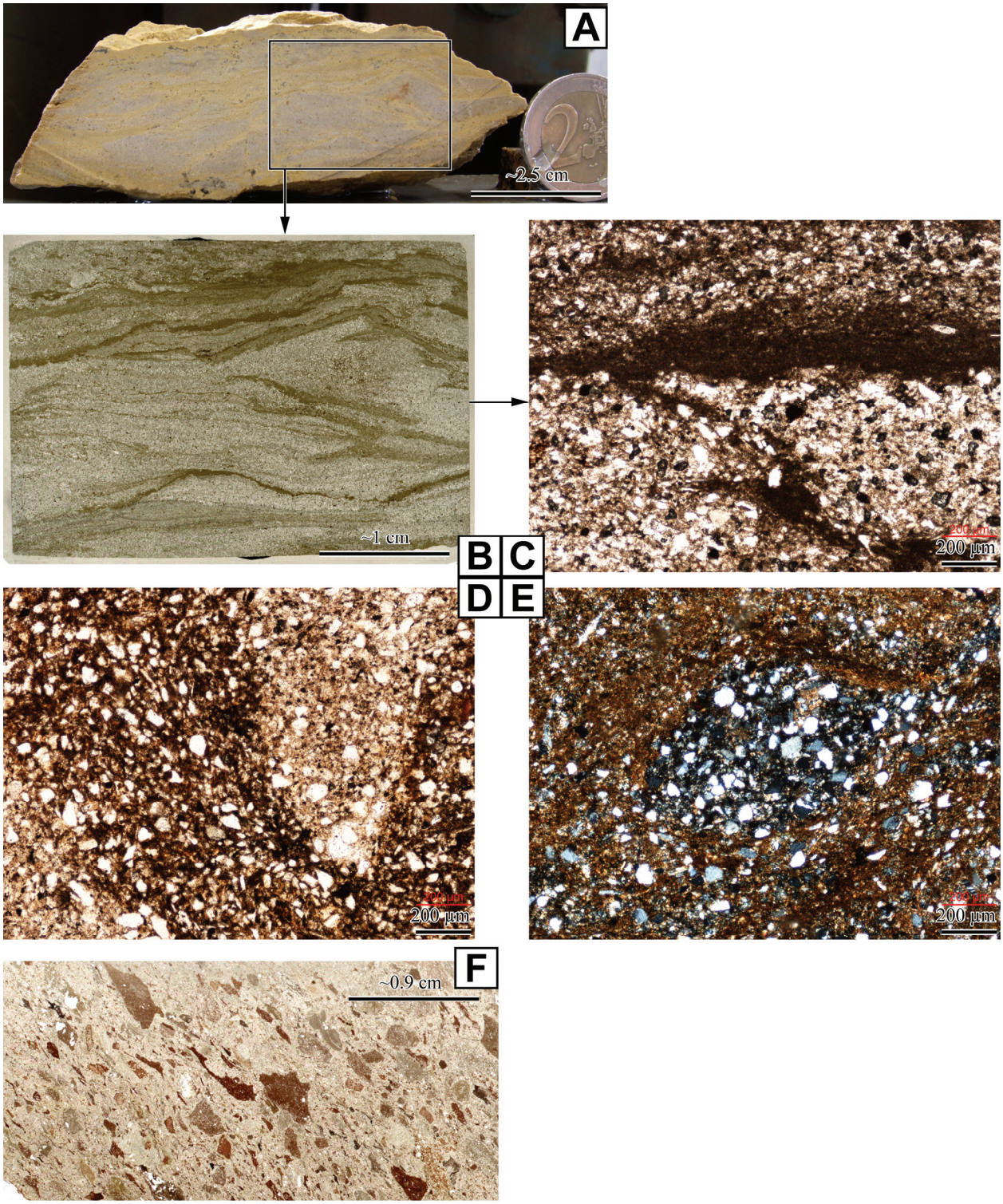

Fig. 7. Field sample (A) and thin sections (B to F) of liquified sediments from the matrix in the Cabanillas area (Zone 3, Type-2 resedimentation facies). In A, B and C, even the sandy-marly material (light-coloured) is plastically deformed as shown in C where it displays ductile deformation. Two types of materials are found in D and E thin sections: one composed by quartz grains and scarce mica grains supported by carbonate and clay, the other one is comprised of quartz grains cemented by carbonate. The marly-rich part of the sediment was fluid, as shown by the preferential orientation of the quartz grains. Quartz aggregates (e.g. in the centre of D) are also plastically deformed. In F the sandy-marly clasts display a markedly preferential orientation. Some of them were probably plastically deformed as shown by their tails that taper off.

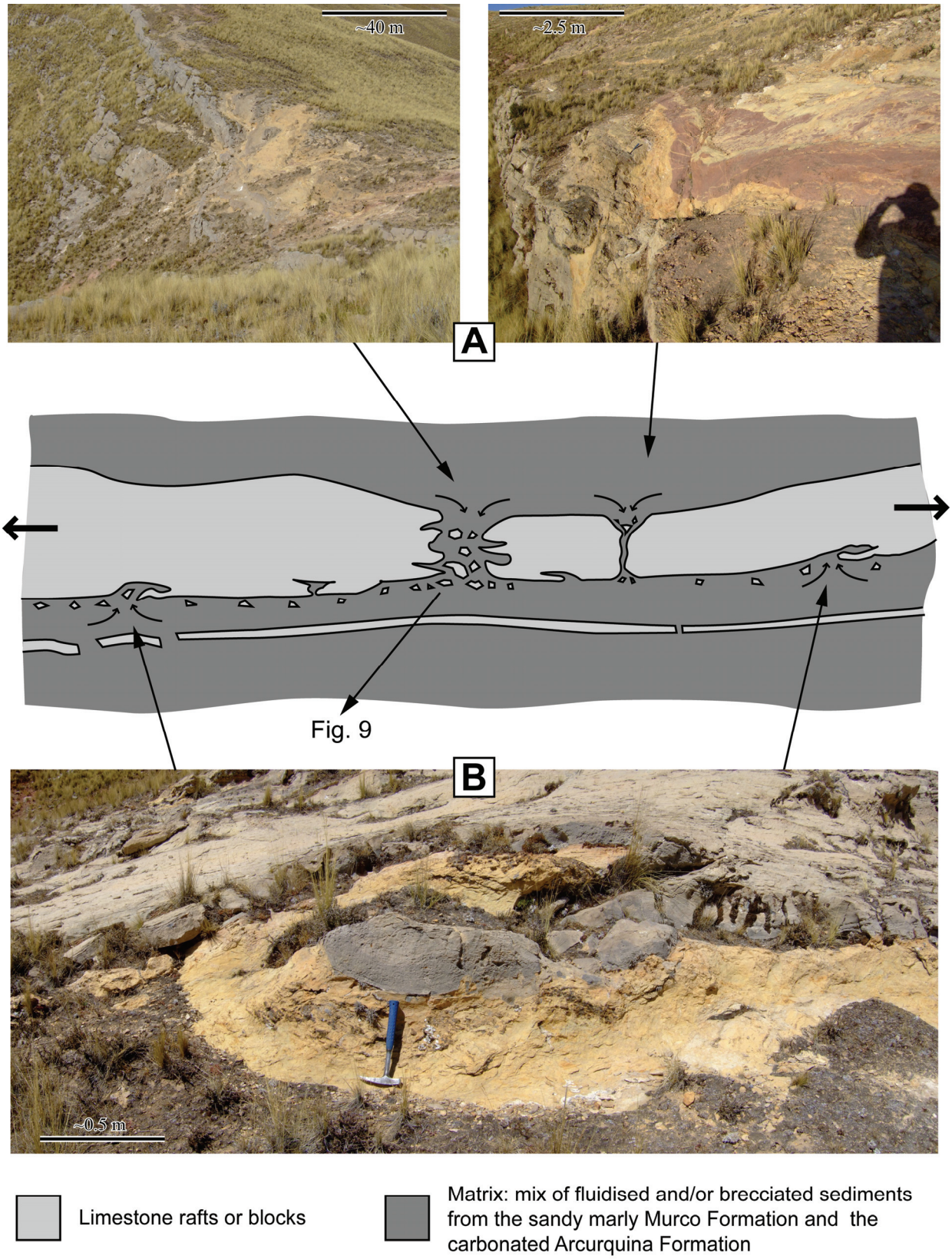

Fig. 8. Injection of the partially liquified sediments at the top (A) and at the base (B) of large limestone rafts, in the Cabanillas area. In case of injections from the top to the bottom (A), sediments frequently cross the whole limestone rafts. Injected sediments at the base (B) never cross the limestone rafts, but they penetrate into the stratification planes and bring down lithified blocks that constitute the abundant limestone clasts present below the rafts.

Fig. 9. Example of matrix-supported breccia found at the base of the large limestone rafts in the Cabanillas area. Clasts are very angular, very heterogeneous in size and derive from the upper limestone rafts (see Fig. 8). Hammer is 32.5 cm-long.

In the Cabanillas and Yanaoco outcrops, the Ayabacas Formation can thus be described as a megabreccia (*sensu* Spence and Tucker, 1997): it displays impressive resedimentation facies, with heterometric, inhomogeneous clasts floating in a sandy-marly, largely liquified matrix material mainly reworked from the Murco Formation.

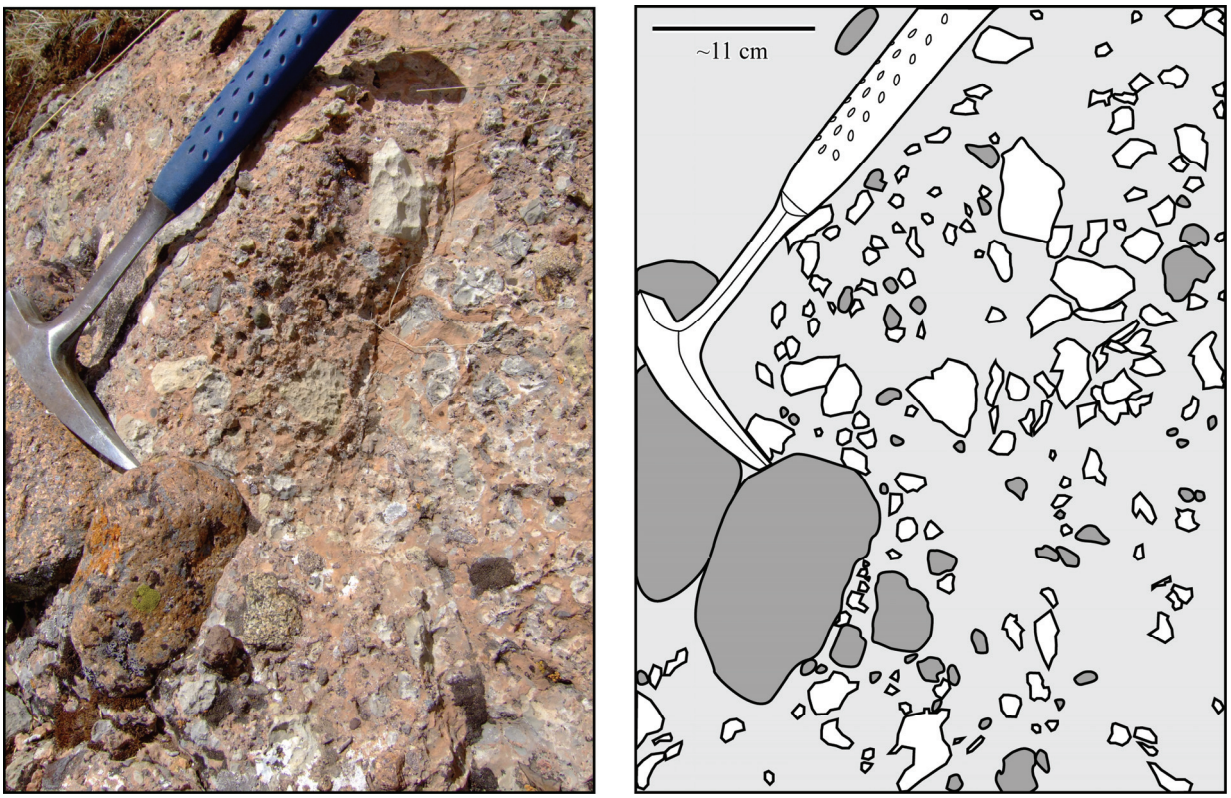

Fig. 10. Photo and interpretative outlines of breccia from the Type-3 resedimentation facies, ~12 km W of Santa Rosa. The matrix-supported breccia is formed by well-rounded clasts of the Mitu Formation and angular heterogeneous clasts (limestones, sandstones, marls) within a marly-sandy matrix.

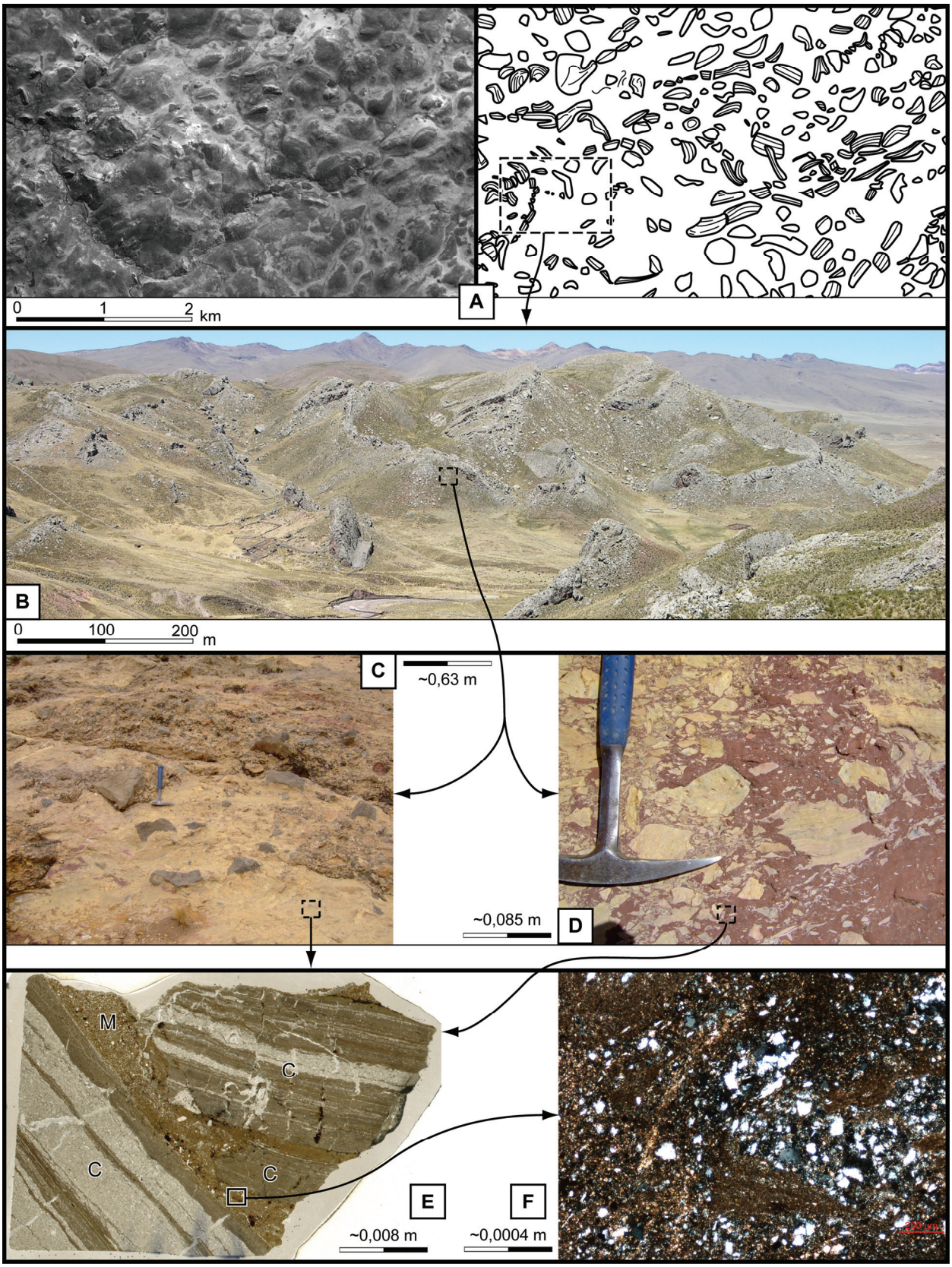

Fig. 11. Deformations and brecciated facies are observed at every scale of observation in the northeastern areas of the Ayabacas Formation: at a multi-kilometric-scale in aerial photo (A); at a kilometric, metric and centimetric scale in the field (B, C and D); at a centimetric or millimetric scale with samples or thin sections (E and F). Such deformations define the Ayabacas Formation as a fractal breccia, at least in its northeastern part (Zone 1 to 3).

3.1.3. Type-3 facies: the Santa Rosa outcrop

South of Santa Rosa, a large area (~150 km²) is covered by the Ayabacas Formation, formed here by an impressive chaos of limestone rafts (10s to 100s of m in size) within a matrix of red mudstone to siltstone. The chaotic aspect is particularly impressive in aerial photograph (Fig. 9 in Callot et al., 2008). In the north-westernmost part of this outcrop (UTM zone 19L 0295000/8382760, 4165 m elevation), the unit includes peculiar matrix-supported breccias. Clasts are diverse and include angular limestone and siliciclastic fragments (although more heterogeneous here than in the typical Type-2 facies), but also volcano-detritic pebbles derived from the Mitu Formation (Permian-Triassic age) (Fig. 10). The Mitu clasts are generally well-rounded, 1-20 cm in size, but smaller or larger (up to 30 cm-long) components were also found. The same facies is exposed very locally in one Cabanillas outcrop, over a few metres.

3.1.4. Fractal (multi-scale) breccias

The northeastern resedimentation facies are also characterized by deformations and a brecciated facies at whichever scale: in aerial photographs (Fig. 11) where the chaotic aspect is obvious, at the outcrop scale with limestone rafts chaotically floating in a matrix (Fig. 11B), which itself consits of partly liquified material including heterogeneous clasts (Fig. 11C,D). Finally, the overall chaotic facies even appears in thin sections (Fig. 11E,F) as a material locally clearly fluidized and including heterogeneous mixed elements (mainly quartz, carbonates and clays). Deformation can be observed at each observation scale (rafts in aerial photos and at outcrop scale, some deformed clasts at metric scale, and clusters of grains in thin section). Thereby the Ayabacas Formation can be defined as a "fractal breccia" in its eastern part, since the same geometric pattern (the brecciated character) is repeated at every observation scale, in strong contrast with tectonic breccias which are localized in the fault zone. The multi-scale brecciation of the Ayabacas Formation was already noted by De Jong (1974) who noticed that "*a continuous transition in size between the smallest clasts in the breccia and the largest blocks is common*". This fractal concept has also been noticed in the present-day Storegga Slide which presents evidence of scale invariant characteristics, in particular geometrical similarity of slide headwalls at a wide range of scales (Haflidason et al., 2004; Micallef et al., 2008).

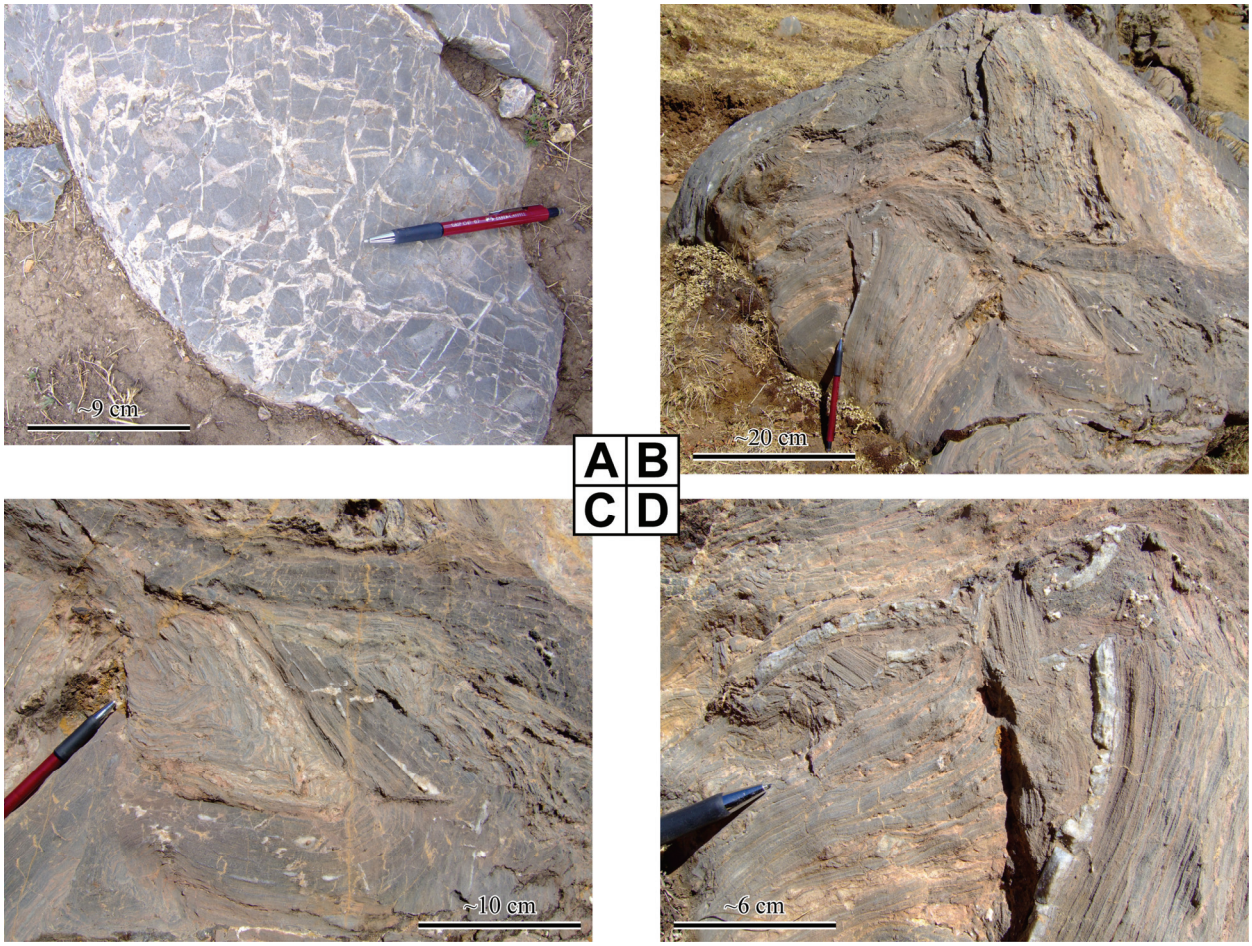

Fig. 12. Carbonate breccia southwest of Espinar (A) and Livitaca (B, C and D). Note in a clast (A) the fractures randomly oriented and filled with calcite. Limestone has sometimes been plastically deformed and then fragmented into clasts (each clast displaying a different deformation) (B, C and D).

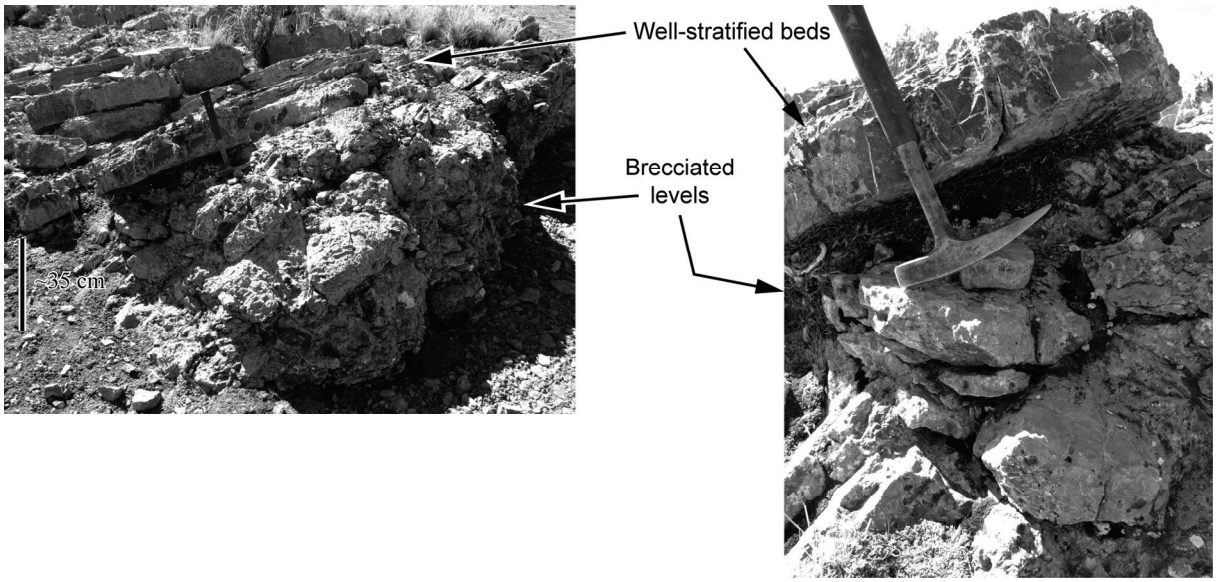

Fig. 13. Alternation of clast-supported carbonate breccias and well-stratified levels near Lago del Colca (~15 km SW of Tisco). Hammer head is 17 cm-long.

3.2. Western resedimentation facies

3.2.1. Type-4 facies: The Livitaca, Espinar and Lago del Colca outcrops

In the outcrops near Livitaca, Espinar and Lago del Colca (~15 km SE of Tisco, Fig. 2), breccias are markedly different from the facies previously described. All Type-4 resedimentation facies share the following features: (i) the material consists almost exclusively of limestones (argillaceous and siliciclastic material being very scarce); (ii) angular limestone clasts are omnipresent; (iii) outcrops are characterized by an alternation of regularly-stratified and brecciated levels; (iv) each brecciated level generally displays clasts from two or three different limestone facies deriving from underlying or overlying beds; (v) breccias are almost always clast-supported; (vi) the space between the clasts is tight and generally filled by carbonate mud, calcite, or a mix of both. A more abundant matrix is rarely observed and usually contains some clay, in particular in the eastern part (Zone 4). The yellow to red mudstones to siltstones, that in the northeast are omnipresent and frequently liquified in the matrix, are rare at Livitaca and Espinar and are not observed at Lago del Colca where only breccias and/or slumps occur.

In the areas near Livitaca and Espinar (Fig. 2), clasts are ~1 mm to 20 cm in size, and a low mud content is locally displayed by the matrix and scarce clastic dykes. Some blocks exhibit randomly oriented tension fractures filled with calcite (Fig. 12A), indicating a hydrostatic stress state during fracturing associated with high fluid pressure at the early time of the deformation of cohesive materials (Cosgrove, 1995). At Lago del Colca, clasts are generally bigger (~ 1 cm to 1 m in size), and some slumps are observed. In all outcrops (Livitaca, Espinar and Lago del Colca) the matrix and/or a part or the totality of some clasts may consist of calcite. The limestone clasts generally present laminations which locally display small-size folds whose style differs from one clast to another (Fig. 12B,C,D). This deformation, often plastic in Zone 4, was acquired prior to the brecciation.

The three outcrops are characterized by an alternation of brecciated and well-stratified levels (Fig. 13), each being a few metres-thick. The thickness of each level and the proportion of stratified beds increase westwards (from Zone 4 to Zone 5). Rafts (10s-100s of metres in size) of stratified layers bounded by brecciated levels are also observed, in particular at Lago del Colca (Fig. 14). Here also some well-stratified levels commonly become gradually and laterally brecciated.

Although less clear, the multi-scale brecciation is also partly visible in zones 4 and 5 in association with Type-4 resedimentation facies. Here the brecciated nature of some beds is

generally well-marked even in aerial photos (*e.g.* Fig. 12 in Callot et al. 2008), at the outcrop scale, and sometimes at the sample scale, but is blurred in thin sections due to calcite recrystallization.

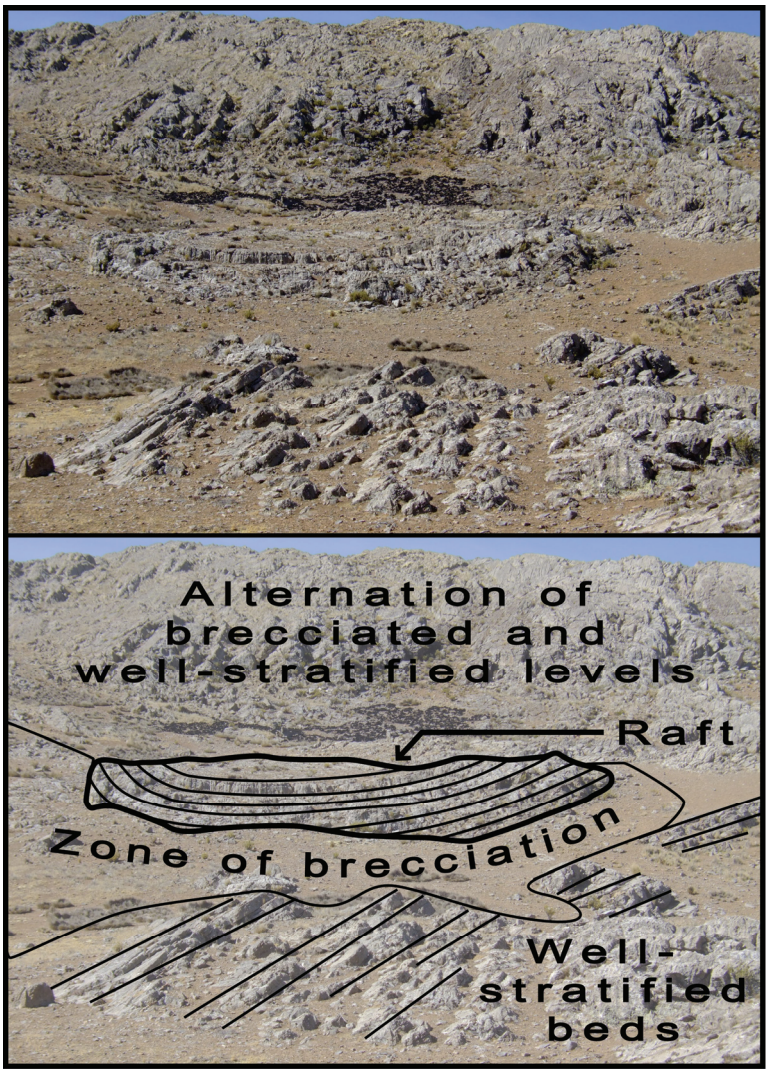

Fig. 14. Example of limestone raft (~30 m-long) within the carbonate mélange near Lago del Colca (~15 km SW of Tisco). The well-stratified raft lies on a brecciated level and is surrounded by well-stratified beds.

3.2.2. Large folds in the Yura area

In the Yura area (Zone 6, Fig. 2), large, >500 m-wide, asymmetrical to overturned WSW-vergent anticlines and related synclines are observed (Callot et al., 2008). The lower part (~130 m) of the succession displays regular beds of even thickness, the overlying 100 m appear essentially regular and only the uppermost ~25-40 m display manifest signs of destabilization (including rafts, piled-up slides, slumps and boudinage structures). Folds are contemporaneous of the collapse since they affect the entire limestone succession but neither the Jurassic-Early Cretaceous substratum nor younger strata.

4) Relationships between resedimentation facies and collapse anatomy

4.1. Contrast between the upslope and downslope resedimentation facies

The organization of the four resedimentation facies is partly related to the organization in six deformational zones exhibited by the Ayabacas Formation (Callot et al., 2008). Type-1, Type-2 and Type-3 facies all consist of limestone and marly-sandy clasts or fragments floating in a mainly marly-sandy matrix, and can be found randomly anywhere in Zone 1 to Zone 3 (Fig. 2). The differences between these three resedimentation facies may result from local variations of initial sedimentation, cementation, fluid trapping, faulting and fluid escape. They can be grouped into one larger type of resedimented structure, only found in the northeastern part of the basin (Fig. 2) and characterized by a sandy-marly composition and the occurrence of liquification. The northeastern facies markedly contrast with Type-4 facies, which are characteristic of zones 4 and 5 and involved a material that almost exclusively consisted of limestone and was generally well-lithified at the time of collapse. Type-4 resedimentation facies seem to slightly evolve from Zone 4 to Zone 5, as clast size and average thickness of brecciated or regularly-stratified units apparently increase westwards. The paucity of outcrops (mainly two in Zone 4 and only one in Zone 5) however hampers a firmer statement.

Marked differences in composition and deformation style between northeastern and southwestern resedimentation facies define a boundary located between zones 3 and 4. It reveals a strong change in the genesis of facies, which is discussed below.

4.2. Motion of the major fault systems before and during the collapse

The two major accidents in the study area, the SFUACC and the CECLLA, have had distinct behaviours and histories, and had different effects on the collapse.

Offset on the SFUACC fault system was limited during Albian to Turonian times since limestone deposits are thin (~20-40 m-thick) on both sides. This assumption of limited offset on the SFUACC before the collapse is reinforced by the fact that the Murco Formation was not deeply buried before the event since in zones 1 to 3 its material was largely reworked in the matrix of the Ayabacas Formation. However, the occurrence in the collapse of large lithified blocks derived from the Angostura and Huancané formations and from Paleozoic strata (up to 100s of m in length and width, and up to several 10s of m in stratigraphic thickness; Callot et al., 2008) implies that these pre-Ayabacas units were exposed to catastrophic erosion. These large blocks are notably observed within 30 km on both sides of

the SFUACC fault system, indicating that offset on this fault system during the collapse was sufficient to expose those units (Fig. 15). Some of these blocks were able to slide over several kilometres, probably supported by a sliding sole.

The major contrast between zones 3 and 4, *i.e.* across the CECLLA fault system, is highlighted by the disappearance of Murco material in the collapse deposit and an increase in thickness for the Arcurquina limestones. The CECLLA fault system was active starting at least in the Early Albian as suggested by higher thicknesses, and thus subsidence, in the western part of the basin. However, no indication of any other collapse prior to the Ayabacas event is observed in the basin, which strongly suggests that downwarping was continuous from the Albian to late Turonian. Furthermore, the broad and diffuse character of the CECLLA structural system (Fig. 2) is likely to have spatially distributed fault offsets over an extended width (Fig. 15), hampering the triggering of catastrophic events before the Ayabacas collapse. In the entire study area, the Murco alluvial deposits and the transgressive Arcurquina limestones onlapped northeastwards. In the western part of the basin more time was thus available for interstitial water to be squeezed out of the accumulating deposits, and so for these to compact. West of the CECLLA, the Arcurquina deposits were thus progressively thicker (up to ~250 m in the Yura area) and more lithified, and the Murco Formation was buried more deeply.

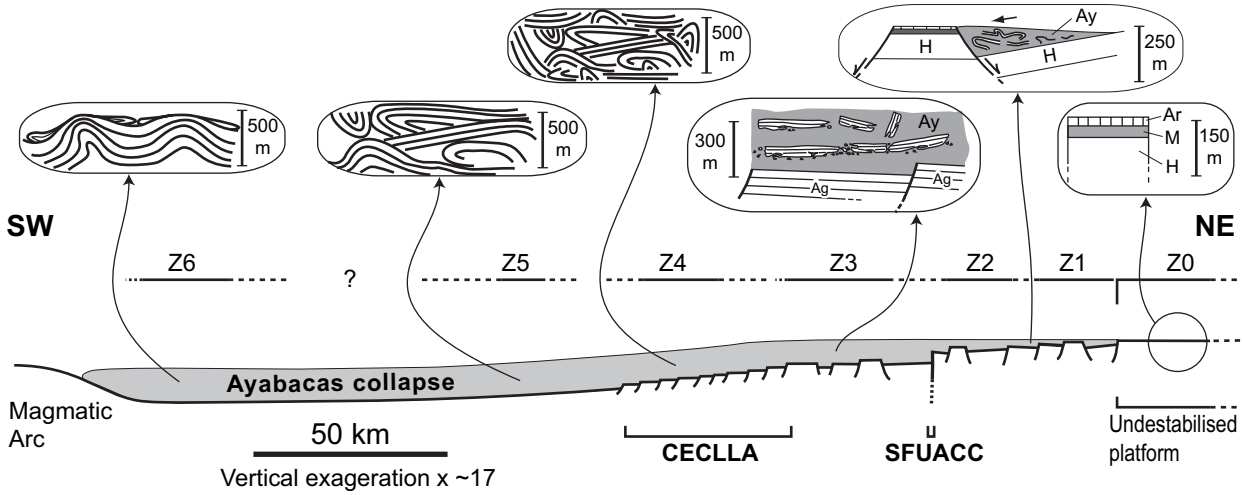

Fig. 15. Distribution of deformational styles across a section of the Ayabacas Body and its substratum, with the position of the magmatic arc and the SFUACC and CECLLA fault systems. Cross section is located in Fig. 2 and its vertical exaggeration is ~17. Each insert zooms in on the area indicated by arrow and includes its own scale bar. H=Huancané Formation; Ag=Angostura Formation; M=Murco Formation; Ar=Arcurquina Formation ; Ay=Ayabacas Formation.

4.3. Lithification state of materials at time of collapse

The diverse components of the Ayabacas Formation displayed different thicknesses and diagenetic states when they have been involved in the collapse. These differences are marked horizontally (from upslope at northeast to southwest dowslope) and vertically (within the sedimentary succession).

4.3.1. NE-to-SW increase in pre-collapse lithification

Northeast of the SFUACC fault system (corresponding approximately to zones 0, 1, and locally 2; Fig. 2) only the second, Late Cenomanian — Late Turonian (~95 - ~90 Ma) transgression is recorded. The Arcurquina Formation, *i.e.* the limestones initially deposited in this area, was thin (≤ 20 m-thick, as observed in both the reworked and non-reworked units). In the Ayabacas Formation, limestone rafts are plastically deformed, limestone clasts within the breccias are generally scarce, and liquification features involving Murco siliciclastic material are common (Yanaoco and Pancarhualla outcrops). These features indicate that the degree of lithification of both the Murco and Arcurquina formations was low at the time of collapse (~90 Ma). However, the occurrence of limestone rafts within the mélange indicates that part of the limestone succession had undergone some cementation shortly after deposition, which is commonly the case in carbonate-rich sediments (Bathurst, 1971), and was thus partially lithified when the collapse occurred. This different behaviour between carbonated and siliciclastic materials is attributed to faster lithification of limestone compared with sandstone (Tucker, 2001). The thickness of the resedimented unit is small (0-100 m).

Between approximately the SFUACC and CECLLA fault systems (corresponding roughly to zones 2 and 3; Fig. 2) the pre-collapse limestone deposits were also thin (generally ~20-30 m-thick, and in any case <40 m-thick) but thickness slightly increased from northeast to southwest. Limestone rafts were clearly plastically deformed in Zone 2 and became progressively more fragmented (but less folded) in Zone 3. Within the breccias angular limestone clasts are very common. The Murco material was largely involved into the collapse matrix and again appears to have been partly liquified. Although both transgressions (Early Albian — Late Albian, ~108.5 - ~102 Ma; Late Cenomanian — Late Turonian, ~95 - ~90 Ma) are recorded in this area, the small thickness variations between limestone rafts northeast and southwest of the SFUACC suggests that the limestone succession deposited during the Albian transgression was thin (probably less than a few metres). Albian limestones must have been cemented at the time of collapse because a ~7 Myr hiatus separated the two

transgressions and at least ~12 Myr elapsed between the end of Albian limestone deposition and the collapse, a time largely sufficient to allow limestone cementation to develop (Bathurst, 1971; Tucker, 2001). This in turn made possible the generation of limestone clasts, through pervasive fracturation of these cemented limestones.

Southwest of the CECLLA fault system (corresponding approximately to zones 4 to 6) subsidence is likely to have been significantly higher (see section 4.2 above). In the westernmost part (Yura area) the Albian transgression is represented by ~130 m of limestones, and the second transgression by another ~135 m. The red to yellow, mudstone to fine sandstone matrix that is present to the east completely disappears west of the CECLLA fault system, indicating that the Murco Formation was not involved in the downslope part of the collapse. In zones 4 and 5 the Ayabacas Formation displays alternating regularly-stratified beds and calcite-rich breccias, whereas in zone 6 (Yura and Chalhuanca areas, Fig. 2) most of the succession is regularly-stratified, indicating a higher degree of lithification in the west at the time of collapse.

This evolution suggests that, prior to the collapse, the Arcurquina limestones presented a progressive increase in lithification degree from northeast to southwest, in relation with an older age of deposition and a higher subsidence and burial in the west. This gradient is also reflected in the direction in which the two transgressions that deposited the limestone succession had developed.

4.3.2. Vertical variations in lithification northeast of the CECLLA

Vertical variations in lithification are most notable upslope, northeast of the CECLLA fault system, where the Murco Formation was involved in the mélange. In the entire basin the red argillaceous and siliciclastic strata of the Murco Formation were overlain by the limestone beds of the Arcurquina Formation before the collapse. In zones 1 to 3 the largely siliciclastic and plastically-deformed matrix of the Ayabacas collapse consists of material reworked from the Murco Formation, which indicates that at least the upper part of this unit had remained water-rich and uncemented, implying a limited diagenetic evolution. On the other hand two observations show that the lower part of the Murco Formation was already compacted and well cemented at the time of collapse: (i) in most cases its base is preserved, without evidence of reworking or even soft-sediment deformation; (ii) angular clasts of red compacted siliciclastic material are common in the Ayabacas matrix and were most probably derived from a cemented part of the Murco Formation. Furthermore, although the significant clay content of the Murco Formation may have been a factor of preliminary lithification (Dapples,

1967), clay-rich sandstone can easily partly crumble when placed in water (Dapples, 1967) and this may have favoured reworking of the Murco material through water incorporation during the collapse (De Blasio et al., 2004). Consequently it is difficult to conclude whether siliciclastic deposits remained uncemented, or had been clay-cemented and were subsequently liquefied by water injection through fracturing of the overlying limestones.

Carbonates also displayed variable degrees of cementation in zones 1 to 3 at the time of collapse. The base of the succession is likely to have been already lithified, in particular between the CECLLA and SFUACC fault systems, as suggested by the abundance of angular limestone clasts and, especially, by the fact that a limestone succession must have been deposited in this area during the first, Albian transgression and had thus probably lithified during the ≥12 Myr that elapsed until the time of collapse (see above). This process may have formed a crust of well-cemented limestones overlying water-rich, uncemented siliciclastic deposits, generating permeability barriers that prevented fluid escape and created pore-pressure gradients (Halley et al., 1983; Spence and Tucker, 1997; Onasch and Kahle, 2002). Rafts were partly cemented at the time of collapse since they conserved some cohesion and did not mix into the matrix. Lithification, however, was not complete: rafts were plastically deformed as they do not exhibit any features of brittle deformation. Finally the significant carbonate content of the matrix in all studied samples indicates that a part of the limestone succession (very likely the uppermost part) was not cemented at all and was incorporated into the liquified matrix.

In the upslope northeastern region, a vertical succession immediately prior to the collapse can thus be reconstructed as follows (Fig. 16) from bottom to top: (i) lithified mudstones to fine argillaceous sandstones at the base of the Murco Formation; (ii) overlying argillaceous siliciclastic deposits of the Murco Formation were potentially liquefiable; (iii) cemented limestones, a few metres-thick at most; (iv) cohesive but not completely lithified limestones, ~20-30 m-thick (the average thickness of the limestone rafts); (v) finally, recently deposited carbonate mud. A confined aquifer (upper part of the Murco Formation) isolated by a cemented cap of limestone (base of the Arcurquina Formation) was thus existing in the pre-collapse succession.

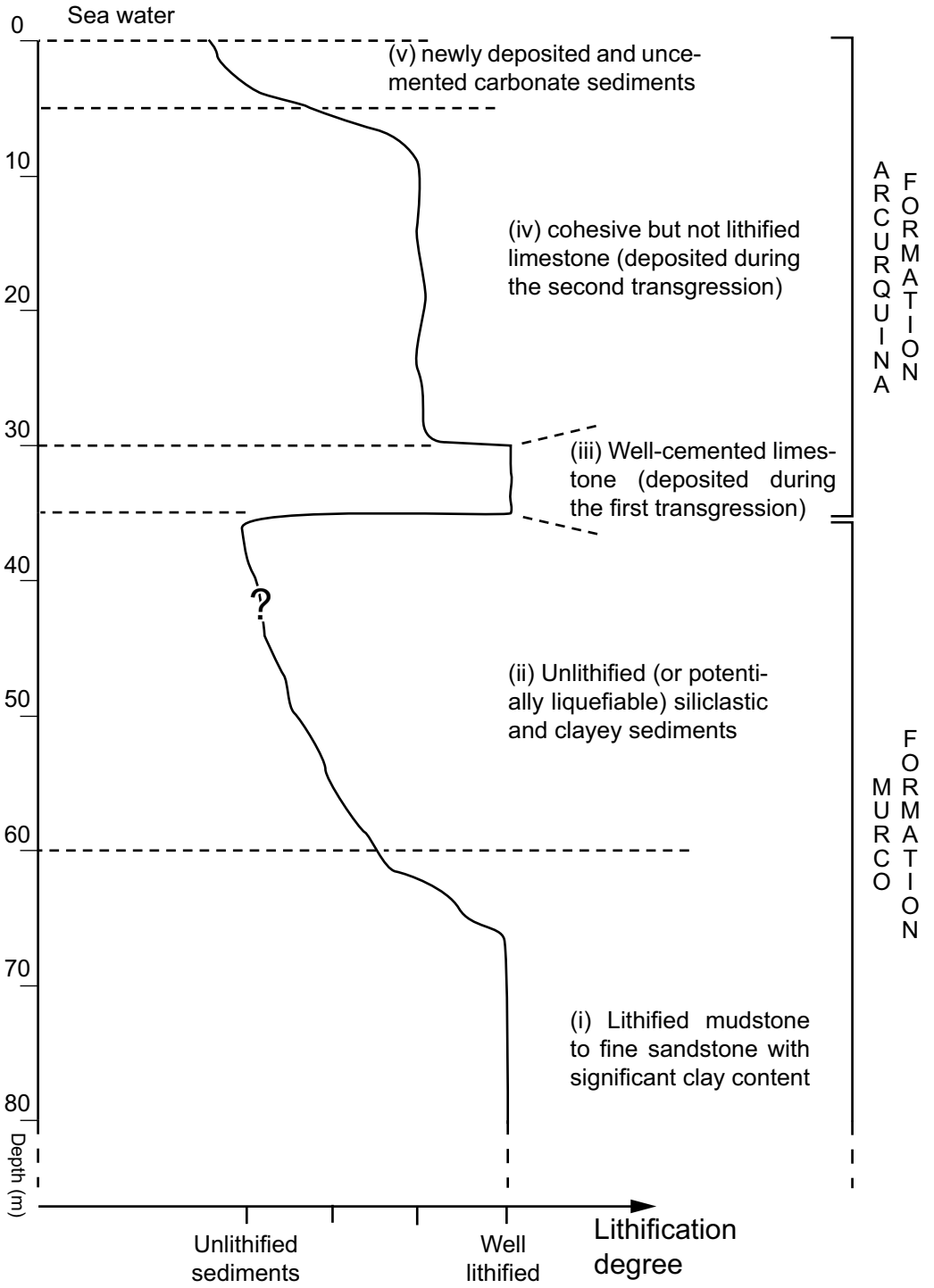

Fig. 16. Degree of lithification and supposed thickness of the Murco and Arcurquina formations in zones 1 to 3 before the collapse. The Arcurquina Formation is well-cemented at its base which has created a cap trapping fluids and preventing lithification in the Murco Formation. The top of the Arcurquina (v) and Murco (iii) formations are not lithified and will be mix together to form the matrix of the Ayabacas Formation. The central part of the Arcurquina Formation (iv) is cohesive but not lithified: it will form the plastically deformed limestone rafts of the Ayabacas Formation. The base of the Arcurquina Formation and a part of the one of the Murco Formation will be fragmented into clasts which are found in the matrix of the Ayabacas Formation.

4.4. Formation of the dykes and rafts in the upslope areas

In Cusco, Yanaoco and Cabanillas (Figs. 11A,B and 8), the matrix was clearly vertically injected at the base of the limestone rafts and then horizontally into some stratification planes, which expanded (Fig. 8B). The injection of an entrapped mix of siliciclastic sediments and fluids has fractured the overlying cemented cap, provoking (or at least helping, *e.g.* Fig. 3D) the fragmentation of the raft bases and the incorporation of limestone clasts into breccias below the rafts. These injections are not observed to cross entire rafts in any of the inspected outcrops, demonstrating that fluid pressures were not sufficient to break across the whole cemented limestone succession. In contrast, downward motions of the liquified matrix formed large dykes that entirely cross the rafts (Fig. 8A). These dykes could not have been caused by injection of pressured liquified sediments from the top and rafts were not hewed out by injection of liquified material. At least in the case of large rafts, it is more likely that they were initially cut by normal faults such as those that affect the substratum of the Ayabacas Formation (Callot et al., 2008) and subsequently fragmented into smaller rafts during their sliding downslope (the spaces opening between rafts being filled by the liquefied matrix), as also suggested by George et al. (1995) in another platform collapse. This interpretation is strengthened by the distribution of raft dimensions along the collapse: rafts are more laterally extended in the proximal part of the collapse (Zone 1) where slopes were limited; fragmentation increases downslope, although rafts are thicker, because slope were more extended and materials slided down for longer time and distance. Neptunian dykes (Montenat et al., 1991, 2007, Moretti and Sabato, 2007) filled by the matrix are observed at the top of limestone rafts, probably formed by the flexure of the cohesive rafts during their transport.

The amount of matrix above the rafts can be significant (>20 m), in particular in the Cabanillas area. It implies that the siliciclastic deposits of the Murco Formation, initially located below the Arcurquina limestones (Fig. 16), were largely reworked, to the point that they came in contact with seawater and were fluidized. The base of the limestone rafts was submitted to ablative friction by the fluidized material and the shear effect of downslope movement (De Blasio et al., 2004) over a weak layer acting as a sliding sole.

4.5. Generation of the limestone breccias in the southwestern region

Type-4 resedimentation facies are located southwest of the CECLLA fault system in zones 5 and 6 and are notably characterized by the predominance of limestone breccias. The process through which these resedimentation facies were generated can be hypothesized from

the field observations described in section 3.2.1 above. The breccias are clast-supported and generally very poor in matrix: the abundant liquified material present in the northeastern region die out into the southwestern region, implying that the supply of unlithified sediments required to form the matrix was becoming limited in this direction. The alternation of brecciated and preserved regularly-stratified levels and the relative lithological homogeneity of the limestone clasts (derived from underlying or overlying beds) indicate that brecciation, although significant, was limited to some levels. In the most advanced stages, brecciation developed during sliding of undeformed rafts at the interface between the rafts and underlying beds (Fig. 14). Some clasts were individually deformed as their internal lamination had been folded prior to brecciation. The conjunction of these elements points to the following scenario: during an early stage of deformation, some levels were folded, generally plastically whereas others remained undeformed (depending on cementation grade), so that deformation was accommodated only by less cemented levels. At a subsequent stage strain grew to the point that undeformed and already folded beds were fractured alike and fragmented to generate the clasts forming the breccias. These resedimentation facies thus express a differential deformation, as some beds resisted deformation whereas underlying and overlying beds were brecciated during sliding. Deformation is not uniformly distributed laterally, as some beds that remained regularly-stratified in undisturbed areas are observed to have progressively crumbled in areas of higher deformation.

4.6. Dying out of deformation at the collapse toe (Arequipa area)

In the Yura area (south of Zone 6SE, Fig. 2), folds affect the entire limestone succession but neither the Jurassic-Early Cretaceous substratum nor younger strata. Folds were thus formed by the collapse and indicate that the detachment surface was located at the interface Murco/Arcurquina formations. These compressional structures absorbed the remaining energy of the sliding and indicate that the collapse was blocked downslope. Such structures are not observed in the Chalhuanca area (north of Zone 6NW, Fig. 2), where it is not clear how the collapse dies out. Here a contact exists between a regularly stratified and unfolded Arcurquina Formation at the base, and limestone masses of a destabilized Ayabacas Formation above. It suggests that the sliding surface was here within the limestone succession and not anymore at the interface Murco/Arcurquina formations as in the south. Coalescence between the SFUACC and CECLLA systems in this area (Figs. 1, 2) suggests that more pronounced scarps and cumulated relief were created here before and during the event (Callot et al.,

2008), burying abruptly the Murco and the lower part of the Arcurquina formations, impeding these formations to be involve in the collapse.

In southern Peru, a magmatic arc was active south of Arequipa but no volcanic deposits are observed prior to the Coniacian and only plutons are recorded (Clark et al., 1990; Soler and Bonhomme, 1990; Jaillard, 1994; Jaillard and Soler, 1996; Sempere et al., submitted). In the Arequipa region, Ayabacas deposits are covered by thick volcanodetritic conglomerates of Coniancian age (Cruz, 2002; Callot et al., 2008). Other data indicate that the magmatic arc started to grow 91 Myr ago (Mukasa, 1986; Sempere et al., submitted), which coincides approximately with the Ayabacas collapse. Compressional structures observed in the Arequipa-Yura region were created by a topographic high, due to the magmatic arc present when the collapse occurred, which formed an impassable barrier and stopped the collapse (Fig. 15). In this area, the collapse is a frontally confined submarine landslide (Frey-Martínez et al., 2006). In the northern part of the study area (near Chalhuanca, Fig. 1), the westermost position of the arc (in respect to the collapse) did not allow it to block the collapse, and could explain why the compressional strucures observed in Yura are not observed there.

4.7. Effect of liquified sediments and stratigraphic position of the sliding surface

Confined aquifers isolated by impermeable cap may initiate catastrophic seafloor instability and create megabreccia deposits, especially in carbonate depositional environments during relative sea-level fall because differential cementation is well developed and overpressure increase in the confined aquifer (Hilbrecht, 1989; Spence and Tucker, 1997). Iin case of the Ayabacas collapse this potential triggering mechanism was not sufficient alone to destabilize the platform since sliding did not occur in any part of the basin until the Ayabacas event, and in particular in the western part of the study area (Arequipa region) where such conditions were probably existing at the end of the Late Albian-Middle Cenomanian relative regression, *i.e.* ~12 Myr before the Ayabacas collapse (Callot et al., 2008). But extensional tectonics abruptly developed near the Turonian-Coniacian transition (after a tectonically quiescent Cenomanian-Turonian period), with resulting normal faults, slope creation and seismicity (Callot et al., 2008). These combined phenomena (nonuniform cementation providing permeability barriers, faults, seismicity and slope creation) caused in the upslope areas soft-sediment deformation, earthquake-triggered liquefaction and, in at least some areas, could lead to failure of the limestone cap under brittle conditions, allowing pore fluids to escape rapidly and in quantities sufficient to cause fluidization (Onasch and Kahle, 2002). The upper part of the Murco Formation, partly liquefied and easily deformable, was prone to ductile

deformation. This material thus provided a shear layer acting as a sliding sole that greatly facilitated the downslope displacement of the cemented limestone rafts and in the vicinity of the SFUACC of other large lithified blocks deriving from pre-Ayabacas units. The base of the limestone rafts was submitted to ablative friction by the fluidized material and the shear effect of downslope movement (De Blasio et al., 2004) and provided small limestone clasts to the breccia. Upslope (northeast of the CECLLA), the sliding surface was located in the Murco Formation, and the Ayabacas Formation is progressively disorganised from zones 1 to 3 with more chaotic and fragmented limestone rafts (Fig. 15).

In contrast, organisation and continuity of limestone masses increase from zones 4 to 6, west of the CECLLA fault system (Fig. 15). Limestone breccias are characterized by the presence of calcite in the clasts or the matrix, implying that materials were subjected to brittle fracturing and not anymore to plastic deformation. Murco sediments were progressively buried more deeply, under one or two hundreds of meters of limestone deposits, increasing their lithification degree and therefore canceling the sliding sole effect they produced in zones 1 to 3. In the Yura area (Zone 6SE) the detachment of the collapse is still located at the interface between Murco and Arcurquina formations which strongly suggests that, in the southern part of the study area, the detachment surface was also at the Murco Fm/Arcurquina Fm interface in zones 4 and 5 despite the CECLLA downwarping. It has been possible probably thanks to the broad character of the CECLLA fault system and the resulting progressive offset of the basin in the southern part of the study area, which is not the case in the northern part (Zone 6NE) where the SFUACC end CECLLA fault systems are coalesced.

5) Conclusions

The Ayabacas collapse displays a number of typical resedimentation facies:

- extensive plurimetric sedimentary dykes at the base of the limestone rafts, expulsing upwards red, marly-sandy, liquified sediments (Type-1 facies);
- matrix-supported breccias with heterometric, inhomogeneous clasts floating in a sandy-marly, largely liquified matrix (Type-2 facies), sometimes associated with rounded clasts of Paleozoic sedimentary rocks (Type-3 facies);
- clast-supported limestone breccias in alternation with well-stratified levels (Type-4 facies).

A strong contrast exists between northeastern and southwestern facies, which can thus be grouped into two main types:

(i) In the eastern half of the basin, namely northeast of the CECLLA, Type-1, Type-2 and Type-3 facies are randomly observed, forming a group characterized by the occurrence of sedimentary dykes, clasts of limestone or marly-sandstone in a mainly marly-sandy matrix. Deformation was most often plastic and large amounts of the matrix were liquified. Most of the matrix and some clasts were derived from the Murco Formation, which was partly to largely involved into the collapse, as its sliding sole was located in this unit. These resedimentation facies are markedly characterized by multi-scale deformation and brecciation at whichever scale, and can therefore be described as multi-scale or fractal breccias.

(ii) West of the CECLLA, only limestone breccias are observed in the Ayabacas Formation (Type-4 facies). The absence of siliciclastic material shows that the Murco Formation was not involved in this western part of the collapse.

Materials were marked by different lithification states prior to the collapse. From northeast to southwest, an increase in lithification degree of the Arcurquina limestones was produced by an older age of deposition and a higher subsidence and burial in the west of the backarc basin. In the northeast part, important variations in the degree of lithification are also inferred to have existed in the sedimentary succession before the collapse. In particular, limestones at the base of the Arcurquina Formation were well-cemented, forming a cap that prevented water to escape from the underlying siliciclastic Murco Formation. Although the collapse was triggered by the activation of normal fault and resulting slope creation and oversteepening (Callot et al., 2008), extent and intensity of the collapse were probably increased by the presence of the unlithified and water-saturated Murco Formation, which acted as a sliding sole (a lubricating layer facilitating sliding). Fracturation, fragmentation and ablation at the base of limestone rafts in contact with this layer generated limestone clasts of all sizes. The carbonate platform was increasingly fragmented from NE to SW across zones 1 to 3, where the sliding sole is well-marked. In contrast, size and continuity of the limestone rafts increase west of the CECLLA in zones 4 to 6, where the Murco is not anymore involved into the collapse and was probably lithified and not acting as a lubricating sliding sole. West of the CECLLA, the sliding surface is located at the interface between the Murco and Arcurquina formations in the southern part of the study area and within the limestone succession in the northern part. In the Yura area (south), the collapse was blocked by a topographic high probably due to an enhancing of the magmatic arc. The ending of the collapse has not been precisely observed in the north area, but the compressional structures affecting the limestone succession in the south are lacking, suggesting that the collapse was not blocked here.

Various elements highlight the importance of the two main fault systems, the SFUACC and the CECLLA which largely controlled subsidence, distribution and thickness of transgressive deposits, degrees of lithification, as well as position of the sliding surface, occurrence of a sliding sole and distribution of deformational facies.

References

Allen, J.R.L., 1982. Sedimentary structures: Their Character and Physical Basis, Vol II. Elsevier, Amsterdam, 663 p.

Alonso, J.L., Marcos, A., Suarez, A., 2006. Structure and organization of the Porma Melange: progressive denudation of a submarine nappe toe by gravitational collapse. American Journal of Science 306, 32-65.

Audebaud, E., 1971. Mise au point sur la stratigraphie et la tectonique des calcaires Cénomaniens du Sud-Est péruvien (formation Ayavacas). Comptes Rendus Académie des Sciences Paris 272, 1059-1062.

Audebaud, E., Capdevila, R., Dalmayrac, B., Debelmas, J., Laubacher, G., Lefèvre, C., Marocco, R., Martinez, C., Mattauer, M., Mégard, F., Paredes, J., Tomasi, P., 1973. Les traits géologiques essentiels des Andes Centrales (Pérou-Bolivie). Revue de géographie physique et de géologie dynamique 15, 73-114.

Bathurst, R.G.C., 1971. Carbonate sediments and their diagenesis. Developments in Sedimentology, vol. 12. Elsevier, Amsterdam, 620 p.

Cabrera La Rosa, A., Petersen, G., 1936. Reconocimiento geológico de los Yacimientos Petrolíferos del Departamento de Puno. Boletín del Cuerpo de Ingenieros de Minas del Perú 115, 100 p.

Callot, P., Sempere, T., Odonne, F., Robert, E., 2007. The Mid-Cretaceous carbonate platform of southern Peru collapsed at the Turonian-Coniacian transition. 4th European Meeting on the Palaeontology and Stratigraphy of Latin America (EMPSLA). Cuadernos del Museo Geominero, Instituto Geológico y Minero de España, Madrid, vol. 8, pp. 75-80.

Callot, P., Sempere, T., Odonne, F., Robert, E., 2008. Giant submarine collapse of a carbonate platform at the Turonian-Coniacian transition: The Ayabacas Formation, southern Peru. Basin Research, in press.

Canals, M., Lastras, G., Urgeles, R., Casamor, J.L., Mienert, J., Cattaneo, A., De Batist, M., Haflidason, H., Imbo, Y., Laberg, J.S., Locat, J., Long, D., Longva, O., Masson, D.G., Sultan, N., Trincardi, F., Bryn, P., 2004. Slope failure dynamics and impacts from seafloor and shallow sub-seafloor geophysical data: case studies from the COSTA project. Marine Geology 213, 9-72.

Carlier, G., Lorand, J.P., Liégeois, J.P., Fornari, M., Soler, P., Carlotto, V., Cárdenas, J., 2005. Potassic-ultrapotassic mafic rocks delineate two lithospheric mantle blocks beneath the southern Peruvian Altiplano. Geology 33, 601-604.

Carlotto, V., Gil, W., Cárdenas, J., Chávez, R., 1996. Geología de los cuadrángulos de Urubamba y Calca hojas 27-r y 27-s. Boletín INGEMMET 65 (serie A), Carta Geológica Nacional, Lima, 245 p.

Carman, J.E., 1927. The Monroe division of rocks in Ohio. Journal of Geology 35, 481-506.

Clark, A.H., Farrar, E., Kontak, D., Langridge, R.J., Arenas, M.J., France, L.J., McBride, S.L., Woodman, P.L., Wasteneys, H.A., Sandeman, H.A., Archibald, D.A., 1990. Geologic and geochronologic constraints of the metallogenic evolution of the Andes of southeastern Peru. In: Skinner, B.J. (Ed.), A special issue devoted to the mineral deposits of Peru. Economic Geology and the Bulletin of the Society of Economic Geologists, vol. 85, pp. 1520-1583.

Cosgrove, J.W., 1995. The expression of hydraulic fracturing in rocks and sediments. In: Ameen, M.S. (Ed.), Fractography: fracture topography as a tool in fracture mechanics and stress analysis. Geological Society, Spec. Publ., vol. 92, pp. 187-196.

Cruz, M., 2002. Estratigrafía y evolución tectono-sedimentaria de los depósitos sin-orogénicos del cuadrángulo de Huambo: Las formaciones Ashua y Huanca, departamento de Arequipa. Tesis de la Universidad Nacional San Agustín de Arequipa, Peru, 127 p.

Dapples, E.C., 1967. Diagenesis of sandstones. In: Larsen, G., Chilingar, G.V. (Eds.), Diagenesis in sediments. Developments in Sedimentology, vol. 8. Elsevier, Amsterdam, pp. 91-125.

De Blasio, F.V., Elverhøi, A., Issler, D., Harbitz, C.B., Bryn, P., Lien, R., 2004. Flow models of natural debris flows originating from overconsolidated clay materials. Marine Geology 213, 439-455.

De Jong, K.A., 1974. Melange (Olistostrome) near Lago Titicaca, Peru. Am. Assoc. Pet. Geol. Bull. 58, 729-741.

Drzewiecki, P.A., Simó, J.A., 2002. Depositional processes, triggering mechanisms and sediment composition of carbonate gravity flow deposits: examples from the Late Cretaceous of the south-central Pyrenees, Spain. Sedimentary Geology 146, 155-189.

Floquet, M., Hennuy, J., 2003. Evolutionary gravity flow deposits in the Middle Turonian – Early Coniacian southern Provence Basin (SE France): origins and depositional processes. In: Locat, J., Mienert, J. (Eds.), Submarine Mass Movements and their Consequences. Kluwer Academic Publishers, Dordrecht, Netherlands, pp. 417-424

Frey-Martínez, J., Cartwright, J., Hall, B., 2005. 3D seismic interpretation of slump complexes: examples from the continental margin of Israel. Basin Research 17, 83-108.

Frey-Martínez, J., Cartwright, J., James, D., 2006. Frontally confined versus frontally emergent submarine landslides: A 3D seismic characterisation. Marine and Petroleum Geology 23, 585-604.

Gee, M.J.R., Masson, D.G, Watts, A.B., Allen, P.A., 1999. The Saharan debris flow: an insight into the mechanics of long runout submarine debris flows. Sedimentology 46, 317-335.

George, A.D., Playford, P.E., Powell, C.McA., 1995. Platform-margin collapse during Famennian reef evolution, Canning Basin, Western Australia. Geology 23, 691-694.

Graziano, R., 2001. The Cretaceous megabreccias of the Gargano Promontory (Apulia, southern Italy): their stratigraphic and genetic meaning in the evolutionary framework of the Apulia Carbonate Platform. Terra Nova 13, 110-116.

Haflidason, H., Sejrup, H.P., Nygård, A., Mienert, J., Bryn, P., Lien, R., Forsberg, C.F., Berg, K., Masson, D., 2004. The Storegga Slide: architecture, geometry and slide-development. Marine Geology 213, 201-234.

Haflidason, H., Lien, R., Sejrup, H.P., Forsberg, C.F., Bryn, P., 2005. The dating and morphometry of the Storegga Slide. Marine and Petroleum Geology 22, 123-136.

Halley, R.B., Harris, P.M., Hine, A.C., 1983. Bank margin environments. In: Scholle P.A., Bebout D.G., Moore C.H. (Eds.), Carbonate Depositional Environments. Am. Assoc. Pet. Geol. Mem., vol. 33, pp. 463-506.

Henrich, R., Hanebuth, T.J.J., Krastel, S., Neubert, N., Wynn, R.B., 2008. Architecture and sediment dynamics of the Mauritania Slide Complex. Marine and Petroleum Geology 25, 17-33.

Hilbrecht, H., 1989. Redeposition of late Cretaceous pelagic sediments controlled by sea-level fluctuations. Geology 17, 1072-1075.

Hine, A.C., Locker, S.D., Tedesco, L.P., Mullins, H.T., Hallock, P., Belknap, D.F., Gonzales, J.L., Neumann, A.C., Snyder, S.W., 1992. Megabreccia shedding from modern, low-relief carbonate platforms, Nicaraguan Rise. Geological Society of America Bulletin 104, 928-943.

Huvenne, V.A.I., Croker, P.F., Henriet, J.P., 2002. A refreshing 3D view of an ancient collapse and slope failure. Terra Nova 14, 33-40.

Jaillard, E., 1994. Kimmeridgian to Paleocene tectonic and geodynamic evolution of the Peruvian (and Ecuadorian) margin. In: Salfity, J.A. (Ed.), Cretaceous tectonics of the Andes. Earth Evolution Sciences Monograph Series, Vieweg Publications, Wiesbaden, pp. 101-167.

Jaillard, E., 1995. La sedimentación Albiana – Turoniana en el Sur del Perú (Arequipa – Puno – Putina). Sociedad Geológica del Perú, Volumen Jubilar Alberto Benavides, 135-157.

Jaillard, E., Sempere, T., 1991. Las secuencias sedimentarias de la Formación Miraflores y su significado cronoestratigráfico. Revista técnica de YPFB 12, 257-264.

Jaillard, E., Arnaud-Vanneau, A., 1993. The Cenomanian – Turonian transition on the Peruvian margin. Cretaceous Research 14, 585-605.

Jaillard, E., Soler, P., 1996. Cretaceous to early Paleogene tectonic evolution of the northern Central Andes (0-18°S) and its relations to geodynamics. Tectonophysics 259, 41-53.

Jaillard, E., Cappetta, H., Ellenberger, P., Feist, M., Grambast-Fessard, N., Lefranc, J.-P., Sigé, B., 1993. The Late Cretaceous Vilquechico Group of southern Peru. Sedimentology, paleontology, biostratigraphy, correlations. Cretaceous Research 14, 623-661.

Jaillard, E., Sempere, T., Soler, P., Carlier, G., Marocco, R., 1995. The role of Tethys in the evolution of the northern Andes between Late Permian and Late Eocene times. In: Nairn A.E.M., Ricou L.-E., Vrielynck B., Dercourt J. (Eds.), The Ocean Basins and Margins, Volume 8: The Tethys Ocean. Plenum Press, New York, pp. 463-492.

Johnson, R.L., 1974. Geology and environmental interpretation of the Upper Cayugan Bass Islands dolomite, Southeastern Michigan. Unpublished M.S. thesis, Ann Arbor, Univ. Michigan, USA, 89 p.

Lucente, C.C., Pini, G.A., 2003. Anatomy and emplacement mechanism of a large submarine slide within a Miocene foredeep in the Northern Apennines, Italy: a field perspective. American Journal of Science 303, 565-602.

Lucente, C.C., Pini, G.A., 2008. Basin-wide mass-wasting complexes as markers of the Oligo-Miocene foredeep-accretionary wedge evolution in the Northern Apennines, Italy. Basin Research 20, 49-71.

Martinsen, O.J., Bakken, B., 1990. Extensional and compressional zones in slumps and slides in the Namurian of County Clare, Ireland. Journal of the Geological Society of London 147, 153-164.

McAdoo, B.G., Pratson, L.F., Orange, D.L., 2000. Submarine landslide geomorphology, US continental slope. Marine Geology 169, 103-136.

Micallef, A., Berndt, C., Masson, D.G., Stow, D.A.V., 2008. Scale invariant characteristics of the Storegga Slide and implications for large-scale submarine movements. Marine Geology 247, 46-60.

Mienert, J., Berndt, C., Laberg, J.S., Vorren, T.O., 2002. Slope Instability of Continental Margins. In: Wefer, G., Billet, D., Hebbeln, D., Jørgensen, B.B., Schlüter, M., van Veering, T. (Eds.), Ocean Margin Systems. SpringerVerlag, Berlin, pp. 179-193.

Montenat, C., Barrier, P., Ott d'Estevou, P., 1991. Some aspects of the recent tectonics in the Strait of Messina, Italy. Tectonophysics 194, 203-215.

Montenat, C., Barrier, P., Ott d′Estevou, P., Hibsch, C., 2007. Seismites: An attempt at critical analysis and classification. Sedimentary Geology 196, 5-30.

Moretti, M., Sabato, L., 2007. Recognition of trigger mechanisms for soft-sediment deformation in the Pleistocene lacustrine deposits of the Sant'Arcangelo Basin (Southern Italy): Seismic shock vs. overloading. Sedimentary Geology 196, 31-45.

Moscardelli, L., Wood, L., 2008. New classification system for mass transport complexes in offshore Trinidad. Basin Research 20, 73-98.

Mukasa, S.B., 1986. Zircon U-Pb ages of super-units in the Coastal batholith, Peru: implications for magmatic and tectonic processes. Geological Society of America Bulletin 97, 241-254.

Mulder, T., Cochonat, P., 1996. Classification of offshore mass movements. Journal of Sedimentary Research 66, 43-57.

Mulder, T., Alexander, J., 2001. The physical character of subaqueous sedimentary density flows and their deposits. Sedimentology 48, 269-299.

Naylor, M.A., 1981. Debris flow (olistostromes) and slumping on a distal passive continental margin: the Palombini limestone-shale sequence of the northern Apennines. Sedimentology 28, 837-852.

Nichols, R.J., 1995. The liquification and remobilization of sandy sediments. In: Hartley, A.J., Prosser D.J. (Eds.), Characterization of Deep Marine Clastic Systems. Geological Society, Spec. Publ., vol. 94, pp. 63-76.

Ogg, J.G., Agterberg, F.P., Gradstein, F.M., 2004. The Cretaceous Period. In: Gradstein F.M., Ogg J.G., Smith A.G. (Eds.), A Geologic Time Scale 2004. Cambridge University Press, Cambridge, pp. 344-383.

Onasch, C.M., Kahle, C.F., 2002. Seismically induced soft-sediment deformation in some Silurian carbonates, eastern U.S. Midcontinent. In: Ettensohn, F.R., Rast, N., Brett, C.E. (Eds.), Ancient seismites. Geological Society of America Special Paper, vol. 359, pp. 165-176.

Payros, A., Pujalte, V., Orue-Etxebarria, X., 1999. The South Pyrenean Eocene carbonate megabreccias revisited: new interpretation based on evidence from the Pamplona Basin. Sedimentary Geology 125, 165-194.

Pino, A., Sempere, T., Jacay, J., Fornari, M., 2004. Estratigrafía, paleografía y paleotectónica del intervalo Paleozoico Superior - Cretáceo inferior en el área de Mal Paso - Palca (Tacna). Publicación Especial Sociedad Geológica del Perú, vol. 5, 15-44.

Popenoe, P., Schmuck, E.A., Dillon, W.P., 1993. The Cape Fear Landslide; slope failure associated with salt diapirism and gas hydrate decomposition. In: Schwab, W.C., Lee, H.J., Twichell, D.C. (Eds.) Submarine Landslides; Selected Studies in the U.S. Exclusive Economic ZoneU.S., Geological Survey Bulletin, pp. 40-53..

Portugal, J., 1964. Geology of the Puno-Santa Lucia area, Department of Puno, Peru. Unpublished Ph.D. Thesis, Univ. Cincinnati, USA, 141 p.

Portugal, J., 1974. Mesozoic and Cenozoic stratigraphy and tectonic events of Puno-Santa Lucia area, Department of Puno, Peru. AAPG Bull. 58, 982-999.

Sempere, T., 1994. Kimmeridgian? to Paleocene tectonic evolution of Bolivia. In: Salfity, J.A. (Ed.), Cretaceous tectonics in the Andes. Earth Evolution Sciences Monograph Series, Vieweg Publications, Wiesbaden, pp. 168-212.

Sempere, T., 1995. Phanerozoic evolution of Bolivia and adjacent regions. In: Tankard, A.J., Suárez, R., Welsink, H.J. (Eds.) Petroleum Basins of South America. Am. Assoc. Pet. Geol. Mem., vol. 62, pp. 207-230.

Sempere, T., Jacay, J., 2006. Estructura tectónica del sur del Perú (antearco, arco, y Altiplano suroccidental). Extended abstract, XIII Congreso Peruano de Geología, Lima, pp. 324-327.

Sempere, T., Jacay, J., 2007. Synorogenic extensional tectonics in the forearc, arc and southwest Altiplano of southern Peru. Eos Trans. AGU, 88 (23), Jt. Assem. Suppl., Abstract U51B-04.

Sempere, T., Jacay, J., Carrillo, M.-A., Gómez, P., Odonne, F., Biraben, V., 2000. Características y génesis de la Formación Ayabacas (Departamentos de

Puno y Cusco). Boletín Sociedad Geológica del Perú 90, 69-76.

Sempere, T., Carlier, G., Soler, P., Fornari, M., Carlotto, V., Jacay, J., Arispe, O., Néraudeau, D., Cardenas, J., Rosas, S., Jiménez, N., 2002a. Late Permian - Middle Jurassic lithospheric thinning in Peru and Bolivia, and its bearing on Andean-age tectonics. Tectonophysics 345, 153-181.

Sempere, T., Jacay, J., Fornari, M., Roperch, P., Acosta, H., Bedoya, C., Cerpa, L., Flores, A., Husson, L., Ibarra, I., Latorre, O., Mamani, M., Meza, P., Odonne, F., Oros, Y., Pino, A., Rodríguez, R., 2002b. Lithospheric-scale transcurrent fault systems in Andean southern Peru. Extended abstract, V International Symposium on Andean Geodynamics, Toulouse, pp. 601-604.

Sempere, T., Acosta, H., Carlotto, V., 2004a. Estratigrafía del Mesozoico y Paleógeno al Norte del Lago. Publicación Especial Sociedad Geológica del Perú, vol. 5, 81-103.

Sempere, T., Jacay, J., Carlotto, V., Martínez, W., Bedoya, C., Fornari, M., Roperch, P., Acosta, H., Acosta, J., Cerpa, L., Flores, A., Ibarra, I., Latorre, O., Mamani, M., Meza, P., Odonne, F., Oros, Y., Pino, A., Rodríguez, R., Husson, L., 2004b. Sistemas transcurrentes de escala litosférica en el Sur del Perú. Publicación Especial Sociedad Geológica del Perú, vol. 5, 105-110.

Sempere, T., Jacay, J., Pino, A., Bertrand, H., Carlotto, V., Fornari, M., García, R., Jiménez, M., Marzoli, A., Meyer, C.A., Rosas, S., Soler, P., 2004c. Estiramiento litosférico del Paleozoico Superior al Cretáceo Medio en el Perú y Bolivia. Publicación Especial Sociedad Geológica del Perú, vol. 5, 45-79.

Sempere, T., Callot, P., Odonne, F., Robert, E., Jacay, J., Rousse, S., Saint-Blanquat, M. de., Dramatic onset of Andean orogeny in Peru 90 Myr ago forced by burst of magmatic arc growth. Submitted.

Sigé, B., Sempere, T., Butler, R.F., Marshall, L.G., Crochet, J.-Y., 2004. Age and stratigraphic reassessment of the fossil-bearing Laguna Umayo red mudstone unit, SE Peru, from regional stratigraphy, fossil record, and paleomagnetism. Geobios 37, 771-794.

Soler, P., Bonhomme, M., 1990. Relations of magmatic activity to plate dynamics in Central Peru from Late Cretaceous to Present. In Kay, S., Rapela, C. (Eds.), Plutonism from Antarctica to Alaska. Geological Society of America Memoir, vol. 241, pp. 173-192.

Sparling, D.R., 1970. The Bass Islands Formation in its type region. Ohio Journal of Sciences 70, 1-33.

Spence, G.H., Tucker, M.E., 1997. Genesis of limestone megabreccias and their significance in carbonate sequence stratigraphic models: A review. Sedimentary Geology 112, 163-193.

Spörli, K.B., Rowland, J.V., 2007. Superposed deformation in turbidites and syn-sedimentary slides of the tectonically active Miocene Waitemata Basin, northern New Zealand. Basin Research 19, 199-216.

Steen, Ø., Andresen, A., 1997. Deformational structures associated with gravitational block gliding: examples from sedimentary olistoliths in the Kalvåg Melange, western Norway. American Journal of Science 297, 56-97.

Strachan, L.J., 2008. Flow transformations in slumps: a case study from the Waitemata Basin, New Zealand. Sedimentology, in press, doi: 10.1111/j.1365-3091.2007.00947.x

Tripsanas, E.K., Piper, D.J.W., Jenner, K.A., Bryant, W.R., 2008. Submarine mass-transport facies: new perspectives on flow processes from cores on the eastern North American margin. Sedimentology 55, 97-136.

Tucker, M. E., 2001. Sedimentary Petrology, An introduction to the origin of sedimentary rocks – Third edition. Blackwell Publishing, Oxford, 262 p.

Vernhet, E., Heubeck, C., Zhu, M.-Y., Zhang J.-M., 2006. Large-scale slope instability at the southern margin of the Ediacaran Yangtze platform (Hunan province, central China). Precambrian Research 148, 32-44.

Vorren, T.O., Laberg, J.S., 2001. Late Quaternary sedimentary processes and environment on the Norwegian-Greenland Sea continental margins. In: Martinsen, O.J., Dreyer, T. (Eds.), Sedimentary Environments Offshore Norway - Palaeozoic to Recent, Elsevier, Amsterdam, pp. 451-456.

Wilson, C.K., Long, D., Bulat, J., 2004. The morphology, setting and processes of the Afen Slide. Marine Geology 213, 149-167.

Wynn, R.B., Masson, D.G., Stow, D.A., Weaver, P.P., 2000. The Northwest African slope apron: a modern analogue for deep-water systems with complex sea floor topography. Marine and Petroleum Geology, 17, 253-265.

III.2. Hypothèse sur l'origine des surpressions de fluides interstitiels dans les zones amont

Les figures indiquant des surpressions de fluides se rencontrent dans les parties amont de la Formation Ayabacas (zones 1 à 3). Les surpressions de fluides interstitiels peuvent apparaître lorsque la sédimentation est plus rapide que l'expulsion des fluides des sédiments. C'est par exemple le cas dans certaines parties du delta du Mississipi où se rencontrent des taux de sédimentation très élevés, jusqu'à 20 m/1000 ans (Prior & Coleman, 1982 ; Adams & Roberts, 1993). Les taux de sédimentation dans le bassin d'arrière-arc du Crétacé moyen du sud-Pérou sont beaucoup plus faibles, en particulier dans les parties amont, au NE du CECLLA. De plus, ils présentent une nette différence (environ un ordre de magnitude) entre le centre du bassin (~ 30 m/million d'année soit ~ 0,03 m/1000 ans au SW du CECLLA) et la partie NE du bassin (~ 3 m/million d'année soit ~ 0.003 m/1000 ans au NE du CECLLA). Ces taux de sédimentation n'ont probablement pas été suffisants pour générer un excès de pression interstitielle de fluides, mais l'importante différence de vitesse de sédimentation a pu induire un écoulement des fluides de l'aval vers l'amont dans la couche perméable formée par la Formation Murco scellée par la couche imperméable formée par la Formation Arcurquina (Fig. 3.1). Cette migration de fluides a engendré des pressions de fluides interstitiels élevées dans les parties amont de la Formation Murco, facilitant la rupture dans cette partie du bassin dans laquelle la couverture calcaire formée par la Formation Arcurquina était la moins épaisse.

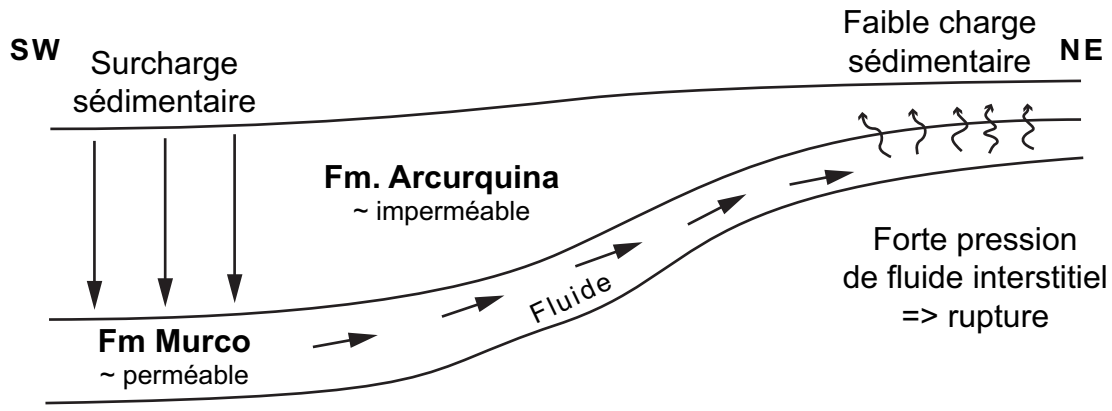

Fig. 3.1 : Genèse de pressions de fluides interstitiels élevées dans les parties amont de la Formation Ayabacas, suite à des taux de sédimentation hétérogènes entraînant une migration du SW vers le NE des fluides piégés dans la Formation Murco. D'après un schéma de Roger Urgeles.

IV.

DISCUSSION SUR L'ORIGINE DU COLLAPSE

IV. Discussion sur l'origine du collapse

IV.1. Les conditions environnementales des grandes zones d'instabilités actuelles comparées à l'Ayabacas

Actuellement, les zones instables dans lesquelles se produisent des glissements sous-marins récurrents ou de grandes dimensions sont :

- la marge nord-ouest européenne (Fig. IV.1 ; Evans et al., 2005), et en particulier la marge de la Norvège, avec par exemple le "Storegga Slide", le "Traenadjupet Slide" (Laberg & Vorren, 2000 ; Haflidason et al., 2004) ou le Bjørnøyrenna Slide (Vorren & Laberg, 2001) : c'est une marge passive, en partie glaciaire, avec un bassin ouvert s'approfondissant jusqu'à plus de 3 000 m de profondeur (Canals et al., 2004 ; Evans et al., 2005). Les glissements semblent pouvoir être reliés aux cycles glaciaires/interglaciaires et en particulier aux périodes de fonte des glaces (Evans et al., 2005 ; Solheim et al., 2005a)

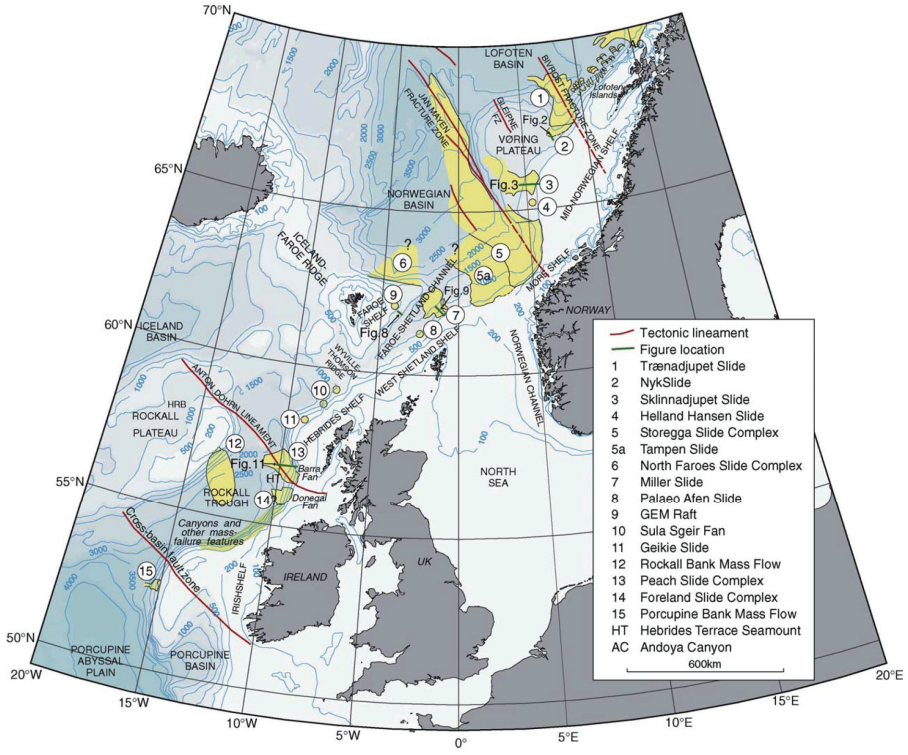

Fig. IV.1 : Carte de la marge nord-ouest européenne et localisation des principaux glissements d'âge Pliocène supérieur à Holocène actuellement connus. D'après Evans et al. (2005).

- le long de la marge ouest-africaine (Gee et al., 1999 ; Talling et al., 2007 ; Henrich et al., 2008) et au large de l'Afrique du Sud (Dingle, 1977, 1980) : ce sont là encore des marges passives, avec des bassins ouverts dépassant parfois les 4 000 m de profondeur.
- dans les cônes sédimentaires à l'embouchure des grands fleuves : Mississipi (McAdoo et al., 2000), Nil (Loncke et al., 2006), Zaïre (Savoye et al., 2000)… Les glissements sont dus à un considérable apport de matériaux et à un effet de surcharge sédimentaire.

Le collapse Ayabacas s'est produit dans des conditions environnementales (plate-forme carbonatée de bassin d'arrière-arc, faible tranche d'eau, taux de sédimentation faible, de seulement ~4 m/Ma dans les parties proximales et de ~20 à ~33 m/Ma dans les parties distales du bassin) nettement différentes de celles des zones qui semblent actuellement propices aux instabilités de grande ampleur. Bien que des glissements surviennent dans des conditions relativement similaires à celles du WPBAB (*e.g.* Mullins et al., 1986 ; Mullins & Hine, 1989 ; George et al., 1995 ; Spence & Tucker, 1997 et références de la Table 1 ; Graziano, 2001 ; Drzewiecki & Simó, 2002 ; Chiocci et al., 2003 ; Floquet & Hennuy, 2003 ; Frey-Martínez et al., 2005, 2006), aucun n'atteint l'ampleur du collapse Ayabacas et tous présentent au moins une caractéristique différente de celles du bassin du WPBAB (taux de sédimentation plus élevé, bassin ouvert, matériaux siliciclastiques et non carbonatés, glissements évoluant en tubidites,...). Le collapse Ayabacas s'est donc produit dans des conditions environnementales qui semblent assez peu propices aux instabilités.

IV.2. Absence de dépôts turbiditiques

La partie aval des dépôts des grands glissements sous-marins (récents ou fossiles) est classiquement turbiditique : *e.g.*, off-shore, le Storegga Slide (Haflidason et al., 2004), le Bjørnøyrenna Slide (Vorren & Laberg, 2001), le Saharan Debris Flow (Gee et al., 1999) ou le Mauritania Slide Complex (Henrich et al., 2008), et, on-shore, les glissements éocènes d'Ainsa (Dreyer et al., 1999) ou les glissements oligo-miocènes dans le nord des Apennins (Lucente & Pini, 2003, 2008).

Cependant, aucun dépôt de turbidites n'a été observé dans la Formation Ayabacas, qui au contraire présente une fragmentation décroissante des dépôts en allant vers l'aval à partir du CECLLA. Dans le sud de la zone d'étude, les dépôts aval de la Formation Ayabacas sont les grands plis de la zone de Yura, qui marquent le blocage du collapse par un seuil topographique. L'absence d'affleurements d'âge Turonien/Coniacien plus à l'ouest ne permet pas d'assurer qu'une zone plus aval ait existé ni qu'aucune turbidite ne s'y soit déposée. Dans la partie nord de la zone d'étude, le seuil topographique n'a pas été mis en évidence et les observations suggèrent que la pente était plus prononcée qu'au sud, mais là non plus il n'a pas été observé de dépôts turbiditiques dans la Formation Ayabacas.

La nature des matériaux impliqués dans le collapse, majoritairement carbonatés, ne semble pas en mesure d'expliquer cette absence de turbidites. En effet, si les sédiments carbonatés se cimentent généralement plus rapidement que la plupart des autres (en particulier les matériaux siliciclastiques) (Dapples, 1967 ; Tucker, 2001), ce qui peut empêcher l'incorporation d'eau et la transformation de la masse glissée en courant de turbidité, les calciturbidites sont couramment observées et certains auteurs considèrent que la cimentation précoce n'a qu'un effet négligeable sur la stabilité de la pente (Spence & Tucker, 1997). Les calciturbidites apparaissent lorsque le taux de sédimentation et la pente sont suffisants pour que les matériaux soient métastables. Des dépôts turbiditiques carbonatés seraient généralement l'indication de glissements récurrents, de dimensions relativement modestes, sur une pente métastable, pendant un certain temps (Spence & Tucker, 1997). Au contraire, l'absence de turbidites et l'existence de la méga-brèche Ayabacas indiquent que la plate-forme carbonatée était stable de l'Aptien au Turonien et a été déstabilisée ensuite.

IV.3. Des dimensions exceptionnelles, mais un ou plusieurs événements ?

La Formation Ayabacas constitue le plus grand dépôt de glissements sédimentaires sous-marins fossiles actuellement connu (Fig. I.15). Ses dimensions sont du même ordre de grandeur que les plus grands glissements actuels, cependant son extension n'est pas parfaitement contrainte. Ainsi, la tête (entre Huancané et Yanaoco) et le pied (zone de Yura) du glissement sont bien définis dans le sud de la zone d'étude, mais assez mal dans le nord (Urubamba-Chalhuanca). En conséquence, les dimensions du collapse Ayabacas avancées (~ 80 000 km² en surface, ~ 10 000 km^3 en volume) sont peut-être des sous-estimations. Il est en revanche difficile de déterminer avec certitude si ces dépôts résultent d'un seul ou de quelques grands glissements mis en place très rapidement, ou bien d'une succession de plusieurs glissements plus modestes se mettant en place en quelques millions d'années, les deux possibilités étant décrites dans la littérature. Il existe en effet de nombreux collapses récents constitués d'un seul grand glissement — *e.g.* le "Saharan Debris Flow" (Gee et al., 1999), le "Agulhas Slump" (Dingle, 1977) — ou de quelques glissements se produisant sur de très courtes périodes (à l'échelle géologique) pour former un collapse géant — *e.g.* le "Storegga Slide", formé à 99% par 5 ruptures en moins de 1 500 ans (Haflidason et al., 2005) —. Mais des successions de glissements de diverses tailles se produisant en quelques millions d'années se rencontrent également : avant le Storegga Slide, d'autres glissements sont survenus dans la même zone entre le Pléistocène Supérieur et l'Holocène, et en particulier il y a environ 0,5 Ma, les auteurs suggérant une alternance entre des périodes de construction de la marge et des périodes de collapse (Solheim et al., 2005a). D'autres exemples existent dans la littérature récente, par exemple off-shore les ~ 40 glissements en ~ 2 Ma des "Israel Slump Complexes" (Frey-Martínez et al., 2005), et on-shore les 10 corps qui se sont déposés entre l'Oligocène supérieur et le Miocène supérieur dans le nord des Apennins (Lucente & Pini, 2008). Lorsqu'il s'agit d'une succession de glissements en quelques millions d'années, les dépôts chaotiques des glissements alternent avec des niveaux régulièrement stratifiés correspondant à la sédimentation normale entre deux événements catastrophiques.

Dans le cas du collapse Ayabacas, l'intervalle de temps pendant lequel les glissements ont pu avoir lieu est au maximum de quelques millions d'années, mais n'a pu être contraint plus précisément (voir section II.1.2). Le moment exact de survenue des glissements ne peut donc être situé avec précision, et cette donnée ne permet pas de déterminer le nombre et la

fréquence d'occurrence des glissements. Cependant, l'ensemble de la Formation Ayabacas est chaotique, marquée par une absence totale de niveaux régulièrement stratifiés séparant des unités chaotiques. De plus, la taille conséquente des radeaux et des blocs transportés suggère que les glissements étaient de grande ampleur et donc peu nombreux. Ces deux observations, bien qu'elles ne soient pas des preuves formelles, suggèrent que les dépôts du collapse Ayabacas résultent de un ou quelques grands glissements, survenant pendant une période assez brève, et considérés à l'échelle des temps géologiques comme un seul événement. Ceci est en accord avec l'absence de turbidites, et implique là encore une brusque déstabilisation de la marge, stable jusqu'alors.

IV.4. Le collapse Ayabacas : une conséquence de changements géodynamiques globaux

Les points précédents montrent que la Formation Ayabacas résulte d'un collapse atypique. Ils indiquent ou suggèrent que ce collapse est un événement unique à l'échelle des temps géologiques, se produisant de façon brusque dans un environnement *a priori* peu favorable aux glissements géants. Dans la littérature, les marges instables (fossiles comme actuelles), se caractérisent par une succession de glissements séparés par des dépôts régulièrement stratifiés correspondant aux périodes peu propices aux ruptures. Au contraire, la Formation Ayabacas correspond à la remobilisation massive des derniers dépôts mis en place dans le bassin, restés remarquablement stables pendant les millions d'années précédant le collapse. La déstabilisation de cette marge *a priori* stable suggère que le collapse soit la conséquence d'événements particuliers, capables de modifier brusquement les conditions de stabilité de la marge.

Dans l'article qui suit sont présentés plusieurs changements et événements se produisant aux alentours de la limite Turonien-Coniacien dans l'ouest de l'Amérique du Sud et dans le Pacifique. Le collapse Ayabacas est considéré comme une conséquence de ces processus géodynamiques qui marquent le début de l'orogenèse des Andes Centrales.

Résumé étendu en français de l'article 4 : Onset of Andean orogeny in Peru 90 Myr ago triggered by burst of magmatic arc growth. *Nature Geoscience*, soumis.

Les Andes Centrales sont le plus grand orogène sur Terre résultant d'une subduction océan-continent, mais leur formation reste sujette à débats. Dans cet article, la conjonction de divers changements et événements aux alentours de 90 Ma permet de proposer un scénario expliquant l'amorce de la croissance orogénique.

La rapide continentalisation du bassin d'arrière-arc de l'ouest du Pérou au Crétacé Supérieur est depuis longtemps considérée comme marquant le début de l'orogenèse andine. Elle fut donc interprétée comme résultant du raccourcissement tectonique de la marge, selon le paradigme dominant, et nommée "phase tectonique péruvienne". Cependant il n'existe pas d'observation directe de raccourcissement tectonique de cet âge et la marge occidentale du Pérou montre essentiellement des structures en extension et en décrochement. La continentalisation est mieux décrite comme une modification brutale de l'enregistrement

stratigraphique et coïncide avec de nombreux changements et événements (détaillés ci-dessous) dans la région et dans l'Océan Pacifique. Notamment elle a été immédiatement précédée par le collapse Ayabacas, raison pour laquelle la discontinuité qui sépare les séries marines de la succession continentale est renommée "discontinuité Ayabacas".

De ~230 à ~90 Ma, le bassin d'arrière-arc de l'ouest du Pérou (WPBAB) se développe en contexte extensif : il s'approfondit vers l'ouest et est plus particulièrement subsident à partir de 110 Ma, lorsque se met en place la plate-forme carbonatée. La discontinuité Ayabacas marque l'arrêt brutal de l'activité de la plate-forme carbonatée albo-turonienne, la quasi-totalité de cette dernière étant de plus entraînée, dans le sud du Pérou, dans le collapse Ayabacas. Après cet événement, les dépôts sont essentiellement continentaux et la polarité du bassin s'inverse, les matériaux provenant de l'ouest et s'étalant vers l'est.

La discontinuité Ayabacas coïncide également avec une activation majeure du volcanisme d'arc, au moins dans le sud Pérou. Avant le collapse, des plutons se mettent en place dans la région d'Ilo, mais aucun enregistrement de roches ou de débris volcaniques n'existe dans le bassin d'arrière-arc entre ~135 et ~90 Ma, suggérant une activité magmatique limitée de l'arc. Au contraire, des laves et des conglomérats volcano-détritiques affleurent en abondance dans le sud du Pérou et jusqu'en Bolivie centrale après la discontinuité Ayabacas. De la même façon, le plutonisme est modeste entre ~150 et 91 Ma et augmente considérablement en volume entre 91 et 70 Ma le long de toute la marge péruvienne. Cette forte croissance de l'activité magmatique, caractérisée par de faibles rapports $^{87}Sr/^{86}Sr$ et donc une source mantellique, concorde par ailleurs avec l'épisode majeur de soulèvement de la côte à 90-80 Ma (déterminé par modélisation et données thermochronologiques). Ce soulèvement résulterait donc d'un épaississement magmatique rapide de l'arc par de considérables transferts de matériaux depuis le manteau. D'autres indices étayent l'hypothèse d'un magmatisme fort et d'un soulèvement de l'arc : d'une part l'altération et l'érosion de ces reliefs proto-andins expliquent les matériaux détritiques et volcano-détritiques rouges qui dominent à l'est après 90 Ma ; d'autre part l'inversion de polarité du bassin implique un soulèvement à l'ouest.

Une telle croissance de l'arc magmatique implique des modifications majeures des conditions de subduction. Une évolution de ces conditions est confirmée par plusieurs événements se produisant dans le Pacifique et dans la zone de subduction entre ~91 et 70 Ma.

Ainsi les plateaux océaniques Caraïbe-Colombie (CCOP) et Gorgona (GOP) se mettent en place respectivement à $91,4 \pm 0,4$ Ma et $88,9 \pm 1,2$ Ma, indiquant une forte anomalie

thermique du manteau permettant d'extraire les grandes quantités de basaltes du CCOP et de générer dans le GOP les seules komatiites phanérozoïques connues sur Terre. De plus l'ensemble de la lithosphère océanique Pacifique a été réchauffé à peu près à partir de la même période et jusqu'à 70 Ma. Ces deux points, qui coïncident avec la mise en place des plutons entre ~91 et 70 Ma au Pérou, impliquent des températures du manteau anormalement élevées et par conséquent une convection accélérée de la cellule Panthalassa (Pacifique). Cette poussée thermique a probablement augmenté la flottabilité de la lithosphère océanique avec pour conséquence une diminution de l'angle de la subduction sous la marge péruvienne.

Une subduction moins inclinée peut entraîner une migration de l'arc magmatique vers l'est, ce qui est bien observé dans l'extrême sud du Pérou. Au nord de la latitude 17°S, la migration de l'arc est néanmoins plus faible ou inexistante. Mais la localisation de l'arc dépend également de la température au sommet de la plaque descendante (et donc de sa vitesse de descente) et/ou de la température dans le coin asthénosphérique. Dans le même temps, la poussée thermique du manteau et l'accélération de la convection de la cellule mantellique Panthalassa peuvent augmenter les températures dans le coin asthénosphérique et/ou la vitesse de subduction, tendant ainsi à limiter les effets de la diminution de l'angle de la subduction et réduisant la migration de l'arc vers l'est.

Ces modifications des conditions de subduction fournissent une explication simple à l'avènement du collapse Ayabacas. La diminution de l'angle de la subduction a augmenté le couplage entre les plaques ce qui, combiné à l'accélération de la vitesse de plongement de la plaque, a induit une flexure temporaire de la lithosphère continentale, créant un basculement vers le sud-ouest de la marge et déclenchant le collapse. Cette interprétation implique que le changement de régime de subduction a été rapide et transitoire, en accord avec les points passés en revue ci-dessus.

Le scénario proposé désigne l'accrétion magmatique dans l'arc comme le contrôle, si ce n'est le moteur, de l'épaississement crustal dans les Andes Centrales depuis le Crétacé Supérieur, en accord avec l'observation que l'épaississement de la croûte est maximal au niveau de l'arc dans la partie occidentale des Andes tandis que le raccourcissement tectonique cénozoïque se limite essentiellement à leur moitié orientale. D'autre part, ce scénario souligne le rôle fondamental de la convection de la cellule mantellique Pacifique dans le contrôle de la production de croûte au niveau de l'arc du Pérou, avec création de croûte juvénile et génération de komatiites, des processus classiquement observés au Précambrien.

Onset of Andean orogeny in Peru 90 Myr ago triggered by burst of magmatic arc growth

Thierry Sempere[1], Pierre Callot[1], Francis Odonne[1], Emmanuel Robert[2], Javier Jacay[3], Sonia Rousse[1] & Michel de Saint-Blanquat[1]

[1]*LMTG, Université de Toulouse, CNRS, IRD, OMP, 14 avenue Edouard Belin, F-31400 Toulouse, France*

[2]*OSUG, Université Joseph Fourier, Institut Dolomieu, 15 rue Maurice Gignoux, F-38031 Grenoble cedex, France*

[3]*EAP Ingeniería Geológica, Universidad Nacional Mayor de San Marcos, Lima, Peru*

The Central Andes are presently on Earth the largest orogen resulting from ocean-continent subduction, but how they have formed remains debated[1]. In particular, it is unclear why in Peru and Bolivia the orogeny started ~90 Myr ago[2–6], and built high mountains only ≤ 26 Myr ago[1], whereas subduction of Panthalassan oceanic plates beneath the western margin of South America has been active for > 450 Myr[7]. Here we report and analyse a significant conjunction of diverse changes and events ~90 Myr ago that illuminates how orogenic growth was initiated in Peru. We observe that in the backarc of southern Peru reversal of basin polarity and regional continentalization[2–6,8] was inaugurated by the giant collapse of the mid-Cretaceous carbonate platform[8], reflecting catastrophic flexuring of the backarc lithosphere, and coincided with resumption of volcanism[3,8], rapid magmatic arc growth[9], and major uplift of the arc crust[10], whereas no coeval tectonic shortening is recorded[1,11]. We point out that major oceanic plateaux were constructed in the East Pacific also ~90 Myr ago[12] during an extensive mantle heat burst[13] which must have accelerated Pacific mantle convection and deeply modified the conditions of subduction and mantle-derived magma production at the Peru arc. The causal chain of processes we identify indicates that magmatic flare-up of the arc, not tectonic shortening, was responsible for initiating Central Andean crustal thickening and growth.

The rapid continentalization of the backarc basin of Peru (Fig. 1) in the Late Cretaceous has long been interpreted to mark the beginning of the Andean orogeny[11,14], and thus the onset of tectonic shortening of the margin[2–6] as the Andes are dominantly viewed to result from this process[1,15]. This interpretation, however, appears largely paradigm-driven as no undisputable direct evidence of coeval tectonic shortening has been observed[1,11], whereas extension and transcurrence have largely dominated the tectonic history of the western Peruvian Andes[1]. Instead of being understood to represent the so-called "Peruvian tectonic phase"[11,14], the backarc continentalization is thus better described as a sharp change in the stratigraphic record, which we refer here as the "Ayabacas discontinuity" for reasons evident below. Throughout western Peru, in what was the Cretaceous backarc, the discontinuity is expressed by a marked lithological change and a complete reversal of basin polarity, reflecting, respectively, an environmental turning point and the emergence of a continuous relief along the arc: mid-Cretaceous marine carbonates deposited in a platform that had been deepening to the west are sharply overlain by reddish, dominantly fine-grained, Senonian-age continental (to locally shallow-marine) deposits derived from the west[2–6,8,11]. Ammonite faunas respectively from below and above the Ayabacas discontinuity date it to near the Turonian-Coniacian boundary[2,5,8] or to the latest Turonian[16], i.e. to between 91 and 89 Myr ago[17], which coincides with a number of changes and events in the region and Pacific ocean (Fig. 2).

From ~230 to ~90 Myr ago, the western Peru backarc basin (WPBAB; Fig. 1) had evolved in a markedly extensional setting, that created and maintained a slope to the west[2–6]. Subsidence significantly increased ~110 Myr ago as a consequence of the western WPBAB evolution toward a state of marginal basin due to considerable lithospheric thinning in central Peru[6,18], a tectonic context that ended with the Ayabacas discontinuity. During the Albian-Turonian interval (~110-90 Myr ago[17]), a carbonate platform developed along the edge of the continental domain, which technically behaved as a kind of passive margin in relation to the much deeper western portion of the basin. Although the narrowing southern extension of the WPBAB was characterized by lower subsidence and less pronounced extensional tectonics and related basic magmatism, the geologic record of southern Peru is especially informative on the upheaval ~90 Myr ago.

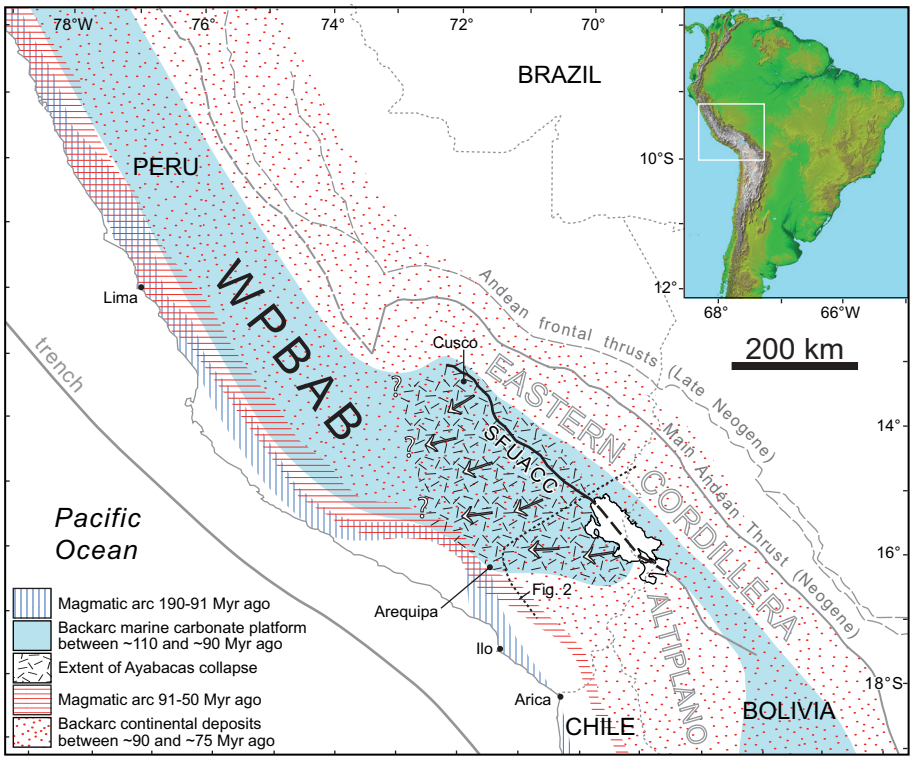

Figure 1 | Locations of magmatic arc and backarc basin across the Ayabacas discontinuity ~90 Myr ago. *WPBAB, West Peruvian backarc basin. SFUACC, Urcos-Ayaviri-Copacabana-Coniri fault system (Spanish abbreviation). Arrows depict approximate local sliding direction during the Ayabacas collapse[8]; question marks delineate the known westernmost extent of collapse. Present-day geological features (trench, coast, names of tectonic domains, faults) appear in graytone. Respective positions of arc magmatism before and after 91 Myr ago illustrate northeasterly arc migration south of 17°S and, to a lesser extent, between 12° and 16°S. Before ~90 Myr ago, the backarc basin was marine and deepened to the southwest (blue); after ~90 Myr ago (red dots), it was mainly continental and fed from the southwest.*

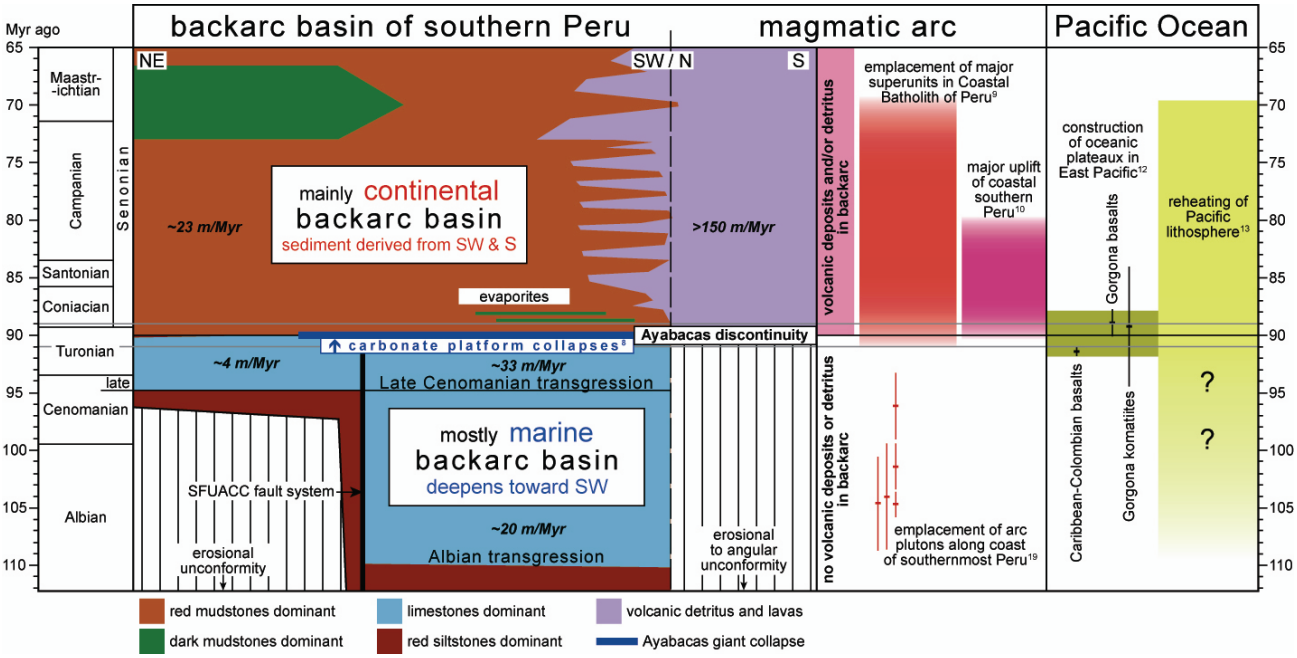

Figure 2 | Synopsis of changes and events ~90 Myr ago in Peru and the Pacific. *Left portion of figure illustrates the Late Cretaceous stratigraphic record in the backarc of southern Peru (see Fig. 1 for approximate location of stratigraphic transect); mean compacted sedimentation rates (expressed in m/Myr) inform on subsidence rate variations in time and space.*

The Ayabacas discontinuity is primarily expressed by the abrupt termination of the Albian-Turonian carbonate platform[2–6,8] (Fig. 2). In southern Peru, this termination was particularly dramatic as most of the platform, which until then had been notably stable, collapsed over >80,000 km^2 down the regional basin slope, i.e. to the southwest and west, involving >10,000 km^3 of mid-Cretaceous limestones and underlying strata, and making the resulting unit, the Ayabacas Formation, one of the largest giant collapses known on Earth[8]. The detailed anatomy of the unit as well as abundant occurrences of hydroplastic breccias and other typically fluidized sediments indicate that this major mass-wasting event was short-lived and submarine[8]. In contrast, the Senonian red strata that overlie the collapse accumulated in alluvial environments[2–6,11]. In the Arequipa area, however, the lower portion of this dominantly red-bed succession include strata deposited in coastal plain to shallow-marine environments[2,6], one of which yielded a Coniacian ammonite confirming that no significant time hiatus was associated with the change from marine to dominantly continental conditions[2,8].

The Ayabacas Formation records the only sedimentary collapse that disrupted the mid-Cretaceous platform of southern Peru. It is noteworthy that this unique catastrophic event in the history of the backarc and margin occurred just before the backarc continentalization. The collapse was apparently triggered by the abrupt activation of extensional faulting over the northeastern slope of the backarc basin, as indicated by field evidence of syn-collapse normal faults and associated block tilting, dominantly displaying down-to-the-southwest kinematics[8]. It is likely that rapid growth of fault scarps and surface tilting created, enhanced, and oversteepened local and regional slopes, enabling sliding. In particular, large blocks of Jurassic and, less commonly, Paleozoic strata, up to 50 m in stratigraphic thickness and to 300 m in length and width, occur in the Ayabacas Formation along the SFUACC fault system (Fig. 1), implying that during the event the basement was exposed to catastrophic removal along significant fault scarps there[8]. Normal faulting in the backarc continued into the Coniacian and formed grabens in which evaporites accumulated, as in central Bolivia[3]. In these regions backarc continentalization was thus associated with extensional, not compressional, faulting.

Most strikingly, the Ayabacas discontinuity also coincided with a major activation of the volcanic arc, at least in southern Peru. Prior to the collapse, the largely marine sub-basin in which stratigraphic units had accumulated since the Early Jurassic connected with the

Panthalassan realm across a modest island-forming magmatic arc: although dioritic to granodioritic plutons were emplaced in the Ilo area between ~109 and ~93 Myr ago[19], no volcanic rocks or detritus are recorded in the backarc basin between ~135 and ~90 Myr ago[3,4,6,8] (Fig. 2), suggesting that magmatic activity in this arc was limited and consisted chiefly of localized intrusions. In contrast, the units younger than the Ayabacas discontinuity display evidence of coeval volcanic activity, including felsic tuff deposits as far as central Bolivia[3,6] and mafic to intermediate volcanodetritic conglomerates in the Arequipa area[8]. South of Arequipa, resumption of volcanic activity and erosion is expressed by the accumulation of >1500 m of volcanodetritic conglomerates and sandstones, derived from the south and thinning northwards into the backarc, that are intercalated with lava flows and unconformably overlie strata of latest Jurassic-earliest Cretaceous age[20] (Fig. 2).

Available data indicate that plutonism in the arc of southern Peru was low between ~150 and 91 Myr ago[9,19]. In contrast, plutonism considerably increased in volume between 91 and 70 Myr ago along the entire Peruvian margin[9,21] (Fig. 2). The initial increase in plutonic volume and coeval onset of major volcanic activity strikingly coincide with the initiation of the major uplift episode (90-80 Myr ago, based on thermochronologic data and modeling[10]) of coastal southern Peru. The Ayabacas discontinuity thus also coincided with a major magmatic input into, and related uplift of, the arc crust: because Mesozoic arc magmas in Peru are characterized by low $^{87}Sr/^{86}Sr$ initial ratios and thus represent additions of material from the mantle to the crust[21], the early Andean uplift and related relief growth must have been achieved by rapid magmatic thickening of the initial arc crust through considerable mass transfer from the mantle.

Indirect evidence for relief formation along the arc, as deduced from the reversal of basin polarity in the backarc, is clearly matched by evidence for coeval magmatic growth and related uplift at the arc. It is likely that alteration and erosion of these emerging proto-Andes provided the reddish detrital material that dominantly accumulated in the backarc after ~90 Myr ago. Furthermore, increased subsidence in the backarc after ~90 Myr ago (Fig. 2) can be explained as a response to the flexuring of the South American lithosphere caused by the loading of the margin produced by the crust rapidly growing and thickening along the arc (Fig. 3).

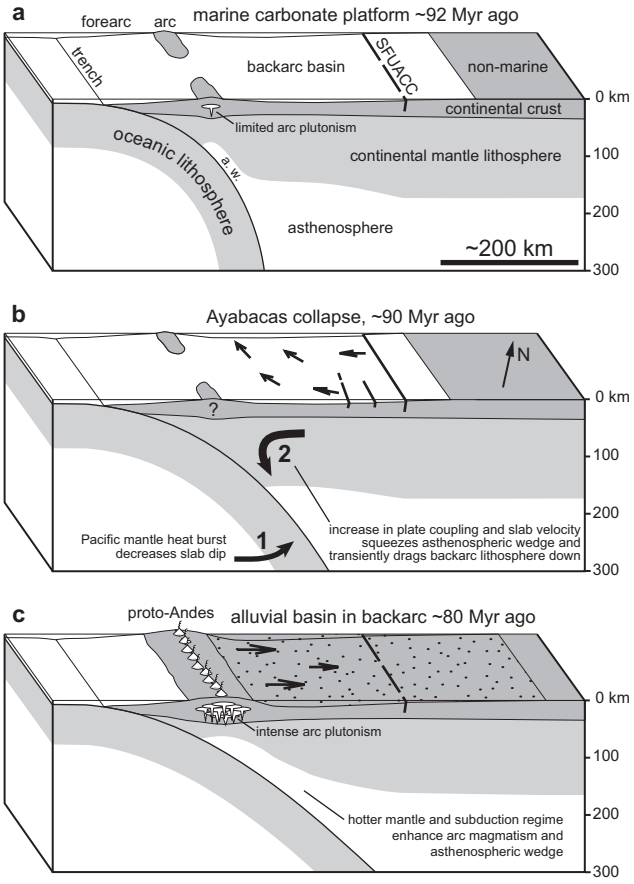

Figure 3 | Changes in subduction regime across the Ayabacas discontinuity in southern Peru. a*, From ~110 to ~90 Myr ago the backarc basin was occupied by a carbonate platform that deepened to the southwest and the arc was the locus of limited plutonism; a. w., asthenospheric wedge; horizontal scale is approximative.* ***b****, During the Ayabacas event, the asthenospheric wedge is inferred to have been transiently squeezed between the oceanic and continental lithospheres due to decreasing slab dip (curved arrow 1); this increased plate coupling and faster subduction caused the backarc lithosphere to be dragged down to the southwest (curved arrow 2), which in turn triggered the Ayabacas collapse at the surface. Arrows in basin (****b****,* ***c****) indicate general sediment transport direction.* ***c****, After ~90 Myr ago the backarc basin was occupied by mostly alluvial environments and fed from the southwest, while the arc rapidly grew and thickened due to massive mass transfer from the mantle and related intense plutonism; following the transient configuration depicted in* ***b****, the asthenospheric wedge is inferred to have re-established and grown due to higher mantle temperatures and subduction velocity.*

Such a rapid magmatic arc growth implies some deep modifications in the conditions of subduction. Although plate motions and velocities cannot be directly estimated for times within the long mid-Cretaceous normal superchron (~124.5-83.5 Myr ago), an insight into this issue appears in the fact that the East Pacific evolution was marked by events strikingly coeval with the Ayabacas discontinuity (Fig. 2). The Caribbean-Colombian (CCOP) and Gorgona (GOP) oceanic plateaux were rapidly constructed 91.4 ± 0.4 and 88.9 ± 1.2 Myr ago, respectively[12], both implying a significant mantle thermal anomaly: large amounts of basalts had to be extracted from the mantle to build the extensive CCOP, and generation in the GOP of the only Phanerozoic komatiites known on Earth required anomalously hot mantle temperatures. Remarkably, both phenomena are compatible with the entire Pacific oceanic

lithosphere having been reheated between approximately ~100 and, more precisely, 70 Myr ago[13]. We infer from the conjunction of these quite anomalous thermal phenomena that the Pacific mantle was affected by an extensive heat burst between ~91 and 70 Myr ago. This implies coeval enhanced and accelerated convection of the Panthalassan (Pacific) cell[7], which would evidently have had some significant effects on the subduction zones along its margins. Major changes in geological evolution are indeed recorded ~90 Myr ago in regions as diverse as China[22] and North America[23], for instance. It is particularly striking that anomalous heating of the East Pacific lithosphere between ~91 and 70 Myr, as we infer here from independent sources[12,13], exactly coincided with emplacement of large plutonic volumes between 91 and 70 Myr ago in Peru[9].

This Pacific heat burst is likely to have made the oceanic lithosphere more buoyant and hence to have tended to decrease the dip of subduction beneath the Peru margin. An easterly migration of the arc should thus be expected, and is indeed observed in southernmost Peru, where plutons younger than ~91 Myr ago form a belt that extends ~70 km northeast of another belt formed by older plutons[24] (Fig. 1). North of 17°S, however, arc migration was smaller or is not detected. But the location of arcs depends on the depth at which the main subduction magmatism develops, which is inversely correlated with the descent speed of the slab and, ultimately, with the temperature at top of the slab or in the mantle wedge[25]. Decrease in slab dip may therefore be accompanied by little or no arc migration in case of sufficient coeval increase in slab velocity and/or mantle temperatures, a phenomenon that is compatible with the idea of accelerated Pacific mantle convection starting ~91 Myr ago. Thus, the limited arc migration north of 17°S and the 91-70 Myr increased plutonism along the Peru arc may conjunctly appear as consequences of the ~91-70 Myr Pacific mantle heat burst and accelerated convection.

Coeval acceleration and decrease in dip of the slab are likely to have transiently destabilized the thermal-tectonic regime at the subduction interface, providing a simple explanation for the unique and intriguing Ayabacas collapse. In this context we infer that decrease in slab dip increased plate coupling, which, combined with slab acceleration, dragged the upper lithosphere down-to-the-southwest, conjunctly causing a transient flexure that triggered the Ayabacas giant collapse in the backarc of southern Peru (Fig. 3). This interpretation implies that the change in subduction regime was rapid. Increasing mantle

temperatures subsequently favoured the re-establishment and growth of the asthenospheric wedge, decreasing plate coupling and increasing arc magmatism (Fig. 3).

The conjunction of extremely diverse coeval phenomena, affecting the Pacific mantle and lithosphere as well as the Peru arc and backarc, leads to a consistent scenario agreeing with the notion that a hotter mantle triggers pulses of rapid subduction which result in massive volcanism and magmatic continental growth at arcs[26]. Between ~91 and 70 Myr ago, a mantle heat burst intensified convection of the Pacific cell[7], which abruptly modified the conditions of subduction and triggered a burst of juvenile crustal production along the Peru margin. Rapid increase in plate coupling and slab velocity transiently flexured and fractured the backarc lithosphere, which destabilized its sedimentary cover into a giant submarine collapse. Massive magmatic transfer of mantle-derived material into the arc crust caused its growth, thickening and uplift, as well as reversal of the backarc basin polarity and subsequent regional continentalization, and maintained backarc subsidence. Given the lack of direct evidence for coeval tectonic shortening of the margin[1,11], it appears that the onset of the Central Andean orogeny in Peru was caused by a marked increase in production of juvenile crust at the arc and, ultimately, by thermal enhancement and acceleration of Pacific mantle convection.

We suggest that, as conjectured earlier[27–30], magmatic accretion at the arc has been a major control, if not the main driver, of Central Andean crustal thickening since the Late Cretaceous, in agreement with the key observation that the crust is thickest across the arc[27,29,30], i.e. in the western half of the Andes, whereas Cenozoic tectonic shortening has been largely restricted to the eastern half[1,27,30]. On the other hand, the key role of Pacific (Panthalassan) mantle convection in controlling crustal production at the Peru arc is reminiscent of how the apparent episodicity of Precambrian crustal growth has been explained[26], and, because some of the phenomena reported here, such as juvenile crust production and komatiite generation, are classical features of the Earth's Precambrian evolution, we wonder whether the period of time and region considered here may provide somewhat of a possible "recent" and short-lived downscaled analogue of a much older geosystem regime.

References

1. Sempere, T., Folguera, A. & Gerbault, M. New insights into Andean evolution: An introduction to contributions from the 6th ISAG symposium (Barcelona, 2005). *Tectonophysics* (2008, in the press).

2. Jaillard, E. Kimmeridgian to Paleocene tectonic and geodynamic evolution of the Peruvian (and Ecuadorian) margin. in *Cretaceous tectonics of the Andes* (ed. Salfity, J.A.) (Earth Evolution Sciences Monographs, Vieweg, Wiesbaden, 1994).

3. Sempere, T. Kimmeridgian? to Paleocene tectonic evolution of Bolivia. in *Cretaceous tectonics of the Andes* (ed. Salfity, J.A.) (Earth Evolution Sciences Monographs, Vieweg, Germany, 1994).

4. Sempere, T. *et al*. Stratigraphy and chronology of Late Cretaceous - Early Paleogene strata in Bolivia and northwest Argentina. *Geological Society of America Bulletin* **109**, 709–727 (1997).

5. Jaillard, E. Sedimentary evolution of an active margin during Middle and Upper Cretaceous times: The north Peruvian margin from late Aptian up to Senonian. *Geologische Rundschau* **76**, 677–697 (1987).

6. Sempere, T. *et al*. Late Permian - Middle Jurassic lithospheric thinning in Peru and Bolivia, and its bearing on Andean-age tectonics. *Tectonophysics* **345**, 153–181 (2002).

7. Collins, W. J. Slab pull, mantle convection, and Pangaean assembly and dispersal. *Earth and Planetary Science Letters* **205**, 225–237 (2003).

8. Callot, P., Sempere, T., Odonne, F. & Robert, E. Giant submarine collapse of a carbonate platform at the Turonian-Coniacian transition: The Ayabacas Formation, southern Peru. *Basin Research* (2008, in the press).

9. Mukasa, S. B. Zircon U-Pb ages of super-units in the Coastal batholith, Peru: Implications for magmatic and tectonic processes. *Geological Society of America Bulletin* **97**, 241–254 (1986).

10. Wipf, M. *Evolution of the Western Cordillera and Coastal Margin of Peru: Evidence from Low-Temperature Thermochronology and Geomorphology*. Thesis, ETH Zurich, no. 16383 (2006).

11. Mégard, F. *Etude Géologique des Andes du Pérou Central* (Travaux et Documents de l'ORSTOM, no. 86, Paris, 1978).

12. Kerr, A. C. & Tarney, J. Tectonic evolution of the Caribbean and northwestern South America: The case for accretion of two Late Cretaceous oceanic plateaus. *Geology* **33**, 269–272 (2005).

13. Ritzwoller, M. H., Shapiro, N. M. & Zhong, S.-J. Cooling history of the Pacific lithosphere. *Earth and Planetary Science Letters* **226**, 69–84 (2004).

14. Steinmann, G. *Geologie von Peru* (Carl Winter, Heidelberg, 1929).

15. Lamb, S. & Davis, P. Cenozoic climate change as a possible cause for the rise of the Andes. *Nature* **425**, 792-797 (2003).

16. Jaillard, E., Bengtson, P. & Dhondt, A. V. Late Cretaceous marine transgressions in Ecuador and northern Peru: A refined stratigraphic framework. *Journal of South American Earth Sciences* **19**, 307–323 (2005).

17. Ogg, J. G., Agterberg, F. P. & Gradstein, F. M. The Cretaceous Period. in *A Geologic Time Scale 2004* (eds Gradstein, F. M., Ogg, J. G. & Smith, A. G.) (Cambridge University Press, Cambridge, 2004).

18. Atherton, M. P. & Webb, S. Volcanic facies, structure, and geochemistry of the marginal basin rocks of central Peru. *Journal of South American Earth Sciences* **2**, 241–261 (1989).

19. Clark, A. H. *et al*. Geologic and geochronologic constraints on the metallogenic evolution of the Andes of southeastern Peru. *Economic Geology* **85**, 1520–1583 (1990).

20. Pino, A., Sempere, T., Jacay, J. Fornari, M. Estratigrafía, paleogeografía y paleotectónica del intervalo Paleozoico superior-Cretáceo inferior en el área de Mal Paso-Palca (Tacna). in *Nuevas*

Contribuciones del IRD y sus Contrapartes al Conocimiento Geológico del Sur del Perú (eds Jacay, J. & Sempere, T.) (Sociedad Geológica del Perú, Special Publication 5, Lima, 2004).

21. Pitcher, W. S., Atherton, M. P., Cobbing, E. J. & Beckinsale, R. D. (eds) *Magmatism at a Plate Edge: the Peruvian Andes* (Blackie, Glasgow & London, 1985).

22. Zhang, Y., Dong, S. & Shi, W. Cretaceous deformation history of the middle Tan-Lu fault zone in Shandong Province, eastern China. *Tectonophysics* **363**, 243–258 (2003).

23. McClelland, W. C. & Oldow, J. S. Late Cretaceous truncation of the western Idaho shear zone in the central North American Cordillera. *Geology* **35**, 723–726 (2007).

24. Roperch, P. *et al*. Counterclockwise rotation of Late Eocene-Oligocene forearc deposits in southern Peru and its significance for oroclinal bending in the Central Andes. *Tectonics* **25**, TC3010, doi:10.1029/2005TC001882 (2006).

25. England, P., Engdahl, R. & Thatcher, W. Systematic variations in the depths of slabs beneath arc volcanoes. *Geophysical Journal International* **156**, 377–408 (2004).

26. O'Neill, C., Lenardic, A., Moresi, L., Torsvik, T. H. & Lee, C.-T. A. Episodic Precambrian subduction. *Earth and Planetary Science Letters* **262**, 552–562 (2007).

27. James, D. E. Plate tectonic model for the evolution of the Central Andes. *Geological Society of America Bulletin* **82**, 3325–3346 (1971).

28. Thorpe, R. S., Francis, P. W. & Harmon, R. S. Andean andesites and crustal growth. *Philosophical Transactions of the Royal Society of London* A **301**, 305–320 (1981).

29. Kono, M., Fukao, Y. & Yamamoto, A. Mountain building in the Central Andes. *Journal of Geophysical Research* **94**, 3891–3905 (1989).

30. James, D. E. & Sacks, I. S. Cenozoic formation of the Central Andes: A geophysical perspective. in *Geology and Ore Deposits of the Central Andes* (ed. Skinner, B. J.) (Society of Economic Geologists, Special Publication 7, 1999).

Acknowledgements

This study was supported by the Institut de recherche pour le développement (IRD) and funds from the CNRS-INSU "GDR Marges" project.

Author contribution

The manuscript was written by T.S. as a development of P.C.'s Ph.D. thesis on the Ayabacas Formation and of ideas discussed with him and other co-authors during the last years. All authors contributed with field work and/or relevant indications and suggestions.

Author information

Correspondence and requests for materials should be addressed to T.S. (sempere@lmtg.obs-mip.fr).

IV.5. Continuité vers le nord du collapse Ayabacas ?

L'hypothèse proposée dans la partie précédente pose la question de la continuité vers le nord du collapse. En effet, la plate-forme carbonatée s'étend aussi dans le centre et le nord du Pérou ainsi qu'en Equateur, mais ne semble pas affectée, d'après la littérature (Jaillard, 1994 ; Toro Álava & Jaillard, 2005 ; Jaillard et al., 2005), de déformations aussi spectaculaires que celles de la Formation Ayabacas. Cependant les modifications des conditions de subduction peuvent avoir eu des effets sur ces dépôts, autres que les changements substantiels des conditions de sédimentation décrits dans la littérature (arrêt ou fort ralentissement de l'activité de la plate-forme carbonatée ; matériaux détritiques ou volcano-détritiques abondants). Une étude de la partie terminale de ces plates-formes en ayant à l'esprit ces nouveaux éléments pourrait permettre de déterminer s'il existe d'autres manifestations des modifications de conditions de la subduction, et pourquoi les plates-formes carbonatées de ces régions n'ont pas subi un collapse aussi considérable que le collapse Ayabacas.

V.

CONCLUSIONS GENERALES

V. Conclusions générales

L'étude de la Formation Ayabacas a confirmé que les déformations particulières affectant cette unité étaient essentiellement contemporaines de la sédimentation et que cette formation est constituée de dépôts de transports en masse sous-marins. Ainsi, il convient dorénavant de bien distinguer les formations Arcurquina et Ayabacas, parfois indifférenciées à cause de leur position stratigraphique similaire :

- La Formation Arcurquina constitue les dépôts non déstabilisés de la plate-forme carbonatée mise en place dans le bassin d'arrière-arc sud péruvien au cours de deux transgressions marines, de l'Albien inférieur à l'Albien supérieur (~108,5 - ~102 Ma) pour la première, et du Cénomanien supérieur au Turonien supérieur (~95 - ~90 Ma) pour la seconde. Elle affleure seulement dans l'est du bassin, ainsi qu'à la base de la succession carbonatée au nord-ouest.
- Affleurant irrégulièrement dans le reste de la zone d'étude, les dépôts de la Formation Ayabacas résultent du collapse de cette plate-forme carbonatée et d'une partie de certaines formations antérieures. Elle constitue une mégabrèche, en particulier dans sa partie est. Une synthèse des données concernant la plate-forme carbonatée ainsi que les unités antérieures et postérieures a permis de déterminer que le collapse s'est produit aux alentours de la limite Turonien-Coniacien (~91-89 Ma), mais l'absence de niveaux régulièrement stratifiés et l'origine du collapse laissent penser qu'il s'agit d'un événement unique et ponctuel à l'échelle des temps géologiques.

L'étude de la Formation Ayabacas à l'échelle du bassin a permis de bien établir qu'il s'agit d'un dépôt de transports en masse sous-marins et d'en définir les caractéristiques :

Les dimensions du collapse, de l'ordre de celles des glissements sous-marins géants actuels, sont considérables : la surface affectée par le collapse est estimée à au moins 80 000 km^2, avec des dépôts, parfois absents à l'amont dans les zones de départ, dépassant les 500 m d'épaisseur dans les zones aval. Le volume de matériaux déplacés est probablement supérieur à 10 000 km^3. Ces dimensions font de la Formation Ayabacas le plus grand glissement sous-marin fossile actuellement connu.

La Formation Ayabacas se structure du nord-est au sud-ouest en six zones basées sur les faciès de déformation. Ces zones s'organisent partiellement autour du SFUACC (au NE) et du CECLLA (au SO), deux importants systèmes structuraux d'échelle lithosphérique, dont les effets étaient déjà documentés pour le Jurassique et le Cénozoïque.

Les zones 1 à 3, principalement au NE du CECLLA à l'amont du collapse, sont constituées de nappes et de radeaux calcaires souvent très plissés, flottant dans un mélange de matériaux généralement rougeâtres provenant en grande partie du remaniement de la Formation Murco et, dans une moindre proportion, de la Formation Arcurquina. Ces matériaux constituent eux-mêmes une brèche, avec des clastes carbonatés et siliciclastiques de toutes tailles flottant dans une matrice pélitique quartzo-marneuse. De grands blocs rigides (plusieurs dizaines de mètres d'épaisseur et centaines de mètres de long), dérivés de formations plus anciennes et lithifiés au moment du collapse, se rencontrent également dans le mélange, notamment au voisinage du SFUACC. Le déplacement des radeaux calcaires et des blocs lithifiés des formations antérieures a été facilité par une semelle de glissement constituée de matériaux resédimentés enclins à se liquifier et à se déformer plastiquement. Cette partie du collapse se caractérise également par une fragmentation progressive et croissante des masses calcaires de l'amont (au nord-est) vers l'aval (au sud-ouest), et par des déformations et des faciès bréchiques quelle que soit l'échelle d'observation, permettant de définir la Formation Ayabacas dans sa partie amont comme une brèche multi-échelle ou "fractale".

Un contraste majeur, qui coïncide approximativement avec la position du CECLLA, existe entre ces zones amont et les parties aval du collapse. Ainsi, les matériaux pélitiques rougeâtres provenant du remaniement de la Formation Murco disparaissent dans les zones 4 et 5, constituées d'un empilement de radeaux et de nappes calcaires, partiellement bréchifiés, dont la taille et la continuité vont croissant vers l'aval. Cette organisation croissante est interprétée comme une conséquence de la disparition de la semelle de glissement dans ces zones.

Enfin la Zone 6 peut être subdivisée en deux parties. Au sud (région de Yura), de grands plis gravitaires affectent toute la pile sédimentaire carbonatée, dont seul le sommet est affecté par des déstabilisations synsédimentaires. Ces plis sont interprétés comme l'amortissement du collapse, frontalement confiné par un seuil topographique probablement dû à la croissance de l'arc volcanique. Au nord (région de Chalhuanca), seule la partie supérieure de la succession carbonatée est là encore affectée par des déformations synsédimentaires. L'absence de structures de compression similaires à celles de la région de Yura suggère que cette partie du collapse n'a pas été bloquée en aval.

Le collapse Ayabacas est atypique (avec notamment une absence de dépôts turbiditiques) et s'est produit dans des conditions environnementales différentes de celles des grands glissements fossiles ou actuels : il a en effet lieu au niveau d'une plate-forme carbonatée de

bassin d'arrière-arc, avec une tranche d'eau peu profonde, et un faible taux de sédimentation. Les marges instables se caractérisent classiquement par une succession de glissements séparés par des dépôts régulièrement stratifiés, tandis que la Formation Ayabacas correspond à la déstabilisation en une seule fois de toute une partie des matériaux d'une marge à priori stable. La singularité de ce collapse résulte de son origine, elle aussi atypique.

Le collapse Ayabacas a en effet immédiatement précédé la continentalisation rapide du bassin d'arrière-arc du sud Pérou, qui depuis longtemps est interprétée comme marquant l'amorce de l'orogenèse andine. Il n'est en fait qu'une des conséquences d'une considérable anomalie thermique affectant la cellule mantellique Pacifique à partir de ~91 Ma. Entre ~91 et 70 Ma cette anomalie thermique a accéléré la convection dans la cellule pacifique, modifiant brusquement les conditions de la subduction et amorçant une production de croûte juvénile le long de l'arc péruvien. L'augmentation rapide du couplage des plaques et l'accélération du plongement de la plaque subductée ont provoqué une flexure brusque et transitoire de la lithosphère continentale dans l'arrière-arc. Le substratum de la Formation Ayabacas a ainsi été découpé en blocs basculés par des failles normales, qui s'observent bien dans la partie supérieure du collapse (zones 1 à 3). Cette tectonique extensive locale en position d'extrados de la flexure lithosphérique, contemporaine des derniers dépôts de la plate-forme carbonatée, a créé des pentes favorables aux glissements et a été le principal élément déclencheur du collapse sous-marin géant. Les transferts massifs de matériaux mantelliques dans l'arc ont par ailleurs causé sa croissance, entraînant un épaississement significatif de sa croûte, un soulèvement de sa surface, puis le dépôt, dans un bassin à la polarité inversée, des matériaux détritiques rouges produits par son altération et son érosion, et caractéristiques de la succession post-Ayabacas.

A l'issue de cette thèse, la Formation Ayabacas a été définie comme résultant de plusieurs glissements en masses sous-marins. Le corps glissé a été décrit morphologiquement et cette étude ouvre plusieurs perspectives :

- Le glissement de grandes masses cohésives, voire lithifiées, a été facilité par une semelle de glissement constituée de matériaux ductiles, facilement déformables. Notamment, il est remarquable que les matériaux silicoclastique de la Formation Murco aient pu être remobilisés et liquifiés plusieurs millions d'années après leur dépôt. Il reste cependant à mieux définir les propriétés de ces matériaux facilitant le glissement : quelle est l'influence des proportions grès/calcaire/argile sur le potentiel de liquification, remobilisation et/ou

déformation plastique ? Quelle est l'influence des fluides ? Comment interagissent-ils avec les matériaux ?

- Les glissements sur les marges passives et actives ou à l'embouchure des grands fleuves sont aujourd'hui classiques, au contraire du glissement Ayabacas qui semble atypique. Dans le cas du collapse Ayabacas, nous avons remarqué qu'il existe un lien chronologique manifeste entre occurrence du glissement sous-marin et modification des conditions de la subduction, voire même changements géodynamiques globaux (réchauffement du manteau et passage à l'échelle du globe d'un régime à dominante extensive à un régime à dominante compressive, variations climatiques à l'échelle du globe). Cette étude semble donc indiquer qu'il existe une relation entre périodes favorables aux glissements sous-marins et processus de géodynamique interne et externe. Un développement intéressant serait de vérifier quelles sont les périodes durant lesquelles se produisent le plus de glissements sous-marins (Crétacé moyen ? Eocène inférieur ? Miocène supérieur ? actuel ?) et s'il est possible de relier ces périodes avec des changements géodynamiques et/ou climatiques.

- Cette genèse des glissements à partir de modifications des modalités de la subduction ou même de changements plus globaux pose le problème de la continuité vers le nord du collapse. Qu'est ce qui explique que le collapse soit majeur dans le sud du Pérou et semble, d'après la littérature, beaucoup moins marqué dans le nord du Pérou et en Equateur. La poursuite de cette étude vers le nord ainsi qu'une étude comparative des deux parties de cette marge pourraient permettre de mieux juger de l'organisation des structures sur toute la marge et de mieux apprécier si cette instabilité est liée à un événement global, régional, ou à un comportement particulier de certains matériaux.

VI.

BIBLIOGRAPHIE

VI. Bibliographie

ABDALLAH, H., SASSI, S., MEISTER, C. & SOUISSI, R. (2000) Stratigraphie séquentielle et paléogéographie à la limite Cénomanien-Turonien dans la région de Gafsa-Chotts (Tunisie centrale). Cretaceous Research, 21, 35-106.

ADAMS, C.E. & ROBERTS, H.H. (1993) A model of the effects of sedimentation rate on the stability of Mississippi Delta sediments. Geo-Marine Letters, 13, 17-23.

ALLEN, J.R.L. (1982) Sedimentary structures: Their Character and Physical Basis, Vol. II., Elsevier, Amsterdam, 663 p.

ALONSO, J.L., MARCOS, A. & SUAREZ, A. (2006) Structure and organization of the Porma Melange: progressive denudation of a submarine nappe toe by gravitational collapse. American Journal of Science, 306, 32-65.

ATHERTON, M.P. (1990) The coastal batholith of Peru: The product of rapid recycling of "new" crust formed within rifted continental margin. Geological Journal, 25, 337-349.

ATHERTON, M.P. & WEBB, S. (1989) Volcanic facies, structure, and geochemistry of the marginal basin rocks of central Peru. Journal of South American Earth Sciences, 2, 241-261.

ATHERTON, M.P. & AGUIRRE, L. (1992) Thermal and geotectonic setting of Cretaceous volcanic rocks near Ica, Peru, in relation to Andean crustal thinning. Journal of South American Earth Sciences, 5, 47-69.

AUDEBAUD, E. (1967) Etude géologique de la région de Sicuani et Ocongate (Cordillère Orientale du Sud Péruvien). Thèse de 3ème cycle, Université de Grenoble, 60 p.

AUDEBAUD, E. (1970) Premières observations sur la tectonique tangentielle polyphasée des terrains secondaires de la Cordillère Orientale du Sud-Est péruvien. Comptes Rendus de l'Académie des Sciences, série D, 270, 3190-3193.

AUDEBAUD, E. (1971a) Mise au point sur la stratigraphie et la tectonique des calcaires Cénomaniens du Sud-Est péruvien (formation Ayavacas). Comptes rendus de l'Académie des Sciences, série D, 272, 1059-1062.

AUDEBAUD, E. (1971b) Photogéologie de reconnaissance et difficultés d'interprétation dans une zone à structure complexe (Cordillère Orientale du Sud du Pérou : hameau Hanchipacha, nord de Sicuani). Photo-interprétation, 5, fascicule 3, Technip, Paris, 15-21.

AUDEBAUD, E. & LAUBACHER, G. (1969) Présence du Tertiaire plissé (groupe Puno) dans la Cordillère Orientale du sud du Pérou. Comptes rendus de l'Académie des Sciences, série D, 269, 2301-2304.

AUDEBAUD, E. & DEBELMAS, J. (1971) Tectonique polyphasée et morphotectonique des terrains Crétacés dans la Cordillère Orientale du Sud péruvien. Etude d'une structure caractéristique. Cahiers ORSTOM, série Géologie, 3, 59-66.

AUDEBAUD, E., CAPDEVILA, R., DALMAYRAC, B., DEBELMAS, J., LAUBACHER, G., LEFEVRE, C., MAROCCO, R., MARTINEZ, C., MATTAUER, M., MEGARD, F., PAREDES, J. & TOMASI, P. (1973) Les traits géologiques essentiels des Andes Centrales (Pérou-Bolivie). Revue de géographie physique et de géologie dynamique, 15, 73-114.

AUDEBAUD, E., LAUBACHER, G. & MAROCCO, R. (1976) Coupe géologique des Andes du Sud du Pérou de l'Océan Pacifique au bouclier brésilien. Geologische Rundschau, 65, 223-264.

BARKER, S.P., HAUGHTON, P.D.W., McCAFFREY, W.D., ARCHER, S.G. & HAKES, B. (2008) Development of rheological heterogeneity in clay-rich high-density turbidity currents: Aptian Britannia Sandstone Member, U.K. continental shelf. Journal of Sedimentary Research, 78, 45-68.

BARLEY, B. (1999) Deepwater problems around the world. The Leading Edge, 18, 488-494.

BARNES, E.M. & LEWIS, K.B. (1991) Sheet slides and rotational failures on a convergent margin: the Kidnappers Slide, New Zealand. Sedimentology, 38, 205-221.

BARTETZKO, A. & KOPF, A.J. (2007) The relationship of undrained shear strength and porosity with depth in shallow (<50 m) marine sediments. Sedimentary Geology, 196, 235-249.

BATHURST, R.G.C. (1971) Carbonate sediments and their diagenesis. Developments in Sedimentology, vol. 12, Elsevier, Amsterdam, 620 p.

BEA, R.G. (1971) How sea floor slides affect offshore structures. Oil Gas Journal, 69, 88-92.

BENAVIDES-CÁCERES, V. (1956) Cretaceous system in northern Peru. Bulletin of the American Museum of Natural History, 108, 353-494.

BENAVIDES-CÁCERES, V. (1962) Estratigrafía pre-Terciaria de la región de Arequipa. Boletín de la Sociedad Geológica del Perú, 38, 5-45.

BJERRUM, L. (1971) Subaqueous slope failures in Norwegian fjords. Norwegian Geotechnical Institute Publication, 88, 1-8.

BOHANNON, R.G. & GARDNER, J.V. (2004) Submarine landslides of San Pedro Escarpment, southwest of Long Beach, California. Marine Geology, 203, 261-268.

BOIT, B. (1926) Dos Neolobites. Boletín de la Sociedad Geológica del Perú, 2, 39-40.

BOND, R.M.G. & MCCLAY, K.R. (1995) Inversion of a Lower Cretaceous extensional basin, south central Pyrenees, Spain. *In*: J.G. Buchanan & P.G. Buchanan (Eds.) Basin Inversion. Geological Society, London, Special Publications, 88, 415-431.

BRANISA, L. (1968) Hallazgo del amonite *Neolobites* en la Caliza Miraflores y de huellas de dinosaurios en la Formación El Molino y su significado para la determinación de la edad del "Grupo Puca". Boletín del Instituto Boliviano del Petróleo, 8, 16-28.

BRUN, J.-P. & FORT, X. (2004) Compressional salt tectonics (Angolan margin). Tectonophysics, 382, 129-150.

BRYANT, W.R., DEFLACKE, A.P. & TRABANT, P.K. (1974) Consolidation of marine clays and carbonates. *In*: Deep Sea Sediments; Physical and Mechanical Properties; Determination of Mechanical Properties in Marine Sediments. Marine Science, 2, 209-244, Plenum, New-York.

von BUCH, L. (1839) Pétrifications recueillies en Amérique par M. Alexandre de Humboldt et par M. Charles Degenhardt. Imprimerie de l'Académie Royale des Sciences, Berlin, 22 p.

BÜNZ, S., MIENERT, J., BRYN, P. & BERG, K. (2005) Fluid flow impact on slope failure from 3D seismic data: a case study in the Storegga Slide. Basin Research, 17, 109-122.

BURG, J.-P., BERNOULLI, D., SMIT, J., DOLATI, A. & BAHROUDI, A. (2008) A giant catastrophic mud-and-debris flow in the Miocene Makran. Terra Nova, 20, 188-193.

CABRERA LA ROSA, A. & PETERSEN, G. (1936) Reconocimiento geológico de los Yacimientos Petrolíferos del Departamento de Puno. Boletín del Cuerpo de Ingenieros de Minas del Perú, 115, 100 p.

CALLOT, P., SEMPERE, T., ODONNE, F. & ROBERT, E. (2007) The Mid-Cretaceous carbonate platform of southern Peru collapsed at the Turonian-Coniacian transition. 4th European Meeting on the Palaeontology and Stratigraphy of Latin America (EMPSLA). Cuadernos del Museo Geominero, Instituto Geológico y Minero de España, Madrid, 8, 75-80.

CALLOT, P., SEMPERE, T., ODONNE, F. & ROBERT, E. (2008) Giant submarine collapse of a carbonate platform at the Turonian-Coniacian transition: The Ayabacas Formation, southern Peru. Basin Research, sous presse.

CALLOT, P., ODONNE, F., DEBROAS, E.-J., MAILLARD, A., DHONT, D., BASILE, C. & HOAREAU, G. 3D Architecture of submarine slide surfaces and associated soft sediment deformation in the Lutetian Sobrarbe deltaic complex (Ainsa, Spanish Pyrenees). Sedimentology, en revision.

CALLOT, P., ODONNE, F. & SEMPERE, T. Causes and consequences of liquification and soft-sediment deformation in a limestone megabreccia: A case study from the Ayabacas giant collapse, southern Peru. Sedimentary Geology, soumis.

CAMERLENGHI, A. & PINI, G.A. (2008) Mud volcanoes, olistostromes and Argille scagliose in the Mediterranean Region. *In*: D. Bernoulli, M.B. Cita & J.A. Mc Kenzie (Eds.) Major Discoveries in Sedimentary Geology in the Mediterranean Realm from a Historical Perspective to New Developments, Special Publication of the International Association of Sedimentologists, 43, 315-350.

CAMPBELL, K.J. (1999) Deepwater geohazards: how significant are they? The Leading Edge, 18, 514-519.

CANALS, M., LASTRAS, G., URGELES, R., CASAMOR, J.L., MIENERT, J., CATTANEO, A., DE BATIST, M., HAFLIDASON, H., IMBO, Y., LABERG, J.S., LOCAT, J., LONG, D., LONGVA, O., MASSON, D.G., SULTAN, N., TRINCARDI, F. & BRYN, P. (2004) Slope failure dynamics and impacts from seafloor and shallow sub-seafloor geophysical data: case studies from the COSTA project. Marine Geology, 213, 9-72.

CARLIER, G., LORAND, J.P., LIÉGEOIS, J.P., FORNARI, M., SOLER, P., CARLOTTO, V., CÁRDENAS, J. (2005) Potassic-ultrapotassic mafic rocks delineate two lithospheric mantle blocks beneath the southern Peruvian Altiplano. Geology, 33, 601-604.

CARLOTTO, V. (2002) Evolution andine et raccourcissement au niveau de Cusco (13-16°S) Pérou. Thèse de Doctorat, Université Joseph Fourier, Grenoble. Géologie Alpine, Mémoire Hors Série, 39, 203 p.

CARLOTTO, V., JAILLARD, E. & MASCLE, G. (1992) Relación entre sedimentación, paleogeografía y tectónica en la región de Cusco (Sur del Perú) entre

el Jurásico Superior-Paleoceno. Boletín de la Sociedad Geológica del Perú, 83, 1-20.

CARLOTTO, V., GIL, W., CÁRDENAS, J. & CHÁVEZ, R. (1996) Geología de los cuadrángulos de Urubamba y Calca hojas 27-r y 27-s. Boletín INGEMMET, 65, serie A, Carta Geológica Nacional, 245 p.

CARMAN, J.E. (1927) The Monroe division of rocks in Ohio. Journal of Geology, 35, 481-506.

CARON, M., ROBASZYNSKI, F., AMEDRO, F., BAUDIN, F., DECONINCK, J.-F., HOCHULI, P.A., VON SALIS-PERCH NIELSEN, K. & TRIBOVILLARD, N. (1999) Estimation de la durée de l'événement anoxique global au passage Cénomanien/Turonien ; approche cyclostratigraphique dans la formation Bahloul en Tunisie centrale. Bulletin de la Société Géologique de France, 170, 145-160.

CARTWRIGHT, J., JAMES, D. & BOLTON, A. (2003) The genesis of polygonal fault systems: a review. *In*: P. Van Rensbergen, R.R. Hillis, A.J. Maltman & C.K. Morley (Eds.), Subsurface Sediment Mobilization. Geological Society, London, Special Publications, 216, 223-243.

CHANOVE, G., MATTAUER, M. & MEGARD, F. (1969) Précisions sur la tectonique tangentielle des terrains secondaires du massif de Pirin (Nord-Ouest du lac Titicaca, Pérou). Comptes Rendus de l'Académie des Sciences, série D, 268, 1698-1701.

CHIOCCI, F. L., MARTORELLI, E. & BOSMAN, A. (2003) Cannibalization of a continental margin by regional scale mass wasting: an example from the central Tyrrhenian Sea. *In*: J. Locat & J. Mienert (Eds.), Submarine Mass Movements and their Consequences. Kluwer Academic Publishers, Dordrecht (Pays-bas), 409-416.

CLAGUE, J.J. (2001) Tsunamis. *In*: G.R. Brooks (Ed.), A Synthesis of Geological Hazards in Canada. Geological Survey of Canada Bulletin, 548, 27-42.

CLARK, A.H., FARRAR, E., KONTAK, D., LANGRIDGE, R.J., ARENAS, M.J., FRANCE, L.J., MCBRIDE, S.L., WOODMAN, P.L., WASTENEYS, H.A., SANDEMAN, H.A., ARCHIBALD, D.A. (1990) Geologic and geochronologic constraints of the metallogenic evolution of the Andes of southeastern Peru. *In*: B.J. Skinner (Ed.) A special issue devoted to the mineral deposits of Peru. Economic Geology and the Bulletin of the Society of Economic Geologists, 85, 1520-1583.

McCLELLAND, W.C. & OLDOW, J.S. (2007) Late Cretaceous truncation of the western Idaho shear zone in the central North American Cordillera. Geology, 35, 723-726.

COCHONAT, P., CADET, J.-P., LALLEMANT, S.J., MAZZOTTI, S., NOUZÉ, H., FOUCHET, C. & FOUCHER, J.-P. (2002) Slope instabilities and gravity processes in fluid migration and tectonically active environment in the eastern Nankai accretionary wedge (KAIKO-Tokai'96 cruise). Marine Geology, 187, 193-202.

COLEMAN, J.M. & PRIOR, D.B. (1988) Mass wasting on continental margins. Annual Review of Earth and Planetary Sciences, 16, 101-119.

COLLINS, W.J. (2003) Slab pull, mantle convection, and Pangaean assembly and dispersal. Earth and Planetary Science Letters, 205, 225-237.

COLLOT, J., LEWIS, K., LAMARCHE, G. & LALLEMAND S. (2001) The giant Ruatoria debris avalanche on the northern Hikurangi margin, New Zealand: Result of oblique seamount subduction. Journal of Geophysical Research, 106, 19271-19298.

COOKE, C.W. (1949) Two Cretaceous echinoids from Peru. Journal of Paleontology, 23, 84-86.

COQUAND, H. (1869) Monographie du genre Ostrea. Terrain crétacé. H. Seven Ed., Marseille, France, 215 p.

COSGROVE, J.W. (1995) The expression of hydraulic fracturing in rocks and sediments. *In*: M.S. Ameen (Ed.), Fractography: fracture topography as a tool in fracture mechanics and stress analysis. Geological Society of London, Special Publications, 92, 187-196.

COUSSOT, P. & MEUNIER, M. (1996) Recognition, classification and mechanical description of debris flows. Earth-Science Reviews, 40, 209-227.

CRUZ, M. (2002) Estratigrafía y evolución tectono-sedimentaria de los depósitos sin-orogénicos del cuadrángulo de Huambo: Las formaciones Ashua y Huanca, departamento de Arequipa. Tesis de la Universidad Nacional San Agustín de Arequipa, 127 p.

DAPPLES, E.C. (1967) Diagenesis of sandstones. *In*: G. Larsen & G.V. Chilingar (Eds.) Diagenesis in sediments. Developments in Sedimentology, vol. 8. Elsevier, Amsterdam, 91-125.

DE BLASIO, F.V., ELVERHØI, A., ISSLER, D., HARBITZ, C.B., BRYN, P., LIEN, R. (2004) Flow models of natural debris flows originating from overconsolidated clay materials. Marine Geology, 213, 439-455.

DE JONG, K.A. (1974) Melange (Olistostrome) near Lago Titicaca, Peru. AAPG Bulletin, 58, 729-741.

DEMERCIAN, S., SZATMARI, P. & COBBOLD, P.R. (1993) Style and pattern of salt diapirs due to thin-skinned gravitational gliding, Campos and Santos basins, offshore Brazil. Tectonophysics, 228, 393-433.

DICKENS, G.R. (2003) Rethinking the global carbon cycle with a large, dynamic and microbially mediated gas hydrate capacitor. Earth & Planetary Science Letters, 213, 169-183.

DICKENS, G.R., CASTILLO, M.M. & WALKER, J.C.G. (1997) A blast of gas in the latest Paleocene: simulating first-order effects of massive dissociation of oceanic methane hydrate. Geology, 25, 259-262.

DINGLE, R.V. (1977) The anatomy of a large submarine slump on a sheared continental margin (SE Africa). Journal of the Geological Society of London, 134, 293-310.

DINGLE, R.V. (1980) Sedimentary basins on the continental margins of southern Africa ; an assessment of their hydrocarbon potential, Erdöl Kohle Erdgas Petrochem., 33 (10), 447-463.

DIXON, R.J., SCHOFIELD, K., ANDERTON, R., REYNOLDS, A.D., ALEXANDER, R.W.S., WILLIAMS, M.C. & DAVIES, K.G. (1995) Sandstone diapirism and clastic intrusion in the Tertiary fans of the Bruce-Beryl Embayment, Quadrant 9, UKCS. Geological Society of London, Special Publications, 94, 77-94.

DORBATH, C., GRANET, M., POUPINET, G. & MARTINEZ, C. (1993) A teleseismic study of the Altiplano and the Eastern Cordillera in northern Bolivia: New constraints on a lithospheric model. Journal of Geophysical Research, 98, 9825-9844.

DOUVILLÉ, H. (1890) Sur la classification des Cératites de la Craie. Bulletin de la Société Géologique de France, série 3, 18, 275-292.

DRZEWIECKI, P.A. & SIMÓ, J.A. (2002) Depositional processes, triggering mechanisms and sediment composition of carbonate gravity flow deposits: examples from the Late Cretaceous of the south-central Pyrenees, Spain. Sedimentary Geology, 146, 155-189.

ELLISON, R.A., KLINCK, B.A. & HAWKINS, M.P. (1989) Deformation events in Andean orogenic cycle in the Altiplano and Western Cordillera, southern Peru. Journal of South American Earth Sciences, 2, 263-276.

ENGLAND, P., ENGDAHL, R. & THATCHER, W. (2004) Systematic variations in the depths of slabs beneath arc volcanoes. Geophysical Journal International, 156, 377-408.

EVANS, S.G. (2001) Landslides. *In*: G.R. Brooks (Ed.), A Synthesis of Geological Hazards in Canada, Geological Survey of Canada Bulletin, 548, 43-79.

EVANS, D., HARRISON, Z., SHANNON, P.M., LABERG, J.S., NIELSEN, T., AYERS, S., HOLMES, R., HOULT, R.J., LINDBERG, B., HAFLIDASON, H., LONG, D., KUIJPERS, A., ANDERSEN, E.S. & BRYN, P. (2005) Palaeoslides and other mass failures of Pliocene to Pleistocene age along the Atlantic continental margin of NW Europe. Marine and Petroleum Geology, 22, 1131-1148.

EVERNDEN, J.F., KRIZ, S. & CHERRONI, C. (1977) Potassium-argon ages of some Bolivian rocks. Economic Geology, 72, 1042-1061.

EYLES, N. & JANUSZCZAK, N. (2007) Syntectonic subaqueous mass flows of the Neoproterozoic Otavi Group, Namibia: where is the evidence of global glaciation? Basin Research, 19, 179-188.

FALIVENE, O., ARBUÉS, P., HOWELL, J., MUÑOZ, J.A., FERNÁNDEZ, O. & MARZO, M. (2006) Hierarchical geocellular facies modelling of a turbidite reservoir analogue from the Eocene of the Ainsa basin, NE Spain. Marine and Petroleum Geology, 23, 679-701.

FERNÁNDEZ, O., MUÑOZ, J.A., ARBUÉS, P., FALIVENE, O. & MARZO, M. (2004) Three-dimensional reconstruction of geological surfaces: An example of growth strata and turbidite systems from the Ainsa basin (Pyrenees, Spain). AAPG Bulletin, 88, 1049-1068.

FINE, I.V., RABINOVICH, A.B., BORNHOLD, B.D., THOMSON, R.E. & KULIKOV, E.A. (2005) The Grand Banks landslide-generated tsunami of November 18, 1929: preliminary analysis and numerical modelling. Marine Geology, 215, 45-57.

FISHER, R.V. (1983) Flow transformations in sediment gravity flows. Geology, 11, 273-274.

FLOQUET, M. & HENNUY, J. (2003) Evolutionary gravity flow deposits in the Middle Turonian – Early Coniacian southern Provence Basin (SE France): origins and depositional processes. *In*: J. Locat & J. Mienert (Eds.), Submarine Mass Movements and their Consequences. Kluwer Academic Publishers, Dordrecht (Pays-bas), 417-424.

FREY-MARTÍNEZ, J., CARTWRIGHT, J. & HALL, B. (2005) 3D seismic interpretation of slump complexes: examples from the continental margin of Israel. Basin Research, 17, 83-108.

FREY-MARTÍNEZ, J., CARTWRIGHT, J. & JAMES, D. (2006) Frontally confined versus frontally emergent submarine landslides: A 3D seismic

characterisation. Marine and Petroleum Geology, 23, 585-604.

FRIÈS, G. & PARIZE, O. (2003) Anatomy of ancient passive margin slope systems: Aptian gravity-driven deposition on the Vocontian palaeomargin, western Alps, south-east France. Sedimentology, 50, 1231-1270.

GARDNER, J.V., PRIOR, D.B. & FIELD, M.E. (1999) Humboldt Slide - a large shear-dominated retrogressive slope failure. Marine Geology, 154, 323-338.

GAWTHORPE, R.L. & CLEMMEY, H. (1985) Geometry of submarine slides in the Bowland Basin (Dinantian) and their relation to debris flows. Journal of the Geological Society of London, 142, 555-565.

GEE, M.J.R., MASSON, D.G, WATTS, A.B. & ALLEN, P.A. (1999) The Saharan debris flow: an insight into the mechanics of long runout submarine debris flows. Sedimentology, 46, 317-335.

GEE, M.J.R., UY, H.S., WARREN, J., MORLEY, C.K. & LAMBIASE, J.J. (2007) The Brunei slide: A giant submarine landslide on the North West Borneo Margin revealed by 3D seismic data. Marine Geology, 246, 9-23.

GENNESSEAUX, M., MAUFFRET, A. & PAUTOT, G. (1980) Les glissements sous-marins de la pente continentale niçoise et la rupture de câbles en mer Ligure (Méditerranée Occidentale). Comptes Rendus de l'Académie des Sciences, Paris, 290, 959-962.

GEORGE, A.D., PLAYFORD, P.E., POWELL, C.McA. (1995) Platform-margin collapse during Famennian reef evolution, Canning Basin, Western Australia. Geology, 23, 691-694.

GEVERS, T.W. (1931) An ancient tillite in SouthWest Africa. Transcript Geological Society of South Africa, 34, 1-17.

GRÀCIA, E., DAÑOBEITIA, J., VERGÉS, J. & PARSIFAL TEAM (2003) Mapping active faults offshore Portugal (368N–388N): implications for seismic hazard assessment along the southwest Iberian margin. Geology, 31, 83-86.

GRADMANN, S., HÜBSCHER, C., BEN-AVRAHAM, Z., GAJEWSKI, D. & NETZEBAND, G. (2005) Salt tectonics off northern Israel. Marine and Petroleum Geology, 22, 597-611.

GRAF, A.A. (2002) Le Cénomanien supérieur en Bolivie: Etude sédimentologique et stratigraphique de la Formation Matilde-Miraflores. Travail de diplôme, Université de Fribourg, Suisse.

GRAF, A.A., STRASSER, A. & CARON, M. (2003) OAE-2 equivalent (Upper Cenomanian) recorded in Bolivian shallow-water sediments. Abstract 11th Swiss Sed. Meeting, Fribourg, 39-40.

GRAZIANO, R. (2001) The Cretaceous megabreccias of the Gargano Promontory (Apulia, southern Italy): their stratigraphic and genetic meaning in the evolutionary framework of the Apulia Carbonate Platform. Terra Nova, 13, 110-116.

GREEN, A. & WERNICKE, B. (1986) Possible large-magnitude Neogene extension on the southern Peruvian Altiplano: Implications for the dynamics of mountain building. Eos Trans. AGU, 67 (44), Jt. Assem. Suppl., Abstract T52C-02.

HAFLIDASON, H., SEJRUP, H.P., NYGÅRD, A., MIENERT, J., BRYN, P., LIEN, R., FORSBERG, C.F., BERG, K. & MASSON, D. (2004) The Storegga Slide: architecture, geometry and slide-development. Marine Geology, 213, 201-234.

HAFLIDASON, H., LIEN, R., SEJRUP, H.P., FORSBERG, C.F. & BRYN, P. (2005) The dating and morphometry of the Storegga Slide. Marine and Petroleum Geology, 22, 123-136.

HALLEY, R.B., HARRIS, P.M., HINE, A.C. (1983). Bank margin environments. *In*: P.A. Scholle, D.G. Bebout & C.H. Moore (Eds.) Carbonate Depositional Environments. American Association of Petroleum Geologists Memoir, 33, 463-506.

HALLWORTH, M.A., PHILLIPS, J.C., HUPPERT, H.E. & SPARKS, R.S.J. (1993) Entrainment in turbulent gravity currents. Nature, 362, 829-831.

HAMAOUI, M. (1965) Type Sections of Cretaceous Formations in the Jerusalem - Bet-Shemesh Area. II. Biostratigraphy. Geological Survey of Israel, Stratigraphic Section, 1, 27-39.

HAMPTON, M.A., LEE, H.J. & LOCAT, J. (1996) Submarine landslides. Reviews of Geophysics, 34, 33-59.

HARDENBOL, J., THIERRY, J., FARLEY, M.B., JACQUIN, T., DE GRACIANSKY, P.-C. & VAIL, P.R. (1998) Mesozoic and Cenozoic sequence chronostratigraphic framework of European basins, chart 1. *In*: P.-C. de Graciansky, J. Hardenbol, T. Jacquin & P.R. Vail (Eds.) Mesozoic and Cenozoic sequence stratigraphy of European basins. SEPM Special Publication, 60, 363-364.

HEEZEN, B.C. & EWING, M. (1952) Turbidity currents and submarine slumps and the 1929 Grand Banks earthquake. Am. J. Sci. 250, 849-873.

HEEZEN, B.C., ERICSON, D.B. & EWING, M. (1954) Further evidence for turbidity current

following the 1929 Grand Banks earthquake. Deep Sea Res. 1, 193-202.

HEIM, A. (1947) Estudios tectónicos en la región del campo petrolífero de Pirín, lado NW del Lago Titicaca. Boletín Oficial de la Dirección de Minas y Petróleo (Ministerio de Fomento), Año XXVI, 79, 47 p.

HENRICH, R., HANEBUTH, T.J.J., KRASTEL, S., NEUBERT, N. & WYNN, R.B. (2008) Architecture and sediment dynamics of the Mauritania Slide Complex. Marine and Petroleum Geology, 25, 17-33.

HILBRECHT, H. (1989) Redeposition of late Cretaceous pelagic sediments controlled by sea-level fluctuations. Geology, 17, 1072-1075.

HINE, A.C., LOCKER, S.D., TEDESCO, L.P., MULLINS, H.T., HALLOCK, P., BELKNAP, D.F., GONZALES, J.L., NEUMANN, A.C., SNYDER, S.W. (1992) Megabreccia shedding from modern, low-relief carbonate platforms, Nicaraguan Rise. Geological Society of America Bulletin, 104, 928-943.

HOFFMAN, P.F. & HARTZ, E.H. (1999) Large, coherent, submarine landslide associated with Pan-African foreland flexure. Geology, 27, 687-690.

HOFFMAN, P.F. & SCHRAG, D.P. (2002) The Snowball Earth hypothesis: testing the limits of global change. Terra Nova, 14, 129-155.

HOFFMAN, P.F., KAUFMAN, A.J., HALVERSON, G.P. & SCHRAG, D.P. (1998) A Neoproterozoic snowball Earth. Science, 281, 1342-1346.

HOSTTAS, J. (1967) Estudio geológico del túnel terminal entre Huambo y Querque. Tesis de la Universidad Nacional San Agustín de Arequipa, 107 p.

HÜNERBACH, V., MASSON, D., et al. (2004) Landslides in the North Atlantic and its adjacent seas: an analysis of their morphology, setting and behaviour. Marine Geology, 213, 343-362.

HUVENNE, V.A.I., CROKER, P.F. & HENRIET, J.P. (2002) A refreshing 3D view of an ancient collapse and slope failure. Terra Nova, 14, 33-40.

HYATT, A. (1903) Pseudoceratites of the Cretaceous. Monographs of the United States Geological Survey, 44, 352 p.

IVERSON, R.M., REID, M.E. & LAHUSEN, R.G. (1997) Debris flow mobilization from landslides. Annual Review of Earth and Planetary Sciences, 25, 85-138.

JAILLARD, E. (1986) La sédimentation crétacée dans les Andes du Pérou central: exemple de la formation Jumasha (Albien moyen-supérieur à Turonien supérieur) dans la région d'Oyón (Département de Lima). Géodynamique, l, 97-108.

JAILLARD, E. (1987) Sedimentary evolution of an active margin during middle and Upper Cretaceous times: the north Peruvian margin from late Aptian up to Senonian. International Journal of Earth Sciences (Geologische Rundschau), 76, 677-697.

JAILLARD, E. (1990) Evolución de la margen andina en el norte del Perú desde el Aptiano superior hasta el Senoniano. Boletín de la Sociedad Geológica del Perú, 81, 3-13.

JAILLARD, E. (1992) La fase peruana (Cretáceo superior) en la margen peruana. Boletín de la Sociedad Geológica del Perú, 83, 81-87.

JAILLARD, E. (1994) Kimmeridgian to Paleocene tectonic and geodynamic evolution of the Peruvian (and Ecuadorian) margin. *In*: J.A. Salfity (Ed.), Cretaceous tectonics of the Andes. Earth Evolution Sciences Monograph Series, Vieweg Publications, Wiesbaden, Allemagne, 101-167.

JAILLARD, E. (1995) La sedimentación Albiana – Turoniana en el Sur del Perú (Arequipa – Puno – Putina). Sociedad Geológica del Perú, Volumen Jubilar Alberto Benavides, 135-157.

JAILLARD, E. & SEMPERE, T. (1991) Las secuencias sedimentarias de la Formación Miraflores y su significado cronoestratigráfico. Revista técnica de YPFB, 12, 257-264.

JAILLARD, E. & ARNAUD-VANNEAU, A. (1993) The Cenomanian – Turonian transition on the Peruvian margin. Cretaceous Research, 14, 585-605.

JAILLARD, E. & SOLER, P. (1996) Cretaceous to early Paleogene tectonic evolution of the northern Central Andes (0-18°S) and its relations to geodynamics. Tectonophysics, 259, 41-53.

JAILLARD, E., CAPPETTA, H., ELLENBERGER, P., FEIST, M., GRAMBAST-FESSARD, N., LEFRANC, J.-P. & SIGE, B. (1993) The Late Cretaceous Vilquechico Group of southern Peru. Sedimentology, paleontology, biostratigraphy, correlations. Cretaceous Research, 14, 623-661.

JAILLARD, E., SEMPERE, T., SOLER, P., CARLIER, G. & MAROCCO, R. (1995) The role of Tethys in the evolution of the northern Andes between Late Permian and Late Eocene times. *In*: A.E.M. Nairn, L.-E. Ricou, B. Vrielynck & J. Dercourt (Eds.) The Ocean Basins and Margins, Volume 8: The Tethys Ocean. Plenum Press, New York, 463-492.

JAILLARD, E., BENGTSON, P. & DHONDT, A.V. (2005) Late Cretaceous marine transgressions in Ecuador and northern Peru: A refined stratigraphic framework. Journal of South American Earth Sciences, 19, 307-323.

JAMES, D.E., (1971) Plate tectonic model for the evolution of the Central Andes. Geological Society of America Bulletin, 82, 3325-3346.

JAMES, D.E. & SACKS, I.S. (1999) Cenozoic formation of the Central Andes: A geophysical perspective. *In*: B.J. Skinner (Ed.), Geology and Ore Deposits of the Central Andes. Society of Economic Geologists Special Publication, 7, 1-25.

JARVIS, I., GALE, A.S., JENKYNS, H.C. & PEARCE, M.A. (2006) Secular variation in Late Cretaceous carbon isotopes: a new δ13C carbonate reference curve for the Cenomanian–Campanian (99.6–70.6 Ma). Geological Magazine, 143, 561-608.

JOHNSON, R.L. (1974) Geology and environmental interpretation of the Upper Cayugan Bass Islands dolomite, Southeastern Michigan. Unpublished M.S. thesis, Ann Arbor, University of Michigan, USA, 89 p.

KALAFATOVICH, V. (1957) Edad de las calizas de la Formación Yuncaypata, Cuzco. Boletín de la Sociedad Geológica del Perú, 32, 127-139.

KENNEDY, W.J. & JUIGNET, P. (1981) Upper Cenomanian Ammonites from the Environs of Saumur, and the Provenance of the Types of Ammonites vibrayeanus and Ammonites geslinianus. Cretaceous Research, 2, 19-49.

KENTER, J.A.M. (1990) Carbonate platform flanks: slope angle and sediment fabric. Sedimentology, 37, 777-794.

KERR, A.C. & TARNEY, J. (2005) Tectonic evolution of the Caribbean and northwestern South America: The case for accretion of two Late Cretaceous oceanic plateaus. Geology, 33, 269-272.

KESSLER, L.G. & BÉDARD, J.H. (2000) Epiclastic volcanic debrites-evidence of flow transformations between avalanche and debris flow processes, Middle Ordovician, Baie Verte Peninsula, Newfoundland, Canada. Precambrian Research, 101, 135-161.

KLINCK, B.A., ELLISON, R.A. & HAWKINS M.P. (1986) The geology of the Cordillera Occidental and Altiplano west of Lake Titicaca, southern Peru. Preliminary report, INGEMMET, Lima, Peru, 353 p.

KNECHTEL, M.M., RICHARDS, E.F. & RATHBUN, M.V. (1947) Mesozoic fossils of the Peruvian Andes. The John Hopkins University studies in geology, 15, 150 p.

KNELLER, B.C. & BUCKEE, C. (2000) The structure and fluid mechanics of turbidity currents: a review of some recent studies and their geological implications. Sedimentology, 47, 62-94.

KONO, M., FUKAO, Y. & YAMAMOTO, A. (1989) Mountain building in the Central Andes. Journal of Geophysical Research, 94, 3891-3905.

KUENEN, P.H. (1952) Estimated size of the Grand Banks turbidity current. Am. J. Sci., 250, 874-884.

LABERG, J.S. & VORREN, T.O. (2000) The Trænadjupet Slide, offshore Norway – morphology, evacuation and triggering mechanisms. Marine Geology, 171, 95-114.

LAJOIE, J. (1972) Slump fold axis orientations: an indication of paleoslope? Journal of Sedimentary Petrology, 42, 584-586.

LAMB, S. & DAVIS, P. (2003) Cenozoic climate change as a possible cause for the rise of the Andes. Nature, 425, 792-797.

LASTRAS, G., CANALS, M., HUGHES-CLARKE, J.E., MORENO, A., DE BATIST, M., MASSON, D.G. & COCHONAT, P. (2002) Seafloor imagery of the BIG'95 debris flow, Western Mediterranean. Geology, 30, 871-874.

LASTRAS, G., CANALS, M., URGELES, R., DE BATIST, M., CALAFAT, A.M. & CASAMOR, J.L. (2004) Characterization of the recent BIG'95 debris flow deposit after a variety of seismic reflection data, Ebro margin, Western Mediterranean Sea. Marine Geology, 213, 235-255.

LAUBACHER, G. (1978) Géologie des Andes péruviennes : Géologie de la Cordillère Orientale et de l'Altiplano au nord et nord-ouest du lac Titicaca (Pérou). Travaux et Documents de l'ORSTOM, 95, 219 p.

LAUBACHER, G. & MAROCCO, R. (1990) La cuenca cretácica del Altiplano peruano: Litoestratigrafía e interpretación secuencial. Boletín de la Sociedad Geológica del Perú, 81, 33-46.

LAVAL, A., CREMER, M., BEGHIN, P. & RAVENNE, C. (1988) Density surges: two-dimensional experiments. Sedimentology, 35, 73-84.

LEE, S.H. & CHOUGH, S.K. (2001) High-resolution (2–7 kHz) acoustic and geometric characters of submarine creep deposits in the South Korea Plateau, East Sea. Sedimentology, 48, 629-644.

LEWIS, K.B. (1971) Slumping on a continental slope inclined at 1-4°. Sedimentology, 16, 97-110.

LISSÓN, C. (1908) Contribución al conocimiento sobre algunos ammonites del Perú. 4th Congreso Científico Latino-Americano, Tipografía del Perú, 22 p.

LISSÓN, C. (1924) Edad de los fósiles peruanos y distribución de sus depósitos. 3rd edition, Lima, 226 p.

LISSÓN, C. & BOIT, B. (1942) Edad de los fósiles peruanos y distribución de sus depósitos. 4th edition, Lima, 320 p.

LOCAT, J. & LEE, H.J. (2002) Submarine landslides: advances and challenges. Canadian Geotechnical Journal, 39, 193-212.

LOCAT, J. & MIENERT, J. (Eds.) (2003) Submarine Mass Movements and Their Consequences. Kluwer Academic Publishers., Dordrecth (Pays-bas), 540 p.

LONCKE, L., GAULLIER, V., MASCLE, J., VENDEVILLE, B. & CAMERA, L. (2006) The Nile deep-sea fan: An example of interacting sedimentation, salt tectonics, and inherited subsalt paleotopographic features. Marine and Petroleum Geology, 23, 297-315.

LONGVA, O., JANBU, N., BLIKRA, L.H. & BOE, R. (2003) The 1996 Finneidfjord Slide, seafloor failure and slide dynamics. *In*: J. Locat & J. Mienert (Eds.), Submarine Mass Movements and their Consequences. Kluwer Academic Publishers, Dordrecht (Pays-bas), 531-538.

LOWE, D.R. (1976) Subaqueous liquefied and fluidized sediment flows and their deposits. Sedimentology, 23, 285-308.

LOWE, D.R. (1982) Sediment gravity flows: II. Depositional models with special reference to the deposits of high-density turbidity currents. Journal of Sedimentary Petrology, 52, 279-297.

LUCENTE, C.C. & PINI, G.A. (2003) Anatomy and emplacement mechanism of a large submarine slide within a Miocene foredeep in the Northern Apennines, Italy: a field perspective. American Journal of Science, 303, 565-602.

LUCENTE, C.C. & PINI, G.A. (2008) Basin-wide mass-wasting complexes as markers of the Oligo-Miocene foredeep-accretionary wedge evolution in the Northern Apennines, Italy. Basin Research, 20, 49-71.

MALTMAN, A.J. & BOLTON, A. (2003) How sediments become mobilized. *In*: P. Van Rensbergen, R.R. Hillis, A.J. Maltman & C.K. Morley (Eds.), Subsurface Sediment Mobilization. Geological Society, London, Special Publications, 216, 9-20.

MANDL, G. & CRANS, W. (1981) Gravitational gliding in deltas. *In*: K.R. McClay & N.J. Price (Eds.), Thrust and Nappe Tectonics. Geological Society, London, Special Publications, 9, 41-54.

MANZI, V., LUGLI, S., RICCI LUCCHI, F. & ROVERI, M. (2005) Deep-water clastic evaporites deposition in the Messinian Adriatic foredeep (northern Appenines, Italy): Did the Mediterranean ever dry out? Sedimentology, 52, 875-902.

MARTIN, H. (1965) Observations on the problem of late Precambrian glacial deposits in southwest Africa. Geologische Rundschau, 54, 115-127.

MARTIN, H., PORADA, H. & WALLISER, O.H. (1985) Mixtite deposits of the Damara sequence, Namibia: problem of interpretation. Palaeogeography, Palaeoclimatology, Palaeoecology, 51, 159-196.

MARTINSEN, O.J. (1989) Styles of soft-sediment deformation on a Namurian (Carboniferous) delta slope, western Irish Namurian Basin, Ireland. *In*: M.K.G. Whateley & K.T. Pickering (Eds.) Deltas: Sites and Traps for Fossil Fuels. Geological Society of London, Special Publications, 41, 167-177.

MARTINSEN, O.J. & BAKKEN, B. (1990) Extensional and compressional zones in slumps and slides in the Namurian of County Clare, Ireland. Journal of the Geological Society of London, 147, 153-164.

MASSON, D.G. (2003) Summary of geophysical techniques. *In*: J. Mienert & P. Weaver (Eds.), European Margin Sediment Dynamics, Side-Scan Sonar and Seismic Images. Springer-Verlag, Berlin, 9-16.

MASSON, D.G., WATTS, A.B., GEE, M.J.R., URGELES, R., MITCHELL, N.C., LE BAS, T.P. & CANALS, M. (2002) Slope failures on the flanks of the western Canary Islands. Earth-Science Reviews, 57, 1-35.

MASSON, D. G., HARBITZ, C. B., WYNN, R. B., PEDERSEN, G. & LOVHOLT, F. (2006) Submarine landslides: processes, triggers and hazard prediction. Philosophical Transactions of the Royal Society A, 364, 2009-2039.

McADOO, B.G., PRATSON, L.F. & ORANGE, D.G. (2000) Submarine landslide geomorphology, US continental slope. Marine Geology, 169, 103-136.

McBRIDE, S.L., ROBERTSON, R.C.R., CLARK, A.H. & FARRAR, E. (1983) Magmatic and metallogenetic episodes in the northern tin belt, Cordillera Real, Bolivia. Geologische Rundschau, 72, 685-713.

McCALL, G.J.H. (1983) Mélanges of the Makran, southeastern Iran. *In*: G.J.H. McCall (Ed.), Ophiolitic and Related Mélanges. Benchmark Papers in Geology, 66. Hutchinson Ross Publishing Company, Stroudsburg, PA., 292-299.

McCALL, G.J.H. & KIDD, R.G.W. (1982) The Makran southeastern Iran: the anatomy of a convergent margin active from Cretaceous to present. *In*: J.K. Leggett (Ed.), Trench-Forearc Geology: Sedimentation and Tectonics of Modern and Ancient Plate Margins. Geological Society of London, Special Publications, 10, 387-397.

MEGARD, F. (1978) Etude géologique des Andes du Pérou central. Travaux et Documents de l'ORSTOM, no. 86, Paris.

MICALLEF, A., BERNDT, C., MASSON, D.G. & STOW, D.A.V. (2008) Scale invariant characteristics of the Storegga Slide and implications for large-scale submarine movements. Marine Geology, 247, 46-60.

MIDDLETON, G.V. & SOUTHARD, J.B. (1984) Mechanics of Sediment Transport, 2nd edidtion SEPM, Eastern Section Short Course 3 Providence, 401 p.

MIENERT, J. & POSEWANG, J. (1999) Evidence of shallow- and deep-water gas hydrate destabilizations in North Atlantic polar continental margin sediments. Geo-Marine Letters, 19, 143-149.

MIENERT, J., BERNDT, C., LABERG, J.S. & VORREN, T.O. (2002) Slope Instability of Continental Margins. *In*: G. Wefer, D. Billet, D. Hebbeln, B.B. Jørgensen, M. Schlüter & T. van Veering (Eds.), Ocean Margin Systems. SpringerVerlag, Berlin, pp. 179-193.

MILLIMAN, J.D. & SYVITSKI, J.P.M. (1992) Geomorphic/tectonic control of sediment discharge to the ocean: the importance of small mountainous rivers. Journal of Geology, 100, 525-544.

MINISINI, D., TRINCARDI, F., ASIOLI, A., CANU, M. & FOGLINI, F. (2007) Morphologic variability of exposed mass-transport deposits on the eastern slope of Gela Basin (Sicily channel). Basin Research, 19, 217-240.

MITCHELL, R.N., BICE, D.M., MONTANARI, A., CLEAVELAND, L.C., CHRISTIANSON, K.T., COCCIONI, R. & HINNOV, L.A. (2008) Oceanic anoxic cycles? Orbital prelude to the Bonarelli Level (OAE 2). Earth and Planetary Science Letters, 267, 1-16.

MONTENAT, C., BARRIER, P. & OTT D'ESTEVOU, P. (1991) Some aspects of the recent tectonics in the Strait of Messina, Italy. Tectonophysics, 194, 203-215.

MONTENAT, C., BARRIER, P., OTT D'ESTEVOU, P. & HIBSCH, C. (2007) Seismites: An attempt at critical analysis and classification. Sedimentary Geology, 196, 5-30.

MOORE, A. (1993) Neogene crustal extension in the southern Peruvian Altiplano: Implications for the dynamics of mountain building. Thèse de Doctorat non publiée, Harvard University, Etats-Unis d'Amérique, 279 p.

MOORE, J.G., CLAGUE, D.A., HOLCOMB, R.T., LIPMAN, P.W., NORMARK, W.R., & TORRESAN, M.E. (1989) Prodigious submarine landslides on the Hawaiian Ridge. Journal of Geophysical Research, 94, 17465-17484.

MORETTI, M. & SABATO, L. (2007) Recognition of trigger mechanisms for soft-sediment deformation in the Pleistocene lacustrine deposits of the Sant'Arcangelo Basin (Southern Italy): Seismic shock vs. overloading. Sedimentary Geology, 196, 31-45.

MOSCARDELLI, L. & WOOD, L. (2008) New classification system for mass transport complexes in offshore Trinidad. Basin Research, 20, 73-98.

MOUNTJOY, E.W., COOK, H.E., PRAY, L.C. & McDANIEL, P.N. (1972) Allochthonous carbonate debris flows worldwide indicators of reef complexes, banks or shelf margins. Reports of the 24th International Geological Congress, Montreal 1972, Section 6, 172-189.

MOURGUES, R. & COBBOLD P.R. (2003) Some tectonic consequences of fluid overpressures and seepage forces as demonstrated by sandbox modelling. Tectonophysics, 376, 75-97.

MUKASA, S.B. (1986) Zircon U-Pb ages of super-units in the Coastal batholith, Peru: implications for magmatic and tectonic processes. Geological Society of America Bulletin, 97, 241-254.

MULDER, T. & ALEXANDER, J. (2001) The physical character of subaqueous sedimentary density flows and their deposits. Sedimentology, 48, 269-299.

MULDER, T. & COCHONAT, P. (1996) Classification of offshore mass movements. J. Sed. Res., 66, 43-57.

MULDER, T. & MORAN, K. (1995) Relationship among submarine instabilities, sea-level variations and the presence of an ice sheet on the continental shelf: an example from the Verrill Canyon area, Scotian Shelf. Paleoceanography, 10, 137-154.

MULDER, T., SAVOYE, B. & SYVITSKI, J.P.M. (1997) Numerical modelling of a mid-sized gravity flow: the 1979 Nice turbidity current (dynamics,

processes, sediment budget and seafloor impact). Sedimentology, 44, 305-326.

MÜLLER, G. (1967) Diagenesis in argillaceous sediments. *In*: G. Larsen & G.V. Chilingar (Eds.), Diagenesis in sediments. Developments in Sedimentology, vol. 8, Elsevier, Amsterdam, 127-177.

MULLINS, H.T., & HINE, A.C. (1989) Scalloped bank margins: Beginning of the end for carbonate platforms? Geology, 17, 30-33.

MULLINS, H.T., GARDULSKI, A.F. & HINE, A.C. (1986) Catastrophic collapse of the west Florida carbonate platform margin: Geology, 14, 167-170.

MURTY, T.S. (1977) Seismic sea waves-tsunamis. Bull. Fish. Res. Board Can., 198, 337 pp.

MYERS, J.S. (1974) Cretaceous stratigraphy and structure, western Andes of Peru between latitudes 10° and 10°30'S. AAPG Bulletin, 58, 474-487.

NADIM, F., KVALSTAD, T.J. & GUTTORMSEN, T. (2005) Quantification of risks associated with seabed instability at Ormen Lange. Marine and Petroleum Geology, 22, 311-318.

NARDIN, T.R., HEIN, F.J., GORSLINE, D.S. & EDWARDS, B.D. (1979) A review of mass movement processes, sediment and acoustic characteristics, and contrasts in slope and base-of-slope systems versus canyon-fan-basin floor systems. *In*: L.J. Doyle & O.H. Pilkey (Eds.), Geology of Continental Slopes. SEPM Special Publication, 27, 61-73.

NAYLOR, M.A. (1981) Debris flow (olistostromes) and slumping on a distal passive continental margin: the Palombini limestone-shale sequence of the northern Apennines. Sedimentology, 28, 837-852.

NEWELL, N.D. (1949) Geology of the Lake Titicaca region, Peru and Bolivia. Geological Society of America Memoir, 36, 111 p.

NICHOLS, R.J. (1995) The liquification and remobilization of sandy sediments. *In*: A.J. Hartley & D.J. Prosser (Eds.), Characterization of Deep Marine Clastic Systems. Geological Society of London, Special Publications, 94, 63-76.

NORMARK, W.R., McGANN, M. & SLITER, R. (2004) Age of Palos Verdes submarine debris avalanche, southern California. Marine Geology, 203, 247-259.

OGG, J.G., AGTERBERG, F.P. & GRADSTEIN, F.M. (2004) The Cretaceous Period. *In*: F.M. Gradstein, J.G. Ogg & A.G. Smith (Eds.) A Geologic Time Scale 2004. Cambridge University Press, Cambridge, 344-383.

OLLIER, G., COCHONAT, P., LÉNAT, J.F. & LABAZUY, P. (1998) Deep-sea volcaniclastic sedimentary systems: an example from La Fournaise volcano, Réunion Island, Indian Ocean. Sedimentology, 45, 293-330.

ONASCH, C.M. & KAHLE, C.F. (2002) Seismically induced soft-sediment deformation in some Silurian carbonates, eastern U.S. Midcontinent. *In*: F.R. Ettensohn, N. Rast & C.E. Brett (Eds.), Ancient seismites. Geological Society of America Special Paper, 359, 165-176.

O'NEILL, C., LENARDIC, A., MORESI, L., TORSVIK, T.H. & LEE, C.-T.A. (2007) Episodic Precambrian subduction. Earth and Planetary Science Letters, 262, 552-562.

d'ORBIGNY, A. (1840-42) Paléontologie française: Terrains crétacés. I. Céphalopodes. Masson Ed., Paris, 1-120 (1840), 121-430 (1841), 431-662 (1842).

ORPIN, A.R. (2004) Holocene sediment deposition on the Poverty-slope margin by the muddy Waipaoa River, East Coast New Zealand. Marine Geology, 209, 69-90.

PAYROS, A., PUJALTE, V. & ORUE-ETXEBARRIA, X. (1999) The South Pyrenean Eocene carbonate megabreccias revisited: new interpretation based on evidence from the Pamplona Basin. Sedimentary Geology, 125, 165-194.

PICKERING, K.T. & CORREGIDOR, J. (2005) Mass-transport complexes (MTCs) and tectonic control on basin-floor submarine fans, Middle Eocene, south Spanish Pyrenees. Journal of Sedimentary Research, 75, 761-783.

PINO, A., SEMPERE, T., JACAY, J. & FORNARI, M. (2004) Estratigrafía, paleografía y paleotectónica del intervalo Paleozoico Superior - Cretáceo inferior en el área de Mal Paso - Palca (Tacna). Publicación Especial Sociedad Geológica del Perú, 5, 15-44.

PIPER, D.J.W. & SAVOYE, B. (1993) Processes of late Quaternary turbidity current flow and deposition on the Var deepsea fan, north-west Mediterranean Sea. Sedimentology, 40, 557-583.

PIPER, D.J.W., COCHONAT, P., OLLIER, G., LE DREZEN, E., MORRISON, M. & BALTZER, A. (1992) Evolution progressive d'un glissement rotationnel en un courant de turbidité : cas du séisme de 1929 des Grands Bancs (Terre Neuve). Comptes Rendus de l'Académie des Sciences, série D, 314, 1057-1064.

PIPER, D.J.W., COCHONAT, P. & MORRISON, M.L. (1999) The sequence of events around the epicenter of the 1929 Grand Banks earthquake: initiation of debris flows and turbidity current inferred from sidescan sonar. Sedimentology, 46, 79-97.

PITCHER, W.S., ATHERTON, M.P., COBBING, E.J. & BECKINSALE, R.D. (Eds) (1985) Magmatism at a Plate Edge: the Peruvian Andes. Blackie & Son, Glasgow & London, 328 p.

PLINK-BJÖRKLUND, P. & STEEL, R.J. (2004) Initiation of turbidity currents: outcrop evidence for Eocene hyperpycnal flow turbidites. Sedimentary Geology, 165, 29-52.

POPENOE, P., SCHMUCK, E.A. & DILLON, W.P. (1993) The Cape Fear Landslide; slope failure associated with salt diapirism and gas hydrate decomposition. *In*: W.C. Schwab, H.J. Lee & D.C. Twichell (Eds.), Submarine Landslides; Selected Studies in the U.S. Exclusive Economic Zone. U.S. Geological Survey Bulletin, 40-53.

PORADA, H. & WITTIG, R. (1983) Turbidites and their significance in the geosynclinal evolution of the Damara Orogen, SouthWest Africa/Namibia. *In*: R.McG. Miller (Ed.), Evolution of the Damara Orogen, Geological Society of South Africa, Special Publication, 11, 21-36.

PORTUGAL, J. (1964) Geology of the Puno-Santa Lucia area, Department of Puno, Peru. Thèse de Doctorat non publiée, Université de Cincinnati, Etats-Unis d'Amérique, 141 p.

PORTUGAL, J. (1974) Mesozoic and Cenozoic stratigraphy and tectonic events of Puno-Santa Lucia area, Department of Puno, Peru. AAPG Bulletin, 58, 982-999.

POSTMA, G. (1983) Water escape structures in the context of a depositional model of a mass flow dominated conglomeratic fan-delta (Abrioja Formation, Pliocene, Almeria Basin, Spain). Sedimentology, 30, 91-103.

POSTMA, G. (1986) Classification for sediment gravity-flow deposits based on flow conditions during sedimentation. Geology, 14, 291-294.

PRIOR, D.B. & COLEMAN, J.M. (1978) Disintegrating retrogressive landslides on very-low-angle subaqueous slopes, Mississippi delta. Marine Geotechnology, 3, 37-60.

PRIOR, D.B. & COLEMAN, J.M. (1982) Active slides and flows in underconsolidated marine sediments on the slope of the Mississippi delta. *In*: S. Saxov & J.K. Nieuwenhuis (Eds.), Marine Slides and Other Mass Movements. Plenum Press, New York, 21-49.

PRIOR, D.B. & COLEMAN, J.M. (1984) Submarine slope instability. *In*: D. Brundsen & D.B. Prior (Eds.), Slope Instability. Wiley, Chichester, New York, 419-455.

PRIOR, D.B. & DOYLE, E.H. (1985) Intra-slope canyon morphology and its modification by rockfall processes, U.S. Atlantic continental margin. Marine Geology, 67, 177-196.

PRIOR, D.B., BORNHOLD, B.D. & JOHNS, M.W. (1984) Depositional characteristics of a submarine debris flow. Journal of Geology, 92, 707-727.

RASSMUSS, J.E. (1935) Informe sobre la región petrolífera de Puno. Boletín de la Dirección de Minas y Petróleo del Ministerio de Fomento del Perú, año 15, 45, 85-105.

RITZWOLLER, M.H., SHAPIRO, N.M. & ZHONG, S.-J. (2004) Cooling history of the Pacific lithosphere. Earth and Planetary Science Letters, 226, 69-84.

ROBERT, E. (2002) La transgression albienne dans le Bassin Andin (Pérou) : biostratigraphie, paléontologie et stratigraphie séquentielle. Strata, 38, 380 p.

ROBERT, E., BULOT, L.G., JAILLARD, E. & PEYBERNÈS, B. (2002) Proposition d'une nouvelle biozonation par ammonites de l'Albien du Bassin andin (Pérou). Comptes Rendus Palevol, 1, 1-9.

ROBERT, E., JAILLARD, E., PEYBERNÈS, B. & BULOT, L.G. (2002) La transgresión albiana en la Cuenca Andina (Perú Central - Ecuador): modelo general y diacrónismo de los depósitos marinos. Boletín de la Sociedad Geológica del Perú, 94, 25-30.

RODINE, J.D. & JOHNSON, M.A. (1976) The ability of debris, heavily freighted with coarse clastic materials, to flow on gentle slopes. Sedimentology, 23, 213-234.

ROEMER, C.F. (1849) Mit besonderer Rücksicht auf deutsche Auswanderung und die physischen Verhältnisse des Landes nach eigener Beobachtung geschildert; mit einem naturwissenschaftlichen Anhänge, und einer topographisch-geognostichen Karte von Texas. Bonn, 464 p.

ROPERCH, P., SEMPERE, T., MACEDO, O., ARRIAGADA, C., FORNARI, M., TAPIA, C., GARCÍA, M. & LAJ, C. (2006) Counterclockwise rotation of Late Eocene-Oligocene forearc deposits in southern Peru and its significance for oroclinal bending in the Central Andes. Tectonics, 25, TC3010, doi:10.1029/2005TC001882.

SAGEMAN, B.B., MEYERS, S.R. & ARTHUR, M.A. (2006) Orbital time scale and new C-isotope record for Cenomanian-Turonian boundary stratotype. Geology, 34, 125-128.

SAVOYE, B., COCHONAT, P., APPRIOUAL, R., BAIN, O., BALTZER, A., BELLEC, V., BEUZART, P., BOURILLET, J.-F., CAGNA, R., CREMER, M., CRUSSON, A., DENNIELOU, B., DIEBLER, D., DROZ, L., ENNES, J.-C., FLOCH, G., GUIOMAR, M., HARMEGNIES, F., KERBRAT, R., KLEIN, B., KUHN, H., LANDURE, J.-Y., LASNIER, C., LE DREZEN, E., LE FORMAL, J.-P., LOPEZ, M., LOUBRIEU, B., MARSSET, T., MIGEON, S., NORMAND, A., NOUZE, H., ONDREAS, H., PELLEAU, P., SAGET, P., SERANNE, M., SIBUET, J.-C., TOFANI, R. & VOISSET, M. (2000) Structure et évolution récente de l'éventail turbiditique du Zaïre : premiers résultats scientifiques des missions d'exploration Zaïango 1 & 2 (marge Congo–Angola). Comptes Rendus de l'Académie des Sciences, série II, 331, 211-220.

SEMPERE, T. (1994) Kimmeridgian? to Paleocene tectonic evolution of Bolivia. *In*: J.A. Salfity (Ed.), Cretaceous tectonics in the Andes. Earth Evolution Sciences Monograph Series, Vieweg Publications, Wiesbaden, Allemagne, 168-212.

SEMPERE, T. (1995) Phanerozoic evolution of Bolivia and adjacent regions. *In*: A.J. Tankard, R. Suárez & H.J. Welsink (Eds.), Petroleum Basins of South America. American Association of Petroleum Geologists Memoir, 62, 207-230.

SEMPERE, T. & JACAY, J. (2006) Estructura tectónica del sur del Perú (antearco, arco, y Altiplano suroccidental). Extended abstract, XIII Congreso Peruano de Geología, Lima, 324-327.

SEMPERE, T. & JACAY, J. (2007) Synorogenic extensional tectonics in the forearc, arc and southwest Altiplano of southern Peru. Eos Trans. AGU, 88 (23), Jt. Assem. Suppl., Abstract U51B-04.

SEMPERE, T., BUTLER, R.F., RICHARDS, D.R., MARSHALL, L.G., SHARP, W. & SWISHER III, C.C. (1997) Stratigraphy and chronology of Late Cretaceous - Early Paleogene strata in Bolivia and northwest Argentina. Geological Society of America Bulletin, 109, 709-727.

SEMPERE, T., JACAY, J., CARRILLO, M.-A., GÓMEZ, P., ODONNE, F. & BIRABEN, V. (2000) Características y génesis de la Formación Ayabacas (Departamentos de Puno y Cusco). Boletín de la Sociedad Geológica del Perú, 90, 69-76.

SEMPERE, T., CARLIER, G., SOLER, P., FORNARI, M., CARLOTTO, V., JACAY, J., ARISPE, O., NÉRAUDEAU, D., CARDENAS, J., ROSAS, S. & JIMÉNEZ, N. (2002a) Late permian - middle Jurassic lithospheric thinning in Peru and Bolivia, and its bearing on Andean-age tectonics. Tectonophysics, 345, 153-181.

SEMPERE, T., JACAY, J., FORNARI, M., ROPERCH, P., ACOSTA, H., BEDOYA, C., CERPA, L., FLORES, A., HUSSON, L., IBARRA, I., LATORRE, O., MAMANI, M., MEZA, P., ODONNE, F., OROS, Y., PINO, A., & RODRÍGUEZ, R. (2002b) Lithospheric-scale transcurrent fault systems in Andean southern Peru. Extended abstract, V International Symposium on Andean Geodynamics, Toulouse, 601-604.

SEMPERE, T., ACOSTA, H. & CARLOTTO, V. (2004a) Estratigrafía del Mesozoico y Paleógeno al Norte del Lago Titicaca. Publicación Especial Sociedad Geológica del Perú, 5, 81-103.

SEMPERE, T., JACAY, J., CARLOTTO, V., MARTÍNEZ, W., BEDOYA, C., FORNARI, M., ROPERCH, P., ACOSTA, H., ACOSTA, J., CERPA, L., FLORES, A., IBARRA, I., LATORRE, O., MAMANI, M., MEZA, P., ODONNE, F., ORÓS, Y., PINO, A. & RODRÍGUEZ, R. (2004b) Sistemas transcurrentes de escala litosférica en el Sur del Perú. Publicación Especial Sociedad Geológica del Perú, 5, 105-110.

SEMPERE, T., JACAY, J., PINO, A., BERTRAND, H., CARLOTTO, V., FORNARI, M., GARCÍA, R., JIMÉNEZ, M., MARZOLI, A., MEYER, C.A., ROSAS, S. & SOLER, P. (2004c) Estiramiento litosférico del Paleozoico Superior al Cretáceo Medio en el Perú y Bolivia. Publicación Especial Sociedad Geológica del Perú, 5, 45-79.

SEMPERE, T., FOLGUERA, A. & GERBAULT, M. (2008) New insights into Andean evolution: An introduction to contributions from the 6th ISAG symposium (Barcelona, 2005). Tectonophysics, sous presse, doi: 10.1016/j.tecto.2008.03.011.

SEMPERE, T., CALLOT, P., ODONNE, O., ROBERT, E., JACAY, J., ROUSSE, S. & SAINT-BLANQUAT, M. de. Dramatic onset of Andean orogeny in Peru 90 Myr ago forced by burst of magmatic arc growth. Soumis.

SHAIKH, M.A., MEADOWS, A. & MEADOWS, P.S. (1998) Biological control of avalanching and slope stability in the intertidal zone. *In*: K.S. Black, D.M. Paterson & A. Cramp (Eds.) Sedimentary Processes in the Intertidal Zone. Geological Society of London, Special Publications, 139, 309-329.

SIGÉ, B., SEMPERE, T., BUTLER, R.F., MARSHALL, L.G. & CROCHET, J.-Y. (2004) Age and stratigraphic reassessment of the fossil-bearing Laguna Umayo red mudstone unit, SE Peru, from regional stratigraphy, fossil record, and paleomagnetism. Geobios, 37, 771-794.

SKEMPTON, A.W. & HUTCHINSON, J.N. (1969) Stability of natural slopes and embankment

foundations. State-of-the-Art Report, *in* Proceedings of the 7th International Conference on Soil Mechanics and Foundation Engineering, Mexico City, vol. 2, 291-340.

SOLER, P. & BONHOMME, M. (1990) Relations of magmatic activity to plate dynamics in Central Peru from Late Cretaceous to Present. *In*: S. Kay & C. Rapela (Eds.) Plutonism from Antarctica to Alaska. Geological Society of America Memoir, 241, 173-192.

SOLHEIM, A., BERG, K., FORSBERG, C.F. & BRYN, P. (2005a) The Storegga Slide complex: repetitive large scale sliding with similar cause and development. Marine and Petroleum Geology, 22, 97-107.

SOLHEIM, A., BRYN, P., SEJRUP, H.P., MIENERT, J. & BERG, K. (2005b) Ormen Lange—an integrated study for the safe development of a deep-water gas field within the Storegga Slide Complex, NE Atlantic continental margin; executive summary. Marine and Petroleum Geology, 22, 1-9.

SPARLING, D.R. (1970) The Bass Islands Formation in its type region. Ohio Journal of Sciences, 70, 1-33.

SPATHOPOULOS, F. (1996) An insight on salt tectonics in the Angola Basin, South Atlantic. *In*: G.I. Aslop, D.J. Blundell & I. Davison (Eds.) Salt Tectonics. Geological Society, London, Special Publications, 92, 187-196.

SPENCE, G.H. & TUCKER, M.E. (1997) Genesis of limestone megabreccias and their significance in carbonate sequence stratigraphic models: A review. Sedimentary Geology, 112, 163-193.

SPÖRLI, K.B. & ROWLAND, J.V. (2007) Superposed deformation in turbidites and syn-sedimentary slides of the tectonically active Miocene Waitemata Basin, northern New Zealand. Basin Research, 19, 199-216.

STEEN, Ø. & ANDRESEN, A. (1997) Deformational structures associated with gravitational block gliding: examples from sedimentary olistoliths in the Kalvåg Melange, western Norway. American Journal of Science, 297, 56-97.

STEINMANN, G. (1929) Geologie von Peru. Carl Winter, Heidelberg, 448 p.

STOW, D.A.V. & MAYALL, M. (2000) Deep-water sedimentary systems: New models for the 21st century. Marine and Petroleum Geology, 17, 125-135.

STRACHAN, L.J. (2008) Flow transformations in slumps: a case study from the Waitemata Basin, New Zealand. Sedimentology, in press, doi: 10.1111/j.1365-3091.2007.00947.x

STRACHAN, J.L. & ALSOP, G.I. (2006) Slump folds as estimators of palaeoslope: a case study from the Fisherstreet Slump of County Clare, Ireland. Basin Research, 18, 451-470.

SULTAN, N., COCHONAT, P., CANALS, M., CATTANEO, A., DENNIELOU, B., HAFLIDASON, H., LABERG, J.S., LONG, D., MIENERT, J., TRINCARDI, F., URGELES, R., VORREN, T.O. & WILSON, C. (2004a) Triggering mechanisms of slope instability processes and sediment failures on continental margins: a geotechnical approach. Marine Geology, 213, 29-321.

SULTAN, N., COCHONAT, P., FOUCHER, J.P. & MIENERT, J. (2004b) Effect of gas hydrates melting on seafloor slope instability. Marine Geology, 213, 379-401.

SYVITSKI, J.P.M. (2003) Supply and flux of sediment along hydrological pathways: research for the 21st Century. Global and Planetary Change, 39, 1-11.

TALLING, P.J., WYNN, R.B., MASSON, D.G., FRENZ, M., CRONIN, B.T., SCHIEBEL, R., AKHMETZHANOV, A.M., DALLMEIER-TIESSEN, S., BENETTI, S., WEAVER, P.P.E., GEORGIOPOULOU, A., ZÜHLSDORFF, C. & AMY, L.A. (2007) Onset of submarine debris flow deposition far from original giant landslide. Nature, 450, 541-544.

THORPE, R.S., FRANCIS, P.W. & HARMON, R.S. (1981) Andean andesites and crustal growth. Philosophical Transactions of the Royal Society of London A, 301, 305-320.

TORO ÁLAVA, J. & JAILLAR, E. (2005) Provenance of the Upper Cretaceous to upper Eocene clastic sediments of the Western Cordillera of Ecuador: Geodynamic implications. Tectonophysics, 399, 279-292.

TRIPSANAS, E.K., PIPER, D.J.W., JENNER, K.A. & BRYANT, W.R. (2008) Submarine mass-transport facies: new perspectives on flow processes from cores on the eastern North American margin. Sedimentology, 55, 97-136.

TUCKER, M. E. (2001) Sedimentary Petrology, An introduction to the origin of sedimentary rocks – Third edition. Blackwell Scientific Publications, Oxford, 262 p.

URGELES, R., CANALS, M., BARAZA, J., ALONSO, B. & MASSON, D.G. (1997) The most recent megalandslides of the Canary Islands: El Golfo debris avalanche and Canary debris flow, west El Hierro island. Journal of Geophysical Research, 102 (B09), 20305-20323.

URGELES, R., MASSON, D.G., CANALS, M., WATTS, A.B. & LE BAS, T. (1999) Recurrent giant landslides on the west flank of La Palma, Canary Islands. Journal of Geophysical Research, 104 (B11), 25331-25348.

VARNES, D.J. (1978) Slope movement types and processes. *In*: R.L. Shuster & R.J. Krizek (Eds.) Landslides-Analysis and Control. National Academy of Sciences, Washington, Special Report, 176, 11-33.

VENDEVILLE, B. & COBBOLD, P.R. (1987) Glissements gravitaires synsédimentaires et failles normales listriques : modèles expérimentaux. Comptes Rendus de l'Académie des Sciences, série II, 305, 1313-1319.

VENDEVILLE, B. & GAULLIER, V. (2003) Role of pore-fluid pressure and slope angle in triggering submarine mass movements: natural examples and pilot experimental models. *In*: J. Locat & J. Mienert (Eds.), Submarine Mass Movements and their Consequences. Kluwer Academic Publishers, Dordrecht (Pays-bas), 137-144.

VERNHET, E., HEUBECK, C., ZHU, M.-Y. & ZHANG, J.-M. (2006) Large-scale slope instability at the southern margin of the Ediacaran Yangtze platform (Hunan province, central China). Precambrian Research, 148, 32-44.

VOGT, P.R., GARDNER, J. & CRANE, K. (1999) The Norwegian-Barents-Svalbard (NBS) continental margin: Introducing a natural laboratory of mass wasting, hydrates, and ascent of sediment, pore water, and methane. Geo-Marine Letters, 19, 2-21.

VOLPI, V., CAMERLENGHI, A., HILLENBRAND, C.-D., REBESCO, M. & IVALDI, R. (2003) Effects of biogenic silica on sediment compaction and slope stability on the Pacific margin of the Antarctic Peninsula. Basin Research, 15, 399-363.

VORREN, T.O. & LABERG, J.S. (2001) Late Quaternary sedimentary processes and environment on the Norwegian-Greenland Sea continental margins. *In*: O.J. Martinsen & T. Dreyer (Eds.) Sedimentary Environments Offshore Norway - Palaeozoic to Recent. Elsevier, Amsterdam, 451-456.

WENDLER, J., KUSS, J. & STEIN, R. (2007) Late Cenomanian carbon isotope stratigraphy of the Levant carbonate platform (Central Jordan): Cyclic patterns and correlations. Geophysical Research Abstracts, 9, EGU2007-A-11163.

WIESE, F. & SCHULZE, F. (2005) The upper Cenomanian (Cretaceous) ammonite Neolobites vibrayeanus (d'Orbigny, 1841) in the Middle East: taxonomic and palaeoecologic remarks. Cretaceous Research, 26, 930-946.

WILSON, C.K., LONG, D. & BULAT, J. (2003) The Afen Slide—a multistaged slope failure in the Faeroe-Shetland Channel. *In*: J. Locat & J. Mienert (Eds.), Submarine Mass Movements and their Consequences. Kluwer Academic Publishers, Dordrecht (Pays-bas), 317-324.

WIPF, M. (2006) Evolution of the Western Cordillera and Coastal Margin of Peru: Evidence from Low-Temperature Thermochronology and Geomorphology. Thèse de doctorat, ETH Zurich, no. 16383, 152 p.

WOODCOCK, N.H. (1979a) Size of submarine slides and their significance. Journal of Structural Geology, 1, 137-142.

WOODCOCK, N.H. (1979b) The use of slump structures as paleoslope orientation estimators. Sedimentology, 26, 83-99.

WRIGHT, C.W., CALLOMAN, J.H. & HOWARTH, M.K. (1996) Treatise on Invertebrate Paleontology. Part L. Mollusca 4 revised, Cephalopoda, Cretaceous Ammonoidea. The Geological Society of America and University of Kansas Press, 362 p.

WRIGHT, J.D., CRAMER, B.S., MILLER, K.G. & KATZ, M.E. (2003) Orbital Cycles, Climate, and Diagenesis Mimic Methane Releases: Results from a High Resolution Study of OAE-2, New Jersey Coastal Plain. Eos Trans. AGU, 84 (46), Jt. Assem. Suppl., Abstract PP42D-03.

WYNN, R.B., MASSON, D.G., STOW, D.A. & WEAVER, P.P. (2000) The Northwest African slope apron: a modern analogue for deep-water systems with complex sea floor topography. Marine and Petroleum Geology, 17, 253-265.

ZHANG, Y., DONG, S. & SHI, W. (2003) Cretaceous deformation history of the middle Tan-Lu fault zone in Shandong Province, eastern China. Tectonophysics, 363, 243-258.

VII.

LISTE DES FIGURES

VII. Liste des figures

VIII.

ANNEXES
Résumé des congrès
Images satellites

Callot P., Carlotto V., Odonne F. & Sempere T. (2006) Progresos en el estudio de la Formación Ayabacas. XIII Congreso Peruano de Geología, Lima, Perú.

PROGRESOS EN EL ESTUDIO DE LA FORMACIÓN AYABACAS

Pierre CALLOT[1], Víctor CARLOTTO[2], Francis ODONNE[3], Thierry SEMPERE[3]

[1] Convenio IRD-INGEMMET, Av. Canadá 1470, San Boja, Lima 41, Perú / LMTG, UMR 5563 CNRS - Université Paul Sabatier - IRD, 31400 Toulouse, Francia (callot@lmtg.obs-mip.fr)
[2] INGEMMET, Av. Canadá 1470, San Boja, Lima 41, Perú (vcarlotto@ingemmet.gob.pe)
[3] LMTG, UMR 5563 CNRS - Université Paul Sabatier - IRD, 31400 Toulouse, Francia (sempere@lmtg.obs-mip.fr)

Abstract – **The Ayabacas Formation is a chaotic unit of ~Turonian age that crops out over more than 50,000 km^2 in the Altiplano and Eastern Cordillera of southern Peru. A number of interpretations have been proposed since the 1940s to explain its peculiar disorganised appearance (fold-and-thrust tectonics, heavy erosion, subaerial sliding, submarine megabreccia). New field observations, including locally large amounts of hydroplastic breccias, synsedimentary normal faults, and folding of poorly-lithified rocks, confirm that it is a subaqueous resedimented unit (megabreccia). Four main facies are defined, which reflect a downslope, WSW-wards increase in fragmentation of the Albian-Cenomanian carbonate platform.**

Introducción

La Formación Ayabacas (~Turoniano) es una unidad resedimentada que se observa sobre un área superior a 50000 km^2 en el Altiplano y la Cordillera Oriental del sur del Perú (Sempere *et al.*, 2000). Su génesis fue explicada de maneras muy diferentes: fallamiento de bloques y erosión intensa (Heim, 1947), tectónica con pliegues y cabalgamientos (Newell, 1949; Chanove *et al.*, 1969), deformación disharmónica y/o polifásica, fracturación causada por karstificación y/o diapirismo de yesos, intrusiones hipovolcánicas (Audebaud, 1971), caos producido por deslizamientos subaéreos (De Jong, 1974) o submarinos (Audebaud, 1967; Sempere *et al.*, 2000). El estudio en curso soporta esta última interpretación, describiendo la Fm Ayabacas como una megabrecha (u olistostromo), es decir el resultado de deslizamientos submarinos de gran amplitud (Spence and Tucker, 1997).

Aunque las interpretaciones son diferentes, la mayoría de los autores hacen descripciones similares, al menos en las zonas estudiadas por ellos: un caos de bloques grandes (50-500 m) que aparentemente "flotan" dentro de una matriz más blanda. Estos bloques, a menudo plegados y en cada posición imaginable, son principalmente de calizas cretáceas (Fm Arcurquina), pero también de otras formaciones anteriores (Fm Huancané, Fm Muni, Fm Sipin, Grupo Mitu, Paleozoico). La matriz es una brecha con clastos grandes y pequeños de calizas y areniscas fracturadas dentro de pelitas multicolores (generalmente rojas) y areniscas. Sin embargo un estudio más exhaustivo muestra que la Fm Ayabacas no es uniforme en cuanto a facies de deslizamiento.

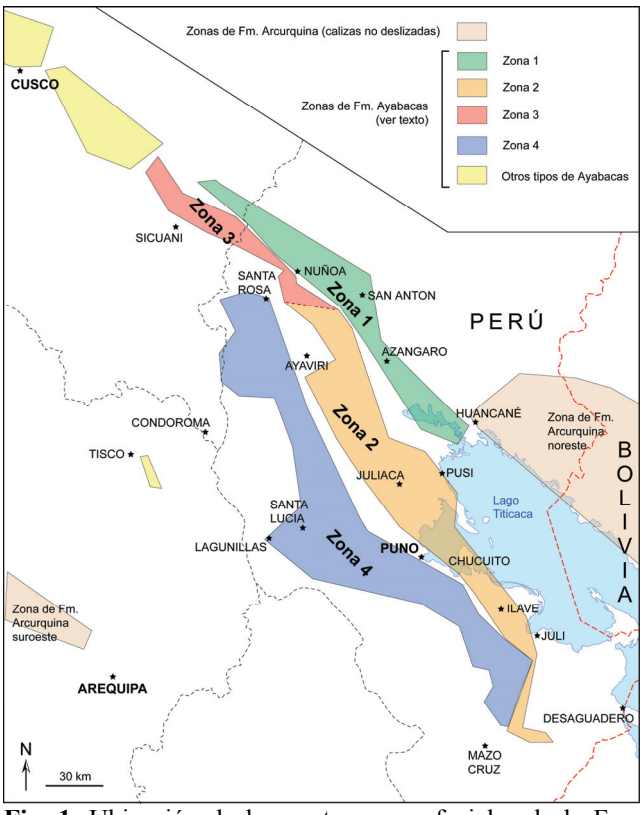

Fig. 1. Ubicación de las cuatro zonas faciales de la Fm Ayabacas.

Diferentes facies en la Formación Ayabacas

Se puede distinguir cuatros zonas faciales en el área de distribución de la Fm Ayabacas, tomando en cuenta que ésta resulta principalmente del deslizamiento de la Fm Arcurquina (**Fig. 1**).

- En los afloramientos del NE, zona 1 (oeste de Huancané, San Antón, Nuñoa, **fig. 1**), la Fm Ayabacas tiene generalmente poco espesor. Consiste de trozos tabulares que se cabalgan (**Fig. 2**), y localmente se puede observar una Fm Ayabacas más desestructurada y de gran espesor, con bloques de calizas fragmentados y plegados, y de vez en cuando con bloques de la Fm Huancané que pueden alcanzar unos centenares de metros. Los cortes estratigráficos de los bloques de calizas de esta zona son similares: su espesor es pequeño, de 10 a 20 metros, y se puede distinguir 5 niveles característicos cuando el bloque es completo (**Fig. 3**). Durante la sedimentación de las calizas, fallas normales habrían basculado bloques del substrato (Fm Huancané y unidades anteriores) y producido el deslizamiento de las calizas (**Fig. 4**); algunas de estas fallas normales fueron reactivadas en compresión durante la deformación andina, como por ejemplo en la región de San Antón.

↑ **Fig. 2.** Larimayo (0354876 – 8396892 – 4081 m), cerca de San Antón. La Fm Ayabacas consiste de trozos tabulares ligeramente plegados que se cabalgan, mientras que las unidades anteriores y posteriores son regulares. Los trozos tabulares de calizas muestran secciones iguales.

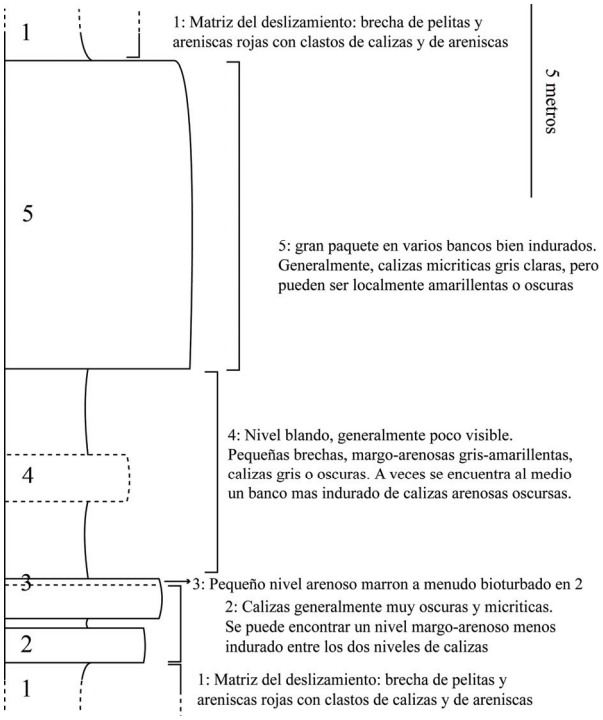

← **Fig. 3.** Corte estratigráfico típico en los bloques de calizas de la Fm Ayabacas, en la zona 1. Los bloques no son siempre completos, ya que puede faltar una parte de la base o del tope.

↓ **Fig. 4.** Antacalla (0317153 – 8412459 – 4288 m), al NO de Nuñoa. La Fm Huancané (abajo) está cortada por una falla a la derecha y basculada hacia el NE. La Fm Ayabacas desliza en la misma dirección y asoma a la izquierda. Arriba el Grupo Vilquechico no está cortado por la falla y sella el conjunto.

- Más al S, zona 2, en una franja que pasa al E de Mazo Cruz y por Juli, Ilave, la Península de Chucuito, Pusi, Juliaca y al E de Santa Rosa (**Fig. 1**), la Fm Ayabacas tiene un gran espesor, y generalmente sus bloques de calizas son muy plegados (**Fig. 5**); en la región de Pusi se pueden encontrar bloques de la Fm Huancané. Los "bloques plegados" de calizas que constituyen la Fm Ayabacas poseen tamaños entre decenas y centenares de metros, pero a veces se pueden seguir en fotos áreas sobre varios kilómetros (**Fig. 6A**) en estructuras generalmente NW-SE. Las secciones de bloques son más espesas que en la zona 1, pero igualmente más heterogéneas.

- En la zona 3, al norte de la carretera entre Santa Rosa y Cusco (**Fig. 1**), la Fm Ayabacas tiene un gran espesor y es muy caótica, con una mezcla de bloques cretáceos (pelitas rojas y calizas) así como grandes bloques de estratos litificados de las Fms Huancané, Muni, Sipín, Grupo Mitu, y Paleozoico.

- La siguiente zona (4) es otra franja ubicada más al S de las tres anteriores, que pasa por la carretera Mazo Cruz-Ilave, al E de Ilave, en Lagunillas y Santa Lucía, y finalmente al S de Santa Rosa (**Fig. 1**). La Fm Ayabacas se presenta a menudo, en el campo y en fotos áreas, con un aspecto ondulado. Consiste de bloques de calizas más espesos pero más pequeños que en la zona 2 y que flotan en una "matriz" de brechas rojizas. Los bloques pueden presentar una orientación (en particular en el gran afloramiento de Ayabacas al S de Santa Rosa), pero generalmente esta zona es más desestructurada que las anteriores. En particular nunca se observan pliegues alargados en fotos áreas. En algunos sitios grandes cantidades de brechas hydroplásticas se ubican debajo de una barra grande de calizas.

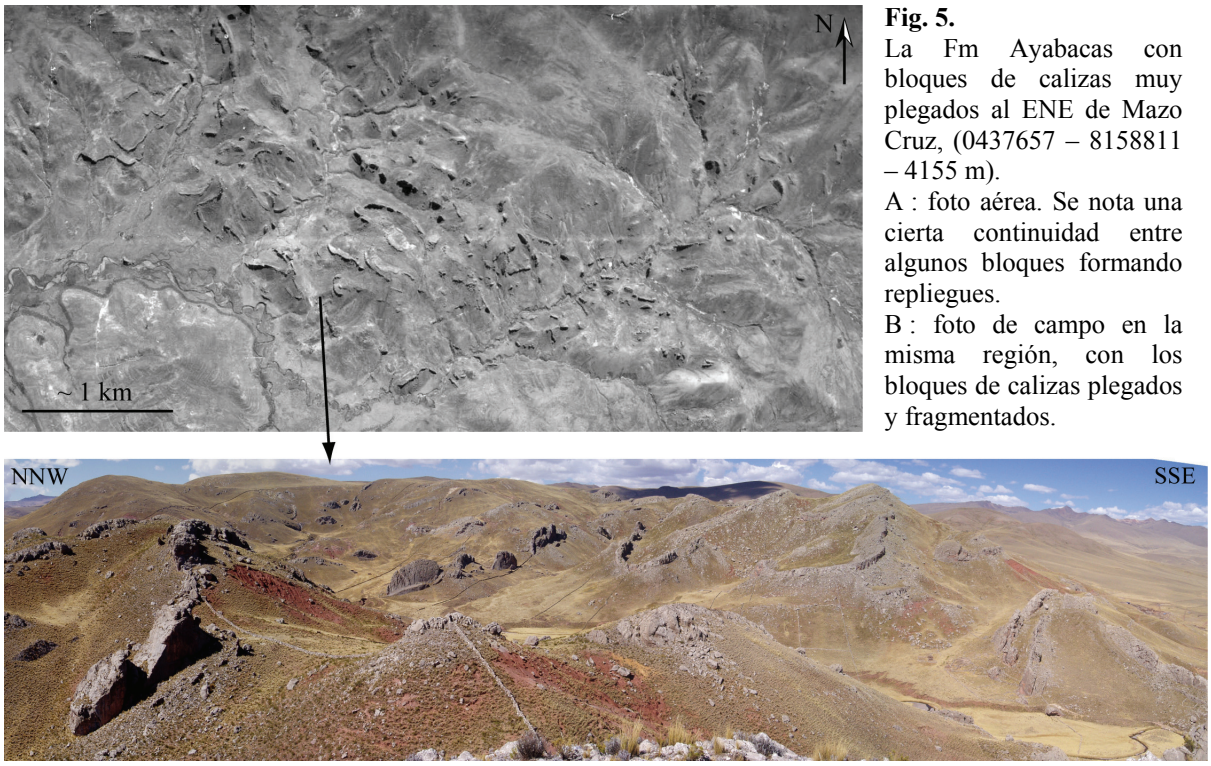

Fig. 5.
La Fm Ayabacas con bloques de calizas muy plegados al ENE de Mazo Cruz, (0437657 – 8158811 – 4155 m).
A : foto aérea. Se nota una cierta continuidad entre algunos bloques formando repliegues.
B : foto de campo en la misma región, con los bloques de calizas plegados y fragmentados.

Un origen marino bien establecido

El aspecto replegado a caótico de la Fm Ayabacas contrasta fuertemente con la regularidad de las unidades subyacente y sobreyacente (**Fig. 2**). Este hecho, constante cuando se observan las relaciones de base y tope, demuestra que la deformación aparente ocurrió durante o poco después de la sedimentación.

En un mismo afloramiento de la Fm Ayabacas, se puede tener bloques vecinos no deformados y plegados con ejes de pliegue totalmente diferentes. Por otra parte las brechas hidroplásticas (**Fig. 6**) que a veces se encuentran separando bloques o trozos tabulares de calizas se formaron en sedimentos saturados de agua (Cosgrove, 1995); estas brechas se inyectaron en los estratos de calizas, que además son atravesados por filones clásticos. En el momento de la deformación los depósitos no estaban totalmente litificados, lo que implica que el deslizamiento ocurrió bajo agua.

Conclusión

La Formación Ayabacas es el resultado de deslizamientos submarinos de gran amplitud (megabrecha). La zonación de las facies a escala de la región de estudio muestra un aumento de la fragmentación hacia el OSO de la plataforma carbonatada albo-cenomaniana, en concordancia con la geometría de la cuenca sedimentaria.

Fig. 6.
A. Entre Juliaca y Santa Lucía (0354166 – 8264089 – 4037 m). Sucesión de estratos de calizas y de brechas hydroplásticas.
B. Detalle. Se nota clastos más litificados de calizas y calizas arenosas flotando en una matriz margo-arenosa fluidificada.

Referencias

Audebaud, E. (1967) Etude géologique de la région de Sicuani et Ocongate (Cordillère Orientale du Sud Péruvien). Thèse de géologie structurale, Grenoble, 60 pp.

Audebaud, E. (1971) Mise au point sur la stratigraphie et la textonique des calcaires cénomaniens du Sud-Est péruvien (formation Ayavacas). C. R. Acad. Sc. Paris, 272: 1059-1062.

Chanove, G., Mattauer, M. and Mégard, F. (1969) Précisions sur la tectonique tangentielle des terrains secondaires du massif de Pirin (Nord-Ouest du lac Titicaca, Pérou). Comptes Rendus Acad. Sci., ser. D, 268: 1698-1701.

Cosgrove, J.W. (1995) The expression of hydraulic fracturing in rocks and sediments. In: Fractography: fracture topography as a tool in fracture mechanics and stress analysis (Ed M.S. Ameen), Geol. Soc. London Spec. Publ., 92, 187-196.

De Jong, K.A. (1974) Melange (Olistostrome) near Lago Titicaca, Peru. Am. As. Petrol. Geol. Bull., 58: 729-741.

Heim, A. (1947) Estudios tectónicos en la región del campo petrolífero de Pirin, lado NW del Lago Titicaca. Dirección Minas y Petróleo Bol., Perú, año 26, no. 79, 45 pp.

Newell, N.D. (1949) Geology of the Lake Titicaca region, Peru and Bolivia. Geol. Soc. America Mem., 36, 111 pp.

Sempere, T., Jacay, J., Carrillo, M.-A., Gómez, P., Odonne, F. and Biraben, V. (2000) Características y génesis de la Formación Ayabacas (Departamentos de Puno y Cusco). Bol. Soc. Geol. Perú, 90: 69-76.

Spence, G.H. and Tucker, M.E. (1997) Genesis of limestone megabreccias and their significance in carbonate sequence stratigraphic models: a review. Sed. Geol., 112: 163-193.

Callot P., Odonne F. & Sempere T. (2007) Giant submarine collapse of a Mid-Cretaceous carbonate platform: the Ayabacas Formation of southern Peru. EGU, *Geophysical Research Abstracts*, Vol. 9, EGU07-A-09563, European Geosciences Union, Vienne, Autriche.

Giant submarine collapse of a carbonate platform at the Cenomanian-Turonian transition: the Ayabacas Formation of southern Peru

P. Callot, F. Odonne, T. Sempere
LMTG – UMR 5563 UR 154 CNRS Université Paul-Sabatier IRD - France
(callot@lmtg.obs-mip.fr)

We have performed a thorough study of the Ayabacas Formation, an impressively disturbed, mainly carbonate unit that crops out irregularly over more than 160,000 km², mainly in the Altiplano and Eastern Cordillera of southern Peru. Its thickness increases from 0 m in the NE to >500 m in the W and SW. This extraordinary unit results from the giant submarine collapse of the major part of a carbonate platform that developed mainly during the late Cenomanian transgression. The collapse occurred slightly later (given that the limestones were only partially lithified when they slid), most likely during the sea-level fall of the post-OAE2, latest Cenomanian – earliest Turonian, major marine regression. The collapse is post-dated by Turonian-Santonian red beds.

The Ayabacas Formation displays 6 main different facies or styles of deformation, which reflect a downslope, WSW-ward increase in fragmentation of the Cenomanian carbonate platform. Facies in parts of the collapse are very similar to 3D seismic images of recent submarine landslides. In the ENE-most area, i.e. the most proximal part of the basin, the thin (~20 m) carbonate platform was not destabilized (zone 0). In zones 1 to 3, normal faults have shaped the pre-Ayabacas substratum into tilted blocks and mixed partially lithified limestones with the underlying unlithified red mudstones and fine sandstones, resulting in a chaos of soft-folded limestone floating in a matrix of mudstones and sedimentary breccias; isolated and rare lithified large blocks of older units may also be found in the slide deposits. Westwards, in zones 4 and 5, limestones were brecciated by hydraulic fracturing and often slid as "sedimentary thrust and fold systems", as described in the literature. In zone 6, the lower part of the unit was not destabilized whereas its upper part is formed by piled-up slides, suggesting that this zone mostly behaved as an accumulation area, in contrast with zones 1-5 characterized by slide origination and/or transport.

The WNW-wards change in slide facies is in agreement with the basin slope as reconstructed from depositional facies and thicknesses. Thicknesses of the initial limestone deposits and of the displaced mass increase WSW-wards. Zones 4 to 6 display recurrent slide events, whereas such distinctions cannot be made in the chaotic mass characteristic of zones 1 to 3. Deformation in zone 5 and 6 characteristically includes large asymmetrical to recumbent folds, whose styles are very distinct from the regional Andean tectonic deformation.

The giant collapse documented by the Ayabacas Formation provides a prime example that large-scale submarine mass movements, similar to those known in current margins, have occurred in the Cretaceous, namely near the Cenomanian-Turonian transition. This particular time in Earth's history was marked by a significant drop in sea level, during which the collapse apparently occurred. This coincidence contributes to the debate over whether rapid sea-level drops have had a role in triggering recent collapses.

E. Díaz-Martínez e I. Rábano (Eds.), *4th European Meeting on the Palaeontology and Stratigraphy of Latin America*
Cuadernos del Museo Geominero, nº 8. Instituto Geológico y Minero de España, Madrid, 2007. ISBN 978-84-7840-707-1

THE MID-CRETACEOUS CARBONATE PLATFORM OF SOUTHERN PERU COLLAPSED AT THE TURONIAN-CONIACIAN TRANSITION

P. Callot[1], T. Sempere[1], F. Odonne[1] and E. Robert [2]

[1] LMTG, Université de Toulouse, CNRS, IRD, OMP, 14 Av. E. Belin, F-31400 Toulouse, France.
callot@lmtg.obs-mip.fr, sempere@lmtg.obs-mip.fr, odonne@lmtg.obs-mip.fr
[2] OSUG, Université Joseph Fourier, Institut Dolomieu, 15 rue Maurice Gignoux, F-38031 Grenoble cedex, France.
emmanuel.robert@ujf-grenoble.fr

Keywords: Submarine collapse, carbonate platform, Turonian-Coniacian boundary, southern Peru.

INTRODUCTION

The Ayabacas Fm of southern Peru consists of an extraordinarily deformed, highly disrupted, chaotic unit that reworks previous deposits and rocks (Cabrera & Petersen, 1936; Portugal, 1974). This enigmatic unit has long been known to be of Cretaceous age. It mainly includes mm- to km-size limestone fragments reworked from the underlying Arcurquina Fm, and can therefore be described as a limestone megabreccia (*sensu* Spence & Tucker, 1997). In the northeastern half of the study area, these fragments are enclosed in a "matrix" of reddish mudstones and siltstones reworked from the Murco Fm, i.e. the unit underlying the Arcurquina Fm. Only limestones are documented in the southwest. In northeastern areas, lithified blocks of Jurassic sandstones and even Paleozoic shales occur. Particularly significant is the common occurrence of fluidised sediments and breccias within the "matrix", implying a submarine collapse process.

The Ayabacas Fm typically lacks regular stratification, in marked contrast with the underlying and overlying units. No undisturbed marine limestone strata occur either within or at the top of the Ayabacas Fm, which is directly overlain by reddish strata of mainly continental origin (Vilquechico Gp and equivalent units). The unit thus forms a single mass wasting body, which displays noteworthy internal facies variations. It irregularly crops out over 60,000 km^2 and is inferred to extend over >80,000 km^2. Its thickness varies from 0 to ≥500 m, and its volume is estimated to be >10,000 km^3 (>10^{13} m^3). Given its dimensions, the Ayabacas appears as the most extensive ancient submarine mass wasting body currently known, and one of the thickest. Its extension and thickness are of the same magnitude as the largest and thickest recent bodies described to date.

GEOLOGICAL SETTING AND CHARACTERISTICS

The Ayabacas Fm and underlying units were deposited in the southern region of the western Peru back-arc basin (WPBAB), which was active in the Jurassic and Cretaceous. This basin had developed in an extensional tectonic context and deepened overall to the west. Subsidence was greatly enhanced in the mid-

Cretaceous, starting in the Early Albian, as a consequence of the western WPBAB evolution toward a state of marginal basin in central Peru, due to considerable lithospheric thinning there (Jaillard, 1994). The edge of the continental domain, along which the Albian-Turonian carbonate platform developed, thus technically behaved as a kind of passive margin in relation to the much deeper sub-basin to the west. A "passive margin" setting similar to that in central Peru can thus be proposed for the carbonate platform in southern Peru, although lithospheric thinning was much less intense in this region.

Redefinition of the Mesozoic stratigraphy of southern Peru (Sempere *et al.*, 2004) resolved serious discrepancies between previous works. Prior to the Ayabacas collapse, the Mesozoic units of southern Peru accumulated in one largely marine basin that deepened to the west: continental to shallow-marine facies were deposited in the northeast and deeper facies in the southwest and west. In contrast, the units younger than the Ayabacas Fm were deposited in an almost exclusively continental basin that was bounded to the southwest by topographic highs, apparently volcanic in nature.

Although the Ayabacas and Arcurquina formations consist of limestones and occupy the same stratigraphic position — overlying the Murco Fm and underlying the Vilquechico Gp and equivalent units —, they must be formally distinguished since the Arcurquina was deposited in regular beds in a stable carbonate platform, whereas the Ayabacas resulted from the reworking of the Arcurquina and previous units: their deposition was therefore neither contemporaneous nor driven by similar processes. Due to these markedly different depositional processes, they display distinct characteristics, which are obvious in the field.

In the Arequipa area, the major mid-Cretaceous transgression is mainly recorded by the ~250 m-thick Arcurquina Fm limestones. In the Altiplano, this transgression peaked with the deposition of the <100 m-thick Arcurquina Fm consisting here of marine, regularly-bedded, thickening-upward, grey to black, organic-rich micritic limestones. The Ayabacas Fm and its typical deformation are post-dated by the Vilquechico Gp (Late Campanian-Early Paleocene, ~700 m-thick). It is noteworthy that the Arcurquina Fm (and equivalent deposits) mostly consists of marine limestones whereas the Lower Vilquechico Fm (and equivalents) is dominated by abundant red mudstones that were deposited in a continental or near-continental environment; in the Central Andean domain, away from the coast, true marine deposits are extremely rare afterwards. The Ayabacas Fm was thus deposited at the very time when the south Peruvian basin underwent a dramatic and permanent change from marine to continental conditions.

BIOCHRONOLOGIC CONSTRAINTS

The age of the Ayabacas Fm is bracketed by the youngest age yielded by the youngest reworked unit, namely the Arcurquina Fm (and its Bolivian and north Peruvian equivalents), and by the oldest age yielded by the overlying units, i.e. the Vilquechico Gp (and equivalents).

In the Lake Titicaca region, the Ayabacas Fm is generally >100 m-thick just southwest of the SFUACC fault system (Ayabacas, Pusi and Puno areas; for locations, see Sempere *et al.*, 2004), where it reworks limestones bearing late Early Albian to Late Cenomanian fossils. In contrast, the Arcurquina Fm is <35 m-thick and has only yielded fossils of Late Cenomanian age in the area located northeast of the SFUACC (Huancané area and western to central Bolivia).

In Bolivia, two units, generally <30 m-thick, are equivalent to the Arcurquina Fm: the Matilde Fm north of Lake Titicaca and the Miraflores Fm in central Bolivia. The Miraflores Fm yielded the ammonite

Neolobites kummeli (Branisa, 1968), now considered as synonym of the Late Cenomanian *N. vibrayeanus* (Wiese & Schulze, 2005). Graf (2002) and Graf *et al.* (2003) described a 33 m-thick section near Mina Matilde, ~90 km southeast of Huancané. These authors identified the purportedly Late Cenomanian planktonic foraminiferum *Asterohedbergella asterospinosa* at several levels in the organic-rich lower half of this section, in agreement with other paleontological data from other parts of the basin. On the basis of this Late Cenomanian age, ?^{13}C data, facies, and biostratigraphic correlations, they assigned most of this portion of the section to the Oceanic Anoxic Event 2 (OAE-2), and, because the termination of OAE-2 is now considered to mark the Cenomanian-Turonian boundary (93.5 Ma; Gradstein *et al.*, 2004), the upper half of the Arcurquina Fm at Mina Matilde should implicitly be of Turonian age. However, attribution of as much as ~14 m of this section to the OAE-2 interval is questionable given the shallow depositional environment and low subsidence; furthermore, *Asterohedbergella asterospinosa* has been shown to also occur in the Turonian (Abdallah *et al.*, 2000). We accept Graf *et al.*'s (2003) identification of OAE-2 in this area, but propose that it is likely to be restricted to one of two conspicuous calcareous shale intervals known in most of this domain, which we denominate 'Nuñoa-1' and 'Nuñoa-2' intervals. Among them, the Nuñoa-1 interval is particularly rich in organic matter, as revealed by its dominantly black coloration and high degree of subsequent *per descensum* bioturbation. We test this hypothesis below.

Southwest of the SFUACC system, limestone blocks of the Arcurquina Fm reworked in the Ayabacas Fm yielded Albian and Cenomanian fossils (Newell, 1949): the oldest age, *viz.* the late Early Albian, is recorded by the ammonite *Glottoceras* sp. (previously assigned to the genus *Knemiceras*; Robert *et al.*, 2002), and the echinid *Heteraster texanus* (Ayabacas locality); the Middle Albian is recorded by the ammonite *Oxytropidoceras* (*Oxytropidoceras*) *peruvianum* (early Middle Albian; Robert *et al.*, 2002) and the echinid *Coenholectypus planatus* (Ayabacas locality); the echinid *Orthopsis titicacana*, common in the Pusi and Puno areas, and the coral *Epistreptophyllum* aff. *budaensis* indicate a Cenomanian age (Newell, 1949); the Late Cenomanian is characterised by the ammonite *Neolobites vibrayeanus* from 4 km northeast of Cusco and 13 km north of Ayabacas.

In the Arequipa area, the Yura section, 200 km southwest of the Ayabacas locality and 40 km northwest of the city of Arequipa, displays both the Arcurquina and Ayabacas formations. The former is ~275 m-thick and makes up most of the limestone succession there, whereas the latter is only ~25 m-thick and unfossiliferous. Diagnostic fossils (Benavides, 1962) were found in the Arcurquina Fm, which consists of two members. The lower member is characterised in its lower part by the common occurrence of *Ostrea minos*, which is found associated with *Glottoceras raimondii* in northern Peru (Chúlec Fm, late Early Albian; Robert *et al.*, 2002); its upper part is dated by the echinid *Coenholectypus planatus*, considered to range from the latest Early Albian to earliest Late Albian. This lower member thus spans the late Early Albian - Middle Albian interval (102-108.5 Ma). In contrast, the upper member has only yielded *Neolobites* sp. (Middle to Late Cenomanian). Diagnostic fossils from the two intervals are only ~30 m apart, revealing that the two members are separated by a chronologic hiatus of ~7 Myr (between at least ~102 and ~95 Ma). We found no evidence of a post-Albian, pre-Late Cenomanian protracted emersion or alteration in the outcropping uppermost part of the lower member, although a mudcracked and silicified surface is indeed observed at the top of this unit.

The Vilquechico Gp of the Lake Titicaca region consists of three formations (Lower, Middle, and Upper Vilquechico), which correlate with dated Bolivian units (Sempere *et al.*, 2004). The Lower Vilquechico Fm generally overlies the Ayabacas Fm and consists of dominantly red mudstones. It is equivalent to the

set formed by the Santonian-Campanian Chaunaca and Coniacian? Aroifilla formations of Bolivia. The Ashua Fm, the Vilquechico equivalent in the Arequipa region, abruptly overlies the Ayabacas Fm and shares a number of characteristics with the Aroifilla Fm of Bolivia. It dominantly consists of red mudstones and includes ≤4 m-thick gypsum bodies, ≤15 m-thick volcaniclastic conglomerates and sandstones, and ≤10 m-thick limestone beds (Cruz, 2002). One of these limestones yielded the ammonite *Paratissotia steinmanni* (Hosttas, 1967). *P. steinmanni* indicated historically the Lenticeras baltai Zone, assigned to the Santonian (Benavides, 1956). But a revision of the faunal association of the Lenticeras baltai Zone, listed by Benavides (1956), questions its true chronostratigraphic position. *Paratissotia* is commonly considered as a Coniacian genus (Wright *et al*., 1996). *P. steinmanni* must therefore be now recognized to indicate the Coniacian. This datum strictly constrains the Ayabacas Fm to be older than the latest Coniacian (~86 Ma).

Central and northern Peru. Thicknesses and reconstructed depositional depths in the WPBAB show an overall increase from southern Peru northwards. Much of the relevant information relative to the mid-Cretaceous stratigraphy and evolution of central and northern Peru is summarized in Jaillard (1994). A first major transgression started in the middle Early Albian (~110 Ma) with ammonite-bearing marine mudstones and sandstones. The first massive limestones are represented by the Chúlec Fm of late Early Albian age (Robert *et al*., 2002), and a >2 km-thick succession of limestones and marls was deposited until the Late Turonian. The west-Peruvian carbonate platform was affected by a relative regression during the Late Albian-Middle Cenomanian interval (102-95 Ma, ~7 Myr). In the entire west-Peruvian basin, a major transgression was initiated in the latest Middle Cenomanian (~95 Ma) and culminated in the Early Turonian (~92.5 Ma). Carbonate-dominated sedimentation continued until the Late Turonian. In northern Peru, the Turonian limestones are sharply overlain by ~300 m of reddish to brown mudstones and fine sandstones, Early Coniacian to Middle Campanian in age, that were deposited in marine to non-marine environments and are thought to reflect the onset of aerial erosion in western areas throughout the Central Andes (Jaillard, 1994). The sharp change from carbonates to reddish mudstones thus occurred approximately at the Turonian-Coniacian boundary (~89 Ma).

DISCUSSION AND CONCLUSION

Age of the Ayabacas Formation. Chronologic constraints available from southern Peru only indicate that deposition of the Ayabacas Fm occurred between the earliest Late Cenomanian and latest Coniacian. However, recognition of the OAE-2 event in the lower and/or middle part of the west-Bolivian equivalent of the Arcurquina Fm (Graf, 2002) strongly suggests that the upper part of the Arcurquina Fm is Turonian in age, although diagnostic Turonian fossils have not been reported yet. The data from southern Peru are consistent with the well-constrained evolution of central and northern Peru. The two major transgressions known in the north, respectively starting in the middle to late Early Albian (~110 Ma) and in the latest Middle Cenomanian (~95 Ma) are recorded southwest of the SFUACC by the late Early and Middle Albian, and Late Cenomanian, faunas found in limestones reworked in the Ayabacas Fm, as well as in the Yura section. The ~7 Myr-long hiatus observed in the Arequipa area is apparently correlative of the Late Albian - Middle Cenomanian regression (~102-~95 Ma) documented in northern Peru. Likewise, the Arcurquina Fm of southern Peru was thus mainly deposited during two distinct transgressive-highstand intervals. Unlike the Albian transgression, which is only recorded southwest of the SFUACC fault system,

the worldwide Late Cenomanian transgression flooded the area northeast of it, even reaching central Bolivia (Sempere, 1995).

In northern as in southern Peru, termination of the carbonate platform and subsequent deposition of dominantly reddish mudstones record a major sedimentary upheaval. This first-order change occurred near the Turonian-Coniacian boundary in northern Peru and, consistent with the regional constraints, it is reasonable to propose that this change took place at about the same time in southern Peru. Because the Ayabacas Fm coincides with this change, post-dating the termination of the carbonate platform and predating the onset of red mudstone deposition, the Ayabacas collapse is likely to have occurred also near the Turonian-Coniacian boundary (~90-89 Ma).

Testing the chronostratigraphic model. The chronostratigraphy proposed above for the Arcurquina Fm northeast of the SFUACC can be tested by calculating a mean compacted sedimentation rate for each of the 9 measured sections and, on this basis, deriving mean ages for the initiation and termination of the Nuñoa-1 and Nuñoa-2 intervals, one of which is supposed to be the local correlative of OAE-2. Assuming that deposition of the Arcurquina Fm in this area started at ~95 Ma (latest Middle Cenomanian or basal Late Cenomanian) and ended at ~89 Ma (Turonian-Coniacian transition), we find that, in southern Peru, compacted depositional rates varied between 2.5 and 3.9 m/Myr northeast of the SFUACC system. Assuming a constant rate at each locality, we calculate the mean ages for initiation and termination of the Nuñoa-1 deposition as 94.4 ± 0.2 and 93.8 ± 0.3 Ma, respectively; and, for Nuñoa-2, as 93.4 ± 0.4 and 92.7 ± 0.4 Ma, respectively. Values relative to the Nuñoa-1 interval fairly agree with available data concerning OAE-2, which was initiated at 94.0 ± 0.2 Ma and terminated at 93.5 ± 0.2 (Caron *et al.*, 1999) or 93.5 ± 0.8 Ma (Gradstein *et al.*, 2004). Such a good agreement strongly suggests that our proposed chronostratigraphy is consistent, and that the organic-rich Nuñoa-1 interval does represent OAE-2 in southern Peru. The overlying portion of the Arcurquina Fm must therefore be considered of Turonian age.

CONCLUSION

The highly disrupted Ayabacas Formation of southern Peru was formed by the giant submarine collapse, at the Turonian-Coniacian transition, of the carbonate platform deposits that had accumulated in the Andean back-arc basin during the Albian-Turonian interval.

REFERENCES

Abdallah, H., Sassi, S., Meister, C. and Souissi, R. (2000). Stratigraphie séquentielle et paléogéographie à la limite Cénomanien-Turonien dans la région de Gafsa-Chotts (Tunisie centrale). Cretaceous Research, 21: 35-106.

Benavides, V. (1956). Cretaceous system in northern Peru. Bull. Amer. Mus. Nat. Hist., 108 : 1-493.

Benavides, V. (1962). Estratigrafía pre-terciaria de la región de Arequipa. Bol. Soc. Geol. Perú, 38: 5-45.

Branisa, L. (1968). Hallazgo del ammonite *Neolobites* en la Caliza Miraflores y de huellas de dinosaurios en la Formación El Molino y su significado para la determinación de la edad del "Grupo Puca". Bol. Inst. Bol. Petr., 8: 16-28.

Cabrera, A. AND Petersen, G. (1936). Reconocimiento geológico de los Yacimientos Petrolíferos del Departamento de Puno. Boletín del Cuerpo de Ingenieros de Minas del Perú, 115, 100 pp.

Caron, M., Robaszynski, F., Amedro, F., Baudin, F., Deconinck, J.-F., Hochuli, P.A., von Salis-Perch Nielsen, K. and Tribovillard, N. (1999). Estimation de la durée de l'événement anoxique global au passage Cénomanien/Turonien; approche cyclostratigraphique dans la formation Bahloul en Tunisie centrale. Bull. Soc. Géol. France, 170: 145-160.

Cruz, M. (2002). Estratigrafía y evolución tectono-sedimentaria de los depósitos sin-orogénicos del cuadrángulo de Huambo: Las formaciones Ashua y Huanca, departamento de Arequipa. Tesis UNSA, Arequipa, 127 pp.

Gradstein, F.M., Ogg, J.G. and Smith, A.G. (2004). A Geologic Time Scale 2004. Cambridge University Press, 589 pp.

Graf, A.A. (2002). Le Cénomanien supérieur en Bolivie: Etude sédimentologique et stratigraphique de la Formation Matilde-Miraflores. Travail de diplôme, U. Fribourg, Suisse.

Graf, A.A., Strasser, A. and Caron, M. (2003). OAE-2 equivalent (Upper Cenomanian) recorded in Bolivian shallow-water sediments. Abs. 11th Swiss Sed. Meeting, Fribourg, 39-40.

Hosttas, J. (1967). Estudio geológico del túnel terminal entre Huambo y Querque. Tesis UNSA, Arequipa, 107 p.

Jaillard, E. (1994). Kimmeridgian to Paleocene tectonic and geodynamic evolution of the Peruvian (and Ecuadorian) margin. In: Cretaceous tectonics of the Andes (J.A.Salfity, ed.). Braunschweig, Vieweg, 101-167.

Newell, N.D. (1949). Geology of the Lake Titicaca region, Peru and Bolivia. Geol. Soc. of Amer. Memoir, 36, 111 pp.

Portugal, J. (1974). Mesozoic and Cenozoic stratigraphy and tectonic events of Puno-Santa Lucia area, Department of Puno, Peru. AAPG Bull., 58: 982-999.

Robert, E., Bulot, L.G., Jaillard, E. and Peybernès, B. (2002). Proposition d'une nouvelle biozonation par ammonites de l'Albien du Bassin andin (Pérou). *C*. R. Palevol, 1: 1-9.

Spence, G.H. and Tucker, M.E. (1997). Genesis of limestone megabreccias and their significance in carbonate sequence stratigraphic models: A review. Sedimentary Geology, 112: 163-193.

Sempere, T. (1995). Phanerozoic evolution of Bolivia and adjacent regions. In: Petroleum Basins of South America (A.J. Tankard, R. Suárez & H.J. Welsink, eds.). AAPG Memoir, 62: 207-230.

Sempere, T., Jacay, J., Carrillo, M.-A., Gómez, P., Odonne, F. and Biraben, V. (2000). Características y génesis de la Formación Ayabacas (Departamentos de Puno y Cusco). Bol. Soc. Geol. Perú, 90: 69-76.

Sempere, T., Acosta, H. and Carlotto, V. (2004). Estratigrafía del Mesozoico y Paleógeno al norte del Lago Titicaca. In: Nuevas contribuciones del IRD y sus contrapartes al conocimiento geológico del sur del Perú (J. Jacay & T. Sempere, eds.), Sociedad Geológica del Perú, Publicación Especial, 5: 81-103.

Wiese, F. and Schulze, F. (2005). The upper Cenomanian (Cretaceous) ammonite *Neolobites vibrayeanus* (d'Orbigny, 1841) in the Middle East: taxonomic and palaeoecologic remarks. Cretaceous Research, 26: 930-946.

Wright, C.W., Calloman, J.H. and Howarth, M.K. (1996). Treatise on Invertebrate Paleontology. Part L. Mollusca 4 revised, Cephalopoda, Cretaceous Ammonoidea. The Geological Society of America and University of Kansas Press, 362 pp.

L'EFFONDREMENT SOUS-MARIN DE LA PLATE-FORME CARBONATÉE DU SUD PÉROU À LA LIMITE TURONIEN-CONIACIEN : LA FORMATION AYABACAS

Pierre CALLOT*, Thierry SEMPERE*, Francis ODONNE*, Emmanuel ROBERT**

*LMTG, UNIVERSITÉ DE TOULOUSE, CNRS, IRD, OMP, 14 av. edouard belin, 31400, Toulouse, France, callot@lmtg.obs-mip.fr, sempere@lmtg.obs-mip.fr, odonne@lmtg.obs-mip.fr
**OSUG, Université joseph fourier, institut dolomieu, 15 rue maurice gignoux, 38031, Grenoble cedex, France, emmanuel.robert@ujf-grenoble.fr

La Formation Ayabacas est une unité resédimentée qui affleure irrégulièrement sur plus de 60 000 km² dans les Cordillères et l'Altiplano du sud du Pérou. Affectée par d'impressionnantes déformations qui contrastent fortement avec les formations sous- et sus-jacente peu perturbées, elle résulte de l'effondrement sous-marin en masse de la plate-forme carbonatée sud-péruvienne à la limite Turonien-Coniacien (~90-89 Ma). Cette dernière s'était déposée dans le bassin d'arrière-arc ouest péruvien lors de deux transgressions entre l'Aptien Supérieur et le Turonien.

A l'extrême NE, dans les parties les plus proximales du bassin, les dépôts ne présentent pas de déformations particulières et ne sont pas déstabilisés (Formation Arcurquina, Zone 0). Puis la Formation Ayabacas s'organise du NE vers le SW selon six zones définies en fonction des faciès de déformation. Dans les zones 1 à 3 la plate-forme carbonatée est marquée par une fragmentation croissante du NE vers le SW. La Formation Ayabacas est ici constituée d'un mélange de radeaux et de nappes sédimentaires carbonatés, de 20 à 40 m d'épaisseur et de 10 m à plusieurs km de long, souvent déformés plastiquement, flottant dans une matrice rougeâtre de boues ou de silts carbonatés et gréseux. Cette matrice contient fréquemment des sédiments fluidisés et des brèches hydroplastiques. Les zones 4 et 5 sont exclusivement carbonatées, et composées de masses de taille croissante en allant vers le SW (jusqu'à plusieurs km) qui s'empilent en "sedimentary thrust and fold systems" (sensus Frey-Martínez et al., 2006). Dans la Zone 6, l'ensemble de la série est affecté par de grands plis gravitationnels asymétriques à vergence SW et seule la partie supérieure de la série est déstabilisée. Les glissements sont contemporains de la croissance des plis puisque leurs produits (slumps, radeaux calcaires,…) se concentrent dans les creux synclinaux.

L'effondrement sous-marin résulte d'une importante activité tectonique en extension qui a engendré seismes et création de pentes favorables aux glissements. Les vitesses de lithification différentes dans les carbonates et les sédiments détritiques ainsi que les surpressions de fluides ont essentiellement facilité le glissement.

L'extension des zones glissées est probablement supérieure à 80 000 km² en plan, l'épaisseur des dépôts varie de 0 m (dans les zones de départ au NE) à plus de 500 m (au SW), et le volume de sédiments déplacés est estimé à plus de 10 000 km3.

FREY-MARTÍNEZ J., CARTWRIGHT J. & JAMES D. (2006) Frontally confined versus frontally emergent submarine landslides: A 3D seismic characterisation. Marine and Petroleum Geology, vol. 23, p. 585-604.

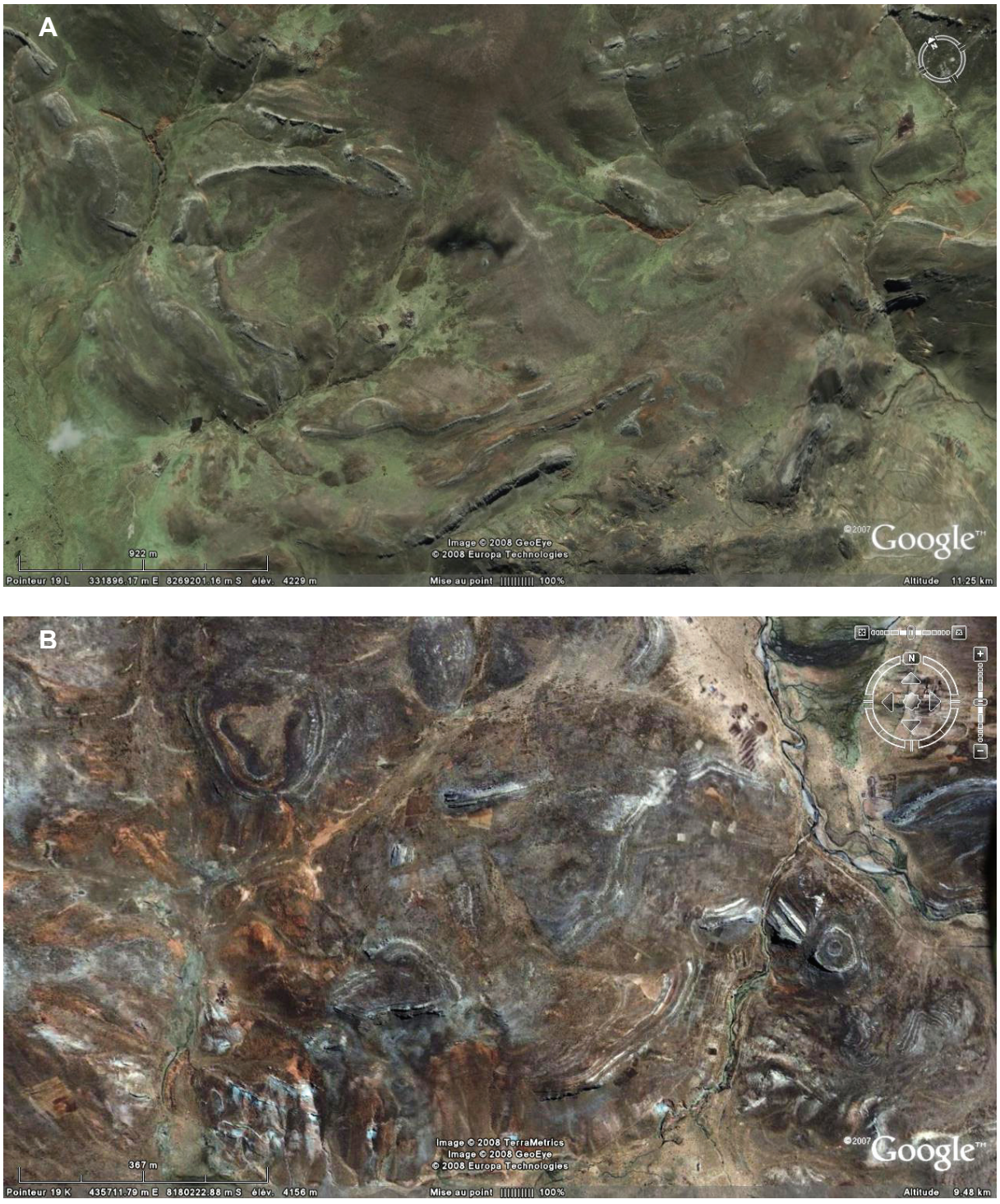

Annexe 2 : Images satellites Google Earth de la Formation Ayabacas, avec les faciès typiques des zones amont (radeaux calcaires peu épais, avec une large extension latérale, flottant dans une matrice pélitique-gréseuse rougeâtre ; image A), des zones centrales (faciès très chaotique, radeaux calcaires très fragmentés flottant dans une matrice pélitique-gréseuse rougeâtre ; images B et C), et des zones plus aval (diminution de la désorganisation, empilement de radeaux calcaires plus épais et avec une plus grande continuité latérale, matériaux presque exclusivement carbonatés ; image D). Il existe un fort contraste entre les déformations de la Formation Ayabacas et les unités sous- et sus-jacente, que l'on note sur l'image C : les Couches Rouges du Crétacé supérieur, régulièrement stratifiées et seulement basculées par la tectonique orogénique andine, reposent sur la Formation Ayabacas chaotique.


C
Image © 2008 TerraMetrics
Image © 2008 GeoEye
© 2008 Europa Technologies
Google
474 m
19 K 455695.25 m E 8153586.46 m S
élév. 4120 m
Altitude 10.09 km


D
N
Image © 2008 GeoEye
© 2008 Europa Technologies
Google
406 m
19 K 434745.19 m E 8168111.31 m S
élév. 4256 m
27 sept. 2003
Altitude 9.67 km

The Ayabacas Formation (Turonian-Coniacian boundary, southern Peru): submarine collapse ensued from the initiation of the Andean orogeny

The Ayabacas Formation, which crops out irregularly over more than 80 000 km^2 in the Andes of southern Peru, is a submarine mass-wasting deposit that displaced more than 10 000 km^3 of sedimentary materials during a single event (at the scale of geological time). It results from the submarine collapse, near the Turonian-Coniacian boundary (~90 Ma), of the carbonate platform. Its dimensions are comparable to those of recent giant slides and the Ayabacas collapse appears as the most extensive fossil submarine mass-wasting body currently known.

Deposits are organised from NE (head) to SW (toe) into six zones, on the basis of deformational facies and in relation with two important structural systems that were reactivated at the time of collapse.

When compared with recent or fossil giant slides, the Ayabacas Formation appears as an atypical collapse because it occurred along an apparently stable backarc margin. The collapse occurred just prior to the rapid continentalization of the backarc basin of Peru, which have long been interpreted to mark the beginning of the Andean orogeny, and was one of the consequences of the significant changes that affected the Pacific mantle convection cell between ~91 and 70 Ma. Along the Peru margin, the conditions of subduction were abruptly modified starting ~91-89 Ma: decrease in slab subduction angle increased plate coupling and slab velocity, which dragged down and flexured the backarc lithosphere. This flexuration normal-faulted the backarc substratum, which triggered the giant collapse of its sedimentary cover.

AUTEUR : Pierre CALLOT

TITRE : La Formation Ayabacas (limite Turonien-Coniacien, Sud-Pérou) : collapse sous-marin en réponse à l'amorce de l'orogenèse andine

DIRECTEURS DE THESE : Francis ODONNE, Thierry SEMPERE

LIEU ET DATE DE SOUTENANCE : 26 juin 2008, Université Paul Sabatier, Observatoire Midi-Pyrénées, 14, av. Edouard Belin, 31400 Toulouse

---

La Formation Ayabacas, qui affleure irrégulièrement sur > 80 000 km^2 dans les Andes du Sud-Pérou, est un dépôt de transport en masse sous-marin déplaçant plus de 10 000 km^3 de sédiments. Elle s'organise en 6 zones, du NE au SW, en relation avec deux importants systèmes structuraux d'échelle lithosphérique, et résulte du collapse de la quasi-totalité de la plate-forme carbonatée à la limite Turonien-Coniacien, lors d'un événement unique à l'échelle des temps géologiques. Ses dimensions, de l'ordre de celles des glissements sous-marins géants, en font le plus grand glissement sous-marin fossile connu. Ce collapse, atypique, précède la continentalisation du bassin, marqueur de l'émergence des Andes. Il résulte de changements géodynamiques à l'échelle de la cellule de convection mantellique Pacifique, en particulier une flexure de la lithosphère et un découpage du substratum ante-Ayabacas en blocs basculés par des failles normales, créant des pentes favorables au collapse de la plate-forme.

MOTS-CLES :
Instabilités sédimentaires ; Glissement sous-marin fossile ; Collapse ; Sud Pérou ; Andes ; Limite Turonien Coniacien ; Déformations synsédimentaires ; Mégabrèche carbonatée ; Plate-forme carbonatée ; Crétacé

DISCIPLINE ADMINISTRATIVE :
Sciences de la Terre

INTITULE ET ADRESSE DU LABORATOIRE :
Laboratoire des Mécanismes et Transferts en Géologie (LMTG), UMR 5563.
Université de Toulouse, CNRS, IRD, OMP, 14 av. Edouard Belin, 31400 Toulouse